Defining and Dissecting Mitochondrial Specific Stress Signalling Pathways in *Arabidopsis thaliana*

Submitted by

Cunman He

(B.Sc. Shandong Agricultural University;

M.Sc. Zhejiang University)

This thesis is submitted in total fulfilment of the requirements for the degree of Doctor of Philosophy

College of Science, Health and Engineering

School of Life Sciences

Department of Animal, Plant and Soil Sciences

La Trobe University

Victoria, Australia

August 2021

TABLE OF CONTENTS

STATEMENT OF AUTHORSHIP

Except where reference is made in the text of the thesis, this thesis contains no other material published elsewhere or extracted in whole or in part from a thesis accepted for the award of any other degree or diploma.

No other person's work has been used without due acknowledgment in the main text of the thesis.

This thesis has not been submitted for the award of any degree or diploma in any other tertiary institution.

Cunman He, 12 August 2021

ACKNOWLEDGEMENTS

I would like to express my sincere and warm gratitude to my principal supervisor Professor Jim Whelan for accepting me to his outstanding lab, for all his expertise and untiring support. His enthusiasm for plant research and hard work set a good example for me. Under his guidance, I learnt critical and scientific thinking which facilitated the completion of my degree.

My sincere thanks also go to my co-supervisor Dr Oliver Berkowitz for his expertise and dedication throughout my study. He not only taught me advanced skills and knowledge in scientific area, but also guided me how to systematically analyse and solve problems in research. His careful mentoring was immensely valuable and provided confidence to continue my research career.

I would like to thank Dr Jennifer Selinski and Dr Yue Xu for their kind guidance, support and help in both science and life, which will be kept in my memory. Thanks to Dr Lim Chee Liew, Dr Reena Narsai and Tim Burge for technical support and professional advice. I would also like to thank all the current and former lab members for a great working environment. Dr Ricarda Jost and Dr Yan Wang gave a lot support and help in the lab, also special thanks to the best cakes prepared by Ricarda. Also, my colleagues Changyu, Marta, Sophia, Ghaz, Emma, Amelia, Harvey, Lu, Xiang, Yanqiao, Andreas, Meiyan, Ritushree, Chunli and all our team members for providing help in my research and life outside the lab. My particular appreciation goes to my MSc advisor Prof. Shou and her recommendation to pursue my PhD in Australia. I also want to acknowledge Dr Mathew Lewsey and Lingling Yin (La Trobe University) for providing seeds of line *proEIN3: EIN3-Ypet* and sharing unpublished data.

A special thank you to my family. I would like to express my deep gratitude to my parents for continuous support and encouragement. My partner Dr Xiaocui Luo provided me with understanding and enormous support especially while I was trapped in China for two months in early 2020 because of the COVID-19 pandemic and the following six lockdowns in Melbourne. Her encouragement as well as my supervisors' strong support kept me going during these difficult times.

Last but not least, I would like to sincerely thank the reviewers of this dissertation for their time and efforts.

This work was supported by a La Trobe University Postgraduate Research Scholarship and a La Trobe University Full Fee Research Scholarship.

ABBREVIATIONS

AA	Antimycin A
ABA	Abscisic acid
ACC	1-aminocyclopropane-1-carboxylic acid
ADP	Adenosine diphosphate
AOX	Alternative oxidase
Col-0	Columbia-0
ChIP	Chromatin immunoprecipitation
CRR	Chloroplast retrograde regulation
CRS	Chloroplast retrograde signalling
DEG	differentially expressed gene
DML	Drought and moderate light
EMS	ethyl methanesulfonate
ER	endoplasmic reticulum
ERF	Ethylene response factor
ET	Ethylene
ETC	Electron transport chain
Fv/Fm	Maximum quantum efficiency of photosystem II
GA	Gibberellin
GUS	β-glucuronidase
H_2O_2	Hydrogen peroxide
IAA	Indole-3-acetic acid
IMM	Inner mitochondrial membrane
IMS	Intermembrane space
LB	Left T-DNA border primer
LP	Left genomic primer
LUC	Luciferase
MDM	Mitochondrial dysfunction motif
MDS	Mitochondrial dysfunction stimulon
MEcPP	Methylerythritol cyclodiphosphate
MIA	Mitochondrial import and assembly
MRR	Mitochondria retrograde regulation
MRS	Mitochondrial retrograde signalling
mtDNA	Mitochondrial DNA
Myxo	Myxothiazol
NGS	Next-generation sequencing

NO	Nitric oxide
$^1O_2$	Singlet oxygen
O_2^-	Superoxide radical
2OG	2-oxoglutarate
2-OGDO	2-oxoglutarate-dependent oxygenases family
OMM	Outer membrane
OXPHOS	Oxidative phosphorylation
PAP	3’-Phosphoadenosine 5’-phosphate
PCD	Programmed cell death
PGE	Plastid gene expression
PPR	Pentatricopeptide-repeat
RAO	Regulator of AOX
REDOX	Reduction/oxidation
ROG	Regulator of OGO
ROS	Reactive oxygen species
RP	Right genomic primer
RTG	Retrograde responsive genes
SA	Salicylic acid
TCA	Tricarboxylic acid cycle
TM	Transmembrane
TOM	Translocase of the outer mitochondrial membrane
UQ	Ubiquinone

ABSTRACT

Mitochondria are essential organelles playing a central role in metabolism, from the production of ATP by oxidative phosphorylation, to a variety of metabolic pathways that provide the building blocks for cell growth. To coordinate and integrate their function to variable cellular needs, mitochondria act as sensors for external and internal stimuli and use a signalling pathway, termed retrograde signalling, to coordinate the expression of organellar and nuclear gene expression.

To further understand how mitochondrial signalling operates, a gene encoding a 2-oxoglutarate Fe(II)-dependent oxygenase (OGO) with sequence similarity to the plant hormone ethylene generating 1-aminocyclopropane-1-carboxylate (ACC) oxidase, was identified that is induced by mitochondrial dysfunction but not high light stress in *Arabidopsis thaliana*. *OGO* is highly expressed in sepals during the flowering stage, and over-expressing plants displayed earlier inflorescence emergence and flowering phenotype. Loss of function mutants for *OGO* are sensitive to combined drought and moderate light treatment while over-expressing lines are more tolerant compared to wild type. *OGO* expression was also up-regulated during leaf senescence and submergence as well as responsive to treatment with the ethylene precursor ACC and biosynthesis inhibitor $AgNO_3$.

A forward genetic screen identified mutants that were impaired in the ability to induce *OGO* on inhibition of mitochondrial function. This identified two genes as putative regulators of *OGO* expression: *SIN3*, encoding an enhancer of ETHYLENE RESPONSE FACTOR 7 activity, and an uncharacterised Acyl-CoA N-acyltransferase.

Furthermore, a time resolved RNA sequencing (RNA-seq) experiment comparing the response of the wild type, a mutant for the ethylene-signalling regulator ETHYLENE INSENSITIVE 3 and an *ogo* mutant after treatment with the complex III inhibitor antimycin A further supported a role for ethylene in mitochondrial signalling. Chromatin immunoprecipitation Sequencing (ChIP-seq) confirmed several ethylene- and auxin related genes as being directly regulated by NAC DOMAIN CONTAINING PROTEIN 17 (ANAC017).

Combined these results identified putative new regulators of mitochondrial signalling and showed that ethylene and auxin are mediating the mitochondrial retrograde response downstream of ANAC017.

1. CHAPTER I - GENERAL INTRODUCTION

1.1 The structure and endosymbiotic origin of mitochondria

Mitochondria are double membrane-bound organelles and present in nearly all eukaryotic cells (Palade, 1953; Duncan et al., 2011). The mitochondrial outer membrane (OMM) is generally permeable, while the inner membrane (IMM) is highly folded into cristae and delimits the mitochondrial lumen (matrix) (Giacomello et al., 2020). The shape and number of mitochondria varies between cells and cell cycle stages with typically rod-shaped or sausage-shaped structure, ranging from 0.5-2 μm in diameter (Palade, 1953; Logan and Leaver, 2000).

According to the widely accepted endosymbiosis theory, mitochondria originated from an endosymbiotic event in which α-proteobacterium-like organism was engulfed by an archaebacterium (Archibald, 2015; Martin et al., 2015; Martijn et al., 2018; Imachi et al., 2020). Sequence comparison studies and bioinformatic analysis of mitochondrial and bacterial genomes strongly supports a single prokaryotic origin (Zimorski et al., 2014). A large number of changes occurred incrementally during the transition from endosymbiotic bacterium to permanent organelle, including the origin of protein import system, insertion of small molecule transporters into mitochondrial membranes, genome reduction, endosymbiotic gene transfer, integration of biochemical pathways and the retargeting of proteins (Roger et al., 2017). Although the majority of the genome inherited from the endosymbiont was either lost or horizontally transferred to the nuclear genome of the host cell during evolution, a core set of proteins is still encoded by the mitochondrial genome (Karlberg et al., 2000; Henze and Martin, 2001; Bjorkholm et al., 2015).

1.2 The plant mitochondrial genome

The mitochondrial genome (mtDNA) is highly variable in size and structure in different species due to DNA loss or migration to the nuclear genome (Roger et al., 2017). Whereas human mtDNA contains 37 genes in a 16.6 kb circular molecule and yeast mtDNA varies from 18.5 kb to 105 kb with a coding capacity similar to animals (30-40 genes), land plants have much larger mtDNA typically around 200-400 kb (Table 1) (Sloan et al., 2012; Chevigny et al., 2020; Imachi et al., 2020). Despite the large size, the plant mitochondrial genome only has less than 100 additional genes compared to animals and yeast due to the majority of the mtDNA being noncoding or repeat sequences (Table 1) (Unseld et al., 1997; Chevigny et al., 2020). First to be entirely sequenced, the *Arabidopsis thaliana* mitochondrial

genome has a size of 367 kb and encodes for 32 proteins such as subunits of multi-protein complexes of respiratory chain, ribosomal proteins, 22 tRNAs and 3 ribosomal RNAs (5S, 18S and 26S rRNAs) (Unseld et al., 1997; Gualberto et al., 2014; Liberatore et al., 2016).

Table 1. Scale comparison of mitochondrial genome size and proteome between different organisms. Table is adapted from Morley and Nielsen (2017); Pfannschmidt et al (2020).

Species	Mitochondrial genome size	Coding capacity	Proteome
A. thaliana	367 kb	164 genes	>2000 proteins
Plasmodium	~6 kb	~ 68 genes	~246 proteins
S. cerevisiae	79 kb	55 genes	1000-3500 proteins
D. melanogaster	19.5 kb	37 genes	>1000 proteins
M. musculus	16 kb	37 genes	>1000 proteins
H. sapiens	16.6 kb	37 genes	>1000 proteins

In contrast, over a thousand plant mitochondrial proteins have been resolved by proteomic analysis, thus most of proteins in mitochondria are encoded in nucleus, synthesized in the cytosol, and then translocated across the mitochondrial membranes (Dolezal et al., 2006). Signals are required to coordinate the gene expression of the mitochondrial and nuclear encoded proteins and protein complex subunits, which is achieved by both anterograde control (nucleus to organelle) and retrograde signalling (organelle to nucleus). (Woodson and Chory, 2008; Pfannschmidt et al., 2020).

Plant mitochondrial genes are transcribed by RNA polymerases with phage-type single submit (Hedtke et al., 1997; Bruce Cahoon and Stern, 2001). There are three RNA polymerases in this group, of which RpoT1 and RpoT2 are targeted to mitochondria in Arabidopsis (Emanuel et al., 2006). The primary transcript is further modified in different ways including editing, splicing and subsequent maturation by 5' and 3' end processing (Perrin et al., 2004). The RNA-binding pentatricopeptide repeat (PPR) proteins are large family in plants and the majority of the 450 PPR proteins are predicted to be targeted to mitochondria in Arabidopsis (Rao et al., 2017; Gutmann et al., 2020). PPR proteins are involved in every known stage between transcription and translation including altering RNA sequence, turnover, cleavage, splicing, editing, translation initiation and association with ribosome (Millar et al., 2008; Fujii and Small, 2011; Gutmann et al., 2020). Cytoplasmic male

sterility (CMS) occurs when flower abnormalities or pollen abortion is caused by a mitochondrial gene mutation of which the majority are PPR proteins (Carlsson et al., 2008). Thus, PPR protein research in Arabidopsis helped to understand the complex phenomenon used in crop breeding to facilitate the production of hybrid seeds (Millar et al., 2008).

1.3 Plant mitochondrial proteome and function

1.3.1 Oxidative phosphorylation and energy metabolism

The plant mitochondrial proteome was reported to contain as many as 2000-3000 different proteins, of which around 1000 mitochondrial proteins have been identified, including subunits of mitochondrial respiratory complexes, phosphorylated proteins, supercomplexes and oxidized proteins (Millar et al., 2005; Rao et al., 2017). The primary role of plant mitochondria is the synthesis of adenosine triphosphate (ATP) via respiratory oxidation of organic acids and transfer electrons to O_2 through the mitochondrial electron transport chain (mETC), in which 205 proteins are involved in Arabidopsis (Raghavendra and Padmasree, 2003; Rao et al., 2017; Zancani et al., 2020) (Figure 1).

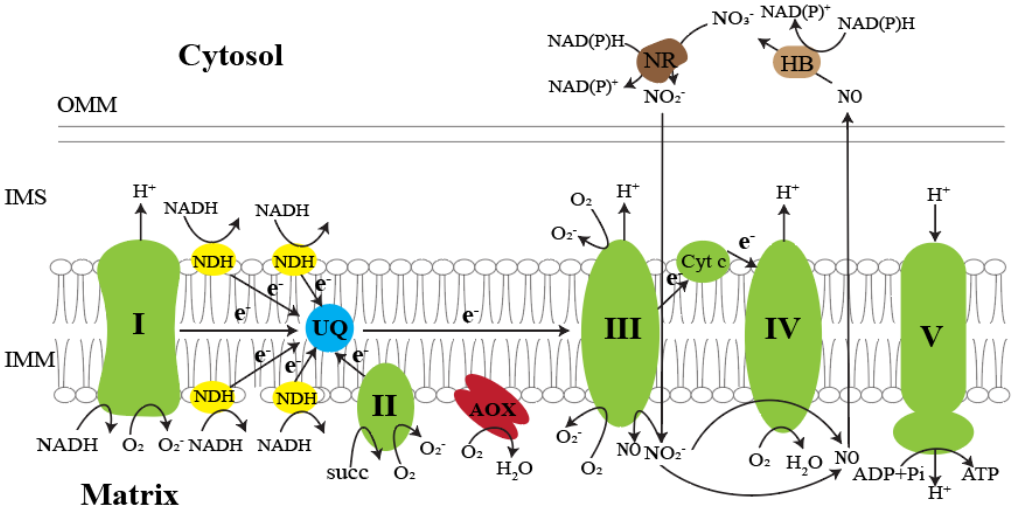

Figure 1. The respiratory electron transport chain in inner membrane of plant mitochondria
Under normal conditions, complexes I, III and IV transfer electrons across the inner mitochondrial membrane (IMM) into the intermembrane space (IMS), producing a proton gradient which drives ATP synthesis. Under stress, alternative oxidase (AOX) catalyses the oxidation of UQH2 and reduces O_2 to H_2O, bypassing complex III, cytochrome *c* and complex IV. Under hypoxia, the NO_2^- act as alternative electron acceptor at complex III and complex IV. Abbreviations: I-V, respiratory complex; I, NADH dehydrogenase; II, succinate dehydrogenase; III, UQ-cytochrome *c* oxidoreductase; IV, cytochrome *c* oxidase; V, F_1F_0 type H^+-ATP synthase; UQ, ubiquinone; NDH, NADH dehydrogenase; NR, nitrate reductase; HB, hemoglobin; OMM, outer mitochondrial membrane; IMM, inner mitochondrial membrane; IMS, intermembrane space; Cyt: cytochrome, succ, succinate. Figure is adapted from Moller et al (2001); Stoimenova et al (2007); Millar et al (2008); Meyer et al (2019).

The main components of the mETC include flavoproteins, FeS proteins, cytochromes, ubiquinone and copper atoms. They consist of four complexes embedded (complex I, III, IV) in or associated (complex II) with the inner membrane: NADH:ubiquinone oxidoreductase – complex I, succinate dehydrogenase – complex II, cytochrome bc1 complex – complex III, and cytochrome c oxidase – complex IV (Fernie et al., 2004; Braun, 2020). Complex I oxidises nicotinamide adenine dinucleotide (NADH) that is generated from the tricarboxylic acid (TCA) cycle and transfers them to ubiquinone (UQ - oxidised) to form ubiquinol UQH2). Likewise, complex II oxidises FADH2 produced in the TCA cycle to reduced UQ to UQH2 (Figure 1). Ubiquinols oxidised by complex III transfer the electrons to the mobile carrier cytochrome *c* (cyt *c*). Reduced cyt *c* is oxidised by complex IV, which uses the electrons to reduce molecular oxygen to water (Breidenbach et al., 1997; Larosa and Remacle, 2018). These reactions are coupled to the creation of an electrochemical gradient across the IMM by the transfer of hydrogen ions across the IMM at complex I, III and IV, and the resulting transmembrane proton gradient is used to generate ATP via complex V (ATP synthase) (Zancani et al., 2020). Alternatively, the cyanide-resistant alternative oxidase (AOX) catalyses the oxidation of UQH_2 and reduces O_2 to H_2O, bypassing complex III, cytochrome *c* and complex IV (Figure 1). As a result, most of the energy is dissipated as heat and a reduction in the production of ATP occurs (Siedow et al., 1995; Ho et al., 2007). Moreover, rotenone-insensitive NADH dehydrogenases (NDAs,NDBs) are also involved in nonenergy conserving bypasses of complex I in Arabidopsis (Soole and Menz, 1995; Michalecka et al., 2003; Antos-Krzeminska and Jarmuszkiewicz, 2019).

1.3.2 Protein import from the cytosol

Given that plant mitochondria contain more than 2000 protein and less than 50 are encoded by the mitochondrial genome, the majority of the mitochondrial proteins are nuclear encoded and translated in the cytoplasm (Murcha et al., 2014). These proteins are maintained in an import-competent form by cytosolic chaperones which direct the precursor to the translocase of outer membrane (TOM) complex (Pfanner and Geissler, 2001; Ghifari et al., 2018). All precursor proteins cross the TOM in the outer membrane (Millar et al., 2008). Four major protein import pathways have been identified in plant mitochondria based on the specific subcompartments they are targeted to (Ghifari et al., 2018). In general import pathway, proteins are directed to the matrix across the TIM17:23 (translocase of the inner membrane) complex which removes the cleavable targeting sequence (Pfanner and Geissler, 2001; Murcha et al., 2003). There are three orthologues of TIM17 in Arabidopsis with the predicted molecular masses of 26, 23 and 14 k Da, among which TIM17-1 has been

characterized to play a role in defining the timing of the germination (Pfanner and Geissler, 2001). The MIA (the intermembrane space import and assembly machinery) is responsible for the import of small intermembrane space proteins with twin cysteine residues (Gnadlinger, 1991; Bolender et al., 2008). Carrier protein with internal signals are imported via TIM22-mediated transport across the inner mitochondrial membrane for insertion in the inner membrane (Pfanner and Geissler, 2001). The sorting and assembly machinery (SAM) complex is located on the outer mitochondrial membrane and responsible for the import/assembly of both α-helical and β-barrel outer membrane proteins such as Tom20 and Tom40, respectively (Neupert and Herrmann, 2007; Stojanovski et al., 2007).

1.4 Organellar signalling

With organellar proteins encoded in separated and compartmentalized genomes, coordinated expression is required to control the stoichiometry of organellar proteins and maintain organelle functions (Woodson and Chory, 2008; Kmiecik et al., 2016; Pfannschmidt et al., 2020). The communication between organelles and the nucleus is crucial for cellular homeostasis as well as stress responses, and ensures gene expression adjust to developmental, tissue-specific, internal and external stimuli. This is more complicated in plants than other eukaryotes due to the additional presence of chloroplasts (Woodson and Chory, 2008; Kmiecik et al., 2016; Pfannschmidt et al., 2020).

There is a two-way communication between organelles and the nucleus, one defined as anterograde (nucleus to organelle) and the other retrograde signalling pathways (organelle to nucleus) (Pfannschmidt et al., 2020). Anterograde signalling is a “top-down” control, where the changes in expression of nuclear genes encoding organellar proteins are directly controlled by developmental and environmental signals transmitted directly to the nucleus. This anterograde regulation occurs at different levels, i.e. by transcriptional and post-translational regulation (Woodson and Chory, 2008). The pathways that influence nuclear gene expression by signals emanating from organelles are defined as retrograde regulation (Woodson and Chory, 2008; Kmiecik et al., 2016). This regulation acts as feedback signals to modulate nuclear gene expression to regulate cellular energy metabolism for optimal growth and survival (Mielecki et al., 2020; Pfannschmidt et al., 2020). While mechanisms involved in retrograde plastid-to-nucleus signalling have been elucidated over the last few decades, the nature of mitochondrial retrograde signalling is still not well understood and needs further characterisation (Kmiecik et al., 2016).

1.4.1 Chloroplast retrograde signalling

The chloroplast retrograde regulation (CRR) pathway has been well established due to its significance and readily observed phenotypes as mutants are often affected in the greening process. The first evidence of signals form plastids was discovered in barley and Pelargonium, where nucleus encoded but plastid located enzymes of the Calvin cycle were reported to be significantly reduced (Beck, 2005; Borner, 2017). Currently, five major classes of plastidial signals have been distinguished depending on where they originate from: (i) plastidial gene expression (PGE); (ii) pigment biosynthesis such as tetrapyrrole biosynthesis and intermediates of carotenoids; (iii) reactive oxygen species (ROS) generation and redox processes in photosynthesis; (iv) metabolite pool changes; (v) signals mediated by dual-localized proteins in both the nucleus and plastids (Pfannschmidt, 2010; Pfannschmidt et al., 2020).

The inhibition of chloroplast biogenesis by plastid translation inhibitor lincomycin (Lin) and carotenoid biosynthesis inhibitor norflurazon (NF) was used to identify and characterize the CRR (Woodson et al., 2013).The genomes uncoupled (gun) mutants, in which the nuclear transcriptional response is uncoupled from chloroplast status, were identified based on an induced expression of *LIGHT HARVESTING CHLOROPHYLL A/B BINDING PROTEIN 1.2* (*LHCB1.2*) following NF treatment (Susek et al., 1993; Zhang et al., 2015). In total six *gun* mutants have been identified in Arabidopsis and five of them (*gun2*-*gun6*) have mutations encoding proteins involved in tetrapyrrole synthesis including heme oxygenase (GUN2), phytochromobilin synthase (GUN3), H subunit of Mg-chelatase (GUN4 and GUN5), GUN6 (results in the induction of ferrochelatase 1) (Mochizuki et al., 2001; Larkin et al., 2003; Woodson et al., 2011). GUN1 encoding a pentatricopeptide-repeat (PPR) protein is located in chloroplast and is the only gun mutant that elevated nuclear gene expression with Lin treatment as well as NF treatment (Hernandez-Verdeja and Strand, 2018). The involvement of GUN1 in chloroplast retrograde signalling pathways linked to plastid gene expression, tetrapyrrole biosynthesis, photosynthetic electron transport and was report to function as a master switch that generates or transduce signals to induced expression of *ABSCISIC ACID INSENSITIVE4* (*ABI4*) (Nott et al., 2006; Koussevitzky et al., 2007). However, a recent study showed that there is no consistent evidence to support the proposal that ABI4 is involve in the chloroplast to nucleus retrograde response downstream of GUN1 (Kacprzak et al., 2019).

Several specific metabolites derived form disturbed plastid metabolism accumulate under stress, such as 3’-phosphoadenosine 5’-phosphate (PAP) and 2-C-methyl-D-erythritol 2,4-cyclodiphosphate (MEcPP). The phosphatase SAL1 degrades and detoxifies PAP which

is maintained at low levels under non-stress conditions (Phua et al., 2018). Under adverse environmental conditions such as drought and high light, an inactivation of redox regulated SAL1 leads to the accumulation of PAP and SAL1-PAP retrograde pathway altering nuclear gene expression (Estavillo et al., 2011; Chan et al., 2016; de Souza et al., 2017). Evidence for a modulation of hormonal signalling by the PAP pathway modulates was provided by enrichment of methyl jasmonate and ABA genes in *sal1* mutant microarray data set as well as overaccumulation of jasmonic acid in *sal1* (Rodriguez et al., 2010). MEcPP as a precursor of isoprenoids produced in plastidial methylerythritol phosphate (MEP) pathway regulates stress-responsive nuclear genes expression (Xiao et al., 2012). MEcPP also alters auxin homeostasis and ethylene concentrations to reprogram plant growth in adaptive responses to adverse growth conditions (Jiang et al., 2018; Jiang et al., 2019; Jiang and Dehesh, 2021). β-cyclocitral (β-CC) as the product of β-carotene oxidation is involved in chloroplast retrograde signalling by enhancing photo-oxidative stress tolerance and salicylic acid (SA) synthesis (Ramel et al., 2012). In addition, accumulation of reactive oxygen species (ROS) like singlet molecular oxygen or superoxide generated in the chloroplast, and other redox-signals serve as important stress signals, which further triggers acclimation responses in the nucleus (Pfannschmidt et al., 2003; Pfannschmidt, 2010; Leister, 2019).

1.4.2 Discovery of mitochondrial retrograde signalling in yeast and mammals

A variety of adverse growth conditions or mutations in genes encoding mitochondrial proteins (mitochondrial encoded or nuclear encoded) alter mitochondrial function In response, mitochondria trigger changes in nuclear gene expression through organelle to nucleus signalling which is referred to as mitochondrial retrograde regulation (MRR) (Brodsky, 1991; Pfannschmidt et al., 2020). The MRR is also an important pathway by which plant mitochondria function as sensors of biotic and abiotic stresses (Liu and Butow, 2006).

Pioneering studies into mitochondrial retrograde signalling were performed in the budding yeast *Saccharomyces cerevisiae* (Parikh et al., 1987; Liu and Butow, 2006). The citrate synthase isoform 2 (CIT2) is a typical target of retrograde responsive genes (RTG) pathway and induced as much as 30-fold when mitochondrial functions are compromised (Liao et al., 1991). Several positive and negative regulators involved in RTG pathway have been identified in a screen for mutants that fail to induce CIT2 (Ellingson et al., 1977; Jia et al., 1997; Liu et al., 2001; Liu et al., 2003). This identified the transcription factor subunits Rtg1p and Rtg3p, the regulatory phosphatase Rtg2p and the ubiquitin-ligase Grr1p (Glucose Repression Resistant) which are positive regulators of classical RTG pathways, while the multiple kinase suppressor Mks1p, seven WD-repeat protein Lst8p and 14-3-3 proteins act

as negative regulators (Roberts et al., 1997; Sekito et al., 2000; Liu et al., 2001; Sekito et al., 2002; Liu et al., 2003; Spielewoy et al., 2004). In addition to the RTG pathway, there are other retrograde signalling pathways in yeast. This includes the AGING FACTOR ONE1 (AFO1) activated retrograde pathway via TARGET OF RAPAMYCIN (TOR1) and perturbation of mitochondrial protein synthesis activated retrograde pathway (Heeren et al., 2009; Caballero et al., 2011). In addition, mitochondrial precursor overaccumulation stress activates the unfolded protein response (UPR) (Wang and Chen, 2015; Wrobel et al., 2015; Weidberg and Amon, 2018; Pfannschmidt et al., 2020). Mitochondrial retrograde signalling in mammalian cells was first revealed in *Mus musculus* (mouse) C2C12 skeletal myoblasts and further confirmed in human lung carcinoma A549 cells (Biswas et al., 1999; Amuthan et al., 2002). To date, reduction of mitochondrial and cellular ATP levels, changes of the cellular NADH/NAD^+ ratio, disequilibrium of cellular oxidative defences and free radical production, and deregulation of cellular Ca^{2+} homeostasis have been recognised as primary mitochondrial dysfunction signals to play an important role in retrograde signalling in mammalian cells (Jones et al., 2012).

1.4.3 The plant mitochondrial retrograde signalling pathway

The existence of plant mitochondrial retrograde response was firstly identified with the *non-chromosomal stripe* (*NCS*) mutants containing an abnormal mitochondrial DNA arrangement and leading to yellow sectors of leaves in *Zea mays* (maize) (Newton and Coe, 1986). This indicated that mitochondrial dysfunction not only changes the gene expression of nuclear encoded proteins but also disturbs the function on a whole cell level (Newton and Coe, 1986). Subsequent studies revealed that the plant MRR plays an essential role in response to stresses (Dutilleul et al., 2003; Dojcinovic et al., 2005; Wang et al., 2020). Mitochondrial function is perturbed by treatment of plants with chemical inhibitors of mitochondrial electron transport such as complex III inhibitors antimycin A (AA) and myxothiazol (myxo) (Alber and Vanlerberghe, 2021). Therefore, experiments using these inhibitors were important to identify genes and proteins involved in the MRR.

Based on microarray-derived transcriptome data sets for mitochondrial perturbation experiments and mutation of genes, 24 mitochondrial dysfunction stimulon (MDS) genes have been identified in *Arabidopsis thaliana* (De Clercq et al., 2013). *Alternative oxidase 1a* (*AOX1a*) is one of these mitochondrial dysfunction stimulon (MDS) genes and its increased expression has established it as a marker of impaired mitochondrial function (Clifton et al., 2006; De Clercq et al., 2013; Ng et al., 2014, Rhoads and Subbaiah, 2007; Selinski et al., 2018). Alternative oxidase (AOX) as a terminal oxidases UQH2 and reduces O_2 to H_2O,

bypassing complex III (Vanlerberghe et al., 2020). As oxidation of substrate by AOX bypasses complex III and IV of the mtETC, the energy is dissipated as heat. It is been studied in a wide range of plant species and by far commonly used as indicator to characterize mitochondrial retrograde signalling (Clifton et al., 2006; Rhoads and Subbaiah, 2007; Ng et al., 2014). AOX is encoded by two nuclear isoforms, AOX1 and AOX2, in dicotyledons, with the AOX2 orthologs seemingly lost in most monocots (Considine et al., 2002; Costa et al., 2017). In Arabidopsis, there are five members of the AOX gene family, *AOX1a, 1b, 1c, 1d and AOX2* (Clifton et al., 2006). AOX maintains the energy homeostasis effectively in a range of metabolic conditions (Yoshida et al., 2008; Vanlerberghe et al., 2009). In plants, when the electron transport ability of the mtETC is reduced or inhibited, electrons leak from complex I and III leading to the generation of ROS and reactive nitrogen species (RNS). AOX activity prevents this over-reduction of the mtETC and leads to concomitant reduction in ROS formation (Millar et al., 2001). AOX activity is regulated on various levels, from transcriptional to post-translational regulation on the protein level to keep its potentially energy-wasting activity under tight control (Selinski et al., 2018). Antimycin A inhibits photosynthetic electron transport, which opens the possibility that the induction of AOX1a by antimycin A can also result from an inhibition of chloroplastidic electron transport activity (Cape et al., 2006; Blanco et al., 2014; Labs et al., 2016). In agreement, AOX plays a role in maintaining photosynthesis under drought or high light conditions (Noguchi and Yoshida, 2008; Dahal and Vanlerberghe, 2017), and it was proposed that this protection partly comes from export of reducing equivalents from chloroplasts to mitochondria via the malate/oxaloacetate shuttle (Zhang et al., 2017).

The *OUTER MITOCHONDRIAL MEMBRANE PROTEIN OF 66 KDA* (OM66) is another MDS gene (De Clercq et al., 2013). It encodes an AAA ATPase (cytochrome bc_1 synthase 1) annotated previously as BCS1 (cytochrome bc1 assembly, AT3G50930). *OM66* is highly induced at a transcript level by both abiotic and biotic stress conditions. Overexpression lines of *OM66* have a curled-leaf phenotype and increased cell death (Zhang et al., 2014). However, there is no major difference in mitochondrial respiratory chain complex abundance in *OM66* mutant plants (Van Aken et al., 2016). The expression level is also highly increased in the mitogen-activated protein kinase (MAPK) cascade signalling mutants such as *mpk4, mekk1, mkk1* and *mkk2*, suggesting interaction of this signalling pathway with the MRR (Van Aken and Van Breusegem, 2015).

Besides *AOX* and *OM66*, for only a few other MDS genes a direct role in mitigating mitochondrial stress has been established (De Clercq et al., 2013). For only about half of these genes their molecular function is known and many are only annotated by sequence

similarity. The latter range from ribosomal proteins, to MULTI-DRUG AND TOXIC COMPOUND EXTRUSION (MATE) efflux carriers, to chaperones and unknown genes (Table 2).

Table 2. List of MDS genes and their annotation

Genes highlighted in red have no established function in the mitochondrial stress response.

Gene name	AGI	Gene annotation (TAIR10)
AT1G05060	AT1G05060	unknown function
UGT74E2	AT1G05680	Uridine diphosphate glycosyltransferase 74E2
AT1G24095	AT1G24095	Putative thiol-disulphide oxidoreductase DCC
ANAC013	AT1G32870	NAC domain protein 13
RPL12	AT2G03130	Ribosomal protein L12
ST1	AT2G03760	sulphotransferase 12
AT2G04050	AT2G04050	MATE efflux family protein
AT2G04070	AT2G04070	MATE efflux family protein
UPOX	AT2G21640	marker for oxidative stress
NAT	AT2G32020	Acyl-CoA N-acyltransferases (NAT) superfamily protein
AT2G41730	AT2G41730	unknown function
ABCB4	AT2G47000	auxin efflux transmembrane transporter
HRE2	AT2G47520	Integrase-type DNA-binding superfamily protein
AOX1a	AT3G22370	alternative oxidase 1A
OXI1	AT3G25250	AGC kinase family protein
PHB4	AT3G27280	prohibitin 4
OM66	AT3G50930	cytochrome BC1 synthesis
CRF6	AT3G61630	cytokinin response factor 6
CYP81D8	AT4G37370	cytochrome P450, family 81, subfamily D, polypeptide 8
At12Cys-2	AT5G09570	Cox19-like CHCH family protein
AT5G14730	AT5G14730	unknown function
OGO	AT5G43450	2-oxoglutarate and Fe(II)-dependent oxygenase, ACO-like
HSP23.5	AT5G51440	HSP20-like chaperones superfamily protein
MGE1	AT5G55200	Co-chaperone GrpE family protein

ANAC013 is a transcription factor that also regulates MDS genes and hence is up-stream in the signalling cascade (De Clercq et al., 2013). *At12Cys-2* (At5g09570) transcript abundance is induced by mitochondrial perturbations and may play a central role in relaying complex I deficiency stress by changing its location between the mitochondria, chloroplasts or the cytosol (Wang et al., 2016). URIDINE DIPHOSPHATE GLYCOSYLTRANSFERASE 74E2 (UGT74E2) and ATP-BINDING CASSETTE B4 (ABCB4) have a function as auxin

conjugase and auxin transporter, respectively, which indicates a crosstalk between mitochondrial signalling and auxin homeostasis (Ivanova et al.; 2014; Kerchev et al., 2014; Noh et al., 2001; Tognetti et al., 2010). Moreover, another two MDS genes link to ethylene. One is MDS gene ethylene response factor (ERF) HYPOXIA RESPONSIVE ERF 2 (HRE2)/ERF71 is a member of the class VII ethylene response transcription factors (ERF) that mediate ethylene-dependent responses under hypoxia in Arabidopsis (Licausi et al., 2010; Lee et al., 2015; Gasch et al., 2016). Among the uncharacterised MDS genes is also a 2-oxoglutarate Fe(II)-dependent oxygenase (AT5G43450, OGO) which is annotated as an ACO-like gene in TAIR10 because of its sequence similarity to the ethylene synthesis enzyme 1-aminocyclopropane-1-carboxylic acid (ACC) oxidase (Vandenbussche et al., 2003; Hagel and Facchini, 2018). This indicates that plant hormones like auxin and ethylene interplay with the mitochondrial retrograde signalling pathway.

1.4.4 Regulators of mitochondrial retrograde signalling in Arabidopsis

Based on AOX being highly up-regulated by antimycin A treatment, components in the MRR have been identified by forward genetic screens in an transgenic Arabidopsis line carrying a construct with the AOX promoter driving a luciferase reporter system. Several mutants termed *regulators of alternative oxidase 1a* (*rao*) with altered luciferase expression were identified and subsequently characterised. CDKE1 (RAO1), a subunit of the kinase module of the mediator complex in plants, is necessary for the regulation of the MRR with stresses like cold and H_2O_2 (Ng et al., 2013). CDKE1 were also reported to interact with a protein kinase 10 (KIN10) in the nucleus which is proposed to be a point of integration of energy and stress signalling during plant growth (Figure 2) (Baena-González et al., 2007). ANAC017/RAO2 is as a positive regulator of *AOX1a*, located at the ER membrane and released to migrate to the nucleus upon mitochondrial perturbation to reprogram retrograde response comprising several hundred genes (Figure 2) (Ng et al., 2013; Meng et al., 2019). Furthermore, several negative regulators of *AOX1a* have been identified, i.e. RAO3 to RAO6, which are involved in auxin signalling (see also 1.6.1) (Ivanova et al., 2014). The transcription factor MYB domain protein 29 (MYB29/RAO7) was shown to repress the MRR as well and its mutation leads to increased *AOX1a* expression compared to the wild type controls (Zhang et al., 2017) (Figure 2)

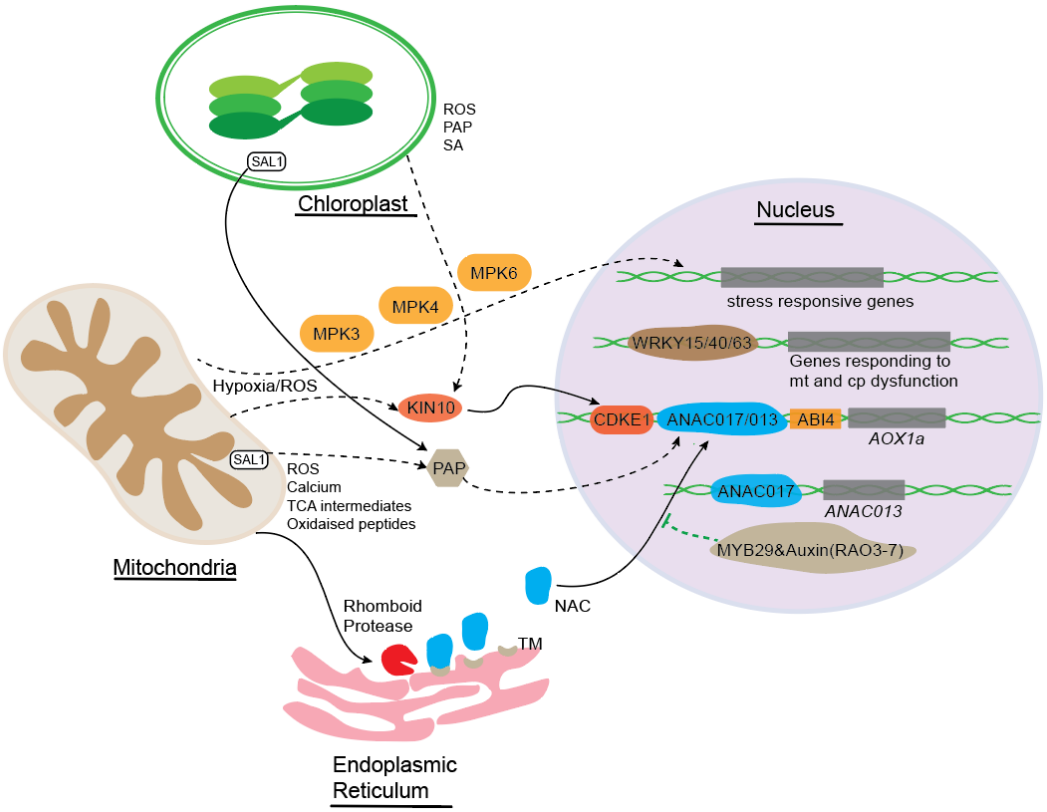

.

Figure 2. Overview of know mitochondrial and chloroplast retrograde signalling
A number of mitochondrial retrograde regulation components (MRR) components have been identified including transcription factors (e.g., NACs, WRKYs, MYBs, ABI4) and kinases (KIN10 and CDKE1) acting as regulators of *AOX1a*. KIN10, ABI4 and CDKE1 are involved in the regulation of both mitochondrial and chloroplast retrograde signalling. Several WRKY transcription factors also respond to both mitochondrial and chloroplast dysfunction. The NAC transcription factor ANAC17, the master regulator of mitochondrial signalling is activating downstream NAC transcription factors such as ANAC13 and other stress responsive proteins in both mitochondria and chloroplasts. Solid line indicates a role that has been experimentally shown. Dashed indicates proposed roles on the basis of transcript abundance changes alone or questioned. MYB29, MYB DOMAIN PROTERIN 29; ANAC, NAC transcription factor 13/17; WRKY 15/40/63, WRKY DOMAIN PROTEIN 15/40/63; CDKE1; CYCLIN-DEPENDENT KINASE E1; ABI4, ABA INSENSITIVE 4; SAL1, phosphate-like protein; PAP, 3'-phosphoadenosine 5'-phosphate; ROS, reactive oxygen species; SA' salicylic acid. Redrawn and modified figure from Ng et al (2014); Wang et al (2020).

Several regulators of *AOX1a* have also been successfully identified by reverse genetic approaches in Arabidopsis. ANAC013 was identified by a yeast one-hybrid screen for transcription factors binding to the promoters of MDS genes and is downstream of ANA017 (Figure 2). However, ANAC013 cannot substitute for the function of ANAC017 after AA treatment (De Clercq et al., 2013). WRKY 40 was identified as a repressor of *AOX1a* retrograde signalling and there is a significant induction of *AOX1a* in *wrky40* knockout lines

compared with wild type under AA treatment or high light stress (Van Aken et al., 2013). WRKY63 is another activator of *AOX1a* and there is a significant induction of *AOX1a* in WRKY63 overexpressing lines (Van Aken et al., 2013). In addition, ABA INSENSITIVE 4 (ABI4) acts as a repressor of *AOX1a* expression under AA treatment, abscisic acid (ABA) and rotenone (Giraud et al., 2009). Moreover, a recent study showed that MYB30 directly binds the promoter of *AOX1a* and up-regulates its expression during the salt stress (Gong et al., 2020).

1.4.5 Interaction of mitochondrial and chloroplast retrograde signalling

In addition to metabolic interaction, mitochondria and chloroplasts share many dual targeted proteins, where the same protein is located in both organelles. There are over 100 dual targeted proteins characterised with as many as 400 predicted to be dual targeted (Mitschke et al., 2009; Xu et al., 2013). ABI4 was linked to both, mitochondrial and chloroplast retrograde signalling, by two separate reports showing its function as a repressor of mitochondrial AOX1a and chloroplastic light-harvesting chlorophyll a/b binding protein (LHCB) (Koussevitzky et al., 2007; Giraud et al., 2009). ABI4 was also reported to be a nuclear component of GUN1-mediated chloroplast retrograde signalling, although its role has been questioned recently (Kacprzak et al., 2019). The phosphatase SAL1 is dual targeting to chloroplasts and mitochondria, which suggested a role of PAP accumulation as a retrograde signalling molecule in both organelles (Van Aken and Pogson, 2017). Moreover, CDKE1 regulates the expression of *AOX1a* and *LHCB2.4* under photosynthetic electron transport chain inhibitors, and its mutant displays impaired ability to recover photosystem efficiency during the initial stages of heterotrophic growth (Blanco et al., 2014), which suggests that CDKE1 integrates both mitochondria and chloroplast retrograde signals (Wang et al., 2020). Signalling pathways from mitochondria to chloroplasts are also integrated by the RADICAL-INDUCED CELL DEATH (RCD1) protein which binds ANAC013 and ANAC017 to repress their activity, leading to a reduced expression of MDS genes (Shapiguzov et al., 2019). This may also explain the observed role of ANAC017 in co-ordinating mitochondrial and some chloroplastic retrograde responses (Van Aken et al., 2016).

1.5 Plant mitochondria and adverse growth conditions

While the biochemical activities of mitochondria have been studied intensively for more than 50 years, in the last decade the role of mitochondria in response to stresses that result in reduction in plant yield, in particular abiotic stresses such as drought, submergence,

excess light and heat have emerged (Atkin and Macherel, 2009; Wang et al., 2018; Che-Othman et al., 2020; Meng et al., 2020; Rashid et al., 2020; Sako et al., 2020; Yu et al., 2020; Scafaro et al., 2021). Several studies have shown that mitochondria are direct targets, sensors and initiators of stresses, from changes in the proteome, altering mitochondrial protein abundance or modification to large-scale changes in the transcriptome encoding mitochondrial proteins (Crawford et al., 2018; Wang et al., 2018; Meng et al., 2020). The role of mitochondria in stress responses is best characterised with reference to AOX, where foundation studies in tobacco, and now in a variety of species, have shown that AOX plays an important role to direct the mitochondrial electron flow, but also to maintain the efficiency of photosynthesis under limiting growth conditions (Dahal et al., 2017; Dahal and Vanlerberghe, 2018). A variety of mitochondrial proteins are consistently induced, or their protein activities altered as hallmarks of mitochondrial perturbation (Schwarzlander and Fuchs, 2017; Wagner et al., 2018; Wang et al., 2018).

In hypoxic conditions such as submergence or in the germinating seed, oxygen is a limiting factor for plant growth as mitochondria depend on oxygen to derive energy from respiration. Transcript abundance changes rapidly when plants are transferred from normal to hypoxic conditions, that occur under conditions such as flooding (Shingaki-Wells et al., 2014; Loreti et al., 2016). In soybean, analysis of mitochondria of plants under flooding stress using proteomics and metabolomics techniques shows that proteins and metabolites related to the TCA cycle were up-regulated, while inner membrane carrier proteins and metabolomics related to complexes III, IV, and V of the respiratory chains were down-regulated (Komatsu et al., 2011). The amounts of NADH and NAD^+ were significantly increased while ATP was decreased by flooding stress. Thus, flooding directly impairs mtETC and decreases carbon flow into the TCA cycle (Komatsu et al., 2011). There is growing evidence demonstrating that mitochondrial Ca^{2+} plays a critical role in initiating anoxic gene expression in many plant species such as maize, barley and Arabidopsis (Nie and Hill, 1997; Tsuji et al., 2000; Klok et al., 2002; Peng et al., 2006). Elevated mtROS that are formed due to the inhibition of both terminal oxidases AOX and complex IV may trigger the release of [Ca^{2+}] leading to changes in gene expression under hypoxic conditions (Ribas-Carbo et al., 1994). Previous work also indicates that sucrose synthase (SUS) interacting with the voltage-dependent anion channel (VDAC) might have a signalling function to communicate the cellular energy status to the nucleus (Daugas et al., 2000). Recent studies showed substantially overlapping transcriptional responses between mitochondrial stress (i.e. antimycin A treatment), submergence and hypoxia, which are

partly controlled by ethylene signalling as well as the mitochondrial retrograde master regulators ANAC017 (Wagner et al., 2018; Meng et al., 2020).

Even though the precise function of plant mitochondria during pathogen attack have not been elucidated yet, there is evidence for the importance of MRR involvement in plants under biotic stress (Van Aken et al., 2013; Colombatti et al., 2014; Burke et al., 2020). The mtROS production increases rapidly during pathogen infection. Elicitors released by plant pathogens induce nuclear gene expression and disrupt mitochondrial function (Krause and Durner, 2004). The bacterial elicitor Harpin acting as an elicitor of bacterial pathogens disrupts mitochondrial ATP synthesis and induces a hypersensitive response (HR) in Arabidopsis suspension cells (Krause and Durner, 2004). This drives the which is a mechanism to limit the spread of microbial pathogens in plants by induction of programmed cell death around the local region surrounding an infection (Zaninotto et al., 2006). It was shown that a strong induction of AOX and a maintenance of high mitochondrial antioxidant manganese superoxide dismutase (MnSOD) activity are caused by infection, indicating that AOX might act as a potential key regulator of a mitochondrial O_2^--based signalling pathway and has an impact on plant responses to bacterial infection (Vanlerberghe, 2013). Evidence shows that the biotic stress-signalling hormone salicylic acid (SA) is both an inhibitor and an uncoupler of mitochondrial electron transport, which suggests that this underlies the induction of some genes by SA. AOX transcript and protein abundance are dramatically induced by SA in thermogenic species, but not Arabidopsis (Rhoads and McIntosh, 1992; Ho et al., 2008). By contrast, the expression of the MDS gene *OM66* is responsive to SA and shows a similar expression pattern as the pathogen-induced PATHOGENESIS-RELATED GENE 1 in several hormone and biotic defence signalling mutants (Ho et al., 2008). OM66 over-expression leads to higher SA content, higher tolerance to *Pseudomonas syringae* (biotrophic pathogen), but higher susceptibility to *Botrytis cinerea* (necrotrophic pathogen) (Van Aken et al., 2013). Expression of the SA marker gene PR-1 is reduced in *om66* mutants. The SA-dependent regulation of OM66 by SA is likely mediated by WRKY transcription factors (Van Aken et al., 2013).

1.6 Interaction between plant hormones and mitochondrial signalling pathways

Plant hormones, including auxin, ethylene, abscisic acid (ABA), cytokinin (CK), gibberellin (GA), jasmonic acid, brassinosteroid (BR) and strigolactone work as signalling substances to regulate plant growth, development, and responses to abiotic and biotic stress

(Vanstraelen and Benková, 2012). Recent studies have shown that mitochondrial retrograde and hormonal signalling pathways interact to optimize plant growth (Figure 3).

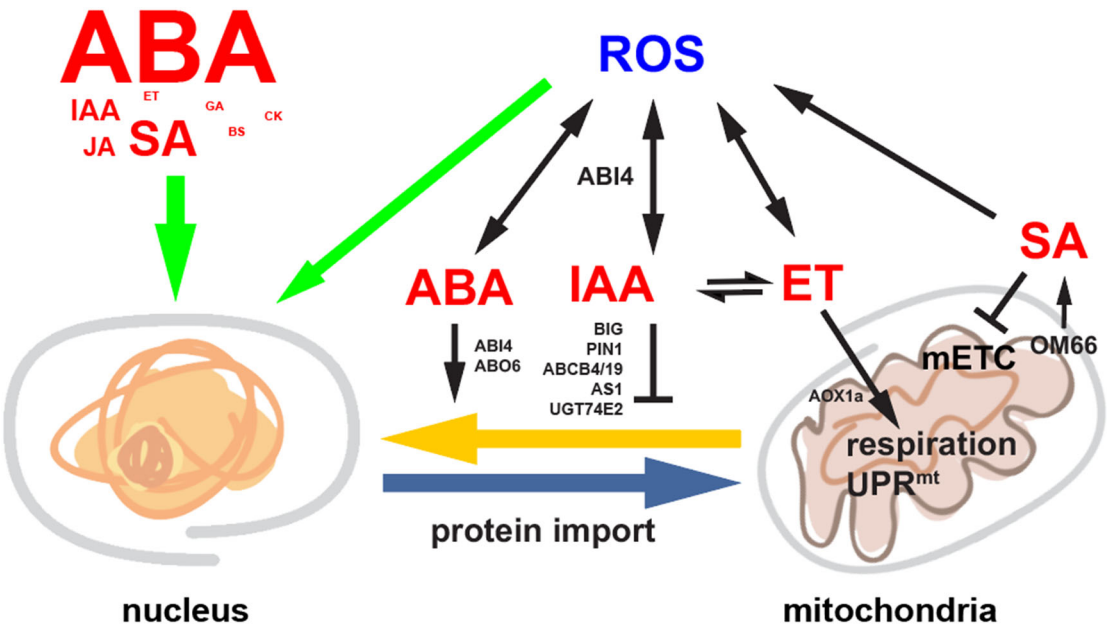

Figure 3. Interaction between hormonal and mitochondrial signalling
Direct control of gene expression by plant hormones and nuclear control of mitochondrial function via protein import are shown as green and blue arrows, respectively. The word cloud represents the extent of the direct transcriptional control of all hormones on the expression of mitochondrial genes. Retrograde signalling and its regulation by hormones with associated genes are indicated by a yellow arrow. Additionally, direct control of mitochondrial function by hormones and their known targets as well as putative feedback mechanisms are shown. For more detailed information on cross-talk between hormone and ROS signalling see recent reviews (Del Rio, 2015; Xia et al., 2015). The intense cross-talk of auxin and ethylene is indicated by reciprocal arrows (Muday et al., 2012). Abbreviations (for gene names see text): ABA: abscisic acid, BS: brassinosteroid, CK: cytokinin, ET: ethylene, GA: gibberellic acid, IAA: auxin, JA: jasmonic acid, mETC: mitochondrial electron transport chain, ROS: reactive oxygen species, SA: salicylic acid. Figure adapted from Berkowitz et al (2016).

Although there is evidence that all major hormones influence mitochondrial function and signalling, it is often still unclear if these are direct regulatory interactions, or if these are indirect consequences of mitochondrial functions impacting growth or developmental processes that subsequently change hormonal homeostasis (Berkowitz et al., 2016; Welchen et al., 2021).

For only a few hormones the molecular mechanism or the role of pathway components has been identified. While ABA was linked early to mitochondrial signalling through the identification of the transcription factor ABI4 as a regulator of *AOX1a* expression

(Giraud et al., 2009), more recently auxin, and also ethylene, are emerging as major hormonal regulators of mitochondrial retrograde signalling (Ivanova et al., 2014; Kerchev et al., 2014; Wang and Auwerx, 2017; Kacprzak et al., 2020; Merendino et al., 2020; Jurdak et al., 2021).

The function of auxin and ethylene as major growth and stress hormones, respectively, and their close interaction, suggests a role of these two hormonal pathways to adjust mitochondrial function to prevailing (adverse) growth conditions and *vice versa* (Muday et al., 2012; Dubois et al., 2018). Therefore, further identification and characterisation of involved components has potential to increase understanding on mitochondrial function and integration with whole plant growth.

1.6.1 Auxin and mitochondrial signalling pathways

After its identification as the plant hormone controlling tropic responses to gravity and light more than 80 years ago (Van Overbeek, 1936; Skoog, 1937), the natural auxin in plants, indole-3-acetic acid (IAA), has been identified as the major hormone regulating plant developmental and growth response including cell division, growth and differentiation (Zhao, 2010; Casanova-Sáez et al., 2021). Early evidence demonstrated that auxin influences the mitochondrial respiratory system to provide sufficient energy and promote plant growth (Albaum and Eichel, 1943; Leonova et al., 1985). Since then, understanding of the genes and biochemical pathways for auxin biosynthesis and signalling has greatly expanded by studies in Arabidopsis, which increased focus on the interplay with mitochondrial signalling. Mitochondria are a major site of ROS production and links between growth control via ROS-auxin interaction has been demonstrated (Kawano, 2003; Pasternak et al., 2005). A mutant for ABO6, encoding a DEXH box RNA helicase regulating the splicing of several genes of mitochondrial complex I, shows increased levels of ROS and decreased auxin levels, providing a mechanism for mitochondrial ROS-mediated growth responses (He et al., 2012). An increase in ROS levels caused by mutation of the mitochondrial inner membrane protease FTSH4 and inhibition of the mETC also leads to altered auxin homeostasis with associated phenotypes (Zhang et al., 2014).

Strong evidence for direct involvement of auxin in the MRR came from a screen for mutants with impaired regulation of *AOX1a* expression under mitochondrial stress. This identified several regulators of *AOX1a* (RAO) that were related to auxin signalling, i.e. the auxin transporters BIG/RAO3, PIN1/RAO4 and ABCB19/RAO5, as well as AS1/RAO6 which is involved in the formation of auxin gradients in leaves (Ivanova et al., 2014). In addition, among the MDS genes highly induced under mitochondrial dysfunction are the auxin

transporter *ABCB4* and the auxin conjugase *UGT74E2* (De Clercq et al., 2013; Kerchev et al., 2014).

Thus, besides ROS mediating the interplay of auxin and mitochondrial function, the MRR is also directly interacting with components of the auxin pathway. This suggests different levels in the auxin pathway, ranging from biosynthesis to signalling, may control the cellular concentration of IAA to modulate the MRR, and a feedback loop also impacts auxin homeostasis. A very brief outline of the auxin pathway is given below to highlight its components and the possible players.

1.6.1.1 Auxin homeostasis and signalling

The concentration of auxin in tissues is controlled by localised biosynthesis (Brumos et al., 2018), conjugation (Casanova-Saez et al., 2021), and directional transport (Hammes et al., 2021). Even though alternative routes via indole-3-acetaldoxime (IAOx) and indole-3-acetamide (IAM) to produce the active auxin IAA are known and complicate the understanding of auxin biosynthesis, the indole-3-pyruvic acid (IPyA) pathway is established as the major route in plants (Figure 4) (Casanova-Saez et al., 2021).

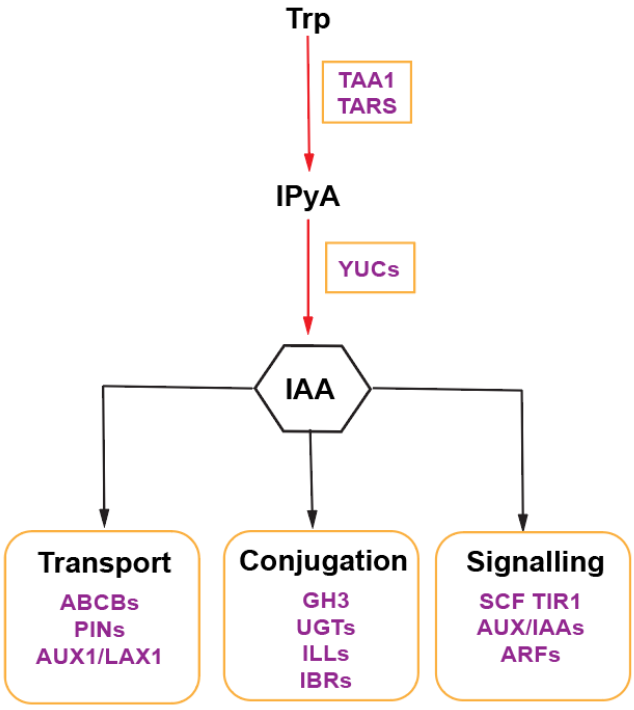

Figure 4. A schematic model of auxin biosynthesis, conjugation, directional transport and signalling in plant

Abbreviations (for gene names and details see text): Trp, tryptophan; IPyA, indole-3-pyruvic acid; IAA, auxin. The red arrows indicate proposed functions of TAA1, TARs and YUCs, respectively. The black arrows indicate process IAA is involved. Figure is adapted from Mashiguchi et al (2011); Leyser (2018); Casanova-Sáez et al (2021).

The prevalent auxin biosynthetic pathway starts with the deamination of the amino acid tryptophan to IPyA catalysed by TAA1 (TRYPTOPHAN AMINOTRANSFERASE OF ARABIDOPSIS1) and TARs (TAA1-RELATED proteins) in the first step (Stepanova et al., 2008; Tao et al., 2008; Yamada et al., 2009). In the second step, IPyA is converted to IAA by the flavin-containing monooxygenases from the YUCCA (YUC) family in the rate limiting and irreversible reaction (Cheng et al., 2007; Mashiguchi et al., 2011). A main source for auxin are classically the apical meristems, but in recent years localised auxin production has been seen as increasingly important (Casanova-Saez et al., 2021). After its formation, IAA is transported through tissues and within the cell by a number of specific transporter systems. Transporters of the AUX1/LAX family mediate the influx of IAA into the cell, while PINFORMED (PIN) proteins are efflux carriers, but some family members also mediate uptake and release of IAA into the ER. ATP BINDING CASSETTE SUBFAMILY B (ABCB) proteins have been linked with long-distance IAA transport and redistribution (Peer et al., 2011). Several reversible and irreversible reactions leading to IAA conjugation with glucose or amino acids catalysed by uridine diphosphate glycosyltransferases (UGTs) and IAA acyl amido synthetases from the GRETCHEN HAGEN 3 (GH3) family convert IAA into storage or inactivated forms to further regulate the levels of active IAA in cells (Peer et al., 2011). The perception of IAA is mediated by the SCF^{TIR} complex as the primary sensor for IAA. The binding of IAA to SCF^{TIR} leads to the activation its E3 ligase domain to ubiquitinate AUX/IAA proteins. This results in the degradation of the AUX/IAA proteins, which are repressors of the auxin signalling, and subsequently enables transcription factors of the auxin response factor (ARF) family to bind to their target genes and activate the transcriptional response (Leyser, 2018).

Given these complexities in the auxin signalling pathways, it is likely that the known interactions of mitochondrial retrograde with auxin signalling are more complex and our understanding may still only cover part of the interaction.

1.6.2 Ethylene and mitochondrial signalling pathway

As described above, progress has been made to analyse the interaction of the auxin and MRR signalling pathways. Much less is known about the impact of ethylene on the MRR. Given the tight interaction of auxin and ethylene signalling pathways (Muday et al., 2012), it seems likely that ethylene has a role in mediating the MRR, either indirectly via auxin, or directly by impacting retrograde signalling. Early studies have demonstrated that the pathogen-induced expression of *AOX1a* could be abolished in the ethylene insensitive mutant *etr1-1* in Arabidopsis (Simons et al., 1999). In tomato plants, AOX RNAi lines

exhibited retarded ripening, respiration, ethylene production and down regulated ripening-relevant genes, which indicated that AOX is involved in ethylene-mediated fruit ripening of tomato (Xu et al., 2012). Under mitochondrial stress that leads to accumulation of misfolded proteins, ethylene also modulates the proteotoxic response (Wang and Auwerx, 2017). A recent study has shown that ethylene regulates Arabidopsis seed dormancy by ethylene impacting on the required ROS production in the mitochondrial electron transport chain. Here, an ethylene-dependent up-regulation of the MRR genes *AOX1a* and *ANAC013* was observed (Bailly, 2021). Furthermore, the involvement of the master regulator of the MRR, ANAC017, in stress responses that rely on the action of ethylene as a signalling molecule, i.e. hypoxia and submergence, also suggests a role of this hormone for the MRR (Wagner et al., 2018; Bui et al., 2020; Meng et al., 2020). Plants overproducing ethylene or exposed to ethylene show decreased growth, while mutation of positive regulators of ethylene signalling are bigger than wild type (Vogel et al., 1998; Qu et al., 2007). Interestingly, this phenocopies ANAC017 overexpression and mutant lines, respectively (Meng et al., 2019). However, Kacprzak et al. (2020) concluded that ANAC017 is not directly involved in ethylene-dependent regulation of the MRR as mutation of two genes involved in the ethylene signalling pathway, *ETHYLENE INSENSITVE (EIN) 2* or *MAP KINASE (MPK) 6*, only partially repressed the MRR.

Thus, knowledge on the interplay between ethylene and mitochondrial signalling pathway is still limited and the molecular basis of their crosstalk and action remains to be further characterised. A brief overview of the ethylene pathway is given below to present components that might be involved.

1.6.2.1 Ethylene homeostasis and signalling

The substrate for ethylene biosynthesis is S-Adenosyl methionine (SAM) which is converted from methionine by SAM synthetase (Ravanel et al., 1998). Both these precursors thus link ethylene biosynthesis with key molecules of primary metabolism. The conversion of SAM to the immediate precursor of ethylene, 1-aminocyclopropane-1-carboxylic acid (ACC), by ACC synthase is the rate limiting step of ethylene synthesis (Yang and Hoffman, 1984). 5-methylthioadenosine (MTA) is also produced in this reaction and recycled back to methionine to maintain the constant concentration of methionine when ethylene is rapidly synthesized. The final step of ethylene synthesis is catalysed by ACC oxidase (ACO) using ACC as substrate and releasing also cyanide (Bleecker and Kende, 2000) (Figure 5).

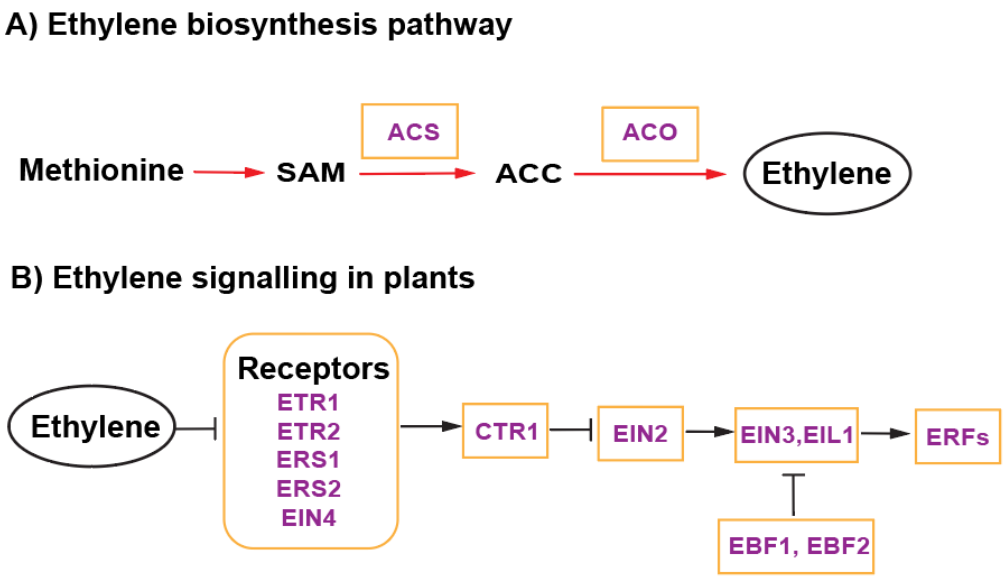

Figure 5. Ethylene biosynthesis and biosynthesis pathway
A) The ethylene biosynthesis pathway in plants in general, B) The ethylene signalling pathway in Arabidopsis. Abbreviations (for gene names see text): SAM, S-Adenosyl methionine; ACC, 1-aminocyclopropane-1-carboxylic acid. Red arrows indicate proposed functions of ACS, ACO, respectively. Black arrows indicate promotion, and black perpendicular line indicates inhibition. Figure is adapted from Wang et al (2002); Binder (2020).

Although the sequence of only two steps leading to ethylene is simple, there is still some discussion regarding the identity and regulation of the two enzymes. This is especially so for ACO owing to its recalcitrance to biochemical purification, *in vitro* production and also debated subcellular localisation (membrane, cytosol). Only six recombinant proteins from four species (tomato, petunia, apple, Arabidopsis) have a confirmed ACO activity *in vitro* and it is therefore questionable if all genes annotated as ACO indeed have this activity or if proteins with similar sequence might also be able to produce ethylene (Houben and Van de Poel, 2019). The latter is especially complicated by the fact that ACO belongs to a large protein family, the 2-oxoglutarate-dependent oxygenases family (2-OGDO), with dozens of highly similar members that are biochemically largely uncharacterised like ACO. Incidentally, one mitochondrial dysfunction stimulon gene (AT5G43450), that is highly induced by antimycin A treatment, is also an uncharacterised 2-oxoglutarate-dependent oxygenase annotated as an ACO-like protein in TAIR10.

Ethylene signalling is triggered by its perception by membrane-localized ethylene receptors with five identified in Arabidopsis (ETR1, ETR2, ERS1, ERS2 and EIN4) (Chang et al., 1993; Hua et al., 1998; Sakai et al., 1998). In the absence of ethylene, these receptors bind the CONSTITUTIVE TRIPLE RESPONSE 1 (CTR1) kinase whereby it is activated and

represses the downstream component EIN2. By contrast, when ethylene is present, CTR1 is inactivated by proteasomal degradation and EIN2 then inhibits the translation of EBF1 and EBF2. The decrease in abundance of these proteins then stabilises the transcription factor ETHYLENE INSENSITIVE3 (EIN3), which is the master regulator of ethylene responsive genes. Therefore, at the end of the signalling pathway and in presence of ethylene, EIN3 binds to the promoter of genes encoding transcript factors of the ETHYLENE RESPONSE FACTOR (ERF) family, which further interact with the GCC box of target genes and activate downstream ethylene responses (Solano et al., 1998). In parallel, the MKK9-MPK3/6 phosphorylation cascade, activated by various stresses, can also increase the activity of ERFs and induce ethylene biosynthesis by phosphorylation of ACS isoforms (Liu and Zhang, 2004; Meng et al., 2013).

The role of ethylene as a stress signalling hormone is well established (Dubois et al., 2018), and from the above it is evident that connections between the MRR, ethylene and auxin have the potential to coordinate whole plant responses to adverse conditions and growth with mitochondrial function.

1.7 Research aims

As described above, mitochondria are essential organelles involved in energy production required for proper growth and responses to adverse environmental conditions. This function is regulated by mitochondria sending signals to the nucleus. However, the intricacies of the MRR and the functions of its components are only now emerging. Although several genes highly induced by mitochondrial dysfunction have been identified, e.g. the MDS genes, for many it is still unknown why they are involved in this response and what their role in mitigating the stress is. Also, although some up-stream regulators such as ANAC017, ANAC013 and some WRKY proteins have been determined as important, it seems likely that additional regulators are needed to fine-tune transcriptional regulation. In addition, how the signalling outputs from mitochondria are dynamically integrated to adjust with cellular homeostasis and overall plant growth is still largely unclear. Recent evidence suggests interplay with plant hormones like auxin and ethylene may play a role.

Therefore, it is my aim to investigate a yet uncharacterised mitochondrial dysfunction stimulon gene (OGO, AT5G43450) belonging to the 2-oxoglutarate Fe(II)-dependent oxygenase family and identify novel regulators (*REGULATORS OF OGO*, *ROG*) of its expression:

1.7.1 Aim 1. Characterization of a mitochondrial dysfunction stimulon gene *2-OXOGLUTARATE FE(II)-DEPENDENT OXYGENASE* (*OGO, AT5G43450*)

A 2-oxoglutarate Fe(II)-dependent oxygenase (*OGO*, *AT5G43450*) is one of the uncharacterised mitochondrial dysfunction stimulon genes, which is responsive to various mitochondrial perturbations and annotated as an ACO-like gene in TAIR10 because of its sequence similarity to ethylene synthesis enzyme 1-aminocyclopropane-1-carboxylic acid (ACC) oxidase (De Clercq et al., 2013). By using a range of molecular techniques and transgenic approaches it is my aim to further characterise this gene and its possible function in the mitochondrial stress response.

1.7.2 Aim 2. Identification of novel regulators of the mitochondrial retrograde response in *Arabidopsis thaliana*

As OGO is yet uncharacterised, it opens up the possibility that its substantial transcriptional regulation by mitochondrial stress involves regulators that have not been identified by previous studies. A forward genetic screen will be used to identify mutants that

are impaired in the ability to induce *OGO* on inhibition of mitochondrial function. The role of OGO as well as its regulators under adverse growth conditions will be also investigated using mutant and overexpression lines, which will allow to define and dissect acclimation responses impacted by mitochondrial signalling pathways.

1.7.3 Aim 3. Survey the fine-tuning of mitochondrial retrograde signalling by ethylene signalling

The potential involvement of OGO in the ethylene pathway as well as additional recent evidence for a function of ethylene in the retrograde signalling pathway suggests a role of this hormone in the regulation of transcriptional responses to mitochondrial dysfunction. A time resolved RNA-seq experiment using wild type, *ETHYLENE INSENSITIVE 3* (*ein3-1*) and *ogo* mutants plants will determine the regulatory hierarchy fine-tuning this process. In addition, the potential role of master regulator ANAC017 in the activation of ethylene and auxin signalling pathways upon mitochondrial dysfunction will be investigated.

In the following, Chapter II will summarise results obtained for Aims 1 and 2, while Chapter III is addressing Aim 3. Both these chapters are organised as draft manuscripts for submission to the Journal of Experimental Botany (Chapter II) and Plant Physiology (Chapter III). While I endeavoured to focus these drafts on their subtopics, some overlap with what was presented already in this general introduction (and the discussion) was unavoidable to make them suitable as a publication in their own right.

1.8 LITERATURE CITED

Albaum HG, Eichel B (1943) The relationship between growth and metabolism in the oat seedling. American Journal of Botany**:** 18-22

Alber NA, Vanlerberghe GC (2021) The flexibility of metabolic interactions between chloroplasts and mitochondria in Nicotiana tabacum leaf. Plant J **106:** 1625-1646

Amuthan G, Biswas G, Ananadatheerthavarada HK, Vijayasarathy C, Shephard HM, Avadhani NG (2002) Mitochondrial stress-induced calcium signaling, phenotypic changes and invasive behavior in human lung carcinoma A549 cells. Oncogene **21:** 7839-7849

Antos-Krzeminska N, Jarmuszkiewicz W (2019) Alternative Type II NAD(P)H Dehydrogenases in the Mitochondria of Protists and Fungi. Protist **170:** 21-37

Archibald JM (2015) Endosymbiosis and Eukaryotic Cell Evolution. Curr Biol **25:** R911-921

Atkin OK, Macherel D (2009) The crucial role of plant mitochondria in orchestrating drought tolerance. Ann Bot **103:** 581-597

Baena-González E, Rolland F, Thevelein JM, Sheen J (2007) A central integrator of transcription networks in plant stress and energy signalling. Nature **448:** 938

Bailly C (2021) Retrograde signalling from the mitochondria to the nucleus translates the positive effect of ethylene on dormancy breaking of Arabidopsis thaliana seeds. New Phytologist **229:** 2192-2205

Beck CF (2005) Signaling pathways from the chloroplast to the nucleus. Planta **222:** 743-756

Berkowitz O, De Clercq I, Van Breusegem F, Whelan J (2016) Interaction between hormonal and mitochondrial signalling during growth, development and in plant defence responses. Plant, cell & environment **39:** 1127-1139

Binder BM (2020) Ethylene signaling in plants. Journal of Biological Chemistry **295:** 7710-7725

Biswas G, Adebanjo OA, Freedman BD, Anandatheerthavarada HK, Vijayasarathy C, Zaidi M, Kotlikoff M, Avadhani NG (1999) Retrograde Ca2+ signaling in C2C12 skeletal myocytes in response to mitochondrial genetic and metabolic stress: a novel mode of inter-organelle crosstalk. EMBO J **18:** 522-533

Bjorkholm P, Harish A, Hagstrom E, Ernst AM, Andersson SG (2015) Mitochondrial genomes are retained by selective constraints on protein targeting. Proc Natl Acad Sci U S A **112:** 10154-10161

Blanco NE, Guinea-Diaz M, Whelan J, Strand A (2014) Interaction between plastid and mitochondrial retrograde signalling pathways during changes to plastid redox status. Philos Trans R Soc Lond B Biol Sci **369:** 20130231

Bleecker AB, Kende H (2000) Ethylene: a gaseous signal molecule in plants. Annual review of cell and developmental biology **16:** 1-18

Bolender N, Sickmann A, Wagner R, Meisinger C, Pfanner N (2008) Multiple pathways for sorting mitochondrial precursor proteins. EMBO Rep **9:** 42-49

Borner T (2017) The discovery of plastid-to-nucleus retrograde signaling-a personal perspective. Protoplasma **254:** 1845-1855

Braun HP (2020) The Oxidative Phosphorylation system of the mitochondria in plants. Mitochondrion **53:** 66-75

Breidenbach RW, Saxton MJ, Hansen LD, Criddle RS (1997) Heat generation and dissipation in plants: can the alternative oxidative phosphorylation pathway serve a thermoregulatory role in plant tissues other than specialized organs? Plant Physiol **114:** 1137-1140

Brodsky FM (1991) What's the score? Nature **352:** 288-289

Bruce Cahoon A, Stern DB (2001) Plastid transcription: a menage a trois? Trends Plant Sci **6:** 45-46

Brumos J, Robles LM, Yun J, Vu TC, Jackson S, Alonso JM, Stepanova AN (2018) Local Auxin Biosynthesis Is a Key Regulator of Plant Development. Dev Cell **47:** 306-318 e305

Bui LT, Shukla V, Giorgi FM, Trivellini A, Perata P, Licausi F, Giuntoli B (2020) Differential submergence tolerance between juvenile and adult Arabidopsis plants involves the ANAC017 transcription factor. Plant J **104:** 979-994

Burke R, Schwarze J, Sherwood OL, Jnaid Y, McCabe PF, Kacprzyk J (2020) Stressed to Death: The Role of Transcription Factors in Plant Programmed Cell Death Induced by Abiotic and Biotic Stimuli. Front Plant Sci **11:** 1235

Caballero A, Ugidos A, Liu B, Oling D, Kvint K, Hao X, Mignat C, Nachin L, Molin M, Nystrom T (2011) Absence of mitochondrial translation control proteins extends life span by activating sirtuin-dependent silencing. Mol Cell **42:** 390-400

Cape JL, Bowman MK, Kramer DM (2006) Understanding the cytochrome bc complexes by what they don't do. The Q-cycle at 30. Trends Plant Sci **11:** 46-55

Carlsson J, Leino M, Sohlberg J, Sundstrom JF, Glimelius K (2008) Mitochondrial regulation of flower development. Mitochondrion **8:** 74-86

Casanova-Saez R, Mateo-Bonmati E, Ljung K (2021) Auxin Metabolism in Plants. Cold Spring Harb Perspect Biol **13**

Chan KX, Phua SY, Crisp P, McQuinn R, Pogson BJ (2016) Learning the Languages of the Chloroplast: Retrograde Signaling and Beyond. Annu Rev Plant Biol **67:** 25-53

Chang C, Kwok SF, Bleecker AB, Meyerowitz EM (1993) Arabidopsis ethylene-response gene ETR1: similarity of product to two-component regulators. Science **262:** 539-544

Che-Othman MH, Jacoby RP, Millar AH, Taylor NL (2020) Wheat mitochondrial respiration shifts from the tricarboxylic acid cycle to the GABA shunt under salt stress. New Phytol **225:** 1166-1180

Cheng Y, Dai X, Zhao Y (2007) Auxin synthesized by the YUCCA flavin monooxygenases is essential for embryogenesis and leaf formation in Arabidopsis. The Plant Cell **19:** 2430-2439

Chevigny N, Schatz-Daas D, Lotfi F, Gualberto JM (2020) DNA Repair and the Stability of the Plant Mitochondrial Genome. Int J Mol Sci **21**

Clifton R, Millar AH, Whelan J (2006) Alternative oxidases in Arabidopsis: a comparative analysis of differential expression in the gene family provides new insights into function of non-phosphorylating bypasses. Biochim Biophys Acta **1757:** 730-741

Colombatti F, Gonzalez DH, Welchen E (2014) Plant mitochondria under pathogen attack: a sigh of relief or a last breath? Mitochondrion **19 Pt B:** 238-244

Considine MJ, Holtzapffel RC, Day DA, Whelan J, Millar AH (2002) Molecular distinction between alternative oxidase from monocots and dicots. Plant Physiol **129:** 949-953

Costa JH, Santos CP, de Sousa ELB, Moreira Netto AN, Saraiva KD, Arnholdt-Schmitt B (2017) In silico identification of alternative oxidase 2 (AOX2) in monocots: A new evolutionary scenario. J Plant Physiol **210:** 58-63

Crawford T, Lehotai N, Strand A (2018) The role of retrograde signals during plant stress responses. J Exp Bot **69:** 2783-2795

Dahal K, Martyn GD, Alber NA, Vanlerberghe GC (2017) Coordinated regulation of photosynthetic and respiratory components is necessary to maintain chloroplast energy balance in varied growth conditions. J Exp Bot **68:** 657-671

Dahal K, Vanlerberghe GC (2017) Alternative oxidase respiration maintains both mitochondrial and chloroplast function during drought. New Phytol **213:** 560-571

Dahal K, Vanlerberghe GC (2018) Growth at Elevated CO2 Requires Acclimation of the Respiratory Chain to Support Photosynthesis. Plant Physiol **178:** 82-100

Daugas E, Nochy D, Ravagnan L, Loeffler M, Susin SA, Zamzami N, Kroemer G (2000) Apoptosis-inducing factor (AIF): a ubiquitous mitochondrial oxidoreductase involved in apoptosis. FEBS Letters **476:** 118-123

De Clercq I, Vermeirssen V, Van Aken O, Vandepoele K, Murcha MW, Law SR, Inze A, Ng S, Ivanova A, Rombaut D, van de Cotte B, Jaspers P, Van de Peer Y, Kangasjarvi J, Whelan J, Van Breusegem F (2013) The membrane-bound NAC transcription factor ANAC013 functions in mitochondrial retrograde regulation of the oxidative stress response in Arabidopsis. Plant Cell **25:** 3472-3490

de Souza A, Wang JZ, Dehesh K (2017) Retrograde Signals: Integrators of Interorganellar Communication and Orchestrators of Plant Development. Annu Rev Plant Biol **68:** 85-108

Del Rio LA (2015) ROS and RNS in plant physiology: an overview. J Exp Bot **66:** 2827-2837

Dojcinovic D, Krosting J, Harris AJ, Wagner DJ, Rhoads DM (2005) Identification of a region of the Arabidopsis AtAOX1a promoter necessary for mitochondrial retrograde regulation of expression. Plant Mol Biol **58:** 159-175

Dolezal P, Likic V, Tachezy J, Lithgow T (2006) Evolution of the molecular machines for protein import into mitochondria. Science **313:** 314-318

Dubois M, Van den Broeck L, Inze D (2018) The Pivotal Role of Ethylene in Plant Growth. Trends Plant Sci **23:** 311-323

Duncan O, Taylor NL, Carrie C, Eubel H, Kubiszewski-Jakubiak S, Zhang B, Narsai R, Millar AH, Whelan J (2011) Multiple lines of evidence localize signaling, morphology, and lipid biosynthesis machinery to the mitochondrial outer membrane of Arabidopsis. Plant Physiol **157:** 1093-1113

Dutilleul C, Garmier M, Noctor G, Mathieu C, Chetrit P, Foyer CH, de Paepe R (2003) Leaf mitochondria modulate whole cell redox homeostasis, set antioxidant capacity, and determine stress resistance through altered signaling and diurnal regulation. Plant Cell **15:** 1212-1226

Ellingson A, Haram K, Sagen N, Solheim E (1977) Transplacental passage of ketamine after intravenous administration. Acta Anaesthesiol Scand **21:** 41-44

Emanuel C, von Groll U, Muller M, Borner T, Weihe A (2006) Development- and tissue-specific expression of the RpoT gene family of Arabidopsis encoding mitochondrial and plastid RNA polymerases. Planta **223:** 998-1009

Estavillo GM, Crisp PA, Pornsiriwong W, Wirtz M, Collinge D, Carrie C, Giraud E, Whelan J, David P, Javot H, Brearley C, Hell R, Marin E, Pogson BJ (2011) Evidence for a SAL1-PAP chloroplast retrograde pathway that functions in drought and high light signaling in Arabidopsis. Plant Cell **23:** 3992-4012

Fernie AR, Carrari F, Sweetlove LJ (2004) Respiratory metabolism: glycolysis, the TCA cycle and mitochondrial electron transport. Curr Opin Plant Biol **7:** 254-261

Fujii S, Small I (2011) The evolution of RNA editing and pentatricopeptide repeat genes. New Phytol **191:** 37-47

Gasch P, Fundinger M, Muller JT, Lee T, Bailey-Serres J, Mustroph A (2016) Redundant ERF-VII Transcription Factors Bind to an Evolutionarily Conserved cis-Motif to Regulate Hypoxia-Responsive Gene Expression in Arabidopsis. Plant Cell **28:** 160-180

Ghifari AS, Gill-Hille M, Murcha MW (2018) Plant mitochondrial protein import: the ins and outs. Biochem J **475:** 2191-2208

Giacomello M, Pyakurel A, Glytsou C, Scorrano L (2020) The cell biology of mitochondrial membrane dynamics. Nat Rev Mol Cell Biol **21:** 204-224

Giraud E, Van Aken O, Ho LH, Whelan J (2009) The transcription factor ABI4 is a regulator of mitochondrial retrograde expression of ALTERNATIVE OXIDASE1a. Plant Physiol **150:** 1286-1296

Gnadlinger K (1991) [Harmonic occlusal concept for functional artificial tooth]. Dent Labor (Munch) **39:** 1607-1610, 1613-1608

Gong Q, Li S, Zheng Y, Duan H, Xiao F, Zhuang Y, He J, Wu G, Zhao S, Zhou H, Lin H (2020) SUMOylation of MYB30 enhances salt tolerance by elevating alternative respiration via transcriptionally upregulating AOX1a in Arabidopsis. Plant J **102:** 1157-1171

Gualberto JM, Mileshina D, Wallet C, Niazi AK, Weber-Lotfi F, Dietrich A (2014) The plant mitochondrial genome: dynamics and maintenance. Biochimie **100:** 107-120

Gutmann B, Royan S, Schallenberg-Rudinger M, Lenz H, Castleden IR, McDowell R, Vacher MA, Tonti-Filippini J, Bond CS, Knoop V, Small ID (2020) The Expansion and Diversification of Pentatricopeptide Repeat RNA-Editing Factors in Plants. Mol Plant **13:** 215-230

Hagel JM, Facchini PJ (2018) Expanding the roles for 2-oxoglutarate-dependent oxygenases in plant metabolism. Nat Prod Rep **35:** 721-734

Hammes UZ, Murphy AS, Schwechheimer C (2021) Auxin Transporters-A Biochemical View. Cold Spring Harb Perspect Biol, DOI: 10.1101/cshperspect.a039875

He J, Duan Y, Hua D, Fan G, Wang L, Liu Y, Chen Z, Han L, Qu L-J, Gong Z (2012) DEXH box RNA helicase–mediated mitochondrial reactive oxygen species production in Arabidopsis mediates crosstalk between abscisic acid and auxin signaling. The Plant Cell **24:** 1815-1833

Hedtke B, Borner T, Weihe A (1997) Mitochondrial and chloroplast phage-type RNA polymerases in Arabidopsis. Science **277:** 809-811

Heeren G, Rinnerthaler M, Laun P, von Seyerl P, Kossler S, Klinger H, Hager M, Bogengruber E, Jarolim S, Simon-Nobbe B, Schuller C, Carmona-Gutierrez D, Breitenbach-Koller L, Muck C, Jansen-Durr P, Criollo A, Kroemer G, Madeo F, Breitenbach M (2009) The mitochondrial ribosomal protein of the large subunit, Afo1p, determines cellular longevity through mitochondrial back-signaling via TOR1. Aging (Albany NY) **1:** 622-636

Henze K, Martin W (2001) How do mitochondrial genes get into the nucleus? Trends Genet **17:** 383-387

Hernandez-Verdeja T, Strand A (2018) Retrograde Signals Navigate the Path to Chloroplast Development. Plant Physiol **176:** 967-976

Ho LH, Giraud E, Lister R, Thirkettle-Watts D, Low J, Clifton R, Howell KA, Carrie C, Donald T, Whelan J (2007) Characterization of the regulatory and expression context of an alternative oxidase gene provides insights into cyanide-insensitive respiration during growth and development. Plant Physiol **143:** 1519-1533

Ho LH, Giraud E, Uggalla V, Lister R, Clifton R, Glen A, Thirkettle-Watts D, Van Aken O, Whelan J (2008) Identification of regulatory pathways controlling gene expression of stress-responsive mitochondrial proteins in Arabidopsis. Plant Physiol **147:** 1858-1873

Houben M, Van de Poel B (2019) 1-Aminocyclopropane-1-Carboxylic Acid Oxidase (ACO): The Enzyme That Makes the Plant Hormone Ethylene. Front Plant Sci **10:** 695

Hua J, Sakai H, Nourizadeh S, Chen QG, Bleecker AB, Ecker JR, Meyerowitz EM (1998) EIN4 and ERS2 are members of the putative ethylene receptor gene family in Arabidopsis. The Plant Cell **10:** 1321-1332

Imachi H, Nobu MK, Nakahara N, Morono Y, Ogawara M, Takaki Y, Takano Y, Uematsu K, Ikuta T, Ito M, Matsui Y, Miyazaki M, Murata K, Saito Y, Sakai S, Song C, Tasumi E, Yamanaka Y, Yamaguchi T, Kamagata Y, Tamaki H, Takai K (2020) Isolation of an archaeon at the prokaryote-eukaryote interface. Nature **577:** 519-525

Ivanova A, Law SR, Narsai R, Duncan O, Lee J-H, Zhang B, Van Aken O, Radomiljac JD, van der Merwe M, Yi K (2014) A functional antagonistic relationship between auxin and mitochondrial retrograde signaling regulates ALTERNATIVE OXIDASE1a expression in Arabidopsis thaliana. Plant physiology**:** pp. 114.237495

Ivanova A, Law SR, Narsai R, Duncan O, Lee JH, Zhang B, Van Aken O, Radomiljac JD, van der Merwe M, Yi K, Whelan J (2014) A Functional Antagonistic Relationship between Auxin and Mitochondrial Retrograde Signaling Regulates Alternative Oxidase1a Expression in Arabidopsis. Plant Physiol **165:** 1233-1254

Jia Y, Rothermel B, Thornton J, Butow RA (1997) A basic helix-loop-helix-leucine zipper transcription complex in yeast functions in a signaling pathway from mitochondria to the nucleus. Mol Cell Biol **17:** 1110-1117

Jiang J, Dehesh K (2021) Plastidial retrograde modulation of light and hormonal signaling: an odyssey. New Phytol **230:** 931-937

Jiang J, Rodriguez-Furlan C, Wang JZ, de Souza A, Ke H, Pasternak T, Lasok H, Ditengou FA, Palme K, Dehesh K (2018) Interplay of the two ancient metabolites auxin and MEcPP regulates adaptive growth. Nat Commun **9:** 2262

Jiang J, Zeng L, Ke H, De La Cruz B, Dehesh K (2019) Orthogonal regulation of phytochrome B abundance by stress-specific plastidial retrograde signaling metabolite. Nat Commun **10:** 2904

Jones AW, Yao Z, Vicencio JM, Karkucinska-Wieckowska A, Szabadkai G (2012) PGC-1 family coactivators and cell fate: roles in cancer, neurodegeneration, cardiovascular disease and retrograde mitochondria-nucleus signalling. Mitochondrion **12:** 86-99

Jurdak R, Launay-Avon A, Paysant-Le Roux C, Bailly C (2021) Retrograde signalling from the mitochondria to the nucleus translates the positive effect of ethylene on dormancy breaking of Arabidopsis thaliana seeds. New Phytol **229:** 2192-2205

Kacprzak SM, Dahlqvist A, Van Aken O (2020) The transcription factor ANAC017 is a key regulator of mitochondrial proteotoxic stress responses in plants. Philos Trans R Soc Lond B Biol Sci **375:** 20190411

Kacprzak SM, Mochizuki N, Naranjo B, Xu D, Leister D, Kleine T, Okamoto H, Terry MJ (2019) Plastid-to-Nucleus Retrograde Signalling during Chloroplast Biogenesis Does Not Require ABI4. Plant Physiol **179:** 18-23

Karlberg O, Canback B, Kurland CG, Andersson SG (2000) The dual origin of the yeast mitochondrial proteome. Yeast **17:** 170-187

Kawano T (2003) Roles of the reactive oxygen species-generating peroxidase reactions in plant defense and growth induction. Plant cell reports **21:** 829-837

Kerchev PI, De Clercq I, Denecker J, Muhlenbock P, Kumpf R, Nguyen L, Audenaert D, Dejonghe W, Van Breusegem F (2014) Mitochondrial perturbation negatively affects auxin signaling. Mol Plant **7:** 1138-1150

Klok EJ, Wilson IW, Wilson D, Chapman SC, Ewing RM, Somerville SC, Peacock WJ, Dolferus R, Dennis ES (2002) Expression Profile Analysis of the Low-Oxygen Response in Arabidopsis Root Cultures. The Plant Cell **14:** 2481-2494

Kmiecik P, Leonardelli M, Teige M (2016) Novel connections in plant organellar signalling link different stress responses and signalling pathways. J Exp Bot **67:** 3793-3807

Komatsu S, Yamamoto A, Nakamura T, Nouri M-Z, Nanjo Y, Nishizawa K, Furukawa K (2011) Comprehensive Analysis of Mitochondria in Roots and Hypocotyls of Soybean under Flooding Stress using Proteomics and Metabolomics Techniques. Journal of Proteome Research **10:** 3993-4004

Koussevitzky S, Nott A, Mockler TC, Hong F, Sachetto-Martins G, Surpin M, Lim J, Mittler R, Chory J (2007) Signals from chloroplasts converge to regulate nuclear gene expression. Science **316:** 715-719

Krause M, Durner J (2004) Harpin inactivates mitochondria in Arabidopsis suspension cells. Mol Plant Microbe Interact **17:** 131-139

Labs M, Ruhle T, Leister D (2016) The antimycin A-sensitive pathway of cyclic electron flow: from 1963 to 2015. Photosynth Res **129:** 231-238

Larkin RM, Alonso JM, Ecker JR, Chory J (2003) GUN4, a regulator of chlorophyll synthesis and intracellular signaling. Science **299:** 902-906

Larosa V, Remacle C (2018) Insights into the respiratory chain and oxidative stress. Biosci Rep **38**

Lee SY, Hwang EY, Seok HY, Tarte VN, Jeong MS, Jang SB, Moon YH (2015) Arabidopsis AtERF71/HRE2 functions as transcriptional activator via cis-acting GCC box or DRE/CRT element and is involved in root development through regulation of root cell expansion. Plant Cell Rep **34:** 223-231

Leister D (2019) Piecing the Puzzle Together: The Central Role of Reactive Oxygen Species and Redox Hubs in Chloroplast Retrograde Signaling. Antioxid Redox Signal **30:** 1206-1219

Leonova L, Gamburg K, Vojnikov V, Varakina N (1985) Promotion of respiration by auxin in the induction of cell division in suspension culture. Journal of Plant Growth Regulation **4:** 169-176

Leyser O (2018) Auxin signaling. Plant physiology **176:** 465-479

Liao XS, Small WC, Srere PA, Butow RA (1991) Intramitochondrial functions regulate nonmitochondrial citrate synthase (CIT2) expression in Saccharomyces cerevisiae. Mol Cell Biol **11:** 38-46

Liberatore KL, Dukowic-Schulze S, Miller ME, Chen C, Kianian SF (2016) The role of mitochondria in plant development and stress tolerance. Free Radic Biol Med **100:** 238-256

Licausi F, van Dongen JT, Giuntoli B, Novi G, Santaniello A, Geigenberger P, Perata P (2010) HRE1 and HRE2, two hypoxia-inducible ethylene response factors, affect anaerobic responses in Arabidopsis thaliana. Plant J **62:** 302-315

Liu Y, Zhang S (2004) Phosphorylation of 1-aminocyclopropane-1-carboxylic acid synthase by MPK6, a stress-responsive mitogen-activated protein kinase, induces ethylene biosynthesis in Arabidopsis. Plant Cell **16:** 3386-3399

Liu Z, Butow RA (2006) Mitochondrial retrograde signaling. Annu Rev Genet **40:** 159-185

Liu Z, Sekito T, Epstein CB, Butow RA (2001) RTG-dependent mitochondria to nucleus signaling is negatively regulated by the seven WD-repeat protein Lst8p. EMBO J **20:** 7209-7219

Liu Z, Sekito T, Spirek M, Thornton J, Butow RA (2003) Retrograde signaling is regulated by the dynamic interaction between Rtg2p and Mks1p. Mol Cell **12:** 401-411

Logan DC, Leaver CJ (2000) Mitochondria-targeted GFP highlights the heterogeneity of mitochondrial shape, size and movement within living plant cells. J Exp Bot **51:** 865-871

Loreti E, van Veen H, Perata P (2016) Plant responses to flooding stress. Curr Opin Plant Biol **33:** 64-71

Martijn J, Vosseberg J, Guy L, Offre P, Ettema TJG (2018) Deep mitochondrial origin outside the sampled alphaproteobacteria. Nature **557:** 101-105

Martin WF, Garg S, Zimorski V (2015) Endosymbiotic theories for eukaryote origin. Philos Trans R Soc Lond B Biol Sci **370:** 20140330

Mashiguchi K, Tanaka K, Sakai T, Sugawara S, Kawaide H, Natsume M, Hanada A, Yaeno T, Shirasu K, Yao H (2011) The main auxin biosynthesis pathway in Arabidopsis. Proceedings of the National Academy of Sciences **108:** 18512-18517

Meng X, Li L, De Clercq I, Narsai R, Xu Y, Hartmann A, Claros DL, Custovic E, Lewsey MG, Whelan J, Berkowitz O (2019) ANAC017 Coordinates Organellar Functions and Stress Responses by Reprogramming Retrograde Signaling. Plant Physiol **180:** 634-653

Meng X, Li L, Narsai R, De Clercq I, Whelan J, Berkowitz O (2020) Mitochondrial signalling is critical for acclimation and adaptation to flooding in Arabidopsis thaliana. Plant J **103:** 227-247

Meng X, Xu J, He Y, Yang KY, Mordorski B, Liu Y, Zhang S (2013) Phosphorylation of an ERF transcription factor by Arabidopsis MPK3/MPK6 regulates plant defense gene induction and fungal resistance. Plant Cell **25:** 1126-1142

Merendino L, Courtois F, Grubler B, Bastien O, Straetmanns V, Chevalier F, Lerbs-Mache S, Lurin C, Pfannschmidt T (2020) Retrograde signals from mitochondria reprogramme skoto-morphogenesis in Arabidopsis thaliana via alternative oxidase 1a. Philos Trans R Soc Lond B Biol Sci **375:** 20190567

Meyer EH, Welchen E, Carrie C (2019) Assembly of the Complexes of the Oxidative Phosphorylation System in Land Plant Mitochondria. Annu Rev Plant Biol **70:** 23-50

Michalecka AM, Svensson AS, Johansson FI, Agius SC, Johanson U, Brennicke A, Binder S, Rasmusson AG (2003) Arabidopsis genes encoding mitochondrial type II NAD(P)H dehydrogenases have different evolutionary origin and show distinct responses to light. Plant Physiol **133:** 642-652

Mielecki J, Gawronski P, Karpinski S (2020) Retrograde Signaling: Understanding the Communication between Organelles. Int J Mol Sci **21**

Millar AH, Heazlewood JL, Kristensen BK, Braun HP, Moller IM (2005) The plant mitochondrial proteome. Trends Plant Sci **10:** 36-43

Millar AH, Small ID, Day DA, Whelan J (2008) Mitochondrial biogenesis and function in Arabidopsis. Arabidopsis Book **6:** e0111

Millar H, Considine MJ, Day DA, Whelan J (2001) Unraveling the role of mitochondria during oxidative stress in plants. IUBMB life **51:** 201-205

Mitschke J, Fuss J, Blum T, Hoglund A, Reski R, Kohlbacher O, Rensing SA (2009) Prediction of dual protein targeting to plant organelles. New Phytol **183:** 224-236

Mochizuki N, Brusslan JA, Larkin R, Nagatani A, Chory J (2001) Arabidopsis genomes uncoupled 5 (GUN5) mutant reveals the involvement of Mg-chelatase H subunit in plastid-to-nucleus signal transduction. Proc Natl Acad Sci U S A **98:** 2053-2058

Moller IM (2001) PLANT MITOCHONDRIA AND OXIDATIVE STRESS: Electron Transport, NADPH Turnover, and Metabolism of Reactive Oxygen Species. Annu Rev Plant Physiol Plant Mol Biol **52:** 561-591

Morley SA, Nielsen BL (2017) Plant mitochondrial DNA. Front Biosci (Landmark Ed) **22:** 1023-1032

Muday GK, Rahman A, Binder BM (2012) Auxin and ethylene: collaborators or competitors? Trends Plant Sci **17:** 181-195

Murcha MW, Kmiec B, Kubiszewski-Jakubiak S, Teixeira PF, Glaser E, Whelan J (2014) Protein import into plant mitochondria: signals, machinery, processing, and regulation. J Exp Bot **65:** 6301-6335

Murcha MW, Lister R, Ho AY, Whelan J (2003) Identification, expression, and import of components 17 and 23 of the inner mitochondrial membrane translocase from Arabidopsis. Plant Physiol **131:** 1737-1747

Neupert W, Herrmann JM (2007) Translocation of proteins into mitochondria. Annu Rev Biochem **76:** 723-749

Newton KJ, Coe EH (1986) Mitochondrial DNA changes in abnormal growth (nonchromosomal stripe) mutants of maize. Proc Natl Acad Sci U S A **83:** 7363-7366

Ng S, De Clercq I, Van Aken O, Law SR, Ivanova A, Willems P, Giraud E, Van Breusegem F, Whelan J (2014) Anterograde and retrograde regulation of nuclear genes encoding mitochondrial proteins during growth, development, and stress. Mol Plant **7:** 1075-1093

Ng S, Ivanova A, Duncan O, Law SR, Van Aken O, De Clercq I, Wang Y, Carrie C, Xu L, Kmiec B (2013) A membrane-bound NAC transcription factor, ANAC017, mediates mitochondrial retrograde signaling in Arabidopsis. The Plant Cell**:** tpc. 113.113985

Nie X, Hill RD (1997) Mitochondrial Respiration and Hemoglobin Gene Expression in Barley Aleurone Tissue. Plant Physiology **114:** 835-840

Noguchi K, Yoshida K (2008) Interaction between photosynthesis and respiration in illuminated leaves. Mitochondrion **8:** 87-99

Noh B, Murphy AS, Spalding EP (2001) Multidrug resistance-like genes of Arabidopsis required for auxin transport and auxin-mediated development. Plant Cell **13:** 2441-2454

Nott A, Jung HS, Koussevitzky S, Chory J (2006) Plastid-to-nucleus retrograde signaling. Annu Rev Plant Biol **57:** 739-759

Palade GE (1953) An electron microscope study of the mitochondrial structure. J Histochem Cytochem **1:** 188-211

Parikh VS, Morgan MM, Scott R, Clements LS, Butow RA (1987) The mitochondrial genotype can influence nuclear gene expression in yeast. Science **235:** 576-580

Pasternak T, Potters G, Caubergs R, Jansen MA (2005) Complementary interactions between oxidative stress and auxins control plant growth responses at plant, organ, and cellular level. Journal of experimental botany **56:** 1991-2001

Peer WA, Blakeslee JJ, Yang H, Murphy AS (2011) Seven things we think we know about auxin transport. Mol Plant **4:** 487-504

Peng S, Bouman B, Visperas RM, Castañeda A, Nie L, Park H-K (2006) Comparison between aerobic and flooded rice in the tropics: Agronomic performance in an eight-season experiment. Field Crops Research **96:** 252-259

Perrin R, Meyer EH, Zaepfel M, Kim YJ, Mache R, Grienenberger JM, Gualberto JM, Gagliardi D (2004) Two exoribonucleases act sequentially to process mature 3'-ends of atp9 mRNAs in Arabidopsis mitochondria. J Biol Chem **279:** 25440-25446

Pfanner N, Geissler A (2001) Versatility of the mitochondrial protein import machinery. Nat Rev Mol Cell Biol **2:** 339-349

Pfannschmidt T (2010) Plastidial retrograde signalling--a true "plastid factor" or just metabolite signatures? Trends Plant Sci **15:** 427-435

Pfannschmidt T, Schutze K, Fey V, Sherameti I, Oelmuller R (2003) Chloroplast redox control of nuclear gene expression--a new class of plastid signals in interorganellar communication. Antioxid Redox Signal **5:** 95-101

Pfannschmidt T, Terry MJ, Van Aken O, Quiros PM (2020) Retrograde signals from endosymbiotic organelles: a common control principle in eukaryotic cells. Philos Trans R Soc Lond B Biol Sci **375:** 20190396

Phua SY, Yan D, Chan KX, Estavillo GM, Nambara E, Pogson BJ (2018) The Arabidopsis SAL1-PAP Pathway: A Case Study for Integrating Chloroplast Retrograde, Light and Hormonal Signaling in Modulating Plant Growth and Development? Front Plant Sci **9:** 1171

Qu X, Hall BP, Gao Z, Schaller GE (2007) A strong constitutive ethylene-response phenotype conferred on Arabidopsis plants containing null mutations in the ethylene receptors ETR1 and ERS1. BMC Plant Biol **7:** 3

Raghavendra AS, Padmasree K (2003) Beneficial interactions of mitochondrial metabolism with photosynthetic carbon assimilation. Trends Plant Sci **8:** 546-553

Ramel F, Birtic S, Ginies C, Soubigou-Taconnat L, Triantaphylides C, Havaux M (2012) Carotenoid oxidation products are stress signals that mediate gene responses to singlet oxygen in plants. Proc Natl Acad Sci U S A **109:** 5535-5540

Rao RS, Salvato F, Thal B, Eubel H, Thelen JJ, Moller IM (2017) The proteome of higher plant mitochondria. Mitochondrion **33:** 22-37

Rashid FAA, Crisp PA, Zhang Y, Berkowitz O, Pogson BJ, Day DA, Masle J, Dewar RC, Whelan J, Atkin OK, Scafaro AP (2020) Molecular and physiological responses during thermal acclimation of leaf photosynthesis and respiration in rice. Plant Cell Environ **43:** 594-610

Ravanel S, Gakière B, Job D, Douce R (1998) The specific features of methionine biosynthesis and metabolism in plants. Proceedings of the National Academy of Sciences **95:** 7805-7812

Rhoads DM, McIntosh L (1992) Salicylic Acid Regulation of Respiration in Higher Plants: Alternative Oxidase Expression. Plant Cell **4:** 1131-1139

Rhoads DM, Subbaiah CC (2007) Mitochondrial retrograde regulation in plants. Mitochondrion **7:** 177-194

Ribas-Carbo M, Berry JA, Azcon-Bieto J, Siedow JN (1994) The reaction of the plant mitochondrial cyanide-resistant alternative oxidase with oxygen. Biochimica et Biophysica Acta (BBA) - Bioenergetics **1188:** 205-212

Roberts RL, Mosch HU, Fink GR (1997) 14-3-3 proteins are essential for RAS/MAPK cascade signaling during pseudohyphal development in S. cerevisiae. Cell **89:** 1055-1065

Rodriguez VM, Chetelat A, Majcherczyk P, Farmer EE (2010) Chloroplastic phosphoadenosine phosphosulfate metabolism regulates basal levels of the prohormone jasmonic acid in Arabidopsis leaves. Plant Physiol **152:** 1335-1345

Roger AJ, Munoz-Gomez SA, Kamikawa R (2017) The Origin and Diversification of Mitochondria. Curr Biol **27:** R1177-R1192

Sakai H, Hua J, Chen QG, Chang C, Medrano LJ, Bleecker AB, Meyerowitz EM (1998) ETR2 is an ETR1-like gene involved in ethylene signaling in Arabidopsis. Proceedings of the National Academy of Sciences **95:** 5812-5817

Sako K, Futamura Y, Shimizu T, Matsui A, Hirano H, Kondoh Y, Muroi M, Aono H, Tanaka M, Honda K, Shimizu K, Kawatani M, Nakano T, Osada H, Noguchi K, Seki M (2020) Inhibition of mitochondrial complex I by the novel compound FSL0260 enhances high salinity-stress tolerance in Arabidopsis thaliana. Sci Rep **10:** 8691

Scafaro AP, Fan Y, Posch BC, Garcia A, Coast O, Atkin OK (2021) Responses of leaf respiration to heatwaves. Plant Cell Environ **44:** 2090-2101

Schwarzlander M, Fuchs P (2017) Plant mitochondrial membranes: adding structure and new functions to respiratory physiology. Curr Opin Plant Biol **40:** 147-157

Sekito T, Liu Z, Thornton J, Butow RA (2002) RTG-dependent mitochondria-to-nucleus signaling is regulated by MKS1 and is linked to formation of yeast prion [URE3]. Mol Biol Cell **13:** 795-804

Sekito T, Thornton J, Butow RA (2000) Mitochondria-to-nuclear signaling is regulated by the subcellular localization of the transcription factors Rtg1p and Rtg3p. Mol Biol Cell **11:** 2103-2115

Selinski J, Scheibe R, Day DA, Whelan J (2018) Alternative Oxidase Is Positive for Plant Performance. Trends Plant Sci **23:** 588-597

Selinski J, Scheibe R, Day DA, Whelan J (2018) Alternative oxidase is positive for plant performance. Trends in plant science

Shapiguzov A, Vainonen JP, Hunter K, Tossavainen H, Tiwari A, Jarvi S, Hellman M, Aarabi F, Alseekh S, Wybouw B, Van Der Kelen K, Nikkanen L, Krasensky-Wrzaczek J, Sipari N, Keinanen M, Tyystjarvi E, Rintamaki E, De Rybel B, Salojarvi J, Van Breusegem F, Fernie AR, Brosche M, Permi P, Aro EM, Wrzaczek M, Kangasjarvi J (2019) Arabidopsis RCD1 coordinates chloroplast and mitochondrial functions through interaction with ANAC transcription factors. Elife **8**

Shingaki-Wells R, Millar AH, Whelan J, Narsai R (2014) What happens to plant mitochondria under low oxygen? An omics review of the responses to low oxygen and reoxygenation. Plant Cell Environ **37:** 2260-2277

Siedow JN, Umbach AL, Moore AL (1995) The active site of the cyanide-resistant oxidase from plant mitochondria contains a binuclear iron center. FEBS Lett **362:** 10-14

Simons BH, Millenaar FF, Mulder L, Van Loon LC, Lambers H (1999) Enhanced expression and activation of the alternative oxidase during infection of Arabidopsis with Pseudomonas syringae pv tomato. Plant Physiol **120:** 529-538

Skoog F (1937) A Deseeded Avena Test Method for Small Amounts of Auxin and Auxin Precursors. J Gen Physiol **20:** 311-334

Sloan DB, Alverson AJ, Chuckalovcak JP, Wu M, McCauley DE, Palmer JD, Taylor DR (2012) Rapid evolution of enormous, multichromosomal genomes in flowering plant mitochondria with exceptionally high mutation rates. PLoS Biol **10:** e1001241

Solano R, Stepanova A, Chao Q, Ecker JR (1998) Nuclear events in ethylene signaling: a transcriptional cascade mediated by ETHYLENE-INSENSITIVE3 and ETHYLENE-RESPONSE-FACTOR1. Genes & development **12:** 3703-3714

Soole KL, Menz RI (1995) Functional molecular aspects of the NADH dehydrogenases of plant mitochondria. J Bioenerg Biomembr **27:** 397-406

Spielewoy N, Flick K, Kalashnikova TI, Walker JR, Wittenberg C (2004) Regulation and recognition of SCFGrr1 targets in the glucose and amino acid signaling pathways. Mol Cell Biol **24:** 8994-9005

Stepanova AN, Robertson-Hoyt J, Yun J, Benavente LM, Xie D-Y, Doležal K, Schlereth A, Jürgens G, Alonso JM (2008) TAA1-mediated auxin biosynthesis is essential for hormone crosstalk and plant development. Cell **133:** 177-191

Stoimenova M, Igamberdiev AU, Gupta KJ, Hill RD (2007) Nitrite-driven anaerobic ATP synthesis in barley and rice root mitochondria. Planta **226:** 465-474

Stojanovski D, Guiard B, Kozjak-Pavlovic V, Pfanner N, Meisinger C (2007) Alternative function for the mitochondrial SAM complex in biogenesis of alpha-helical TOM proteins. J Cell Biol **179:** 881-893

Susek RE, Ausubel FM, Chory J (1993) Signal transduction mutants of Arabidopsis uncouple nuclear CAB and RBCS gene expression from chloroplast development. Cell **74:** 787-799

Tao Y, Ferrer J-L, Ljung K, Pojer F, Hong F, Long JA, Li L, Moreno JE, Bowman ME, Ivans LJ (2008) Rapid synthesis of auxin via a new tryptophan-dependent pathway is required for shade avoidance in plants. Cell **133:** 164-176

Tognetti VB, Van Aken O, Morreel K, Vandenbroucke K, van de Cotte B, De Clercq I, Chiwocha S, Fenske R, Prinsen E, Boerjan W, Genty B, Stubbs KA, Inze D, Van Breusegem F (2010) Perturbation of indole-3-butyric acid homeostasis by the UDP-glucosyltransferase UGT74E2 modulates Arabidopsis architecture and water stress tolerance. Plant Cell **22:** 2660-2679

Tsuji Y, Ayaki H, Whitman SP, Morrow CS, Torti SV, Torti FM (2000) Coordinate Transcriptional and Translational Regulation of Ferritin in Response to Oxidative Stress. Molecular and Cellular Biology **20:** 5818-5827

Unseld M, Marienfeld JR, Brandt P, Brennicke A (1997) The mitochondrial genome of Arabidopsis thaliana contains 57 genes in 366,924 nucleotides. Nat Genet **15:** 57-61

Van Aken O, De Clercq I, Ivanova A, Law SR, Van Breusegem F, Millar AH, Whelan J (2016) Mitochondrial and Chloroplast Stress Responses Are Modulated in Distinct Touch and Chemical Inhibition Phases. Plant Physiol **171:** 2150-2165

Van Aken O, De Clercq I, Ivanova A, Law SR, Van Breusegem F, Millar AH, Whelan J (2016) Mitochondrial and Chloroplast Stress Responses Are Modulated in Distinct Touch and Chemical Inhibition Phases. Plant Physiology **171:** 2150-2165

Van Aken O, Pogson BJ (2017) Convergence of mitochondrial and chloroplastic ANAC017/PAP-dependent retrograde signalling pathways and suppression of programmed cell death. Cell Death Differ **24:** 955-960

Van Aken O, Van Breusegem F (2015) Licensed to Kill: Mitochondria, Chloroplasts, and Cell Death. Trends in Plant Science **20:** 754-766

Van Aken O, Zhang B, Law S, Narsai R, Whelan J (2013) AtWRKY40 and AtWRKY63 modulate the expression of stress-responsive nuclear genes encoding mitochondrial and chloroplast proteins. Plant Physiol **162:** 254-271

Van Overbeek J (1936) Growth Substance Curvatures of Avena in Light and Dark. J Gen Physiol **20:** 283-309

Vandenbussche F, Vriezen WH, Smalle J, Laarhoven LJ, Harren FJ, Van Der Straeten D (2003) Ethylene and auxin control the Arabidopsis response to decreased light intensity. Plant Physiol **133:** 517-527

Vanlerberghe G (2013) Alternative Oxidase: A Mitochondrial Respiratory Pathway to Maintain Metabolic and Signaling Homeostasis during Abiotic and Biotic Stress in Plants. International Journal of Molecular Sciences **14:** 6805

Vanlerberghe GC, Cvetkovska M, Wang J (2009) Is the maintenance of homeostatic mitochondrial signaling during stress a physiological role for alternative oxidase? Physiologia Plantarum **137:** 392-406

Vanlerberghe GC, Dahal K, Alber NA, Chadee A (2020) Photosynthesis, respiration and growth: A carbon and energy balancing act for alternative oxidase. Mitochondrion **52:** 197-211

Vanstraelen M, Benková E (2012) Hormonal interactions in the regulation of plant development. Annual review of cell and developmental biology **28:** 463-487

Vogel JP, Woeste KE, Theologis A, Kieber JJ (1998) Recessive and dominant mutations in the ethylene biosynthetic gene ACS5 of Arabidopsis confer cytokinin insensitivity and ethylene overproduction, respectively. Proc Natl Acad Sci U S A **95:** 4766-4771

Wagner S, Van Aken O, Elsasser M, Schwarzlander M (2018) Mitochondrial Energy Signaling and Its Role in the Low-Oxygen Stress Response of Plants. Plant Physiol **176:** 1156-1170

Wang KL-C, Li H, Ecker JR (2002) Ethylene biosynthesis and signaling networks. The plant cell **14:** S131-S151

Wang X, Auwerx J (2017) Systems Phytohormone Responses to Mitochondrial Proteotoxic Stress. Mol Cell **68:** 540-551 e545

Wang X, Chen XJ (2015) A cytosolic network suppressing mitochondria-mediated proteostatic stress and cell death. Nature **524:** 481-484

Wang Y, Berkowitz O, Selinski J, Xu Y, Hartmann A, Whelan J (2018) Stress responsive mitochondrial proteins in Arabidopsis thaliana. Free Radic Biol Med **122:** 28-39

Wang Y, Lyu W, Berkowitz O, Radomiljac JD, Law SR, Murcha MW, Carrie C, Teixeira PF, Kmiec B, Duncan O, Van Aken O, Narsai R, Glaser E, Huang S, Roessner U, Millar AH, Whelan J (2016) Inactivation of Mitochondrial Complex I Induces the Expression of a Twin Cysteine Protein that Targets and Affects Cytosolic, Chloroplastidic and Mitochondrial Function. Mol Plant **9:** 696-710

Wang Y, Selinski J, Mao C, Zhu Y, Berkowitz O, Whelan J (2020) Linking mitochondrial and chloroplast retrograde signalling in plants. Philos Trans R Soc Lond B Biol Sci **375:** 20190410

Weidberg H, Amon A (2018) MitoCPR-A surveillance pathway that protects mitochondria in response to protein import stress. Science **360**

Welchen E, Canal MV, Gras DE, Gonzalez DH (2021) Cross-talk between mitochondrial function, growth, and stress signalling pathways in plants. J Exp Bot **72:** 4102-4118

Woodson JD, Chory J (2008) Coordination of gene expression between organellar and nuclear genomes. Nat Rev Genet **9:** 383-395

Woodson JD, Perez-Ruiz JM, Chory J (2011) Heme synthesis by plastid ferrochelatase I regulates nuclear gene expression in plants. Curr Biol **21:** 897-903

Woodson JD, Perez-Ruiz JM, Schmitz RJ, Ecker JR, Chory J (2013) Sigma factor-mediated plastid retrograde signals control nuclear gene expression. Plant J **73:** 1-13

Wrobel L, Topf U, Bragoszewski P, Wiese S, Sztolsztener ME, Oeljeklaus S, Varabyova A, Lirski M, Chroscicki P, Mroczek S, Januszewicz E, Dziembowski A, Koblowska M, Warscheid B, Chacinska A (2015) Mistargeted mitochondrial proteins activate a proteostatic response in the cytosol. Nature **524:** 485-488

Xia XJ, Zhou YH, Shi K, Zhou J, Foyer CH, Yu JQ (2015) Interplay between reactive oxygen species and hormones in the control of plant development and stress tolerance. J Exp Bot **66:** 2839-2856

Xiao Y, Savchenko T, Baidoo EE, Chehab WE, Hayden DM, Tolstikov V, Corwin JA, Kliebenstein DJ, Keasling JD, Dehesh K (2012) Retrograde signaling by the plastidial metabolite MEcPP regulates expression of nuclear stress-response genes. Cell **149:** 1525-1535

Xu F, Yuan S, Zhang D-W, Lv X, Lin H-H (2012) The role of alternative oxidase in tomato fruit ripening and its regulatory interaction with ethylene. Journal of experimental botany **63:** 5705-5716

Xu L, Carrie C, Law SR, Murcha MW, Whelan J (2013) Acquisition, conservation, and loss of dual-targeted proteins in land plants. Plant Physiol **161:** 644-662

Yamada M, Greenham K, Prigge MJ, Jensen PJ, Estelle M (2009) The TRANSPORT INHIBITOR RESPONSE2 gene is required for auxin synthesis and diverse aspects of plant development. Plant physiology **151:** 168-179

Yang SF, Hoffman NE (1984) Ethylene biosynthesis and its regulation in higher plants. Annual review of plant physiology **35:** 155-189

Yoshida K, Watanabe C, Kato Y, Sakamoto W, Noguchi K (2008) Influence of chloroplastic photo-oxidative stress on mitochondrial alternative oxidase capacity and respiratory properties: a case study with Arabidopsis yellow variegated 2. Plant and Cell Physiology **49:** 592-603

Yu B, Ma J, Li J, Wang D, Wang Z, Wang S (2020) Mitochondrial phosphatase PGAM5 modulates cellular senescence by regulating mitochondrial dynamics. Nat Commun **11:** 2549

Zancani M, Braidot E, Filippi A, Lippe G (2020) Structural and functional properties of plant mitochondrial F-ATP synthase. Mitochondrion **53:** 178-193

Zaninotto F, Camera SL, Polverari A, Delledonne M (2006) Cross Talk between Reactive Nitrogen and Oxygen Species during the Hypersensitive Disease Resistance Response. Plant Physiology **141:** 379-383

Zhang B, Van Aken O, Thatcher L, De Clercq I, Duncan O, Law SR, Murcha MW, van der Merwe M, Seifi HS, Carrie C, Cazzonelli C, Radomiljac J, Hofte M, Singh KB, Van Breusegem F, Whelan J (2014) The mitochondrial outer membrane AAA ATPase AtOM66 affects cell death and pathogen resistance in Arabidopsis thaliana. Plant J **80:** 709-727

Zhang S, Wu J, Yuan D, Zhang D, Huang Z, Xiao L, Yang C (2014) Perturbation of auxin homeostasis caused by mitochondrial FtSH4 gene-mediated peroxidase accumulation regulates Arabidopsis architecture. Molecular Plant **7:** 856-873

Zhang X, Ivanova A, Vandepoele K, Radomiljac J, Van de Velde J, Berkowitz O, Willems P, Xu Y, Ng S, Van Aken O, Duncan O, Zhang B, Storme V, Chan KX, Vaneechoutte D, Pogson BJ, Van Breusegem F, Whelan J, De Clercq I (2017) The Transcription Factor MYB29 Is a Regulator of ALTERNATIVE OXIDASE1a. Plant Physiol **173:** 1824-1843

Zhang ZS, Liu MJ, Scheibe R, Selinski J, Zhang LT, Yang C, Meng XL, Gao HY (2017) Contribution of the Alternative Respiratory Pathway to PSII Photoprotection in C3 and C4 Plants. Mol Plant **10:** 131-142

Zhang ZW, Zhang GC, Zhu F, Zhang DW, Yuan S (2015) The roles of tetrapyrroles in plastid retrograde signaling and tolerance to environmental stresses. Planta **242:** 1263-1276

Zhao Y (2010) Auxin biosynthesis and its role in plant development. Annual review of plant biology **61:** 49-64
Zimorski V, Ku C, Martin WF, Gould SB (2014) Endosymbiotic theory for organelle origins. Curr Opin Microbiol **22:** 38-48

2. CHAPTER II - CHARACTERISATION OF A *2-OXOGLUTARATE FE(II)-DEPENDENT OXYGENASE* (*OGO*) INDUCED BY MITOCHONDRIAL DYSFUNCTION IDENTIFIES NOVEL REGULATORS OF MITOCHONDRIAL SIGNALLING

Author for Contact:
Oliver Berkowitz
La Trobe University
School of Life Sciences
Department of Animal, Plant and Soil Science
AgriBio, Centre for AgriBioscience
Bundoora, Victoria 3086, Australia
E-mail: o.berkowitz@latrobe.edu.au
Tel.: +61 3 9032 7490

Authors and affiliations

Cunman He[1,2], Lim Chee Liew[1], Yue Xu[1], Botao Zhang[1], Mathew G. Lewsey[1], James Whelan[1,2], Oliver Berkowitz[1,2]

[1]Department of Animal, Plant and Soil Science, La Trobe University, Bundoora, Victoria 3086, Australia

[2]ARC Centre of Excellence in Plant Energy Biology, La Trobe University, Bundoora, Victoria 3086, Australia

One sentence summary:

Functional characterisation of a gene encoding a *2-oxoglutarate Fe(II)-dependent oxygenase* (*OGO*) identifies novel regulators involved in the mitochondrial signalling pathway that confer tolerance to adverse growth conditions.

AUTHOR CONTRIBUTIONS:

OB, CH and JW designed the research. CH performed generation of transgenic lines, genotyping, phenotyping, EMS mutant screening and mapping, GUS staining assay and protoplast preparation, CH and OB performed phenotyping and fluorescence microscopy, CH, LCL, YX performed the ChIP experiment, and BZ carried out EMS mutagenesis. CH, LCL, OB, and JW analyzed or interpreted the data; MGL provided unpublished data and material. CH drafted the manuscript. OB and JW revised the manuscript.

FUNDING INFORMATION:

This work was supported by the facilities of the Australian Research Council Centre of Excellence Program (CE140100008, ARC Centre of Excellence in Plant Energy Biology; JW; ARC Discovery Grant DP200102452; JW).

EMAIL ADDRESS OF AUTHOR FOR CONTACT:

o.berkowitz@latrobe.edu.au

ABSTRACT

The energy generating plant organelles mitochondria and chloroplasts are crucial for the acclimation of plants to adverse growth conditions. Imbalances in their function trigger a signalling pathway, the retrograde response, to adjust nuclear gene expression and mitigate organelle dysfunction. Identification and characterisation of many components of the mitochondrial retrograde signalling pathway is still scarce. Here, we demonstrate that a one of the highly induced mitochondrial dysfunction genes, a 2-oxoglutarate Fe(ii)-dependent oxygenase (OGO, AT5G43450), responds specifically to perturbation of mitochondrial function. The annotation of OGO as an ACO-like based on its sequence similarity with the ethylene forming enzyme 1-aminocyclopropane-1-carboxylic acid (ACC) oxidase suggested a role of ethylene in the regulation of OGO. Increased sensitivity of *ogo* mutant lines to treatment with the ethylene precursor ACC in a root growth assay, and early bolting and senescence of OGO overexpression lines further supported a role of ethylene. Furthermore, chromatin immunoprecipitation followed by PCR (ChIP-qPCR) demonstrated binding of the master regulators of ethylene and mitochondrial stress signalling, EIN3 and ANAC017, respectively, to the promoter of OGO. A mutant screen led to the identification of two regulators of OGO expression with no previous role in the in the retrograde signalling pathway. SIN3/ROG2 is a subunit of the histone deacetylase (HAD) complexes HDA6 and HDA19 and interacts with a member of the ethylene-responsive element binding factor family ERF7. ROG4/AT2G36720 is a potential positively regulator of RNA polymerase II. In conclusion, characterisation of OGO indicated ethylene as a signalling molecule in the mitochondrial retrograde response and identified two novel regulators of this pathway.

INTRODUCTION

Plant mitochondria and chloroplast are in a prime position to sense and respond to adverse growth conditions. They turn over metabolic intermediates and provide the energy in form of ATP and reductive equivalents for growth and stress responses. Hence they are intimately connected with metabolic changes necessary for acclimation to maintain cellular homeostasis and function. In response to a variety of adverse growth conditions both organelles trigger alterations in nuclear gene expression via organelle to nuclear signalling, which is referred as retrograde signalling (Woodson and Chory, 2008; Kmiecik et al., 2016; de Souza et al., 2017; Crawford et al., 2018; Pfannschmidt et al., 2020; Wang et al., 2020). Although components of these signalling pathways have been identified over the past decade, the extent of responses observed under impaired mitochondrial and chloroplastic function, ranging from the transcriptional to the whole plant level, suggests our understanding is still limited.

Chloroplast retrograde regulation (CRR) is well studied and established largely due to the readily observable phenotype of mutants that are affected in the greening process. For plastid retrograde regulation, signals are classified into five major groups: plastidial gene expression (PGE), the tetrapyrrole intermediate biosynthesis, reactive oxygen species (ROS), redox processes in photosynthesis, and signals mediated by dual-localized proteins in both the nucleus and plastids (Strand et al., 2003; Pfannschmidt, 2010; Chan et al., 2016). The tetrapyrrole intermediate signalling pathway has been characterized by identification of several *genomes uncoupled* (*gun*) mutants, *gun1-gun6* in *Arabidopsis thaliana* (Mochizuki et al., 2001; Larkin et al., 2003; Woodson et al., 2011). The inhibition of chloroplast biogenesis by plastid translation inhibitor lincomycin (Lin) and carotenoid biosynthesis inhibitor norflurazon (NF), as well as high light treatment were used to identify and characterize the CRR (Woodson et al., 2013; Gollan and Aro, 2020). GUN1 as a chloroplast-localized pentatricopeptide-repeat (PPR) protein, is linked to the plastid gene expression, tetrapyrrole biosynthesis, photosynthetic electron transport. It was reported to act as a master switch that generates or transduces signals to induce the *ABSCISIC ACID INSENSITIVE4* (*ABI4)* to coordinate the expression of nuclear encoded photosynthetic genes (Koussevitzky et al., 2007). However, the role of ABI4 in relation to the chloroplast-to-nucleus retrograde response has been questioned (Kacprzak et al., 2019). Besides, the 3'(2'), 5'-bisphosphate nucleotidase (SAL1)-PAP and MEP 2-C-methyl-D-erythritol 2,4-cyclodiphosphate (MEcPP) as plastidial metabolites are retrograde signals and involved in plant adaption to adverse growth conditions (Estavillo et al., 2011; Xiao et al., 2012).

Similar to chloroplasts, mitochondria also regulate nuclear encoded genes via mitochondrial retrograde regulation (MRR) (Liu and Butow, 2006; Ng et al., 2014; Kleine and Leister, 2016). Antimycin A (AA) and myxothiazol (myxo) are chemical inhibitors of complex III in mitochondrial electron transport chain, which trigger mitochondrial dysfunction and activate the MRR to alter gene expression. Even though antimycin A (AA) is recognized as a compound for inhibition of mitochondrial function it also impacts cyclic electron transport during photosynthesis (Hertle et al., 2013). Cyanide-resistant alternative oxidase (AOX) catalyses the oxidation at the level of ubiquinone (UQ), bypassing complex III, cytochrome c and complex IV and is significantly induced to mitigate the impaired electron flow under AA and myxo treatment. The high responsiveness of the *AOX1a* gene provided a pre-eminent model for MRR in plants to identify regulators by forward genetic screen using a luciferase reporter system (Millar et al., 2011; Wang et al., 2020). Several Regulators of *Alternative Oxidase 1a* termed RAO have been identified and characterized in Arabidopsis (Ng et al., 2013; Ng et al., 2013; Ivanova et al., 2014; Zhang et al., 2017). CDKE1 (RAO1) as a subunit of the kinase module of the mediator complex in plants, is necessary for the response to cellular stresses like H_2O_2 and cold (Ng et al., 2013). CDKE1 also interacts with a protein kinase 10 (KIN10) in the nucleus which is proposed to be a point of integration of energy and stress signalling during plant growth (Baena-Gonzalez et al., 2007). The membrane domain-containing Arabidopsis NAC domain transcription factor 17 (ANAC017/RAO2) is the key regulator of the MRR. ANAC017 as a positive regulator of several genes of the MRR, including AOX1a, located at the endoplasmic reticulum (ER) membrane and translocates to the nucleus upon perturbation of mitochondrial function (Ng et al., 2013). Furthermore, several negative regulators of AOX1a, RAO3 to RAO6, are involved in auxin signalling (Ivanova et al., 2014). The transcription factor MYB domain protein 29 (MYB29/RAO7) was shown to participate in MRR and its mutation leads to increased AOX1a expression compared to the wild type controls (Zhang et al., 2017). MYB30 induces AOX1a expression under salt stress (Gong et al., 2020). WRKY40 and WTKY63 are a repressor and activator of *AOX1a*, respectively, under antimycin A and high light treatment and link both organellar signalling pathways (Van Aken et al., 2013). *ABA INSENSITIVE 4* (*ABI4*) interacts with the *AOX1a* promoter and acts as a repressor (Giraud et al., 2009).

Several mitochondrial dysfunction stimulon (MDS) genes including *AOX1a*, *OUTER MITOCHONDRIAL MEMBRANE PROTEIN OF 66 KDA* (*OM66*) and *UPREGULATED BY OXIDATIVE STRESS* (*UPOX*), have been identified by their high up-regulation under AA treatment. Yeast one-hybrid analysis has revealed a promoter motif within the promoter of

these MDS genes which is bound by several ANACs including ANAC013 and ANAC017 (De Clercq et al., 2013). Among the MDS genes are also *URIDINE DIPHOSPHATE GLYCOSYLTRANSFERASE 74E2* (*UGT74E2*) and *ATP-BINDING CASSETTE B4* (*ABCB4*) that have a function as auxin conjugase and auxin transporter respectively (Noh et al., 2001; Tognetti et al., 2010), while *HYPOXIA RESPONSIVE ERF 2* (*HRE2*)/*ERF71* is involved in ethylene signal transduction. However, few of the 24 MDS genes have an established function in the MRR, either because their role is unclear from the molecular function (e.g. MULTI-DRUG AND TOXIC COMPOUND EXTRUSION proteins, ribosomal protein L12) or their molecular function is unknown.

In this study, we characterize one MDS, *a 2-oxoglutarate Fe(II)-dependent oxygenase* (*OGO*), which has not been analysed previously and is annotated as ACO-like because of its similarity to the ethylene forming 1-aminocyclopropane-1-carboxylic acid *oxidase* (*ACO*). Loss-of-function mutants of *OGO* are also more sensitive to external treatment with the ethylene precursor 1-aminocyclopropane-1-carboxylic acid. We show that *OGO* is directly targeted by the master regulators of the MRR and ethylene signalling, ANAC017 and ETHYLENE INSENSITIVE 3 (EIN3), respectively. A forward genetic screen identified two mutants that were impaired in the ability to induce *OGO* on inhibition of mitochondrial function. Mutants for the underlying genes (*SIN3/ROG2*, *ROG4/ AT2G36720*) and for *OGO* are sensitive to combined drought and moderate light treatment while over-expressing lines are more tolerant when compared to wild type. Combined these results provide evidence for an interplay of the mitochondrial retrograde and ethylene signalling pathways, with OGO a possible downstream target of both, and two novel regulators of the mitochondrial retrograde signalling pathway.

RESULTS

Mitochondrial stress-specific induction of a *2-oxoglutarate and Fe(II)-dependent oxygenase* (*OGO*, *AT5G43450*)

Many chemical or abiotic stress treatments affect both energy generating organelles, i.e. mitochondria and chloroplasts, and impair their function. This complicates the identification of organelle-specific signalling pathways and their components. Using bio-informatic analyses on publicly available microarray datasets, several genes whose transcripts are specifically induced by either antimycin A or high light treatment were identified (Figure 1), suggesting these genes are preferentially regulated by the mitochondrial or chloroplast retrograde pathways, respectively. Several heat-shock protein (HSP) family genes, *HEAT SHOCK PROTEIN 17.6A* (*HSP17.6A*, *AT1G59860*), *HEAT SHOCK PROTEIN 17.6B* (*HSP17.6B*, AT2G29500), *HEAT SHOCK PROTEIN 17.6C* (*HSP17.6C*, *AT1G53540*) and *HEAT SHOCK PROTEIN 26.5* (*HSP26.5*, *AT1G52560*) were significantly responsive to high light treatment only, with 142-, 48-, 358-, 441-fold induction respectively ($P<0.001$), while not significantly altered by antimycin A treatment. These were therefore recognized as chloroplast specific stress marker genes (Figure 1). By contrast, the mitochondrial dysfunction stimulon (MDS) gene *OUTER MITOCHONDRIAL MEMBRANE PROTEIN OF 66 KDa* (*OM66*, *At3g50930*) was the most antimycin-responsive gene and induced by 46-fold, but it did not specifically respond to high light stress. Thus, OM66 is a stress marker on the basis of a specific mitochondrial perturbation response, in agreement with an earlier report (Zhang et al., 2014). Several other genes specific for a mitochondrial stress response were *AT1G76600*, *GLYCOLIPID TRANSFER PROTEIN* (*GLTP*, *AT4G39670*), *UDP-GLUCOSYL TRANSFERASE 73B3* (*UGT73B3*, *AT4G34131*) and *AT5G43450*, which were significantly ($P<0.001$) induced by antimycin A by 18-, 34-, 16-, 12-fold, respectively, but not significantly altered by high light treatment (Figure 1).

The *AT5G43450* gene was previously identified as a member of the MDS genes (De Clercq et al., 2013) but is largely uncharacterized. It belongs to the 2-oxoglutarate and Fe(II)-dependent oxygenase family (2-OGDO) and hence was named OGO. The family members have been implicated in a variety of molecular functions ranging from ethylene synthesis, auxin oxidation to gibberellic and flavanol synthesis (Kawai et al., 2014). *OGO* was initially identified and cloned because of its sequence similarity to the ethylene forming enzyme 1-aminocyclopropane-1-carboxylic acid (ACC) oxidase (ACO) (Trentmann and Kende, 1995; Vandenbussche et al., 2003) and is annotated as ACO-like in TAIR. To confirm the mitochondrial stress-specific expression of OGO, a reporter line was generated to be able

to visualise OGO expression non-invasively. The reporter line carries a construct for the expression of the firefly luciferase (LUC) coding region under the control of the OGO promoter (1 kb upstream region form the translation start codon) (Figure 2A). Treatment with antimycin A and myxothiazol led to strong induction of LUC expression as indicated by the increase bioluminescence signals obtained after application of the LUC substrate luciferin, while mock treatment (initial spray with water, followed by luciferin) gave no increase bioluminescence (Figure 2B,C). Importantly, high light treatment also failed to induce LUC expression, confirming the induction of OGO expression by mitochondrial stress only (Figure 2B,C), as already suggested by the analysis of publicly available expression data (Figure 1).

The results provided evidence that the *OGO* gene might have a role specifically in the mitochondrial stress response as it was not responsive to high light treatment and it possibly has links to hormonal signalling pathways.

In silico sequence and expression analysis of the 2-oxoglutarate and Fe(II)-dependent oxygenase (OGO) and close homologs

The OGO protein was placed into the DOXC subclass of the 2-OGDO protein family which largely includes biosynthetic enzymes with varying substrates (Kawai et al., 2014). However, for the 100 family members in Arabidopsis, only for about a third a molecular function has been attributed and mostly only on sequence similarity (Kawai et al., 2014). For few the enzymatic activity has been validated *in vitro*. For example, for the five annotated isoforms of the ethylene forming enzyme ACO in Arabidopsis, only the ACO2 protein has a confirmed activity (Houben and Van de Poel, 2019). A sequence alignment for members of this subclass with sequence similarity to OGO and with a wide range of molecular functions (ethylene biosynthesis, auxin oxidation, gibberellic acid, jasmonic acid and flavanol biosynthesis) showed substantial divergence among the proteins (Figure 3A and 3B). Even for the five ACO isoforms amino acid conservation was limited outside the conserved 2-oxoglutarate binding and oxygenase domains. OGO shares the sequence conservation for these domains but also substantial sequence variation outside of these domains. Hence, sequence analyses provide only limited information on the function of these proteins because of their restricted biochemical characterisation that is not yet detailed enough to make predictions from sequence alone.

To investigate the gene expression and regulation of *OGO* and other members of the 2-OGDO family, a comparative transcript analysis utilizing microarrays and transcriptome data using Genevestigator was performed (Figure 3C) (Hruz et al., 2008). *OGO* is induced by many treatments, underlining its importance in mitochondrial stress response and

signalling. Under 50 µM antimycin A (complex III inhibitor) and 10 µM oligomycin (complex V inhibitor) treatment (Data set ID AT-00664 and AT-00522), there is a 12-fold and 29-fold induction on transcript level, respectively, with *ACC OXIDASE 4* (*ACO4*), DIOXYGENASE FOR *AUXIN OXIDATION* (*DAO1*) and *JASMONIC ACID OXIDASE (JAO) 2* (*JAO2*) having a similar pattern, suggesting that ethylene, auxin or jasmonic acid production might be induced by mitochondrial dysfunction. This is further supported as *OGO*, *JAO2* and *JAO4* transcript levels were less induced in a mutant line (*rao2-1*) for the mitochondrial retrograde signalling master regulator ANAC017 under antimycin A and H_2O_2 treatment. This suggests that *OGO* is downstream of ANAC017 (Dataset ID AT-00664). Previous studies revealed that the adaptation to submergence is dependent on the mitochondrial retrograde signalling pathway and hypoxia impacts mitochondrial respiration (Wagner et al., 2018; Meng et al., 2020). Hypoxia treatment (0.1% O_2) induces *OGO* by 44-fold- change, and *ACO4*, *FLAVONOL SYNTHASE* 1 (*FLS1*), *JAO2*, *JAO4*, and *FLAVANONE 3-HYDROXYLASE* (*F3H*) were also induced during the process (Data set ID AT-00447). The ETHYLENE RESPONSE FACTOR (ERF) 73/HYPOXIA RESPONSIVE ERF (HRE)1 was reported to function in stress responses to hypoxia and submergence modulating the ethylene response (Yang et al., 2011). *OGO* was repressed in a *35S:HRE1* overexpression line under hypoxia stress on the transcript level, which indicates that *OGO* might be involved in ethylene dependent hypoxia/submergence stress responses (Data set ID AT-00396). EIN3 and EIN3-LIKE1 (EIL1) are key transcription factors in the ethylene response, and EIN2 is the transducer of ethylene signalling (Guo and Ecker, 2003; Li et al., 2015). *OGO* was downregulated in the *ein3eil1* and *ein2-1* mutants (Data set ID AT-00450 and AT-00597), which is similar to the pattern of several ACC oxidase (*ACO2*, *ACO4* and *ACO5*) and indicates that *OGO* could be involved in ethylene signalling pathway downstream of EIN3/EIL1 or EIN2.

Cytosolic localization of 2-oxoglutarate and Fe(II)-dependent oxygenase (OGO)

To further determine the function/role of OGO, the subcellar localization of the OGO protein was determined (Figure 4). For this, constructs for the expression of the OGO protein tagged with the fluorescent RFP or GFP protein at the C-terminus and under the control of the CaMV 35S were generated. As controls, corresponding constructs to express a RBCS-GFP fusion protein (chloroplast control), GFP-PTS fusion (peroxisomal control), SHMT-GFP fusion (mitochondrial control) were also used (Wachter et al., 2005). These constructs were then transiently expressed in transfected Arabidopsis protoplasts and analysed by confocal laser scanning microscopy. While all control fusion proteins were locating as expected, the

detected fluorescence signals revealed that the OGO protein was in the cytoplasm (Figure 4). This suggests that the induction of OGO under mitochondrial stress is not directly involved in processes in the mitochondria but rather that OGO has a function in linking mitochondria with other cellular processes via a cytosolic activity. Given that OGO is annotated as an ACO-like protein, its localisation is in agreement with a cytosolic localisation of ACOs reported previously and of many members of the 2-OGDO family in general (Kawai et al., 2014; Houben and Van de Poel, 2019).

Expression of *2-oxoglutarate and Fe(II)-dependent oxygenase* (*OGO*) in different tissues and developmental stages

To investigate the tissue-specific expression pattern of *OGO*, reporter lines expressing the β-glucuronidase (GUS) protein under the control of the native *OGO* promoter (1kb upstream of the start codon) were generated. Histochemical staining for GUS activity was performed in these *proOGO-GUS* transgenic plants using twelve-days old seedlings as well as mature and flowering plants (Figure 5). GUS signal was visible in the leaf tip and vasculature, hydathodes, leaf tip mesophyll (Figure 5A,B,C), sepals in flowers (Figure 5E,F), stigma of young siliques (Figure 5G,H) and parts of the root (Figure 5I-K). A previous study using the DR5:GUS auxin reporter lines showed GUS to be mainly localized in serrate initiation site, leaf tips, developing vasculature and edge of cotyledon (Bao et al., 2004), which is a similar *OGO* expression. This may indicate that *OGO* expression might be related to auxin levels. For flowers, *OGO* expression indicated by high GUS activity was evident in the sepal and not detectable in stamens, carpels, or petals (Figure 5E,F). In mature siliques, no GUS activity was detected in ovule, while in developing siliques GUS activity was present in the remnants of the stigma (Figure 5G and H). For the root, GUS activity was only strong in the mature zone of laterals (Figure 5I), and in those with comparably weaker activity in the root tip (Figure 5J) and throughout all tissues (Figure 4K). Interestingly, ChIP-seq data shows that the transcription factor ETHYLENE RESPONSE DNA-BINDING FACTOR (EDF2) directly binds to the *OGO* promoter region under ethylene treatment (Mathew G. Lewsey (La Trobe University), unpublished data). The EDFs are important downstream genes of the ethylene signalling pathways in Arabidopsis (Alonso et al., 2003; Patterson and Bleecker, 2004; Chen et al., 2015). The sepal-specific expression pattern of *EDF2* was similar with *OGO* expression in the flower (Chen et al., 2015). These results suggest that *OGO* is regulated by ethylene signalling pathways with targeting by EDF2. Overall, these results provide evidence that OGO could play a role in the auxin or ethylene signalling pathways.

Characterization of mutant and overexpression lines for *2-oxoglutarate and Fe(II)-dependent oxygenase* (*OGO)*

To further investigate the potential role of OGO for mitochondrial and hormonal signalling, *OGO* mutant and overexpression lines were characterised. Two viable T-DNA insertion lines (SALK_107806 and SAIL_306_F10) were obtained for *OGO*. PCR and sequencing results showed both insertions are located in an exon region, with *ogo-1* (SALK_107806) at the position +499 bp (downstream) of the translational start site and *ogo-2* (SAIL_306_F10) at the position +870 bp from the translational start site (Figure 6A). Homozygous mutants were identified in the T3 generation and further confirmed by PCR analysis of genomic DNA (Figure 6B). In addition, RNA-seq data (see Chapter III for details) also confirmed that no functional transcripts were generated in both lines (Figure 6C). For *ogo-1* the expression was only residual and no reads were detectable past the insertion site. For *ogo-2* reads were present, but a break in overlapping read alignments around the T-DNA insertion site, which was not apparent in the wild type, showed no functional transcript was being made. Transgenic lines overexpressing a full-length coding sequence of *OGO* under the control of the CaMV 35S promoter were also generated and homozygous lines identified for phenotyping. Expression of the *OGO* gene in the two representative overexpression lines *OGO OE-1* and *OGO OE-2* was determined by qRT-PCR (Figure 6D). Both lines have approximately 16-fold higher *OGO* expression than the wild type (Figure 6D).

Detailed growth analysis was conducted in 14-h-light/10-h-dark cycle on the two *ogo* mutant lines and the two overexpressing lines and the leaf stage progression (two leaves, stage 1.02; four leaves, stage 1.04; eight leaves, stage 1.08; ten leaves, stage 1.10, fourteen leaves, stage 1.14), inflorescence emergence (first flower buds visible, stage 5.1) and flower production (stage 6.0) were determined (Figure 7A) (Boyes et al., 2001). There were no substantial differences between genotypes during the vegetative development. However, the inflorescence emergence and flower production stages were delayed in *ogo-1* and *ogo-2* when compared to Col-0 ($P<0.05$). The opposite was observed with the two *OGO* overexpression lines ($P<0.05$) which bolted earlier than wild type (Figure 7B). Consequently, flowers emerged earlier in these two lines and senescence of leaves and siliques was also prior to wild type, suggesting accelerated development after transition to reproductive stage and into senescence. Altered inflorescence development and leaf senescence have been attributed to ethylene signalling (Dubois et al., 2018), and the decreased expression of *OGO* in ethylene signalling mutants (Figure 3B) together with altered timing of these processes

by *OGO* mutation and overexpression also suggest a relationship of *OGO* function and its induction under mitochondrial dysfunction with ethylene signalling.

Previous studies demonstrated that ethylene plays an important role in the transition from vegetative growth to flowering to senescence in Arabidopsis (Jing et al., 2002; Ogawara et al., 2003; van der Graaff et al., 2006; Li et al., 2013). For example, ethylene-related mutants *ein3-1*, *ein2-1* and *etr1* showed delayed flowering compared with the wild type (Ogawara et al., 2003), similar to *ogo*-1 and *ogo-2*. As *OGO* is also down-regulated in ethylene mutants *ein3-1* and *ein2-1* (Figure 3B), these results provide further evidence that *OGO* could be involved in ethylene biosynthesis or signalling in Arabidopsis.

Phenotypic effects of exogenous application of 1-aminocyclopropane-1-carboxylic acid (ACC), aminoethoxyvinylglycine (AVG) and 1-naphthylacetic acid (NAA) on *OGO* mutants, *rao2-1* and *ein3-1* root growth

To investigate whether a lack of *OGO* interferes with ethylene- or auxin-related root growth, the response of wild type, *OGO* mutants (*ogo-1*, *ogo-2*), the *rao2-1* mutant of the master regulator of mitochondrial signalling ANAC017 (*ANAC017* EMS mutant, (Ng et al., 2013)), and the *ein3-1* (*ETHYLENE INSENSITIVE 3* mutant) were compared when grown in the presence of varying concentrations of the ethylene precursor 1-aminocyclopropane-1-carboxylic acid (ACC) (Vanderstraeten et al., 2019), ethylene biosynthesis inhibitor aminoethoxyvinylglycine (1 µM AVG) and the synthetic auxin 1-naphthylacetic acid (0.2 µM NAA). For this, each of these genotypes were precultured on the control medium seedlings for 5 days, then seedlings were transferred to media containing the chemicals and the growth of roots was monitored for a further 16 days for phenotype assessment (Figure 8), or for a further 8 days for quantitative measurements (Figures 9). In the absence of any added chemicals and in the presence of AVG, the five genotypes showed no major differences in their phenotypes. The addition of NAA to the medium increased lateral root growth in all genotypes as expected for an auxin response (Laskowski et al., 1995), but without causing differences among genotypes (Figure 8). Interestingly, the ACC treatments used in this experiment increased shoot growth in all genotypes. Although ethylene is usually considered as a growth inhibiting hormone (Dubois et al., 2018), low concentrations below about 10 µM have a promoting effect in some species (Lee and Reid, 1997; Fiorani et al., 2002). ACC treatment visibly decreased root growth at the higher concentrations of 5 µM and 10 µM (Figure 8), in agreement with a previous study (Vanderstraeten et al., 2019).

Quantification of root elongation after transfer corroborated the phenotypic observations (Figure 9). No differences among genotypes were observed on the control

medium and medium supplemented with NAA or AVG. For the ACC treatments, the *ein3-1* mutant showed limited growth inhibition in agreement with its identification as ethylene insensitive and the role of EIN3 in ethylene perception (Chao et al., 1997). The mitochondrial signalling mutant *rao2-1* and both *ogo* mutants showed increased ethylene sensitivity as the increase in root growth was less than for wild type (Figure 9A). These results were also evident from an ACC response curve for the concentrations used (Figure 9B).

Therefore, these ACC dose-response experiments revealed that loss of function of the mitochondrial dysfunction stimulon gene *OGO* and the mitochondrial signalling regulator *ANAC017* leads to increased sensitive to ethylene, providing evidence for the interplay of mitochondrial retrograde and ethylene signalling pathways to affect plant growth.

ETHYLENE INSENSITIVE 3 (EIN3) targets several mitochondria-related genes

To investigate if the master transcriptional factor of the ethylene pathway ETHYLENE INSENSITIVE 3 (EIN3) directly targets *OGO* and other mitochondria-related genes, a ChIP-qPCR experiment was performed. Putative EIN3 binding sites in the vicinity of the genes were extracted from a previous ChIP-seq experiment (O'Malley et al., 2016). For *OGO* and *HRE2* these were located 300 bp and 200 bp up-stream of the translational start sites, respectively, while for *AOX1a* a putative binding site was 300 bp downstream of the 3'-UTR. For this, twelve-days old transgenic Arabidopsis seedlings expressing a translational fusion of a yellow fluorescent protein (Ypet) and *EIN3* under the control of native promoter (*proEIN3:EIN3-Ypet,* provided by Mathew G. Lewsey, unpublished) were treated with ACC to increase tissue levels of ethylene as well as AA and myxothiazol to induce mitochondrial stress. The results showed that promoter region of the MDS gene *OGO* and the 3'-region directly downstream of *AOX1a* had increased binding of EIN3 after ACC treatment and to a lesser degree also after AA treatments, but not myxothiazol treatment. For another MDS gene analysed, HYPOXIA RESPONSIVE ERF (ETHYLENE RESPONSE FACTOR) 2/ERF71, and the control gene ACTIN2, no EIN3 binding was detectable (Figure 10). For *AOX1a* binding of EIN3 to its 3'-region was also observed after myxothiazol treatment.

Overall, the results demonstrate that EIN3 targets the mitochondrial stress-related gene *OGO* which suggests crosstalk between mitochondrial and ethylene signalling pathways.

ANAC017 is a positive regulator of *2-oxoglutarate and Fe(II)-dependent oxygenase* (*OGO*)

The mitochondrial dysfunction motif (MDM) was defined as a *cis*-regulatory element in the upstream region of mitochondrial dysfunction stimulon (MDS) genes and is responsive

to various mitochondrial perturbation (De Clercq et al., 2013). Hierarchical clustering of 34 MDS genes shows that *OGO* is clustering with a group of genes that are affected by chemical treatments and mutant lines, sharing a similar expression pattern with *ANAC013*, *HRE2* (*ATERF71*) and the mitochondrial retrograde signalling maker gene *AOX1a* (De Clercq et al., 2013). Two MDM elements (CTTGNNNNNCA[AC]G) were identified in the 1-kb region upstream of the OGO start codon that are potential binding sites for ANAC013 and ANAC017 (Figure 11A) (De Clercq et al., 2013). ANAC017 directly binds the *AOX1a* promoter to mediate its expression under antimycin A treatment (De Clercq et al., 2013). The *OGO:LUC* line (Figure 2) was crossed with the *rao2-1* knock-out line of ANAC017 and the F2 progeny (*OGO:LUC* x *rao2-1*) were used to investigate if *OGO* was also regulated by ANAC017 under perturbation of mitochondrial function. As controls two reporter lines expressing the luciferase gene under the control of the *AOX1a* (*Col:LUC*) and *OGO* (*OGO:LUC*) promoter, respectively, were grown on B5 plates and sprayed with 50 µM antimycin A (AA). Subsequently luciferin was applied and LUC reporter activity was visualized in a bioluminescence imager 6 h post treatment. Both reporter lines show the expected strong induction of LUC expression in response to the activation of the mitochondrial retrograde response by AA (Figure 11B). For *OGO:LUC* x *rao2-1* plants no induction of LUC activity was detectable, indicating a regulation of *OGO* by ANAC017 (Figure 11B).

In addition, from the same experiment samples were harvested 3 h after the AA treatment of the *OGO:LUC* line and transcript abundance was analysed by qRT-PCR with *UBIQUITIN 21* (*UBC21*) as a reference gene (Figure 11C). *LUC* and *OGO* transcript abundance was significantly lower in the *OGO:LUC* x *rao2-1* line compared to the *OGO:LUC* line ($P < 0.001$). Expression data for *OGO* was also retrieved from a previous experiment using ANAC017 (over)expressing lines (Meng et al., 2019). The transgenic lines (over)expressing a constitutively active form of ANAC017 lacking the transmembrane domain (ΔTM / ΔTMOE2 and ΔTMOE3) or a full-length ANAC017 (OE2, OE3) showed a opposite pattern to the *OGO:LUC* x *rao2-1* line. *OGO* expression level was 5.3-, 5.1-, 34.1-, 20.1-, 28.1-fold higher in *ANAC017△TM, ANAC017△TMOE2, ANAC017△TMOE3, ANAC017OE2* and *ANAC017OE3* compared to the wild type (Figure 11D) (Meng et al., 2019).

To validate the direct regulation of *OGO* by ANAC017, the ability of ANAC017 to bind to the *OGO* promoter was assessed by a ChIP-qPCR experiment. For this, twelve-day old transgenic Arabidopsis seedlings expressing a green fluorescent protein (GFP)-tagged version of ANAC017 under the control of the native ANAC017 promoter (*proANAC017-GFP-*

ANAC017) were generated, treated with AA and ChIP-qPCR conducted using an anti-GFP antibody. The results showed that the MDM-containing promoter regions of *OGO, AOX1a* and *UP-REGULATED PROTEINS BY OXIDATIVE STRESS* (*UPOX*) bind ANAC017. Their binding was 330-, 57- and 566-fold enriched, respectively, under AA treatment when compared to mock treated controls (Figure 11E).

Taken together, the data demonstrate that ANAC017 is a positive regulator of *OGO*, as well as *AOX1a* and *UPOX*, by directly binding to its promoter under mitochondrial stress.

Identification of ROG2 and ROG4 as transcriptional regulators of *2-oxoglutarate and Fe(II)-dependent oxygenase* (*OGO*)

To further characterize the function of OGO in the mitochondrial stress response and to identify potential novel regulators involved, a mutant screen was carried out following established methodology that led to the identification of regulators of *AOX1a* (Ng et al., 2013; Ivanova et al., 2014). Here, seeds of *OGO:LUC* plants were subjected to ethyl methanesulfonate (EMS) mutagenesis and the progeny of the mutagenized *OGO:LUC* population were screened for an inability to induce *LUC* after treatment with 50 µM AA. From the screened population of about 10,000 plants, mutants that failed to induce the luciferase gene were selected and grown to the next generation for confirmation. Of eleven plants initially identified, four showed a consistent reduction in LUC expression and two mutant plants were further analysed. These two mutant lines, named regulator of OGO (*rog) 2 and rog4* showed a greatly reduced induction of LUC after AA treatment (Figure 12A and Figure 12B). The increase in bioluminescence observed in the *OGO:LUC* lines was reduced by fourfold in *rog2* and by two-fold in the *rog4* background ($P<0.001$) (Figure 12C). Notably, LUC signal intensity was also threefold lower in the *rog2* background compared with *OGO:LUC* in control conditions (Figure 12C).

Subsequently, next-generation sequencing was used as described previously to identify the potentially underlying mutations in *rog2* and *rog4* (Ng et al., 2013; Ivanova et al., 2014). From a list of candidate mutations only those that affected the sequence of the underlying protein to likely result in a loss-of-function were retained. This led to the identification of a candidate mutation in each of the two mutants which generated a premature stop codon in the coding sequence of the underlying genes. A mutation in *rog2* was mapped to a candidate point mutation in the *SIN3* (AT1G24190) gene and *rog4* to the candidate point mutation in a gene encoding an uncharacterised *acyl-CoA N-acyltransferase* (AT2G36720) (Figure 12D). The point mutations in *rog2* and *rog4* were further confirmed by Sanger sequencing (Figure 12E).

To further validate that the impaired ability to induce *OGO* in the *rog2* mutant line was caused by a loss-of-function of *SIN3*, two T-DNA lines (SALK_028140 and SAIL_242_H10) were subsequently obtained and preliminarily characterised (Figure 13A). *OGO* and *AOX1a* transcript abundance were examined by qRT-PCR in *OGO:LUC* and independent *rog2/sin3* mutant lines: *rog2* representing the identified EMS mutant, the T-DNA insertion line *rog2 KO-1* (SALK_028140) and another T-DNA insertion line *rog2 KO-2* (SAIL_242_H10). In addition, SIN3 overexpressing lines (*35S:ROG2-1*, *35S ROG2-2* and *35S:ROG2-3*) were generated by transformation with a construct containing the coding sequence of SIN3 in front of the CaMV35S promoter. Twelve-days old seedlings of these genotypes were exposed to 50 µM AA or water (-AA). Samples were harvested 3 h after the treatment and transcript abundance was analysed by qRT-PCR with *UBIQUITIN* (*UBC*) as reference gene. For the mock treatment expression of *LUC*, *OGO* and *AOX1a* was lower in the mutant lines suggesting ROG2/SIN3 influences their expression already under standard growth conditions, while expression of *OGO* was highly increased in the *35S-SIN3* lines as expected (between 15 to 18-fold) and *AOX1a* expressions unchanged in these three lines (Figure 13A). Induction of *LUC*, *OGO* and *AOX1a* after AA treatment was attenuated by about 2- to 3-fold in all three *rog2* mutant lines and accentuated in the *ROG2* overexpressing lines by 2-fold compared when compared to *OGO:LUC*, respectively (Figure 13A). Hence, characterisation of these T-DNA and overexpression lines confirmed the regulation of *OGO* by ROG2 (SIN3) observed in the EMS mutagenised *rog2* line.

Similarly, to further confirm that impaired ability to induce *OGO* in *rog4* mutant line was caused by a specific inactivation of the *acyl-CoA N-acyltransferase* (AT2G36720), two T-DNA lines *rog4 KO-1* (SALK_025328C) and *rog4 KO-2* (SALKSEQ_77499) were also obtained for subsequent analyses. *LUC*, *OGO* and *AOX1a* transcript abundance were examined by qRT-PCR after AA and mock treatments as described above in *OGO:LUC* and the two independent *rog4* T-DNA insertion lines (Figure 13B). In contrast to the *rog2* mutant lines, changes in expression of the three genes tested were minor but trending towards a mild up-regulation (statistically significant for AOX1a only, $p<0.05$,). The three genes were strongly up-regulated by 30 to 60-fold in the *OGO:LUC* line as expected after AA treatment ($P<0.001$), while in the three mutant lines this induction was 2-fold lower (Figure 13B). The analyses of the T-DNA lines thus confirmed the regulation of OGO by ROG4 observed in the *rog4* line.

Taken together, the preliminary characterisation of mutant and overexpression lines as described above indicated a role of ROG2/SIN3 and ROG4 in the regulation of two mitochondrial stress-responsive genes *OGO* and *AOX1a*. For both ROG2 and ROG4 the

mode of action remains to be elucidated. ROG2 has been implicated in chromatin modification and also interacts with *ETHYLENE-RESPONSIVE TRANSCRIPTION FACTOR* (*ERF7*) (Song et al., 2005). These functions could directly explain a role in the transcriptional control of genes such as *OGO* or *AOX1a*, possibly involving ethylene. ROG4 is uncharacterised and been annotated by sequence similarity as a acyl-CoA N-acyltransferase with RING/FYVE/PHD-type zinc finger domain-containing protein (TAIR10), which positively regulate RNA polymerase II and hence this might impact gene expression for target genes.

Mutation of OGO and its regulators impacts drought stress tolerance

It was previously reported that both *anac017* and *aox1a* mutant plants are more sensitive to combined drought and moderate light stress (Giraud et al., 2008; Ng et al., 2013). Also, the regulator of *OGO* expression ROG2/SIN3 has a role in drought tolerance (Song et al., 2005). As ANAC017 and ROG2/4 are regulators of *OGO* expression as shown above, the effect of stress on mutants and/or overexpression lines for *OGO*, *ROG2*, *ROG4*, *ANAC017* and *AOX1a* was investigated and compared to the wild type Col-0 and also the *OGO:LUC* line as the genetic background of the *rog2* and *rog4* mutants. For this, plants were grown for 26 days under standard growth conditions (14 h at 120 µmol m^{-2} s^{-1} light/10 h dark), then transferred to moderate light stress (14 h of 400 µmol m^{-2} s-^{1}) and water was also withheld. After 13 days of this combined drought and moderate light (DML) stress, plants were transferred back to standard growth conditions and watering resumed to evaluate recovery. Plant growth and maximum quantum yield of photo system II (Fv/FM) were measured using an automated phenotyping platform, while relative water content (RWC) was also quantified manually.

Phenotypically, the genotypes Col-0, *OGO OE-1*, *OGO OE-2*, *ANAC017 OE-3*, *AOX1A OE*, *OGO:LUC* were tolerant to the DML stress and recovered, while loss of function *OGO* mutant (*ogo-1* and *ogo-2*) all three *rog2* mutants were more sensitive and the other genotypes, i.e. all three *rog4* mutants , *rao2-1* and *aox1a*, did not recover at all (Figure 14). Quantification of Fv/Fm, RWC and leaf areas confirmed these visual classifications. Under control conditions there were no quantitative difference between genotypes for Fv/Fm and relative water content (RWC) (Figure 15). The overexpression lines *OGO OE-1*, *OGO OE-2*, *ANAC017 OE-3* and *AOX1A OE* maintained higher Fv/Fm values than Col-0 and *OGO:LUC*, and all of these genotype recovered to pre-stress values. For the three *rog2* mutants the Fv/Fm recovered but was consistently lower than for the genotypes above, while the remaining genotypes (*ogo-1*, *ogo-2*, *rog4* mutants, *rao2-1*, *aox1a*) had rapidly

decreasing Fv/Fm values after withdrawal of water and showed very limited recovery (Figure 15). The RWC confirmed the classification of genotypes by Fv/Fm. Under control conditions, the quantification of leaf areas showed genotype-specific differences reflecting their varying growth rates. The *ANAC017 OE-3* line had the lowest leaf area consistent with its previously reported growth retardation (Meng et al., 2019). The *rog4* mutant also showed slower growth than the other genotypes for which the difference was limited to about 15 % variation (Figure 15). At the beginning of DML stress imposition, it affected the measured leaf areas of genotypes to varying degrees, but at the end of the stress treatments (13 days) all genotypes had almost identical and very low leaf area. This was a result of the water loss leading to substantial wilting (Figure 14), which also hampered the accurate measurement of leaf area by the top view sensor array. However, after rewatering and return to normal growth conditions the recovery a of leaf areas was consistent with the tolerance assessment of genotypes by Fv/Fm and RWC.

Taken together, the results confirm earlier reports that altered expression or loss-of-function of genes involved in the mitochondrial stress response, i.e. ANAC017 and AOX1a, affects the ability to acclimate to adverse growth conditions (Giraud et al., 2008; Ng et al., 2013; Meng et al., 2020). The findings presented above extend this to another MDS gene, *OGO*, as well as to its newly identified regulators ROG2/SIN3 and ROG4 for which mutation led to decreased and overexpression of OGO to increased DML stress tolerance, respectively. The identification of these novel players in mitochondrial stress signalling has the potential to increase our understanding on the regulation of mitochondrial function under changing growth conditions.

DISCUSSION

In plants growing under adverse environmental conditions, mitochondrial function can be disturbed, leading to the emission of signals to the nucleus to coordinate cellular homeostasis and activate tolerance responses, which is termed as mitochondrial retrograde regulation (MRR) (Woodson and Chory, 2008; Kmiecik et al., 2016; Pfannschmidt et al., 2020). Identification of novel components of this signalling pathway increases the understanding on how different organisational units within the cell communicate with each other about their functional status and the integration of these on the cellular and whole plant level.

In this study, a *2-oxoglutarate and Fe(II)-dependent oxygenase* (*OGO*, *AT5G43450*) showed low but consistent detectable expression under normal growth conditions and substantially induction after treatment with antimycin A and myxothiazol but not high light. This contrasts with other marker genes, such as *AOX1a*, which are often also responsive to chloroplastic stress, such as excessive light, as their function is interlinked with both organelles (ZHANG et al., 2010; Fu et al., 2012). The response of *OGO* is therefore more specific for the mitochondrial signalling pathway than for many other mitochondrial stress genes. *OGO* belongs to the 2-oxoglutarate and Fe(II)-dependent oxygenase family (2-OGDO) which is the second largest enzyme family in plants (Kawai et al., 2014; Hagel and Facchini, 2018). Of 479 family members in six plant models ranging from green algae to angiosperms, only around 90 of them has been characterized in the literature (Kawai et al., 2014). In Arabidopsis, around 130 family members are known, but only a minority has a validated enzymatic activity. Its members are involved in various oxygenation and hydroxylation reactions such as 1-aminocyclopropane-1-carboxylic acid (ACC) oxidases (ACO), gibberellin 3-oxidase (GA3OX) and flavanone 3-hydroxylases (FNSI) (Kawai et al., 2014). *OGO* is annotated as an *ACO*-like gene by its sequence similarity to ethylene synthesis enzyme 1-aminocyclopropane-1-carboxylic acid (ACC) oxidase. Analysis of microarray data for *OGO* showed downregulation in ethylene-insensitive mutants mutant *ein2-1* and *ein3eil1* mutant similar to the pattern of several *ACC oxidase* (*ACO2*, *ACO4* and *ACO5*), indicating a potential association of *OGO* downstream of the ethylene signalling pathway. The *OGO* promoter also binds the ethylene-induced transcription factor ETHYLENE RESPONSE DNA BINDING FACTOR 2 and both share a similar expression pattern in flowers (Koyama, 2014; Chen et al., 2015). This further suggests a role of OGO in ethylene signalling pathway besides its responsiveness to mitochondrial perturbation. Further biochemical characterisation of OGO will be crucial to establish the enzymatic

activity of the protein. Isoforms of ACO proteins, and of the 2-OGDO protein family in general, have been recalcitrant to purification or bacterial overexpression and hence few members of this protein family have a validated enzymatic activity (Kawai et al., 2014). While our attempts to overexpress OGO in a bacterial system were successful in gaining OGO protein, its purification in a native, active form were unsuccessful as it accumulated in inclusion bodies (Supplemental Figure 1). Hence further optimisation of the expression system will be necessary to obtain an active enzyme and to directly test for its enzyme activity. Given the broad substrate range of the 2-OGDO protein family it cannot be ruled out that OGO has a different enzymatic activity and that the observed relation to ethylene is indirect. Given that other members of the 2-OGDO family are also using auxin or jasmonic acid as substrate, it is possible that OGO has an activity that integrates other hormonal signalling pathways with ethylene signalling.

A forward genetic screen identified two mutants that were impaired in the ability to induce OGO on inhibition of mitochondrial function, which were termed as REGULATORS OF OGO (ROG) 2 and 4. The *rog2* mutation was mapped to the transcriptional repressor SIN3, which was reported as a subunit of the histone deacetylase (HAD) complexes HDA6 and HDA19 and to interact with a member of the ethylene-responsive element binding factor family ERF7 (Knoepfler and Eisenman, 1999; Brubaker et al., 2000; Song et al., 2005). These histone deacetylases control transcriptional repression by changing the accessibility of DNA for transcription factors (Kadosh and Struhl, 1998; Rundlett et al., 1998; Tanaka et al., 2008). HDA19 regulates ethylene and jasmonic acid-dependent regulation of gene expression in pathogen response. Similar to OGO, mutants of SIN3 and HDA19 also flower earlier (Zhou et al., 2005). SIN3 and the histone deacetylase HDA19 enhance the transcription repression activity of ERF7, and plants overexpressing ERF7 display decreased drought tolerance (Song et al., 2005). In this study, *rog2* (*SIN3*) mutant lines and two T-DNA insertion lines showed increased sensitivity to combined drought and moderate light stress which was mirrored by mutant plants (*ogo-1* and *ogo-2*) lacking OGO. In addition, knock-down lines of SIN3 and ERF7 also show increased sensitivity to ABA during seed germination (Song et al., 2005). Mitochondrial biogenesis is a key process during the germination of seeds and hence the connection of OGO with SIN3 and ERF7 might be related to these phenotypes (Carrie et al., 2013; Law et al., 2014). ROG4/ AT2G36720 is uncharacterised and been annotated by sequence similarity as an acyl-CoA N-acyltransferase with RING/FYVE/PHD-type zinc finger domain-containing protein (TAIR10), which positively regulate RNA polymerase II. Hence this might impact gene expression for target genes such as *OGO*. The closest protein with sequence similarity to ROG4 and with

a known function is REPRESSOR OF SILENCING 4 (ROS4). This protein is a histone H3 acetyltransferase and regulating DNA methylation (Miao et al., 2020; Liu et al., 2021). Hence the characterisation of OGO and its regulators provides links between the MRR, ethylene and chromatin modifications.

The transcription factor ETHYLENE INSENSITIVE3 (EIN3), together with its close homolog ETHYLENE INSENSITIVE3-LIKE 1, are the master regulator of ethylene responsive genes by controlling the transcriptional cascade after ethylene perception (Chang et al., 2013). In this study, the promoter region of *OGO* was identified as binding EIN3, which demonstrated *OGO* is a target of the ethylene signalling pathway downstream of EIN3. The mitochondrial dysfunction responsive genes *AOX1a* and *HRE2*/*ERF71* were also targeted by EIN3, which further showed ethylene signalling is potentially involved in MRR. While EIN3 binding to the *HRE2/ERF71* gene occurred in its promoter region and hence suggests direct regulation of its expression, for *AOX1a* binding was observed in the region 300 bp downstream of the gene. It therefore remains to be confirmed if this EIN3 binding site has a direct regulatory function on *AOX1a*, or if this confers regulation of the gene downstream of *AOX1a* which encodes the circadian clock regulator TIME FOR COFFEE. Regulatory elements downstream of plant genes have been reported previously. These are thought to be important for efficient termination of transcription and polyadenylation (Xing et al., 2010). A regulatory role of EIN3 was however confirmed by a reduced induction of *OGO* and *AOX1a* in the *ein3-1* mutant (Chapter III, Figure 5F). More evidence for a regulation of the MRR by ethylene comes from the altered sensitivity in root growth assay of the OGO and ANAC017 mutant lines after exogenous application ethylene precursor 1-aminocyclopropane-1-carboxylic acid (ACC). More detailed evidence for the interaction of ethylene and the MRR, including OGO, is presented in Chapter III.

In conclusion, this study has identified and characterised the mitochondrial dysfunction-inducible *2-oxoglutarate and Fe(II)-dependent oxygenase OGO* (*AT5G43450*) that had an unknown function in the MRR. Phenotypes of mutant and over-expressing plants suggest a role of OGO in stress tolerance and developmental processes. A forward genetic screen identified two regulators of OGO (ROG2 and ROG4), which are novel regulators linked to the mitochondrial stress signalling pathway. Furthermore, characterisation of these genes suggests modulation of the MRR by ethylene.

MATERIAL AND METHODS

Plant material

Two T-DNA insertion lines for *ogo* (SALK_107806 and SAIL_306_F10), *rog2* (SALK_028140 and SAIL_242_H10), *rog4* (SALK_025328C and SALKSEQ_77499), *ein3-1* (N8052) were obtained from the Nottingham Arabidopsis Stock Centre (NASC). T-DNA insertion homozygous lines are verified by left and right gene-specific primers (LP and RP), and T-DNA specific primer (LB) (Supplemental table 1). The accurate T-DNA insert location was confirmed by PCR and sequencing as well as RNA-seq for ogo-1 and ogo-2. The *rao2-1*, *ANAC017 OE-3*, *AOX1A OE* and *aox1a* lines were characterized previously (Giraud et al., 2008; Ng et al., 2013; Meng et al., 2019). For the *OGO:LUC* line, the -1102 bp OGO promoter region upstream of the translation start site was cloned in front of the reporter gene *LUCIFERASE* (*LUC*) and the construct stably transformed into *Arabidopsis thaliana* Columbia-0 (Col-0) (Supplemental Table 1 for cloning primers). *OGO* overexpressing plants were generated by amplifying the OGO full length coding sequence, insertion into the vector pK7FWG2 (Karimi et al., 2002), and transforming the construct into wild-type Arabidopsis Col-0 by floral dipping (Clough and Bent, 1998) (Supplemental Table 1 for cloning primers).

Plant growth and treatment

Seeds were sterilised, stratified for 48 h at 4°C in the dark and sown on Gamborg's B5 medium (PhytoTechnology, Austratec) supplemented with 2%(m/v) Sucrose, 3.21 g/L Gamborg's B5 salts (Austratec), 2 mM MES hydrate (Sigma-Aldrich), and 0.80% (w/v) Difco agar (BD Biosciences), pH 5.8, at 23°C under 100 µmol m^{-2} s^{-1} light in a 16-h/8-h light/dark photoperiod. For soil-based growth, all the lines were sown in a vermiculite, perlite and soil mixture (1:1:3). Plants were grown in growth chambers at 23°C, 65% relative humidity, under 100 µmol m^{-2} s^{-1} light in a 14-h/10-h light/dark photoperiod unless stated otherwise.

EMS mutagenesis and mutant screen

EMS mutagenesis and screening were performed as previously described (Ng et al., 2013a). Homozygous *OGO:LUC* seeds were mutagenized for 16 h in 100 mL 0.25% (v/v) ethyl methane sulfonate, then washed in water over 6 h. Seeds were sown on soil and grown in growth chambers at 23°C, 100 µmol m^{-2} s^{-1}, 16 h light/8 h dark. Seeds were harvested from 5000 M1 plants and approximately 10,000 M2 plants, representing10 pooled family populations were screened by luciferase imaging in the initial screen. Plants were grown for 14 days on Gamborg's B5 growth media and treated with 50 µM antimycin A + 0.01% Tween20 and returned to normal growth conditions. After 6 h, 2.5 mM luciferin (GoldBio) solution was applied to plants and luminescence was measured using bioluminescence

imaging system (Bio-Rad). 106 mutants that failed to induce luciferase expression were selected and grown to the next generation, in which 11 out of 106 mutants were confirmed. Furthermore, the mutant was backcrossed once to *OGO:LUC* and 30 progeny plants also failed to induce luciferase expression. Mutations were shortlisted only if pooled back-cross lines contained the same mutation with next generation sequencing.

Genomic DNA is isolated by DNeasy Plant Maxi kit (Qiagen 24) from 600mg – 1000 mg seedlings (more than 50 seedlings) in 14 days and precipitated, according to manufacturers' instruction. 20 µL of genomic DNA at 2.5 ng/µL (50 ng total) was used as input and libraries were generated using Nextera® DNA Library prep kits (Illumina). The quality of libraries was checked by Agilent bioanalyzer and quantified using Qubit (Invitrogen) before Next-Generation Sequencing on a NextSeq500 platform (Illumina) with a read-length of 84 bp. The raw data was processed on the Galaxy server (https://usegalaxy.org/). Reads for *OGO:LUC* and *rog* mutants were mapped to TAIR 10 reference genome with Bowtie2. Potential PCR duplicates were removed by RmDup tool and SNP calls were generated using bcftools and mpileup tool. Putative causative mutations were filtered on base call quality, mapping quality scores, their location in coding regions of genes and potential impact on protein function. Putative causative mutations were filtered on base call quality, mapping quality scores, their location in coding regions of genes and potential impact on protein function. For *rog2* mutant, 154 SNPs with G to A translations and 370 SNPs with C to T translations were called. For *rog4* mutant, 1161 SNPs with G to A translations and 640 SNPs were called. Only nonsense and missense mutations in coding regions and likely impacting protein function were retained leaving 5 putative candidate mutations for *rog2* mutant and 4 putative candidate mutations for *rog4* mutant. For these, T-DNA mutant lines were obtained to confirm regulation of OGO expression by the impacted mutated gene.

Phenotypic Analysis

Soil-based growth stage progression was performed according to (Boyes et al., 2001). Plant growth analysis and maximum quantum yield of photosystem II (Fv/Fm) determination was performed in a PlantScreen phenotyping system (Photon Systems Instruments, Czech Republic). For Fv/Fm measurements plants were dark adapted for 20 mins. Relative water content (RWC) was determined for whole rosettes. The fresh weight (FW) of the whole rosette was weighed followed by complete submergence in water for 24 hours at 4°C in darkness, and then the turgid weight (TW) was measured. Subsequently, the rosette was

dried at 65 °C for 48 hours with the dry weight (DW) measured. The RWC of samples were calculated using the equations: RWC = (FW-DW) / (TW-DW) x 100.

RNA extraction and Quantitative RT-PCR

RNA isolation, cDNA synthesis, and quantitative RT-PCR (qRT-PCR) were performed as described previously with minor modifications (Meng et al., 2019). Samples were grounding using a Tissue Lyser II (Qiagen) and total RNA was isolated using Spectrum™ Plant Total RNA Kit (Sigma-Aldrich) according to manufacturer's instruction. Genomic DNA was removed by on-column DNase treatment (Sigma-Aldrich) and 1 µg of total RNA was used for cDNA synthesis using Tetro cDNA synthesis kit (Bioline) according to manufacturer's instructions. Quantitative PCR were performed using QuantStudio 12K Flex Real-Time PCR System (Applied Biosystems) and SYBR Green PCR Master Mix (Thermo Fisher Scientific, USA), each reaction was independently done in triplicate. The reference genes were *UBIQUITIN-CONJUGATING ENZYME21 (AT5G25760)* (Czechowski et al., 2005). The gene specific primers were designed using QuantPrime (Arvidsson et al., 2008) and their sequence are provided in Supplemental Table 1.

Protoplast Preparation and Fluorescence Microscopy

The cDNAs for the coding regions of *OGO* was combined with pDONR 221 entry clone by BP reaction gateway cloning method, and entry clone was subsequently the combined into p2GWF7 destination vector by LR reaction (Invitrogen). Protoplasts were isolated from the true leaves of 4- week-old Arabidopsis grown in soil by plant Tape-Arabidopsis Sandwich methods.(Wu et al., 2009). A 20 µg of plasmids were transformed into 0.1 mL W5 solution with 2×10^5 cells / mL Protoplasts were incubated in 0.11 mL 40% PEG solution in the dark for 20 min. Protoplast were washed twice with 0.44 mL 40% PEG and incubated in 12-well plates at room temperature in dark for 12 h. Fluorescence were imaged with an LD C-Apochromat 40x/1.1 water or objective in multi-track channel and images were processed using ZEN 2.3 lite (blue edition, Carl Zeiss Microscopy).

Generation of *proOGO-GUS* lines and staining assay

The 1kb *OGO* promoter were amplified from Col-0 leaf DNA samples. The pGPTV-BAR vector was linearized by restriction enzyme HindIII, XbaI and combined with *OGO* promoter fragment using Gibson assembly method according to manufacturers' instruction (New England Biolabs®). The recombined vector was transformed into Arabidopsis thaliana Columbia-0 (Col-0) to generate *proOGO:GUS* lines and single insertion, homozygous lines were screened on 5 µg/mL BASTA Gamborg's B5 medium.

Tissues of transgenic plants expressing *proOGO::GUS* were infiltrated with 10 mM sodium phosphate (pH 7.2), 0.3% (v/v) Triton X-100 and 250 µg 5-bromo-4-chloro-3-indoxyl-b-D-glucuronide cyclohexylammonium salt (X-Gluc, GoldBio) solution and then incubated in darkness at 37°C for indicated times (Jefferson et al., 1987). Samples were destained with 70% ethanol and images were collected on Carl Zeiss microscope (Axiocam) or one a flatbed scanner (Microtek Artix 3200XL).

CHIP-qPCR

For ANAC017 ChIP-qPCR, the 2-kb OGO promoter ANAC017 (*proANAC017*) region upstream of the translation start site was cloned into the vector pDONR™ P4-P1r (Invitrogen). GFP-Linker was cloned into pDONR221 (Invitrogen), the ORF of ANAC017 without start codon was amplified by PCR from Arabidopsis Col-0 cDNA and cloned into pDONR P2r-P3 (Invitrogen). Three entry vectors were recombined into the Multisite destination vector pK7m34GW to generate final construct proANAC017: GFP-ANAC017 using Gateway technology according to the manufacturer's instructions (Invitrogen). The construct was stably transformed into Arabidopsis thaliana Columbia-0 (Col-0) to generate *ProANAC017: GFP-ANAC017* transgenic lines and single insertion homozygous line was obtained by screening on 35 µg/mL Kanamycin Gamborg's B5 medium. Subsequently, independent representative lines with consistent expression patterns were identified. The *proEIN3: EIN3-Ypet* line was kindly provided by Dr Mathew Lewsey (unpublished).

The ChIP experiments were performed as described with minor modifications (Bowler et al., 2004; De Clercq et al., 2013). *ProANAC017: GFP-ANAC017* or *proEIN3: EIN3-Ypet* were grown for 12 days on B5 medium in plates. Seedings were spray-treated with indicated concentrations of antimycin A (AA) + 0.01% Tween20, myxothiazol + 0.01% Tween20, ACC + 0.01% Tween20 or 0.01% Tween20 as mock for 3 h. Approximately 2 g of the whole seedlings was harvested, rinsed twice with 10mM HEPES-NaOH and cross-linked with 1% (v/v) formaldehyde in a vacuum for 20 min. A final concentration of 0.134 M glycine (Sigma-Aldrich) and vacuum were applied for 2 min. The chromatin DNA was isolated and fragmented by sonication with a Bioruptor chiller sonicator (Diagenode) at 4°C, resulting in fragments of 500 bp at average. The chromatin DNA was precleared with 80 µL Dynal Protein A magnetic beads (10001D, Thermo Fisher Scientific) for at least 2 h at 4ºC with gentle agitation. 70 µL diluted samples (1% input sample) was used as input chromatin controls after pre-clearing. The remainder was split into two samples and immunoprecipitated by 5 µL anti-GFP antibody (10 µg antiGFP, Thermo Fisher Scientific A11122 (2 µg/µL)) coupled to 50 µL Dynal Protein A magnetic beads and the other without antibody. The samples were incubated overnight on rotating platform at 4°C. Proteins were

reverse cross-linked and DNA was purified by column method using PCR Purification Kit according to the manufacture (Qiagen).

Quantitative PCR were performed using QuantStudio 12K Flex Real-Time PCR System (Applied Biosystems) and SYBR Green PCR Master Mix, each reaction was independently done in triplicate. Data were normalized against its respective amount of chromatin used in the INPUT and were represented in %INPUT (%IP).

Accessions

Sequence data from this article can be found in the Arabidopsis Genome Initiative or GenBank/EMBL databases under the following accession numbers: *OGO* (At5g43450), *AOX1a* (At3g22370), *RAO2/ANAC017* (At1g34190), *UBC21* (AT5G25760), *ACT2* (AT3G18780) *OM66* (AT3G50930), *GLTP* (AT4G39670), *UGT73B3* (AT4G34131), *HSP23.6* (AT4G25200), *HSP17.6B* (AT2G29500), *HSP17.6C* (AT1G53540), *HSP26.5* (AT1G52560), *SIN3/ROG2* (AT1G24190), *ROG4* (AT2G36720), *EIN3* (AT3G20770), *HRE2/ERF71* (AT2G47520).

FIGURES

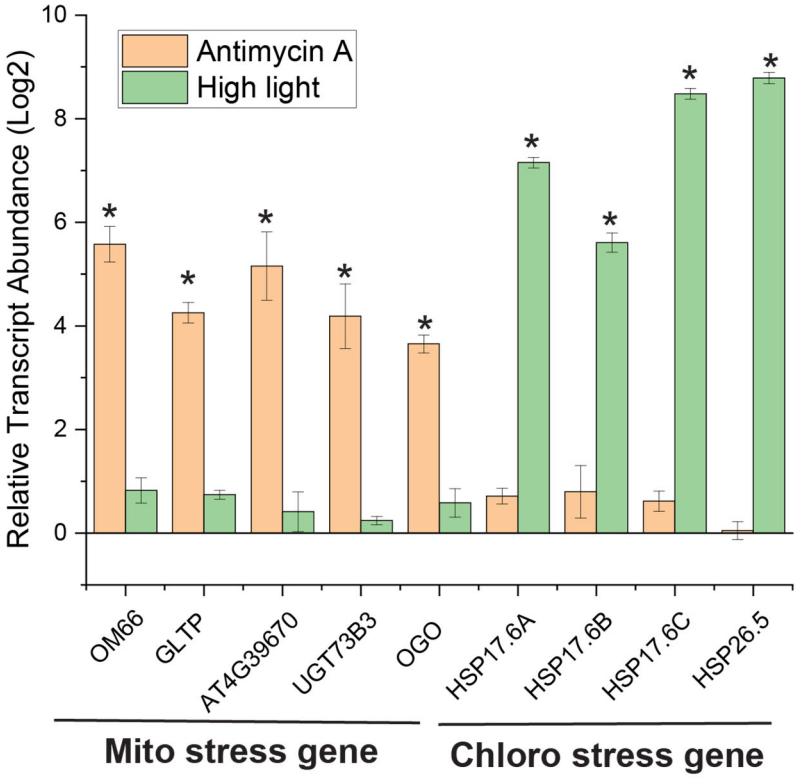

Figure 1. Mitochondrial stress-specific induction of a *2-oxoglutarate and Fe(II)-dependent oxygenase* (*OGO*, *AT5G43450*)

2-oxoglutarate and Fe(II)-dependent oxygenase (*OGO, AT5G43450*) is specifically induced by perturbation of mitochondrial function (antimycin A treatment) but not chloroplast dysfunction (high light treatment). The bar chart represents the relative transcript abundance for *OUTER MITOCHONDRIAL MEMBRANE PROTEIN OF 66 KDa* (*OM66*, *At3G50930*), *AT1G76600*, *GLYCOLIPID TRANSFER PROTEIN* (*GLTP*, *AT4G39670*), *UDP-GLUCOSYL TRANSFERASE 73B3* (*UGT73B3*, *AT4G34131*), a *2-oxoglutarate and Fe(II)-dependent oxygenase* (*OGO*, *AT5G43450*), *HEAT SHOCK PROTEIN 17.6A* (*HSP17.6A*, *AT1G59860*), *HEAT SHOCK PROTEIN 17.6B* (*HSP17.6B*, *AT2G29500*), *HEAT SHOCK PROTEIN 17.6C* (*HSP17.6C*, *AT1G53540*) and *HEAT SHOCK PROTEIN 26.5* (*HSP26.5*, *AT1G52560*). Shown are the means ± SE of the log2 (fold changes) for a comparison of treatment versus control of three biological replicates, with asterisks indicating a statistically significant difference (Student's t-test, $P < 0.001$). Publicly available gene expression data (antimycin A: Dataset ID AT-00561; high light: Data set ID AT-00682) were retrieved using the Genevestigator platform (Hruz et al., 2008).

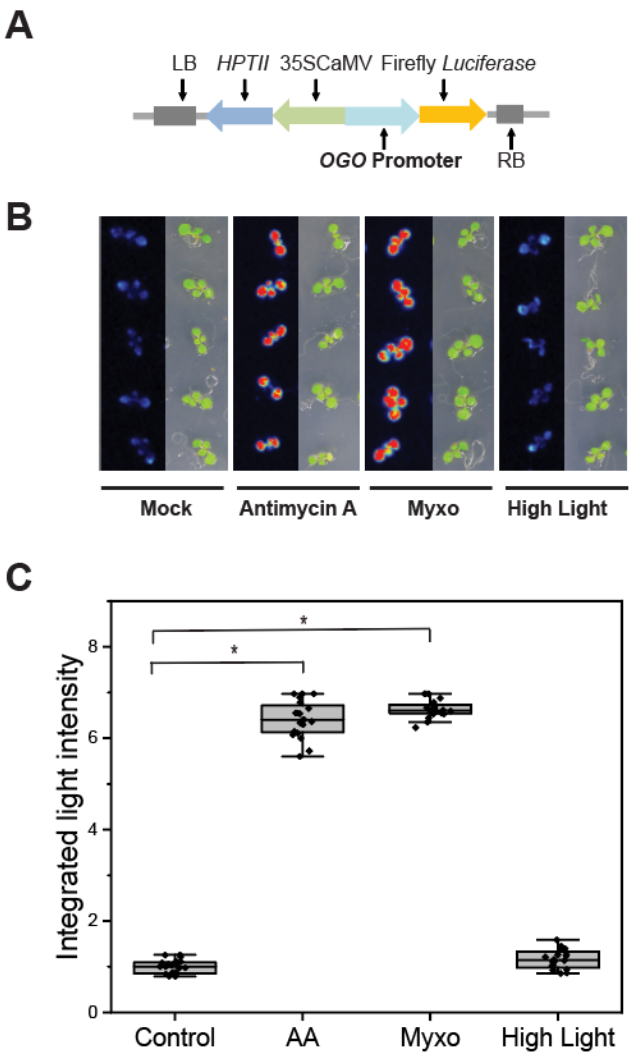

Figure 2. Non-invasive monitoring of *OGO* expression by bioluminescence in a luciferase reporter line

A) A schematic diagram for the construct used to generate reporter lines for the *2-oxoglutarate (2-OG) and Fe(II)-dependent oxygenase OGO* (*AT5G43450*) promoter driving the expression of a luciferase reporter gene (*OGO:LUC*). The *OGO* promoter consists of the region 1102 bp upstream of the translational start site of *OGO* including the *OGO* 5'UTR. LB, T-DNA left border sequences; RB, T-DNA right border sequences. HPTII, hygromycin phosphotransferase II; 35S CaMV, 35S Cauliflower mosaic virus promoter; Firefly Luciferase. B) Twelve-day-old seedlings of *OGO:LUC* were sprayed with water (mock treatment), 50 µM antimycin A (AA), 50 µM myxothiazol (myxo) or exposed to 1000 µmol m^{-2} s^{-1} light to inhibit mitochondrial function (AA and myxo) and perturb chloroplast function (high light). After 3 h, Luciferin (2.5 mM) was applied and the LUC reporter activity was visualized in a Bio-rad ChemiDocTM MP imager after 6 h of treatment. Red colour of seedlings indicates saturating bioluminescence as a consequence of highly induced LUC expression. C) The processed images were analyzed for quantification of LUC expression using the Image Lab software 6.0. Error bars denote ± SE of three biological replicates with 5-7 seedlings pooled from one plate for each replicate. Significant differences were identified by one-way ANOVA followed by Tukey's multiple comparison test and indicated with an asterisk (*, P< 0.001).

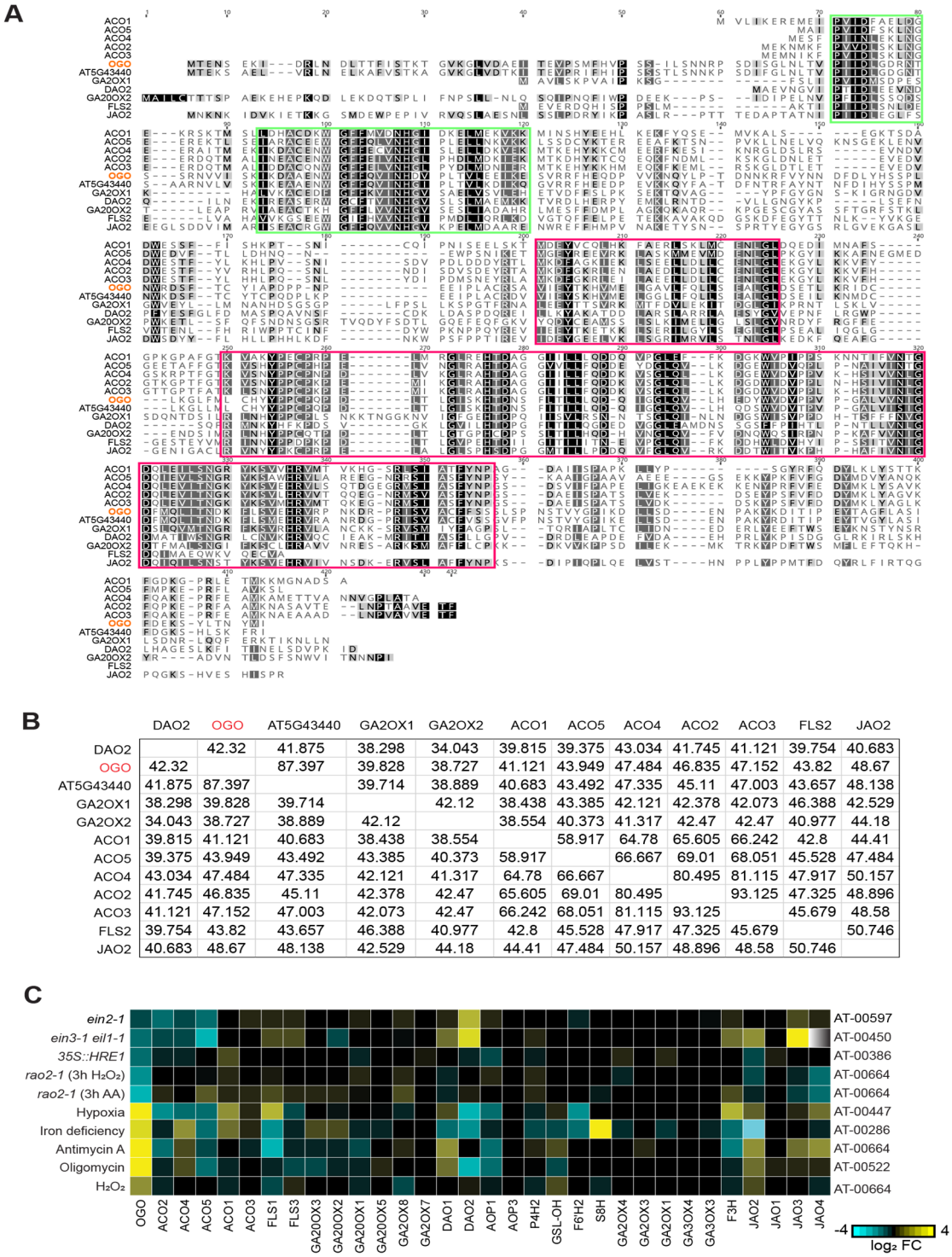

Figure 3. Phylogenetic analysis of the 2-oxoglutarate and Fe(II)-dependent oxygenase protein family in *Arabidopsis thaliana*

A. Protein sequence alignment for selected members of the 2-oxoglutarate and Fe(II)-dependent oxygenase protein family in Arabidopsis. Included are the five 1-aminocyclopropane-1-carboxylic acid oxidase (ACO) isoforms, OGO (AT5G43450), a protein with the highest sequence similarity to OGO in Arabidopsis (AT5G43440), two proteins involved in gibberellic acid synthesis (GA2OX1, GA20OX2), the auxin oxidase DIOXYGENASE FOR AUXIN OXIDATION 1 (DAO2), FLAVONOL SYNTHASE 2 (FLS2) and JASMONIC ACID OXIDASE 2 (JAO2). Shading of amino acids indicates their similarity across the proteins. Green and red boxes indicated the conserved 2-oxoglutarate binding and the oxygenase domains, respectively. B. Protein similarities (based on the blossom 90 matrix) for selected members of the 2-oxoglutarate and Fe(II)-dependent oxygenase protein family in Arabidopsis C. Heatmap showing expression of *OGO*-related genes in various experiments involving oxidative stress (H_2O_2), mitochondrial stress (antimycin A, oligomycin), mitochondrial retrograde signalling mutants (*rao2-1*), hypoxia or ethylene-related mutants (*35S-HRE1*, *ein3-1 eil1* and *ein2-1*). Publicly available gene expression data was retrieved using the Genevestigator platform (Hruz et al., 2008) and data set IDs are indicated on the right.

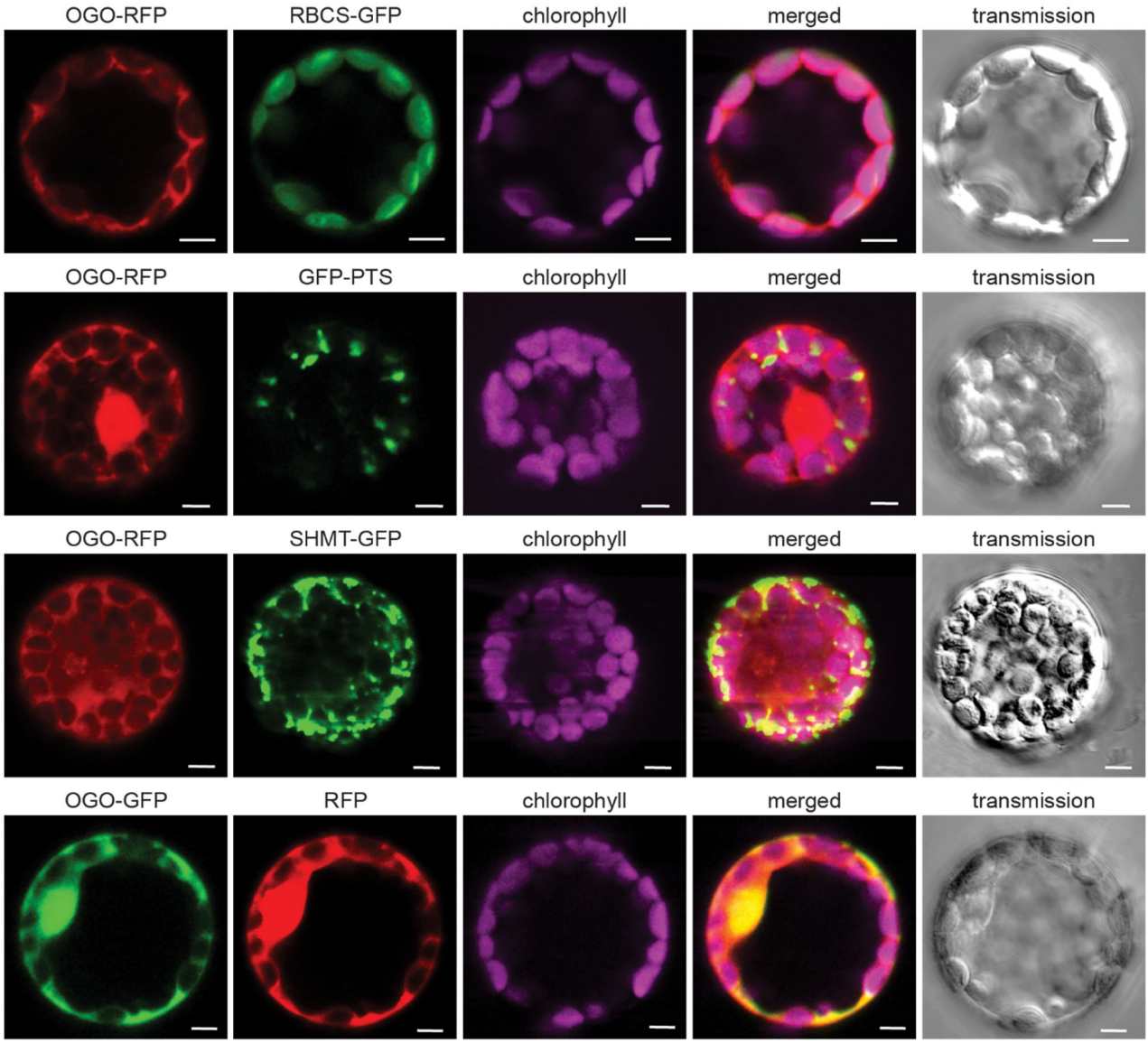

Figure 4. Cytosolic localization of 2-oxoglutarate and Fe(II)-dependent oxygenase (OGO)
The OGO protein was tagged with the fluorescent RFP or GFP protein at the C-terminus and expressed under the control of the cauliflower mosaic virus 35S promoter to assess the subcellar localization. Constructs were co-transformed into Arabidopsis protoplast together with control constructs for peroxisomal localisation (*GFP-PTS*), mitochondrial localisation (*SHMT-GFP*) and chloroplast localisation (*RBCS-GFP*) (Wachter et al., 2005). Shown are representative images after confocal laser scanning microscopy for three channels (GFP, RFP, chlorophyll), their merged images and for transmission. Scale bar indicates 5µm.

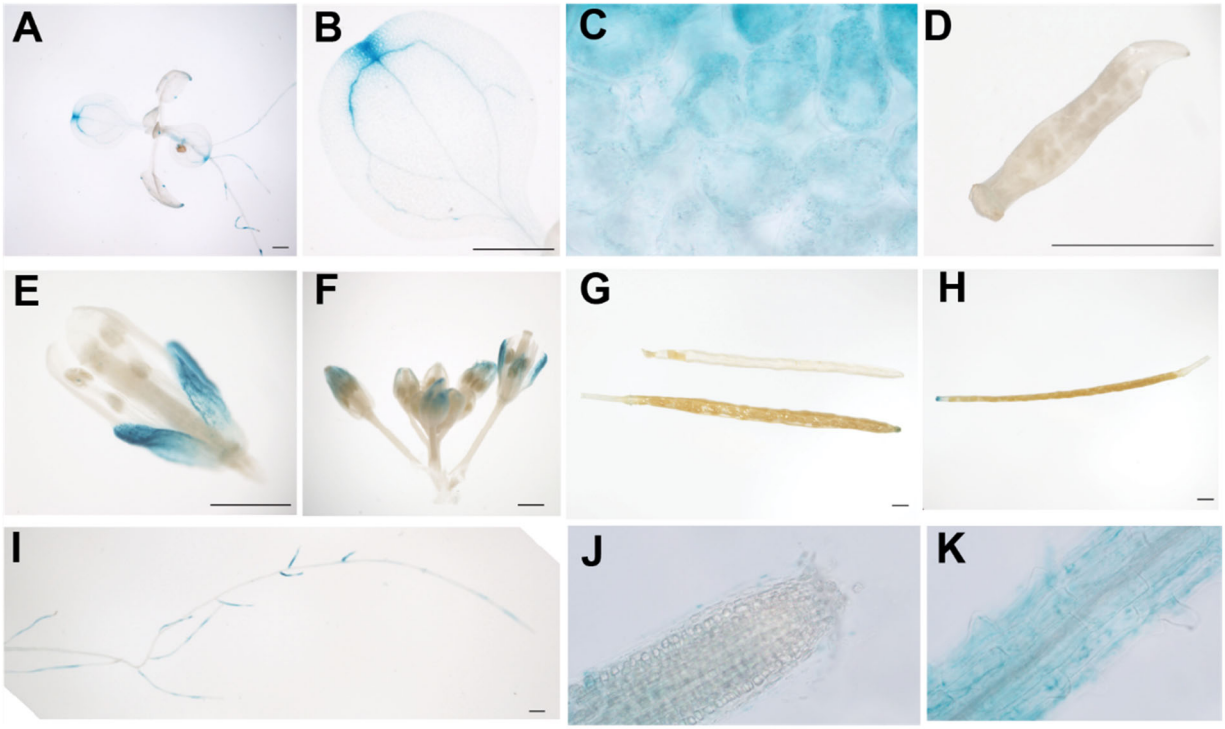

Figure 5. Expression of *2-oxoglutarate and Fe(II)-dependent oxygenase* (*OGO*) in different tissues and developmental stages

OGO expression was determined in various tissues of transgenic Arabidopsis plants harbouring a *proOGO-GUS* construct. Plant were visualised after infiltration with Xgluc staining solution, 12 h incubation at 37°C and subsequent removal of chlorophyll (see methods for details). A. Twelve-day-old whole seedling. B. Leaf of a twelve-day-old seedling. C. Twelve-day-old seedling leaf tip mesophyll cells. D. Ovary. E. Flower. F. Inflorescence. G and H. Silique. I. Twelve-day-old seedling root. J. Root tip. K Root mature zone. Scale bar = 1 mm.

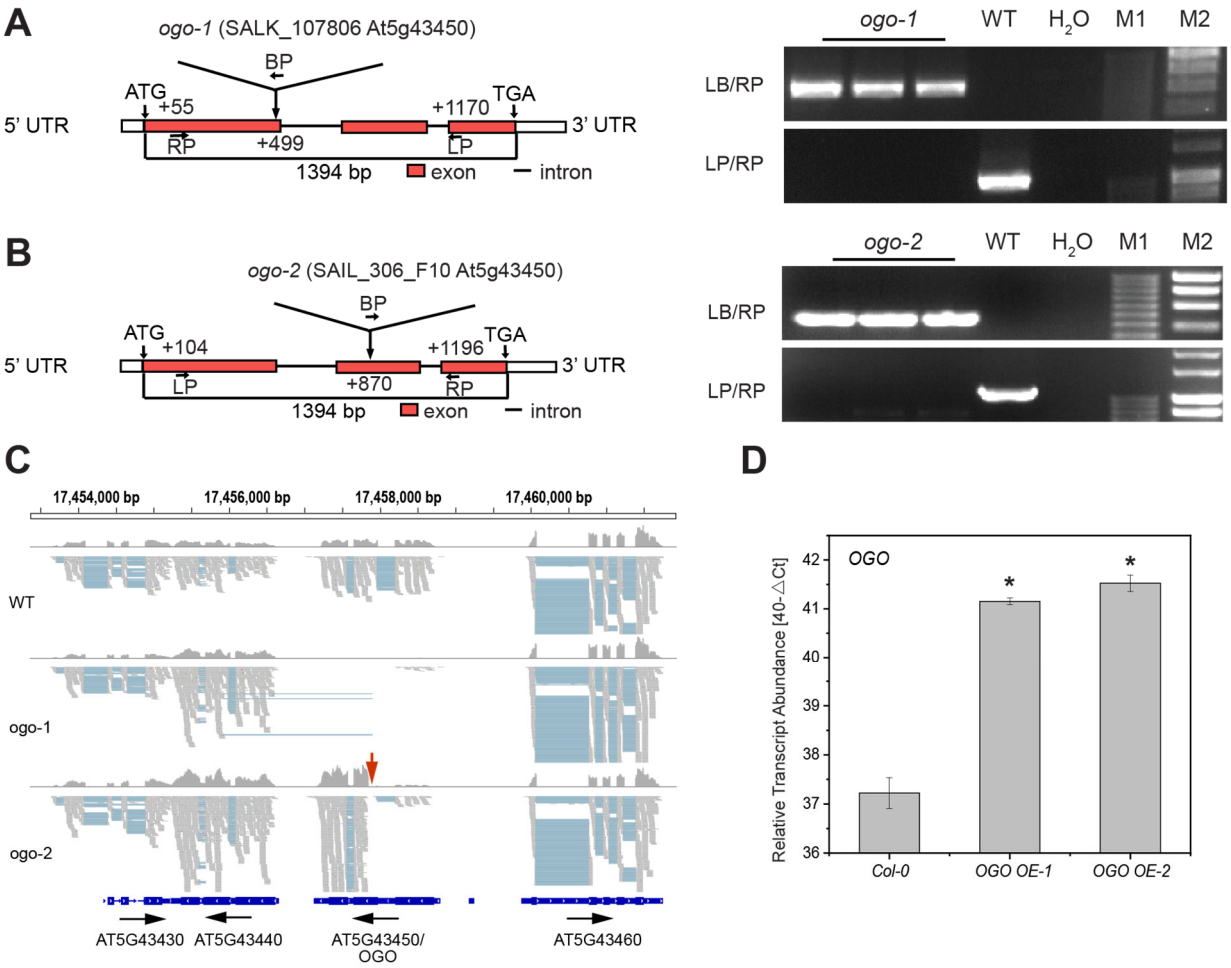

Figure 6. Characterization of mutant and overexpression lines for *2-oxoglutarate and Fe(II)-dependent oxygenase* (*OGO*)

Characterisation of *ogo-1* and *ogo-2* mutant and overexpression lines (*OGO OE-1*, *OGO OE-2*) for the 2-oxoglutarate and Fe(II)-dependent oxygenase (*OGO*). A,B) The left panels show a schematic representation of T-DNA integration in the two mutant lines. The right panels show confirmation by PCR analysis of genomic DNA. For each *ogo* line three plants were analysed. WT: wild type, M1: DNA ladder (100 bp), M2: DNA ladder (1000 bp). C) Genome browser view of RNA-seq reads around the OGO locus for wild type, *ogo-1* and *ogo-2*. For *ogo-2* the red arrow highlights a break in the read alignments around the T-DNA insertion site, indicating no functional transcript is being made in this mutant line. D) Expression of the *OGO* gene in the two overexpression lines *OGO OE-1* and *OGO OE-2* was determined by qRT-PCR with the relative transcript abundance given as 40-ΔCt values (Bari et al., 2006). Both lines have approximately 16-fold higher OGO expression than the wild type. Given are means ± SE of three biological replicates with asterisks indicating a statistically significant difference by one-way ANOVA followed by Tukey's multiple comparison test (*, $P < 0.001$).

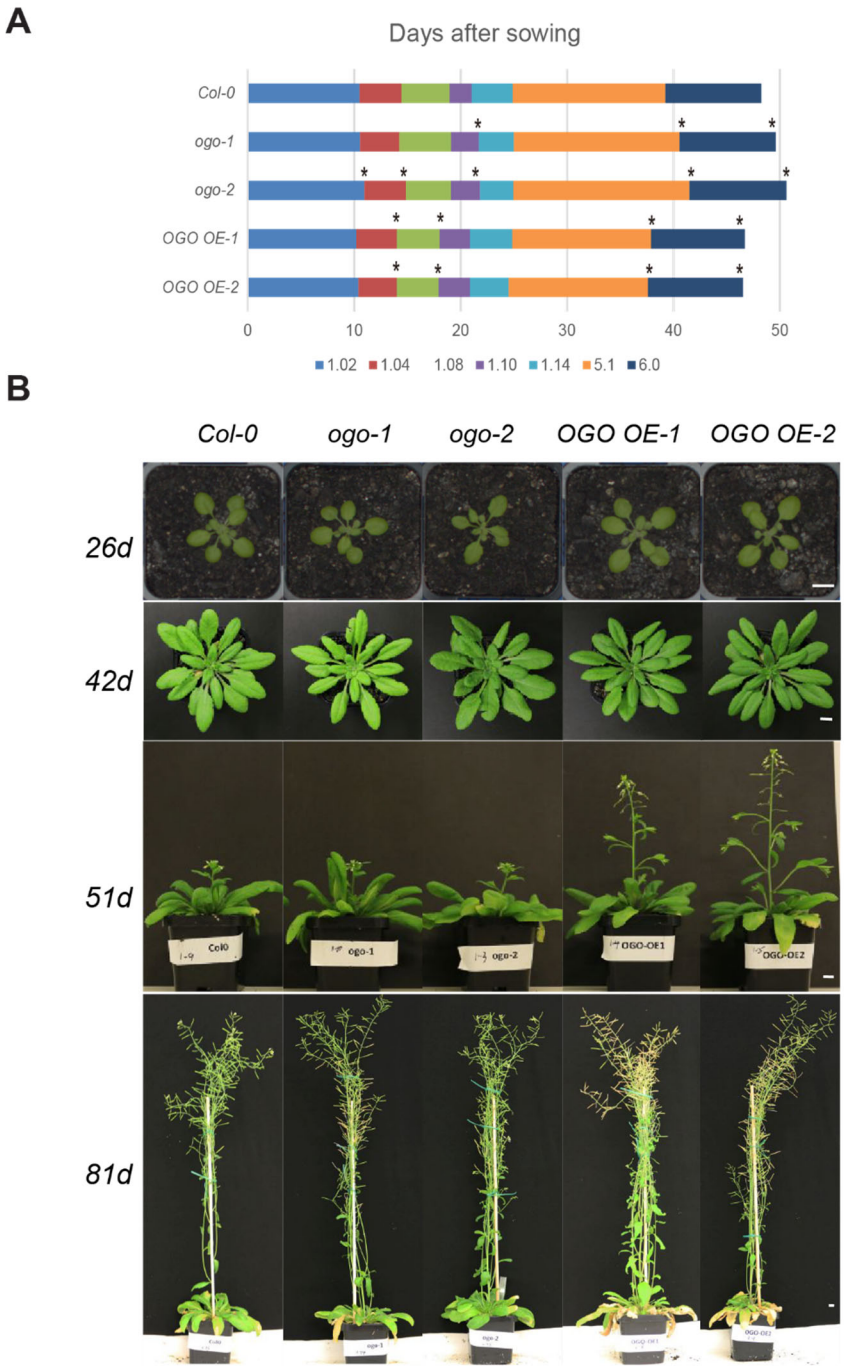

Figure 7. Phenotypic characterization of mutant and overexpression lines for *2-oxoglutarate and Fe(II)-dependent oxygenase* (*OGO*)

A. Soil-based growth stage progression in the 5 analyzed genotypes according to (Boyes et al., 2001). Stage 1.02 (2 rosette leaves >1 mm in length), stage 1.04 (4 rosette leaves >1 mm in length), stage 1.08 (8 rosette leaves >1 mm in length), stage 1.10 (10 rosette leaves >1 mm in length), stage 1.14 (14 rosette leaves >1 mm in length), stage 5.1, first flower buds visible, stage 6.0, First flower open. Significant differences were identified by one-way ANOVA followed by Tukey's multiple comparison test and indicated with an asterisk (*, P< 0.05). B) Representative images are shown for wild type (Col-0), OGO mutant plants (*ogo-1*, *ogo-2*) and over-expressing lines (*OGO OE-1*, *OGO OE-2*) grown on soil in a 14-h-light/10-h-dark cycle. At least 20 plants per genotype were used for phenotypic analysis. Bar = 1 cm. Days are relative to the day of sowing after a 3 day stratification at 4°C.

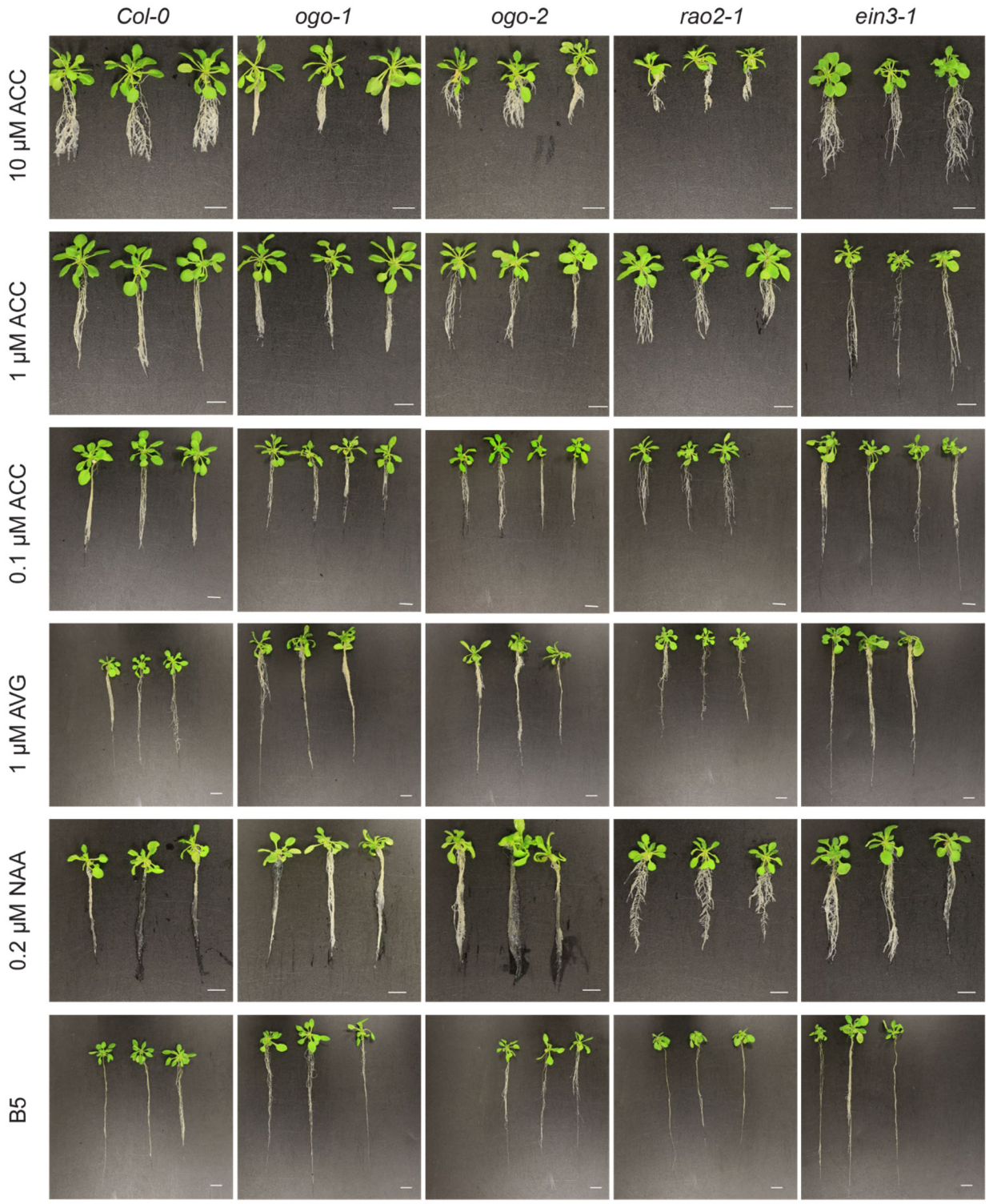

Figure 8. Phenotypic effects of exogenous application of 1-aminocyclopropane-1-carboxylic acid (ACC), aminoethoxyvinylglycine (AVG) and1-naphthylacetic acid (NAA) on OGO mutants, *rao2-1* and *ein3-1* root growth

Seeds of wild type, OGO mutants (*ogo-1*, *ogo-2*), *rao2-1* (*ANAC017* EMS mutant), *ein3-1* (*ETHYLENE INSENITVE 3* mutant) were germinated on B5 medium until primary root length around 2 cm and then transferred to new medium either supplemented or not supplemented with ACC (1-aminocyclopropane-1-carboxylic acid), AVG (aminoethoxyvinylglycine) and NAA (1-naphthylacetic acid). Representative plants were imaged at indicated time points and supplement concentrations. Bar = 1 cm.

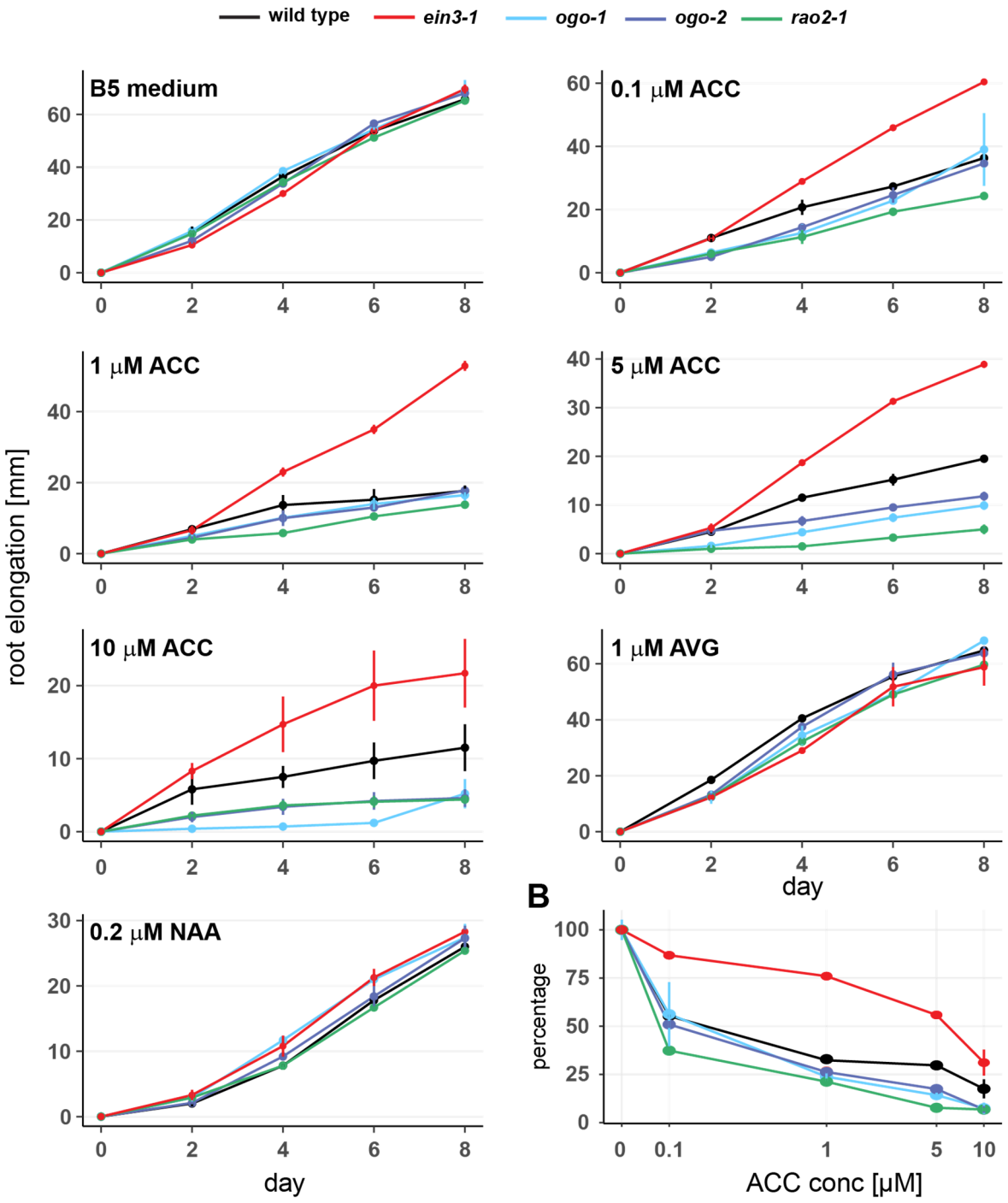

Figure 9. Quantitative effect of exogenous application of 1-aminocyclopropane-1-carboxylic acid (ACC), Aminoethoxyvinylglycine (AVG) and1-naphthylacetic acid (NAA) on *OGO* mutants, *rao2-1* and *ein3-1* root elongation

Seeds of wild type, OGO mutants (*ogo-1*, *ogo-2*), *rao2-1* (ANAC017 EMS mutant), *ein3-1* (*ETHYLENE INSENITVE 3* mutant) were germinated on B5 medium until primary root length around 2 cm and then transferred to new medium either supplemented or not supplemented with ACC (1-aminocyclopropane-1-carboxylic acid), AVG (aminoethoxyvinylglycine) and NAA (1-naphthylacetic acid) at indicated concentrations (see also Figure 8). A. Root elongation after transfer was measured over 8 days. B. Relative root elongation in % of the control treatment (unsupplemented B5 medium). Error bars denote ± SE of three biological replicates with 3-5 seedlings from one plate for each replicate.

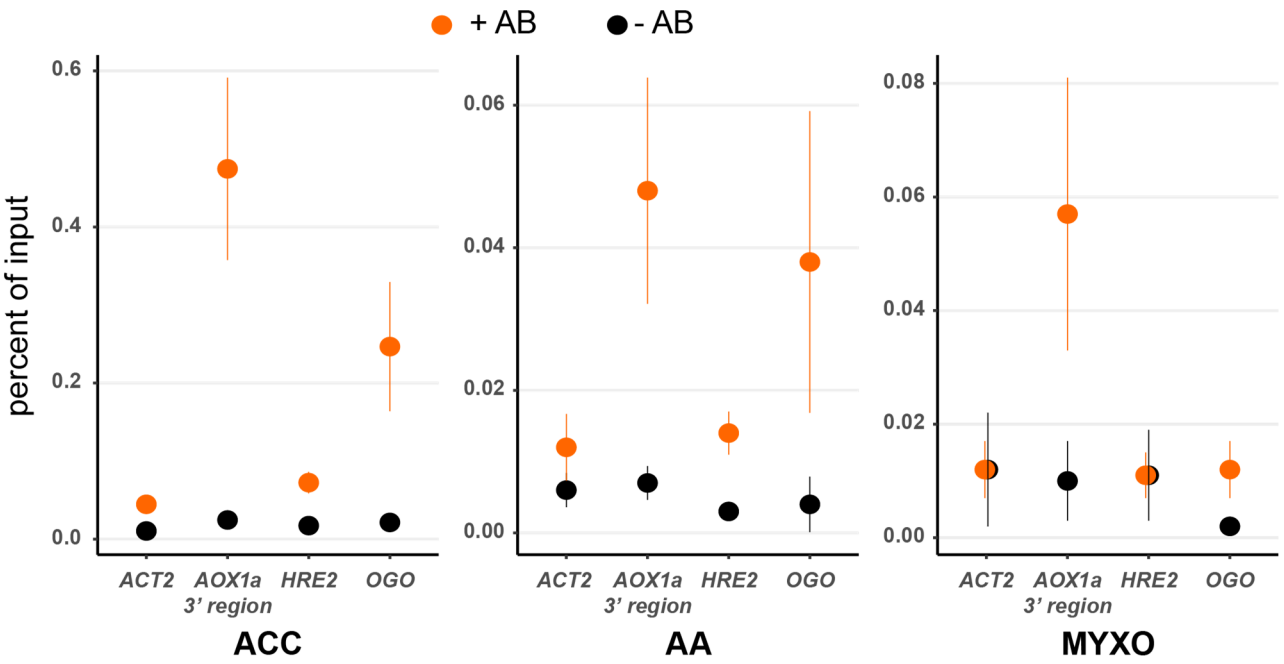

Figure 10. ETHYLENE INSENSITIVE 3 (EIN3) is targeting to mitochondria-related genes
The binding of EIN3 to the promoters of *ACT2*, *HRE2*, *OGO* and the region 300 bp downstream of *AOX1a* gene was determined by ChIP-qPCR analysis on plants treated with either 100 µM 1-aminocyclopropane-1-carboxylic acid (ACC), 50 µM antimycin A (AA) and 50 µM Myxothiazol (myxo). Shown is the enrichment (in percent of input) after ChIP-qPCR using *proEIN3-EIN3-Ypet* seedlings in the presence (+AB) or absence (-AB) of anti-GFP antibodies. ACTIN2 fragments were used as negative controls. Shown are means ± SE of three biological replicates.

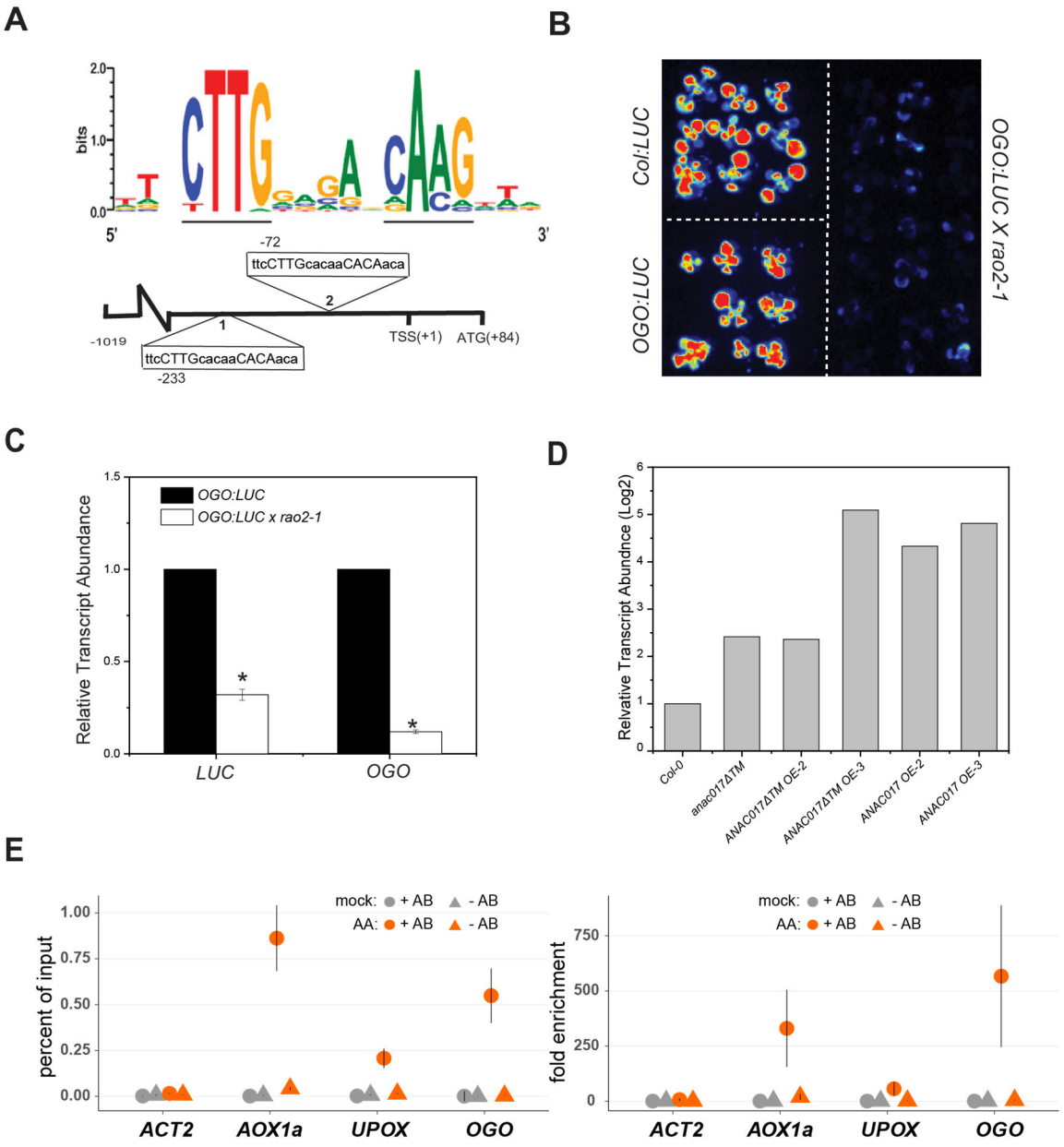

Figure 11. ANAC017 is a positive regulator of *2-oxoglutarate and Fe(II)-dependent oxygenase* (*OGO*)
A. Position weight matrix for the mitochondrial dysfunction motif (MDM) which is the binding motif for ANAC017 (De Clercq et al., 2013). ii) Schematic diagram of two identified MDMs in the *OGO* promoter. TSS, transcriptional start site. B. Two reporter lines expressing the luciferase gene under the control of the *AOX1a* (*Col:LUC*) and *OGO* (*OGO:LUC*) promoter, respectively, were grown on B5 plates and sprayed with 50 µM antimycin A (AA) . Subsequently Luciferin was applied and LUC reporter activity was visualized in Biorad bioluminescence imager 6 h post treatment. Both reporter lines show the expected strong induction of LUC expression in response to the activation of the mitochondrial retrograde response by AA. For the progeny (*OGO:LUC* x *rao2-1*) of a cross of the *OGO:LUC* reporter line and a mutant line of ANAC017 (*rao2-1*) no induction of LUC activity was detectable, indicating a regulation of *OGO* by ANAC017. C. *LUC* and *OGO* transcript abundance determined by qRT- PCR in twelves-day old seedlings of *OGO:LUC* and *rao2-1* lines sprayed with mock (deionized water) or 50 µM AA. Relative transcript abundance (fold changes) in mock- and AA-treated plants determined by qRT-PCR are shown. For three biological replicates the significant differences were identified by one-way ANOVA followed by Tukey's multiple comparison test and indicated with an asterisk (*, P< 0.001). D. *OGO* transcript abundance in transgenic lines (over)expressing a constitutively active form of ANAC017 lacking the transmembrane domain (ΔTM / ΔTM OE-2 and ΔTM OE-3) or a full-length ANAC017 (OE-2, OE-3). Data was extracted from a previous publication (Meng et al., 2019). E. Binding of ANAC017 to the promoters of three MDS genes (*AOX1a, UPOX, OGO*) and *ACTIN2* as negative control was analysed in transgenic lines expressing a GFP-ANAC017 fusion protein under the control of the native ANAC017 promoter (*proANAC017-GFP-ANAC017*). Twelve-day old seedlings of *proANAC017-GFP-ANAC017* line sprayed with mock (deionized water) or 50 µM AA for 3 h. ChIP-qPCR targeted the predicted MDM in the promoters of the analysed genes in the presence (+AB) or absence (-AB) of anti-GFP antibody. Increased binding of ANAC017 after AA treatment when compared to mock treatment is expressed as percentage of DNA input (left panel) and fold enrichment (right panel). Values shown are means ± SE determined for three biological replicates.

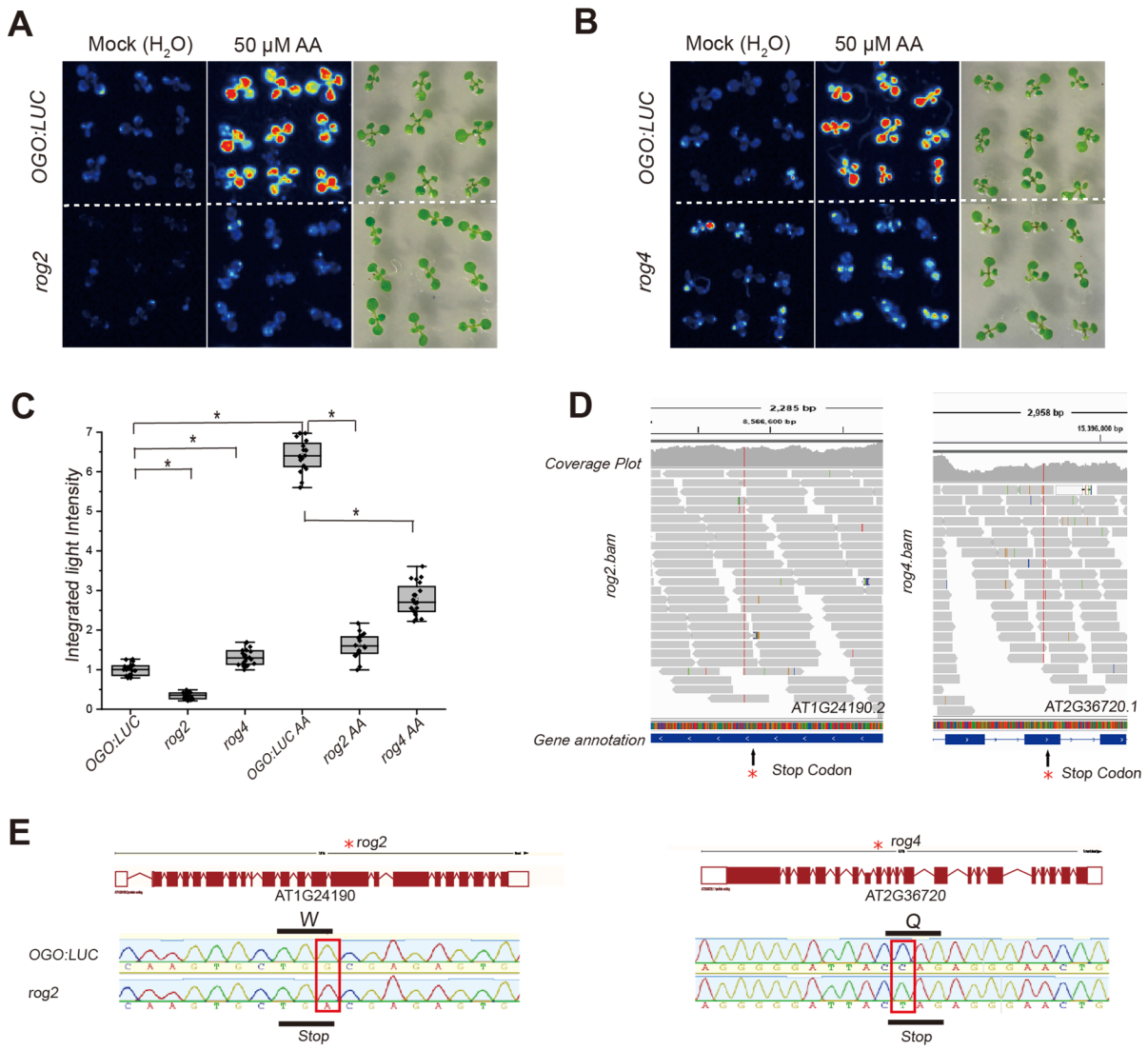

Figure 12. Identification of ROG2 and ROG4 as regulators of *2-oxoglutarate and Fe(II)-dependent oxygenase* (*OGO*)

A. Twelve-day-old seedlings of *OGO:LUC* and *rog2* (*regulator of OGO 2*) were sprayed with or Mock (H_2O) 50 µM antimycin A (+AA) to elicit a mitochondrial retrograde response. Luciferin (2.5 mM) was applied and the LUC reporter activity was visualized in a Bio-rad ChemiDocTM MP imager after 6 h of AA treatment. B. Twelve-day-old seedlings of *OGO:LUC* and *rog4* (*regulator of OGO 4*) were sprayed with or Mock (H_2O) 50 µM antimycin A (+AA) to elicit a mitochondrial retrograde response. Luciferin (2.5 mM) was applied and the LUC reporter activity was visualized in a Bio-rad ChemiDocTM MP imager after 6 h of AA treatment. C. The processed images were analyzed for quantification of LUC expression using the Image Lab software 6.0. Error bars denote means ± S.E of three biological replicates with 5-7 seedlings pooled from one plate for each replicate. Significant differences were identified by one-way ANOVA followed by Tukey's multiple comparison test and indicated with an asterisk (*, P< 0.001). D. Next generation sequence analysis identifying a candidate mutation in *SIN3* (*AT1G24190*) for *rog2* and a gene annotated as an acyl-CoA N-acyltransferase (*ROG4*, *AT2G36720*) for rog4. E. Sanger sequence chromatographs confirming a nucleotide change of G to A within the At1g24190 locus and C to T within AT2G36720, which both leading to a stop codon. The asterisks denote the position of the mutation in the two genes.

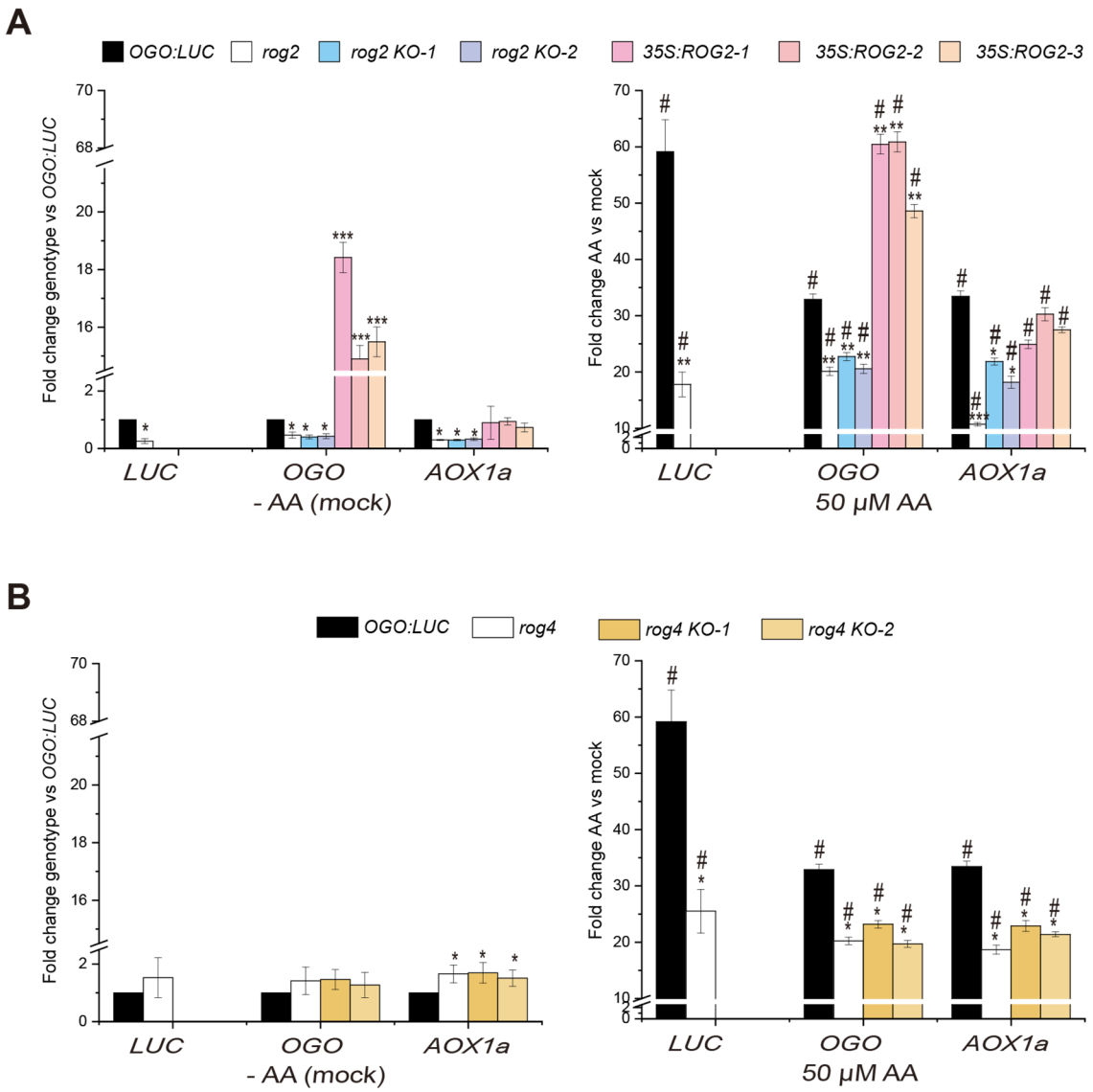

Figure 13. Confirmation of ROG2 and ROG4 as regulators of *2-oxoglutarate and Fe(II)-dependent oxygenase* (*OGO*)

A. Determination of *LUC*, *OGO* and *AOX1a* transcript abundance in *rog2*, two *ROG2/SIN3* T-DNA insertion lines (*rog2 KO-1* and *rog2 KO-2*) and three independent overexpressing lines (*35S:ROG2-1*, *35S:ROG2-2*, *35S:ROG2-3*). *Luciferase* (*LUC*), *OGO* and *AOX1a* transcript abundance under Mock (i) and 50 µM antimycin A (ii) treatment was quantified by qRT-PCR. Twelve-day-old seedlings were exposed to mock (H2O) or 50 µM antimycin A (+AA) and were harvested at 3 h. B. Characterization of *LUC*, *OGO* and *AOX1a* transcript abundance in *rog4*, and T-DNA insertion lines (*rog4 KO-1* and *rog4 KO-2*) for the *ROG4* (*At2G36720*) gene encoding an acyl-CoA N-acyltransferase. *Luciferase* (*LUC*), *OGO* and *AOX1a* transcript abundance under mock and 50 µM antimycin A (given are fold changes compared to *OGO:LUC* under mock condition) treatment. Twelve-day-old seedlings were exposed to mock (water) or antimycin A (+AA) and were harvested at 3 h and transcript abundance analyzed by qRT-PCR. Bars charts in A) and B) represent the means ± SE of three to four biological replicates and asterisks indicate a significant difference of *LUC*, *OGO* or *AOX1a* transcript abundance between *OGO:LUC* and the other genotypes in mock or AA treatments (*, P< 0.05; **, P< 0.01; ***, P< 0.001). Hashes indicate a statistically significant difference of *LUC*, *OGO* or *AOX1a* transcript abundance between mock and AA treatments ($^{\#}$, P< 0.001). Significant differences were identified by one-way ANOVA followed by Tukey's multiple comparison test.

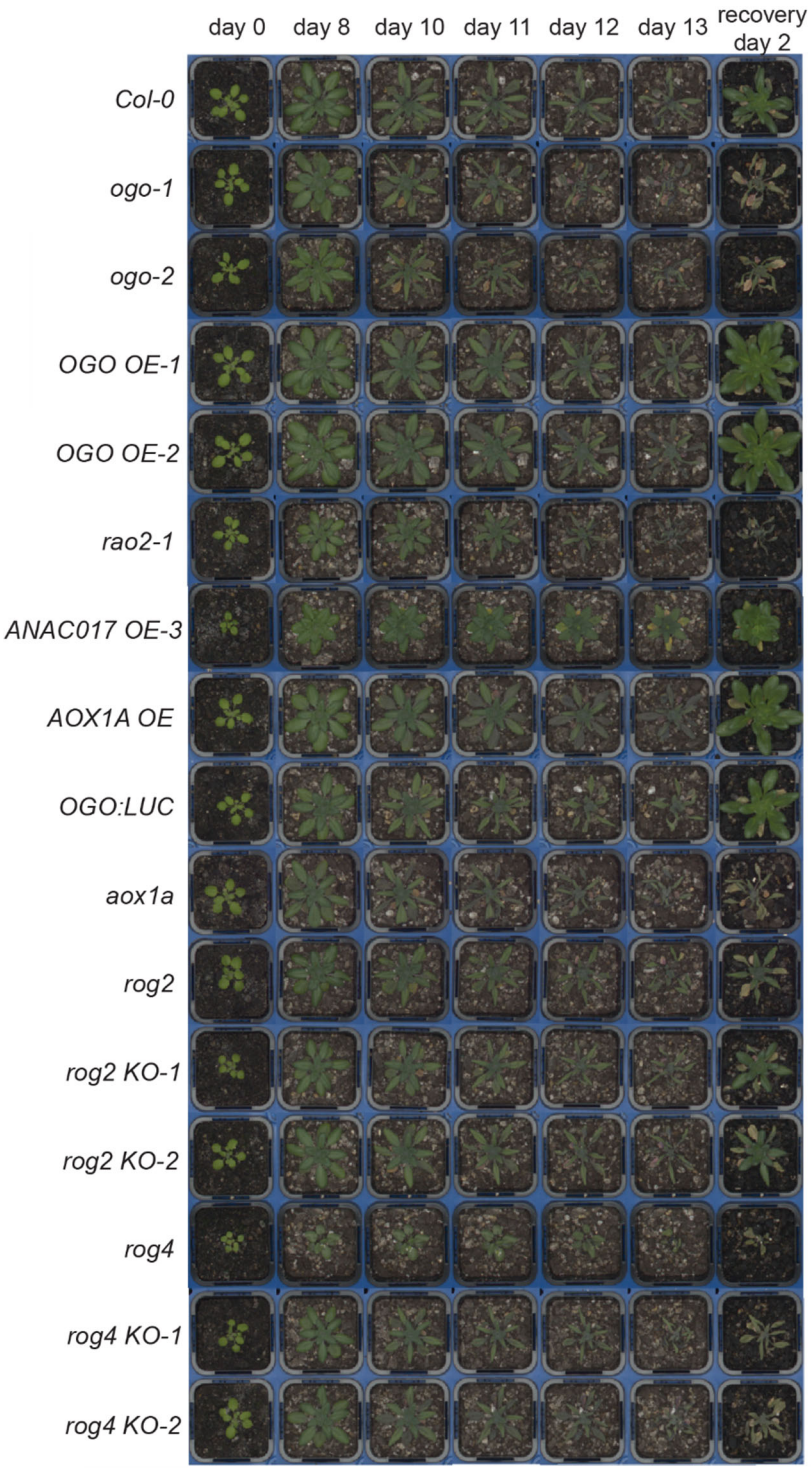

Figure 14. Phenotypes of mutant and overexpressing lines for genes involved in mitochondrial stress signalling under combined drought and moderate light stress

Wild-type (Col-0), loss of function *OGO* mutants (*ogo-1*, *ogo-2*), OGO overexpressing lines (*OGO OE-1*, *OGO OE-2*), *rao2-1* (*ANAC017* EMS mutant), ANAC017 overexpressing line (*ANAC17 OE-3*), AOX1a overexpressing line *AOX1A OE*, *OGO:LUC*, *aox1a*, *rog2* mutant, T-DNA insertion lines *rog2 KO-1* and *rog2 KO-2*, *rog4* mutant, and T-DNA insertion lines *rog4 KO-1* and *rog4 KO-2* were grown under normal conditions (14 h at 120 µmol m-2 s-1 light/10 h dark, 22°C dark) for 26 d. For the drought and moderate light (DML) treatment plants were then transferred to 400 µmol m^{-2} s^{-1} 14h light/10 h dark and water was withheld for 13 days followed by rewatering and return to standard growth conditions for another 3 days to recover. Plants were imaged in a PlantScreen phenotyping platforms (PSI, Czech Republic) at different time points as indicated and one representative plant is shown for each timepoint. See Figure 15 for quantitative parameters.

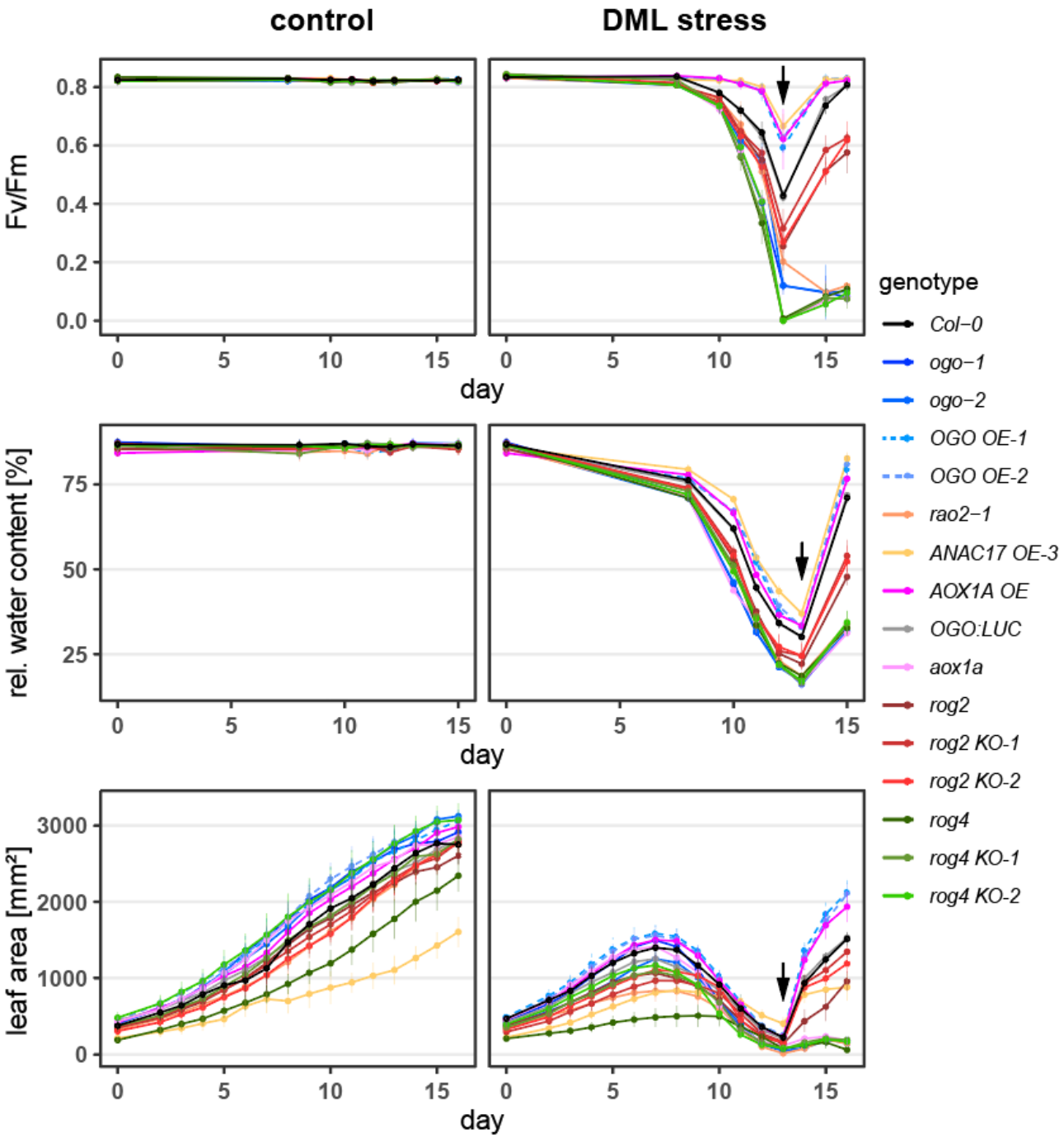

Figure 15. Quantification of physiological parameters of mutant and overexpressing lines for genes involved in mitochondrial stress signalling under combined drought and moderate light stress
Wild-type (Col-0), loss of function *OGO* mutants (*ogo-1*, *ogo-2*), OGO overexpressing lines (*OGO OE-1*, *OGO OE-2*), *rao2-1* (*ANAC017* EMS mutant), ANAC017 overexpressing line (*ANAC17 OE-3*), AOX1A overexpressing line *AOX1A OE*, *OGO:LUC*, *aox1a*, *rog2* mutant, T-DNA insertion lines *rog2 KO-1* and *rog2 KO-2*, *rog4* mutant, and T-DNA insertion lines *rog4 KO-1* and *rog4 KO-2* were grown under normal conditions (14 h at 120 µmol m^{-2} s^{-1} light/10 h dark, 22°C dark) for 26 d. For the drought and moderate light (DML) treatment plants were then transferred to 400 µmol m^{-2} s^{-1} 14h light/10 h dark and water was withheld for 13 days followed by rewatering and return to standard growth conditions for another 3 days to recover. Control plants remained at the standard growth conditions for the whole-time course. The arrows indicate the day watering resumed. Plant images and Fv/Fm values were determined and processed using a PlantScreen phenotyping platform (PSI, Czech Repulic) for the different time points indicated. See Figure 14 for phenotypes.

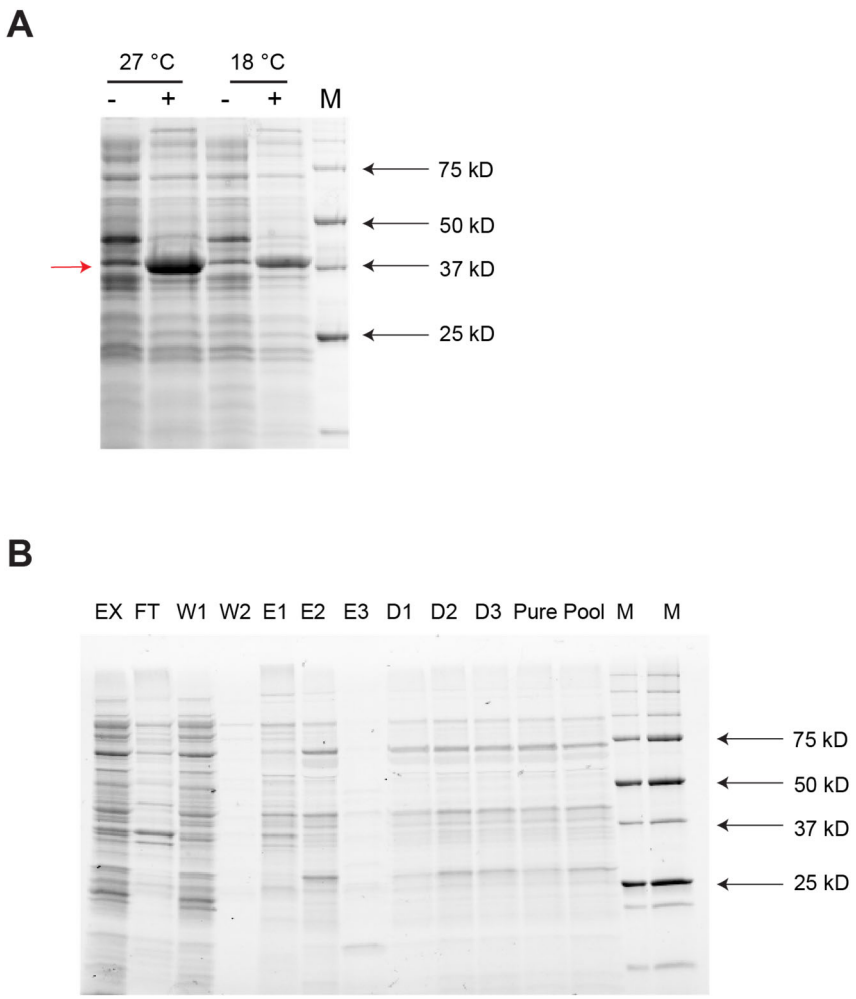

Supplemental Figure 1. Analysis of OGO expression in bacteria and purification of recombinant OGO protein

A. E. coli strain BL21(DE3) were transformed with the plasmid 6xHis-OGO-pDESTTM 17, grown overnight and subcultured for expression of OGO. Bacterial cells were harvested before (0 h) and after (8 h) induction with 0.4 mM IPTG and further growth at 27°C and 18°C, respectively. Cells were ruptured by repeated freeze/thawing in loading buffer and then separated on 8–16% Criterion™ TGX™ Precast Midi Protein Gel (Biorad). The red arrow indicates the position of the OGO protein band after expression. B. Native purification of OGO protein. Using the same culture conditions as in A), the bacterial lysate containing OGO was subjected to affinity chromatography after extraction of soluble proteins (following the pET System Manual, Novagen). No 6xHis-OGO protein was detectable in the elution steps. This experiment is only one example of several attempts using varying optimisation strategies. Ex: extract, FT: column flow through, W: column wash, E: elution, D: denaturing elution, M: Protein ladder.

SUPPLEMENTAL MATERIAL

Supplemental table S1. Primers used in this study.

(a) Genotyping primers

Primer name	Sequence (5'- 3')
SALK LBb1.3	ATTTTGCCGATTTCGGAAC
SAIL LB1	GCCTTTTCAGAAATGGATAAATAGCCTTGCTTCC
SALK_107806-LP	CGCTCAAGAACTTATCGTTCG
SALK_107806-RP	CGACGAAGACAGGAGTGAAAG
SAIL_306_F10-LP	TCCTAGCATGTTTCATGTCCC
SAIL_306_F10-RP	TTTGTTCGGTCGTACCCTATG
SALK_028140_LP1	AAAAGCCAAATCCTTTGTTGC
SALK_028140_RP1	GCCAAGTTTGAAGATGACTGC
SAIL_242_H10_LP2	TAGATGCGATGTGAAAGGGAC
SAIL_242_H10_RP2	ATAAGCCCGATGTGACATCTG
SALK_025328C_LP15	TTGAATACACCATGCTCGATG
SALK_025328C_RP15	TAGGCCATATTTGTATTGCGG
SALKSEQ_77499_LP16	AATCTTTGACGTTTGTTTTTGC
SALKSEQ_77499_RP16	TAGGCCATATTTGTATTGCGG

(b) Primers for qRT-PCR

Primer name	Sequence (5'- 3')
UBC21_RT_For	TTGTGCCATTGAATTGAACCC
UBC21_RT_Rev	CTGCGACTCAGGGAATCTTCTA
OGO_RT_For	TTGCTCCAGATCCTCCGAATCC
OGO_RT_Rev	GTGTATTCGATCACCGCACTCCTG
LUC_RT_For	TCACGCAGGCAGTTCTATGA
LUC_RT_Rev	TCACGCAGGCAGTTCTATGA
AOX1A_RT_For	GATTACTGGAGGCTTCCTGCTG
AOX1A_RT_Rev	CACGACCTTGGTAGTGAATATCAG

(c) Primers for Primers for ChIP qRT-PCR

Primer name	Sequence (5'- 3')
ACTIN2_ChIP_For	ACTACGAGCAGGAGATGGAAACCT
ACTIN2_ChIP_Rev	GCAGCTTCCATTCCCACAAACGAG
OGO_ChIP_For	AAATTCCTTGCACAACACTC
OGO_ChIP_Rev	CTCAAGAAGAAGAGGAAGATTC
AOX1A_ChIP_For	AGCTCTTGGCGACCACGCAA
AOX1A_ChIP_Rev	CCCTTGTGGTCATGAGAGAGACT
AOX1A_3UTR_ChIP_For	GAGACTCTCTCTTATGCCACCAA
AOX1A_3UTR_ChIP_Rev	TGAGGTATGTGGAAGCCTTTTT
HRE2_ChIP_For	TGCAAAAGGTTATAGAGCACACAG
HRE2_ChIP_Rev	TGAACCGAGTCCTAAAAGAGAA

(d) Primers used to clone OGO cDNA

Primer name	Sequence (5'- 3')
attB1F_OGOCDS_For	GGGGACAAGTTTGTACAAAAAAGCAGGCTTCATGACAGAGAATTCTGAAAAAAT
attB2R_OGOCDS_Rev	GGGGACCACTTTGTACAAGAAAGCTGGGTTTCCACCTCCGGATCCTATCATGTAAT

(e) Primers used to clone OGO cDNA

Primer name	Sequence (5'- 3')
OGO_LUC_F	CTGAGGATCCACTCCCAACGAGAAACT
OGO_LUC_R	CTGACCATGGAGATTCTGTTTTTTGTTGTTGTTC
OGO_GUS_F	TGCTTGCGGCAGCGTGAAGCTTACTCCCAACGAGAAACTATATT
OGO_GUS_R	TACCCGGGGATCGATCCTCTAGAGTTTTTTTCTTTTTTTCTTTCTTTC

ACKNOWLEDGEMENTS

We thank Asha Haslem for technical assistance with RNA-seq library generation, the La Trobe University Bioimaging Platform for confocal microscopy equipment and the La Trobe University Genomics Platform for access to next-generation sequencing equipment.

LITERATURE CITED

Alonso JM, Stepanova AN, Leisse TJ, Kim CJ, Chen H, Shinn P, Stevenson DK, Zimmerman J, Barajas P, Cheuk R, Gadrinab C, Heller C, Jeske A, Koesema E, Meyers CC, Parker H, Prednis L, Ansari Y, Choy N, Deen H, Geralt M, Hazari N, Hom E, Karnes M, Mulholland C, Ndubaku R, Schmidt I, Guzman P, Aguilar-Henonin L, Schmid M, Weigel D, Carter DE, Marchand T, Risseeuw E, Brogden D, Zeko A, Crosby WL, Berry CC, Ecker JR (2003) Genome-wide insertional mutagenesis of Arabidopsis thaliana. Science **301:** 653-657

Arvidsson S, Kwasniewski M, Riaño-Pachón DM, Mueller-Roeber B (2008) QuantPrime–a flexible tool for reliable high-throughput primer design for quantitative PCR. BMC bioinformatics **9:** 1-15

Baena-Gonzalez E, Rolland F, Thevelein JM, Sheen J (2007) A central integrator of transcription networks in plant stress and energy signalling. Nature **448:** 938-942

Bao F, Shen J, Brady SR, Muday GK, Asami T, Yang Z (2004) Brassinosteroids interact with auxin to promote lateral root development in Arabidopsis. Plant physiology **134:** 1624-1631

Bari R, Datt Pant B, Stitt M, Scheible WR (2006) PHO2, microRNA399, and PHR1 define a phosphate-signaling pathway in plants. Plant Physiol **141:** 988-999

Bowler C, Benvenuto G, Laflamme P, Molino D, Probst AV, Tariq M, Paszkowski J (2004) Chromatin techniques for plant cells. The Plant Journal **39:** 776-789

Boyes DC, Zayed AM, Ascenzi R, McCaskill AJ, Hoffman NE, Davis KR, Gorlach J (2001) Growth stage-based phenotypic analysis of Arabidopsis: a model for high throughput functional genomics in plants. Plant Cell **13:** 1499-1510

Boyes DC, Zayed AM, Ascenzi R, McCaskill AJ, Hoffman NE, Davis KR, Görlach J (2001) Growth stage–based phenotypic analysis of Arabidopsis: a model for high throughput functional genomics in plants. The Plant Cell **13:** 1499-1510

Brubaker K, Cowley SM, Huang K, Loo L, Yochum GS, Ayer DE, Eisenman RN, Radhakrishnan I (2000) Solution structure of the interacting domains of the Mad-Sin3 complex: implications for recruitment of a chromatin-modifying complex. Cell **103:** 655-665

Carrie C, Murcha MW, Giraud E, Ng S, Zhang MF, Narsai R, Whelan J (2013) How do plants make mitochondria? Planta **237:** 429-439

Chan KX, Phua SY, Crisp P, McQuinn R, Pogson BJ (2016) Learning the Languages of the Chloroplast: Retrograde Signaling and Beyond. Annu Rev Plant Biol **67:** 25-53

Chang KN, Zhong S, Weirauch MT, Hon G, Pelizzola M, Li H, Huang SS, Schmitz RJ, Urich MA, Kuo D, Nery JR, Qiao H, Yang A, Jamali A, Chen H, Ideker T, Ren B, Bar-Joseph Z, Hughes TR, Ecker JR (2013) Temporal transcriptional response to ethylene gas drives growth hormone cross-regulation in Arabidopsis. Elife **2:** e00675

Chao Q, Rothenberg M, Solano R, Roman G, Terzaghi W, Ecker JR (1997) Activation of the ethylene gas response pathway in Arabidopsis by the nuclear protein ETHYLENE-INSENSITIVE3 and related proteins. Cell **89:** 1133-1144

Chen WH, Li PF, Chen MK, Lee YI, Yang CH (2015) FOREVER YOUNG FLOWER Negatively Regulates Ethylene Response DNA-Binding Factors by Activating an Ethylene-Responsive Factor to Control Arabidopsis Floral Organ Senescence and Abscission. Plant Physiol **168:** 1666-1683

Clough SJ, Bent AF (1998) Floral dip: a simplified method for Agrobacterium-mediated transformation of Arabidopsis thaliana. The plant journal **16:** 735-743

Crawford T, Lehotai N, Strand A (2018) The role of retrograde signals during plant stress responses. J Exp Bot **69:** 2783-2795

Czechowski T, Stitt M, Altmann T, Udvardi MK, Scheible W-R (2005) Genome-wide identification and testing of superior reference genes for transcript normalization in Arabidopsis. Plant physiology **139:** 5-17

De Clercq I, Vermeirssen V, Van Aken O, Vandepoele K, Murcha MW, Law SR, Inze A, Ng S, Ivanova A, Rombaut D, van de Cotte B, Jaspers P, Van de Peer Y, Kangasjarvi J, Whelan J, Van Breusegem F (2013) The membrane-bound NAC transcription factor ANAC013 functions in mitochondrial retrograde regulation of the oxidative stress response in Arabidopsis. Plant Cell **25:** 3472-3490

de Souza A, Wang JZ, Dehesh K (2017) Retrograde Signals: Integrators of Interorganellar Communication and Orchestrators of Plant Development. Annu Rev Plant Biol **68:** 85-108

Dubois M, Van den Broeck L, Inze D (2018) The Pivotal Role of Ethylene in Plant Growth. Trends Plant Sci **23:** 311-323

Estavillo GM, Crisp PA, Pornsiriwong W, Wirtz M, Collinge D, Carrie C, Giraud E, Whelan J, David P, Javot H, Brearley C, Hell R, Marin E, Pogson BJ (2011) Evidence for a SAL1-PAP chloroplast retrograde pathway that functions in drought and high light signaling in Arabidopsis. Plant Cell **23:** 3992-4012

Fiorani F, Bogemann GM, Visser EJ, Lambers H, Voesenek LA (2002) Ethylene emission and responsiveness to applied ethylene vary among Poa species that inherently differ in leaf elongation rates. Plant Physiol **129:** 1382-1390

Fu A, Liu H, Yu F, Kambakam S, Luan S, Rodermel S (2012) Alternative oxidases (AOX1a and AOX2) can functionally substitute for plastid terminal oxidase in Arabidopsis chloroplasts. The Plant Cell **24:** 1579-1595

Giraud E, Ho LH, Clifton R, Carroll A, Estavillo G, Tan Y-F, Howell KA, Ivanova A, Pogson BJ, Millar AH (2008) The absence of ALTERNATIVE OXIDASE1a in Arabidopsis results in acute sensitivity to combined light and drought stress. Plant physiology **147:** 595-610

Giraud E, Ho LH, Clifton R, Carroll A, Estavillo G, Tan YF, Howell KA, Ivanova A, Pogson BJ, Millar AH, Whelan J (2008) The absence of ALTERNATIVE OXIDASE1a in Arabidopsis results in acute sensitivity to combined light and drought stress. Plant Physiol **147:** 595-610

Giraud E, Van Aken O, Ho LH, Whelan J (2009) The transcription factor ABI4 is a regulator of mitochondrial retrograde expression of ALTERNATIVE OXIDASE1a. Plant Physiol **150:** 1286-1296

Gollan PJ, Aro EM (2020) Photosynthetic signalling during high light stress and recovery: targets and dynamics. Philos Trans R Soc Lond B Biol Sci **375:** 20190406

Gong Q, Li S, Zheng Y, Duan H, Xiao F, Zhuang Y, He J, Wu G, Zhao S, Zhou H, Lin H (2020) SUMOylation of MYB30 enhances salt tolerance by elevating alternative respiration via transcriptionally upregulating AOX1a in Arabidopsis. Plant J **102:** 1157-1171

Guo H, Ecker JR (2003) Plant responses to ethylene gas are mediated by SCF(EBF1/EBF2)-dependent proteolysis of EIN3 transcription factor. Cell **115:** 667-677

Hagel JM, Facchini PJ (2018) Expanding the roles for 2-oxoglutarate-dependent oxygenases in plant metabolism. Nat Prod Rep **35:** 721-734

Hertle AP, Blunder T, Wunder T, Pesaresi P, Pribil M, Armbruster U, Leister D (2013) PGRL1 is the elusive ferredoxin-plastoquinone reductase in photosynthetic cyclic electron flow. Mol Cell **49:** 511-523

Houben M, Van de Poel B (2019) 1-Aminocyclopropane-1-Carboxylic Acid Oxidase (ACO): The Enzyme That Makes the Plant Hormone Ethylene. Front Plant Sci **10:** 695

Hruz T, Laule O, Szabo G, Wessendorp F, Bleuler S, Oertle L, Widmayer P, Gruissem W, Zimmermann P (2008) Genevestigator v3: a reference expression database for the meta-analysis of transcriptomes. Adv Bioinformatics **2008:** 420747

Ivanova A, Law SR, Narsai R, Duncan O, Lee JH, Zhang B, Van Aken O, Radomiljac JD, van der Merwe M, Yi K, Whelan J (2014) A Functional Antagonistic Relationship between Auxin and Mitochondrial Retrograde Signaling Regulates Alternative Oxidase1a Expression in Arabidopsis. Plant Physiol **165:** 1233-1254

Jefferson RA, Kavanagh TA, Bevan MW (1987) GUS fusions: beta-glucuronidase as a sensitive and versatile gene fusion marker in higher plants. The EMBO journal **6:** 3901-3907

Jing HC, Sturre MJ, Hille J, Dijkwel PP (2002) Arabidopsis onset of leaf death mutants identify a regulatory pathway controlling leaf senescence. Plant J **32:** 51-63

Kacprzak SM, Mochizuki N, Naranjo B, Xu D, Leister D, Kleine T, Okamoto H, Terry MJ (2019) Plastid-to-Nucleus Retrograde Signalling during Chloroplast Biogenesis Does Not Require ABI4. Plant Physiol **179:** 18-23

Kadosh D, Struhl K (1998) Targeted recruitment of the Sin3-Rpd3 histone deacetylase complex generates a highly localized domain of repressed chromatin in vivo. Mol Cell Biol **18:** 5121-5127

Kawai Y, Ono E, Mizutani M (2014) Evolution and diversity of the 2-oxoglutarate-dependent dioxygenase superfamily in plants. Plant J **78:** 328-343

Kleine T, Leister D (2016) Retrograde signaling: Organelles go networking. Biochim Biophys Acta **1857:** 1313-1325

Kmiecik P, Leonardelli M, Teige M (2016) Novel connections in plant organellar signalling link different stress responses and signalling pathways. J Exp Bot **67:** 3793-3807

Knoepfler PS, Eisenman RN (1999) Sin meets NuRD and other tails of repression. Cell **99:** 447-450

Koussevitzky S, Nott A, Mockler TC, Hong F, Sachetto-Martins G, Surpin M, Lim J, Mittler R, Chory J (2007) Signals from chloroplasts converge to regulate nuclear gene expression. Science **316:** 715-719

Koyama T (2014) The roles of ethylene and transcription factors in the regulation of onset of leaf senescence. Front Plant Sci **5:** 650

Larkin RM, Alonso JM, Ecker JR, Chory J (2003) GUN4, a regulator of chlorophyll synthesis and intracellular signaling. Science **299:** 902-906

Laskowski MJ, Williams ME, Nusbaum HC, Sussex IM (1995) Formation of lateral root meristems is a two-stage process. Development **121:** 3303-3310

Law SR, Narsai R, Whelan J (2014) Mitochondrial biogenesis in plants during seed germination. Mitochondrion **19 Pt B:** 214-221

Lee SH, Reid DM (1997) The role of endogenous ethylene in the expansion of Helianthus annuus leaves. Can J Bot **75:** 501-508

Li W, Ma M, Feng Y, Li H, Wang Y, Ma Y, Li M, An F, Guo H (2015) EIN2-directed translational regulation of ethylene signaling in Arabidopsis. Cell **163:** 670-683

Li Z, Peng J, Wen X, Guo H (2013) Ethylene-insensitive3 is a senescence-associated gene that accelerates age-dependent leaf senescence by directly repressing miR164 transcription in Arabidopsis. Plant Cell **25:** 3311-3328

Liu P, Nie WF, Xiong X, Wang Y, Jiang Y, Huang P, Lin X, Qin G, Huang H, Niu Q, Du J, Lang Z, Lozano-Duran R, Zhu JK (2021) A novel protein complex that regulates active DNA demethylation in Arabidopsis. J Integr Plant Biol **63:** 772-786

Liu Z, Butow RA (2006) Mitochondrial retrograde signaling. Annu Rev Genet **40:** 159-185

Meng X, Li L, De Clercq I, Narsai R, Xu Y, Hartmann A, Claros DL, Custovic E, Lewsey MG, Whelan J (2019) ANAC017 coordinates organellar functions and stress responses by reprogramming retrograde signaling. Plant physiology **180:** 634-653

Meng X, Li L, De Clercq I, Narsai R, Xu Y, Hartmann A, Claros DL, Custovic E, Lewsey MG, Whelan J, Berkowitz O (2019) ANAC017 Coordinates Organellar Functions and Stress Responses by Reprogramming Retrograde Signaling. Plant Physiol **180:** 634-653

Meng X, Li L, Narsai R, De Clercq I, Whelan J, Berkowitz O (2020) Mitochondrial signalling is critical for acclimation and adaptation to flooding in Arabidopsis thaliana. Plant J **103:** 227-247

Miao W, Dai J, La Y, Lu C, Zhang J, Hong X, Zhou S, Wang Q, Wang X, Rui Q, Tan F, La H (2020) Characterization and fine mapping of Arabidopsis RLL3, a locus required for DNA demethylation pathway. Mol Genet Genomics **295:** 81-93

Millar AH, Whelan J, Soole KL, Day DA (2011) Organization and regulation of mitochondrial respiration in plants. Annu Rev Plant Biol **62:** 79-104

Mochizuki N, Brusslan JA, Larkin R, Nagatani A, Chory J (2001) Arabidopsis genomes uncoupled 5 (GUN5) mutant reveals the involvement of Mg-chelatase H subunit in plastid-to-nucleus signal transduction. Proc Natl Acad Sci U S A **98:** 2053-2058

Ng S, De Clercq I, Van Aken O, Law SR, Ivanova A, Willems P, Giraud E, Van Breusegem F, Whelan J (2014) Anterograde and retrograde regulation of nuclear genes encoding mitochondrial proteins during growth, development, and stress. Mol Plant **7:** 1075-1093

Ng S, Giraud E, Duncan O, Law SR, Wang Y, Xu L, Narsai R, Carrie C, Walker H, Day DA, Blanco NE, Strand A, Whelan J, Ivanova A (2013) Cyclin-dependent kinase E1 (CDKE1) provides a cellular switch in plants between growth and stress responses. J Biol Chem **288:** 3449-3459

Ng S, Ivanova A, Duncan O, Law SR, Van Aken O, De Clercq I, Wang Y, Carrie C, Xu L, Kmiec B, Walker H, Van Breusegem F, Whelan J, Giraud E (2013) A membrane-bound NAC transcription factor, ANAC017, mediates mitochondrial retrograde signaling in Arabidopsis. Plant Cell **25:** 3450-3471

Noh B, Murphy AS, Spalding EP (2001) Multidrug resistance-like genes of Arabidopsis required for auxin transport and auxin-mediated development. Plant Cell **13:** 2441-2454

O'Malley RC, Huang SC, Song L, Lewsey MG, Bartlett A, Nery JR, Galli M, Gallavotti A, Ecker JR (2016) Cistrome and Epicistrome Features Shape the Regulatory DNA Landscape. Cell **165:** 1280-1292

Ogawara T, Higashi K, Kamada H, Ezura H (2003) Ethylene advances the transition from vegetative growth to flowering in Arabidopsis thaliana. J Plant Physiol **160:** 1335-1340

Patterson SE, Bleecker AB (2004) Ethylene-dependent and -independent processes associated with floral organ abscission in Arabidopsis. Plant Physiol **134:** 194-203

Pfannschmidt T (2010) Plastidial retrograde signalling--a true "plastid factor" or just metabolite signatures? Trends Plant Sci **15:** 427-435

Pfannschmidt T, Terry MJ, Van Aken O, Quiros PM (2020) Retrograde signals from endosymbiotic organelles: a common control principle in eukaryotic cells. Philos Trans R Soc Lond B Biol Sci **375:** 20190396

Rundlett SE, Carmen AA, Suka N, Turner BM, Grunstein M (1998) Transcriptional repression by UME6 involves deacetylation of lysine 5 of histone H4 by RPD3. Nature **392:** 831-835

Song CP, Agarwal M, Ohta M, Guo Y, Halfter U, Wang P, Zhu JK (2005) Role of an Arabidopsis AP2/EREBP-type transcriptional repressor in abscisic acid and drought stress responses. Plant Cell **17:** 2384-2396

Strand A, Asami T, Alonso J, Ecker JR, Chory J (2003) Chloroplast to nucleus communication triggered by accumulation of Mg-protoporphyrinIX. Nature **421:** 79-83

Tanaka M, Kikuchi A, Kamada H (2008) The Arabidopsis histone deacetylases HDA6 and HDA19 contribute to the repression of embryonic properties after germination. Plant Physiol **146:** 149-161

Tognetti VB, Van Aken O, Morreel K, Vandenbroucke K, van de Cotte B, De Clercq I, Chiwocha S, Fenske R, Prinsen E, Boerjan W, Genty B, Stubbs KA, Inze D, Van Breusegem F (2010) Perturbation of indole-3-butyric acid homeostasis by the UDP-glucosyltransferase UGT74E2 modulates Arabidopsis architecture and water stress tolerance. Plant Cell **22:** 2660-2679

Trentmann SM, Kende H (1995) Analysis of Arabidopsis cDNA that shows homology to the tomato E8 cDNA. Plant Mol Biol **29:** 161-166

Van Aken O, Zhang B, Law S, Narsai R, Whelan J (2013) AtWRKY40 and AtWRKY63 modulate the expression of stress-responsive nuclear genes encoding mitochondrial and chloroplast proteins. Plant Physiol **162:** 254-271

van der Graaff E, Schwacke R, Schneider A, Desimone M, Flugge UI, Kunze R (2006) Transcription analysis of arabidopsis membrane transporters and hormone pathways during developmental and induced leaf senescence. Plant Physiol **141:** 776-792

Vandenbussche F, Vriezen WH, Smalle J, Laarhoven LJ, Harren FJ, Van Der Straeten D (2003) Ethylene and auxin control the Arabidopsis response to decreased light intensity. Plant Physiol **133:** 517-527

Vanderstraeten L, Depaepe T, Bertrand S, Van Der Straeten D (2019) The Ethylene Precursor ACC Affects Early Vegetative Development Independently of Ethylene Signaling. Front Plant Sci **10:** 1591

Wachter A, Wolf S, Steininger H, Bogs J, Rausch T (2005) Differential targeting of GSH1 and GSH2 is achieved by multiple transcription initiation: implications for the compartmentation of glutathione biosynthesis in the Brassicaceae. Plant J **41:** 15-30

Wagner S, Van Aken O, Elsasser M, Schwarzlander M (2018) Mitochondrial Energy Signaling and Its Role in the Low-Oxygen Stress Response of Plants. Plant Physiol **176:** 1156-1170

Wang Y, Selinski J, Mao C, Zhu Y, Berkowitz O, Whelan J (2020) Linking mitochondrial and chloroplast retrograde signalling in plants. Philos Trans R Soc Lond B Biol Sci **375:** 20190410

Woodson JD, Chory J (2008) Coordination of gene expression between organellar and nuclear genomes. Nat Rev Genet **9:** 383-395

Woodson JD, Perez-Ruiz JM, Chory J (2011) Heme synthesis by plastid ferrochelatase I regulates nuclear gene expression in plants. Curr Biol **21:** 897-903

Woodson JD, Perez-Ruiz JM, Schmitz RJ, Ecker JR, Chory J (2013) Sigma factor-mediated plastid retrograde signals control nuclear gene expression. Plant J **73:** 1-13

Wu F-H, Shen S-C, Lee L-Y, Lee S-H, Chan M-T, Lin C-S (2009) Tape-Arabidopsis Sandwich-a simpler Arabidopsis protoplast isolation method. Plant methods **5:** 1-10

Xiao Y, Savchenko T, Baidoo EE, Chehab WE, Hayden DM, Tolstikov V, Corwin JA, Kliebenstein DJ, Keasling JD, Dehesh K (2012) Retrograde signaling by the plastidial metabolite MEcPP regulates expression of nuclear stress-response genes. Cell **149:** 1525-1535

Xing A, Moon BP, Mills KM, Falco SC, Li Z (2010) Revealing frequent alternative polyadenylation and widespread low-level transcription read-through of novel plant transcription terminators. Plant Biotechnol J **8:** 772-782

Yang CY, Hsu FC, Li JP, Wang NN, Shih MC (2011) The AP2/ERF transcription factor AtERF73/HRE1 modulates ethylene responses during hypoxia in Arabidopsis. Plant Physiol **156:** 202-212

Zhang B, Van Aken O, Thatcher L, De Clercq I, Duncan O, Law SR, Murcha MW, van der Merwe M, Seifi HS, Carrie C, Cazzonelli C, Radomiljac J, Hofte M, Singh KB,

Van Breusegem F, Whelan J (2014) The mitochondrial outer membrane AAA ATPase AtOM66 affects cell death and pathogen resistance in Arabidopsis thaliana. Plant J **80:** 709-727

ZHANG DW, Xu F, ZHANG ZW, CHEN YE, DU JB, JIA SD, Yuan S, LIN HH (2010) Effects of light on cyanide-resistant respiration and alternative oxidase function in Arabidopsis seedlings. Plant, Cell & Environment **33:** 2121-2131

Zhang X, Ivanova A, Vandepoele K, Radomiljac J, Van de Velde J, Berkowitz O, Willems P, Xu Y, Ng S, Van Aken O, Duncan O, Zhang B, Storme V, Chan KX, Vaneechoutte D, Pogson BJ, Van Breusegem F, Whelan J, De Clercq I (2017) The Transcription Factor MYB29 Is a Regulator of ALTERNATIVE OXIDASE1a. Plant Physiol **173:** 1824-1843

Zhou C, Zhang L, Duan J, Miki B, Wu K (2005) HISTONE DEACETYLASE19 is involved in jasmonic acid and ethylene signaling of pathogen response in Arabidopsis. Plant Cell **17:** 1196-1204

3. CHAPTER III - THE TRANSCRIPTION FACTOR ANAC017 FINE-TUNES THE TRANSCRIPTIONAL RESPONSE TO MITOCHONDRIAL DYSFUNCTION BY DIRECTLY TARGETING ETHYLENE AND AUXIN SIGNALLING PATHWAYS

Author for Contact:

Oliver Berkowitz

La Trobe University

School of Life Sciences

Department of Animal, Plant and Soil Science

AgriBio, Centre for AgriBioscience

Bundoora, Victoria 3086, Australia

E-mail: o.berkowitz@latrobe.edu.au

Tel.: +61 3 9032 7490

Authors and affiliations

Cunman He[1,2], Lim Chee Liew[1], Lingling Yin[1], Mathew G. Lewsey[1], James Whelan[1,2], Oliver Berkowitz[1,2]

[1]Department of Animal, Plant and Soil Science, La Trobe University, Bundoora, Victoria 3086, Australia

ARC Centre of Excellence in Plant Energy Biology, La Trobe University, Bundoora, Victoria 3086, Australia

One sentence summary:

The transcription factors ANAC017 fine-tune mitochondrial retrograde signalling by controlling the transcriptional response to mitochondrial dysfunction by directly targeting ethylene- and auxin related signalling components.

AUTHOR CONTRIBUTIONS

OB, CH and JW designed the research. CH performed generation of transgenic lines, genotyping, GUS staining assay. CH and OB performed time-resolved RNA-seq experiment and data analyses. CH, LCL and LY performed ChIP-Seq experiment. CH, LCL, LY, OB, MGL and JW collected, analysed or interpreted the data; OB, CH and JW wrote the manuscript with contributions by all authors.

FUNDING INFORMATION:

This work was supported by the facilities of the Australian Research Council Centre of Excellence Program (CE140100008, ARC Centre of Excellence in Plant Energy Biology; JW; ARC Discovery Grant DP200102452; JW).

EMAIL ADDRESS OF AUTHOR FOR CONTACT:

o.berkowitz@latrobe.edu.au

ABSTRACT

Mitochondria are ideally positioned in plant cells to sense changes in energy status and metabolism in response to changing environmental conditions, but also to drive the associated acclimation processes. Thus, retrograde signalling from mitochondria to the nucleus is crucial to regulate gene expression, with the transcription factor ANAC017 a master regulator. Here we show that ANAC017 directly regulates the expression of several genes of the ethylene and auxin pathways, including *MAP KINASE KINASE 9*, *1-AMINO-CYCLOPROPANE-1-CARBOXYLATE SYNTHASE 2* and *YUCCA 5*, by chromatin immunoprecipitation followed by sequencing (ChIP-seq). Initial characterisation of a mitochondrial dysfunction stimulon gene, AT4G43450 (*OGO*), also showed induced expression in plants treated with the ethylene precursor 1-amino-cyclopropane-1-carboxylate and during two ethylene-mediated processes, i.e. senescence and submergence. A time resolved RNA-seq experiment using wild type as well as *ein3-1* and *ogo* mutant plants treated with the inhibitor of mitochondrial electron transport antimycin A demonstrated that an activation of ethylene signalling precedes the stimulation of auxin signalling in the mitochondrial stress response. Part of this transcriptional cascade is mediated by the ethylene-signalling regulator ETHYLENE INSENSITIVE 3. A dynamic regulatory events model suggested that distinct transcription factors drive the primary stress-response to maintain mitochondrial function, while a different set of transcription factors controls a more subtle and diverse response to adjust growth. In summary, our findings support a feed-back model for the dual control and fine-tuning of mitochondrial retrograde signalling by ethylene and auxin downstream of ANAC017. This allows adjustment of plant growth under limiting growth conditions.

INTRODUCTION

Mitochondria maintain plant energy homeostasis and adjust metabolism to the prevailing growth conditions through oxidative phosphorylation and the central role of the tricarboxylic acid cycle (TCA). These functions are also crucial for plants to respond to changes in environmental conditions and acclimate to adverse growth conditions. In accordance with this, a role of mitochondria to sense stresses allows the integration with the overall cellular response largely driven from the nucleus. Mitochondria relay their status to the nucleus via a pathway termed mitochondrial retrograde response (MRR) that adjusts the expression of nuclear genes to optimize mitochondrial function. This is also co-ordinated with a function paralleled by chloroplasts and partly overlapping signalling pathways (Crawford et al., 2018; Wang et al., 2020; Dopp et al., 2021).

Triggering mitochondrial dysfunction, e.g. by chemical inhibitors of mitochondrial electron transport such as antimycin A (AA; complex III) and myxothiazol (complex III), or by mutation of genes, has allowed for the identification of many stress-responsive genes through genetic and transcriptomic approaches (Wang et al., 2018). This led to the early identification of 24 mitochondrial dysfunction stimulon (MDS) genes based on their high induction when mitochondrial function was impaired (De Clercq et al., 2013). Together with a forward genetic screen for regulators of the mitochondrial stress marker gene *ALTERNATIVE OXIDASE 1A* (*AOX1a*), also part of the MDS, revealed several key transcription factors (TFs) involved in the regulation (Ng et al., 2013). These TFs, ANAC013 and ANAC017, belong to the Arabidopsis NAC domain (ANAC)-containing family located at the ER membrane and their targeted MDS genes share a common binding motif (De Clercq et al., 2013; Ng et al., 2013). ANAC013 and ANAC017 are released from the ER upon mitochondrial stress by a yet unknown mechanism, potentially by a rhomboid protease, to translocate to the nucleus and activate the down-stream stress response. This response directly regulates the expression of hundreds of genes as evidenced by attenuated transcriptional responses in corresponding mutant lines and increased expression of genes in *ANAC017* overexpressing lines (Ng et al., 2013; Van Aken et al., 2016; Meng et al., 2019). However, it is unknown how many of these genes are directly targeted by ANAC013 or ANAC017, and which genes are further downstream in the transcriptional cascade. Analysis of ANC017 binding sites by DNA affinity purification sequencing (DAP-seq) using genomic and demethylated genomic DNA estimated about 3000 and 8000 genes, respectively, are putative target genes (O'Malley et al., 2016). However, this *in vitro* binding method likely overestimates numbers and may not reflect the native ANAC017 binding affinity under

mitochondrial stress *in planta*. A central role of ANAC017 is also evident from its function in regulating some chloroplast retrograde responses and it is therefore a convergence point for organellar signalling pathways (Van Aken et al., 2016). For example, overexpression of ANAC017 leads to substantial repression of chloroplast functions, likely to maintain overall cellular homeostasis when mitochondrial activity becomes limiting (Meng et al., 2019).

For few of the 24 MDS genes and their encoded proteins a role in mitigating mitochondrial stress has been established, while for many their immediate role in this process is not directly obvious from their molecular function. AOX1a and NAD(P)H DEHYDROGENASE B4 (NDB4) are part of the alternative pathway in the electron transport chain and prevent its detrimental overreduction under adverse conditions (Clifton et al., 2006; Smith et al., 2011). The induction and alternative localisation of At12Cys-2 (At5g09570) provides a mechanism to specifically signal mitochondrial dysfunction upon a reduction in complex I abundance (Wang et al., 2016). Another two MDS genes, *ATP-BINDING CASSETTE B4* (*ABCB4*) and *URIDINE DIPHOSPHATE GLYCOSYLTRANSFERASE 74E2* (*UGT74E2*), are directly linked to auxin homeostasis through their activities as auxin transporter and auxin conjugase, respectively (Noh et al., 2001; Tognetti et al., 2010). Apart from these MDS genes, a role of auxin in the regulation of the mitochondrial function was also established by a screen for mutants with impaired MRR which identified the auxin transporters BIG, PINFORMED (PIN) 1 and ATP-BINDING CASSETTE (ABC) B19 as well as ASYMETRIC LEAVES 1, the latter being involved in the establishment of auxin gradients in the leaf. Together, these findings provided evidence for a feedback loop and antagonistic relationship between the MRR and auxin (Ivanova et al., 2014; Kerchev et al., 2014). Furthermore, two MDS genes have a relationship to ethylene. The ethylene response factor (ERF) HYPOXIA RESPONSIVE ERF 2 (HRE2)/ERF71 belongs to the class VII ERFs that participate in the oxygen status-sensing N-end rule pathway and modulates ethylene responses under hypoxia (Licausi et al., 2010; Gasch et al., 2015). The gene *At5g43450* encodes for an uncharacterized member of the 2-oxoglutarate (2OG) and Fe(II)-dependent oxygenase family and is annotated as an ACO-like gene in TAIR10 because of its sequence similarity to the ethylene biosynthesis enzyme ACC oxidase (ACO) (Trentmann and Kende, 1995; Vandenbussche et al., 2003). Recent studies have provided more evidence for an involvement of ethylene in mitochondrial stress responses. Ethylene modulates the proteotoxic response when impaired mitochondrial function results in the accumulation of misfolded proteins (Wang and Auwerx, 2017; Kacprzak et al., 2020). Impaired mitochondrial translation in a mutant deficient in the organellar polymerase RPOTmp leads to an AOX1a-dependent phenotype reminiscent of the triple-response observed for ethylene-treated wild

type plants (Merendino et al., 2020). Ethylene also activates the MRR to increase ROS production during seed germination to break dormancy (Jurdak et al., 2021). In addition, a substantially overlapping transcriptional response between hypoxia and submergence, both largely controlled by ethylene signalling but also MRR regulators such as ANAC017, with AA- induced mitochondrial dysfunction suggests a role of ethylene in the MRR pathway (Wagner et al., 2018; Meng et al., 2020). A mechanistic understanding for an ethylene-modulated MRR pathway is currently scarce. Kacprzak et al. (2020) showed a stimulation of AA-induced gene expression in an ethylene-overproducing mutant (*eto1-1*), while mutants for the signalling components ETHYLENE INSENSITIVE 2 and MITOGEN ACTIVATED KINASE (MPK) 6 showed no difference to wild type. The authors concluded that ethylene promotes the MRR independent of ANAC017. Results from RNA-seq data of laser capture microdissected leaf tissue suggested a more localised interaction of ethylene and auxin influencing AA-induced transcription (Berkowitz et al., 2021).

Here, we further investigate the role of ethylene on the mitochondrial signalling pathway. We first characterized the ACO-like MDS gene AT4G43450, termed OGO here, and show its induced expression by ACC treatments and during two ethylene-mediated processes, i.e. senescence and submergence stress. A time resolved RNA-seq experiment using AA treated plants revealed an activation of ethylene signalling precedes the stimulation of auxin signalling in the mitochondrial stress response. Furthermore, this transcriptional response was strongly attenuated in a mutant line for the key regulator of ethylene-induced gene expression EIN3. ChIP-seq experiments demonstrated that ANAC017 directly binds to the promoters of several ethylene- and auxin-related genes, including the genes encoding the MAP KINASE KINASE 9 (MKK9), the ethylene biosynthesis enzyme 1-AMINO-CYCLOPROPANE-1-CARBOXYLATE SYNTHASE 2 and the auxin biosynthesis enzyme YUCCA5, providing a mechanism to fine-tune the MRR by these important plant hormones. Thus, our data provides first evidence that ANAC017 is not only a regulator of genes mitigating mitochondrial stress such as AOX1a, but also regulates the expression of several genes involved in the biosynthesis and signalling of ethylene and auxin. Especially the direct targeting of MKK9 and ACS2 by ANAC017 provides a mechanism for ethylene-mediated modulation of retrograde signalling that also involves EIN3. This explains the contribution of ANAC017 to many stress responses depending on mitochondrial function and ethylene signalling such as senescence, hypoxia or submergence (Kim et al., 2018; Wagner et al., 2018; Meng et al., 2019; Bui et al., 2020; Meng et al., 2020; Broda et al., 2021).

RESULTS

An *AOX1A* co-expression network identifies genes related to ethylene signalling

The treatment of plants with antimycin A to inhibit complex III and induce mitochondrial dysfunction has helped greatly to elucidate mechanisms in mitochondrial retrograde signalling (Wang et al., 2020). This allowed for the identification of key genes involved in the response, such as the mitochondrial stress marker gene *AOX1a*. The differential co-expression of genes is another indicator for a similar role of groups of genes as they are present at the same time and in the same tissues even before the onset of stress, and they also concertedly change across varying growth conditions (Wolfe et al., 2005). We have used the CoNekT tool, which incorporates 913 RNA-seq data sets of Arabidopsis for a variety of tissues and developmental stages, to generate a co-expression neighbourhood network around *AOX1a* (Proost and Mutwil, 2018). This identified 12 genes co-expressed with *AOX1a* based on stringent parameters using a Pearson correlation coefficient above 0.5 and a highest reciprocal rank of above 100 (Figure 1A). Only 5 of the 24 mitochondrial dysfunction stimulon (MDS) genes, which are highly up-regulated by AA treatment (De Clercq et al., 2013), were part of this network. Of these, *HRE2/ERF71* and *At5g43450* had the closest connection to *AOX1a* in this network (Figure 1A). Interestingly, both genes having an association to ethylene signalling. HRE2 is a class VII ERF involved in the oxygen-sensing N-end rule pathway and involved in hypoxia responses (Gasch et al., 2015). The gene *At5g43450*, a 2-oxoglutarate (2OG) and Fe(II)-dependent oxygenase subsequently named *OGO*, shares sequence similarity with the ethylene biosynthesis enzyme ACC oxidase (ACO) (Trentmann and Kende, 1995; Vandenbussche et al., 2003). Additional evidence for a role of ethylene in directly connecting the three genes comes from a ChIP-seq experiment showing the binding of HRE2 to the promoters of *AOX1a* and *OGO* under hypoxia (Figure 1B) (Lee and Bailey-Serres, 2019). We further retrieved the expression data of the three genes from publicly available data sets relating to ethylene (treatment with ethylene gas and the biosynthesis inhibitor $AgNO_3$), hypoxia/anoxia and mitochondrial stress (antimycin, oligomycin) using the Genevestigator tool (Hruz et al., 2008). The three genes showed substantial up-regulation across these experiments (Figure 1C), providing additional evidence for their co-expression and involvement of ethylene in their transcriptional regulation.

To further characterise OGO and confirm its ethylene-dependent changes in expression we generated and analysed *proOGO-GUS* reporter lines. As expected from its MDS membership, GUS activity in these lines was increased by AA treatment, but also by

treatment with the ethylene precursor 1-aminocyclopropane-1-carboxylic acid (ACC) (Figure 2A). Consistent with this, AA and ACC treatments also led to increased *OGO* transcript levels, similar to the known marker genes *AOX1a* and *ETHYLENE BINDING FACTOR 2*, respectively, in wild type Col-0 as quantified by qRT-PCR (Figure 2B, C). Given ethylene is an important driver of leaf senescence (Kim et al., 2017), *OGO* expression was also monitored across leaf developmental stages and after dark-induced senescence (Figure 3A,B). In the reporter lines GUS activity was detectable in the oldest leaves, while no GUS was detected in young and mature leaves. Similarly, *OGO* transcript levels increased with leaf age when quantified by qRT-PCR by about 4-fold from young to old leaves (Figure 3A). This was mirrored by the senescence marker genes *STAY-GREEN 1* (*SGR1*) and *PHEOPHORBIDE A OXYGENASE* (*PAO*), while expression of the gene for *RIBULOSE BISPHOSPHATE CARBOXYLASE SMALL CHAIN 1A* (*RBCS1A*) declined (Figure 3A). In experiments using dark-induced senescence, GUS activity in reporter lines and *OGO* transcript levels increased the longer the leaves were kept in the dark (Figure 3B). Expression of marker genes *SRG1* and *PAO* also increased consistent with their role in senescence, while *RBCS1A* expression decreased. Another stress for which ethylene is an important signalling component, but also depends on mitochondrial signalling, is submergence (Loreti et al., 2016; Meng et al., 2020). We therefore also subjected wild-type plants, an OGO knockout mutant (*ogo-1*) and the *ein3-1* mutant, carrying a knock-out allele of the master regulator in ethylene signalling EIN3, to submergence and desubmergence treatments. Both the *ogo-1* and *ein3-1* mutant showed a more severe phenotype than the wild type (Figure 4A). Quantification of chlorophyll concentrations and the maximum quantum yield of photosystem II (Fv/Fm) also confirmed that *ogo-1* and *ein3-1* were more impacted by the treatments than the wild type (Figure 4B). Expression of *OGO* also increased in both genotypes as determined by qRT-PCR (Figure 4C). Taken together, these results suggested a regulation of MDS genes AOX1a and OGO by ethylene.

Transcriptional responses to mitochondrial dysfunction involve an ethylene response preceding auxin signalling

To determine if and to what extend ethylene signalling regulates mitochondrial dysfunction responses, we sampled seedlings of the wild type Col-0, *ein3-1* and *ogo-1* mutant after spraying with the mitochondrial complex III inhibitor antimycin A (AA) at 0, 30, 60, 120, 180, 270, and 360 mins after treatment. A mock treatment was also performed in parallel to account for the known touch response occurring after spray treatments (Van Aken

et al., 2016; Xu et al., 2019). Subsequently, RNA-seq was carried out for these three genotypes across the two treatment time courses.

For the comparison of AA and mock treatments at the same time point, the number of differentially expressed genes (DEGs; |log2 (fold change)| > 1, FDR<0.05) was the lowest in *ein3-1*, while *ogo-1* had generally a higher number of DEGs than wild type, especially at early (60, 120 mins) and late (360 mins) time points (Figure 5A; Supplemental Table 1). Overlaps in DEGs across the genotypes were limited for the two earliest time points and then increased, with *ogo-1* maintaining the highest number of specific DEGs throughout the time course (Figure 5A). The four largest intersects contained only *ogo-1*-specific DEGs and a GO term enrichment analysis determined that they were related to ribosome biogenesis, translation and chloroplast avoidance movement (Figure 5B; Supplemental Table 3). The associated genes for the former two GO terms were largely encoding ribosomal or nucleolar proteins, while the latter encoded proteins (*J-DOMAIN PROTEIN REQUIRED FOR CHLOROPLAST ACCUMULATION RESPONSE 1*, *PHOTOTROPIN 1*, *PLASTID MOVEMENT IMPAIRED 1* and 2) that adjust the localisation of chloroplasts to environmental factors (Kong and Wada, 2014). The *ein3-1* mutant shared almost all its DEGs with the other two genotypes and had only a very small number of specific DEGs (Figure 5A).

Based on their expression in the mock and AA treatments, the DEGs identified across the genotypes were separated into six clusters by a self-organising maps (SOM) clustering algorithm (Figure 5C). DEGs in clusters 1, 2 and 3 included the DEGs with limited changes in expression in response to the two treatments and minor differences between genotypes. While DEGs in cluster 4 were strongly induced early after treatment with AA in wild type and *ogo-1*, these DEGs were also responsive to the mock treatment and hence are touch-induced. Correspondingly, several marker genes for touch responses such as TOUCH3, TOUCH4 and WRKY40 were in the cluster 4 gene list (Supplemental Table 2). For this cluster the changes in gene expression were short-lived with a peak already at 30 to 60 mins, and for *ein3-1* the transcriptional response of these genes was attenuated (Figure 5C). Although the role of ethylene and its signalling pathway for touch responses is somewhat controversial (Braam, 2005), our results and other recent work (Wu et al., 2020) suggest a function of EIN3 for controlling gene expression upon touch.

In contrast to cluster 4, DEGs in cluster 5 and 6 showed only very limited or no touch-responsiveness, respectively (Figure 5B). Therefore, their considerable changes in expression are a specific response to mitochondrial dysfunction induced by the AA treatment. DEGs in cluster 5 responded earlier to AA than DEGs in cluster 6, peaking around 180 to

270 mins post-treatment after which their expression declined. Expression of genes in cluster 6 started to respond 120 mins after AA treatment and continuously increased to plateau around 270 mins for Col-0 and *ogo-1*. For both these clusters, the induction of DEGs was lower in *ein3-1* than in Col-0 or *ogo-1*, and also already decreased after 270 min for genes in cluster 6. Cross-referencing the gene lists for clusters 1 to 6 with known targets of EIN3 identified by ChIP-seq (Chang et al., 2013) showed that genes in cluster 5 were enriched ($p<0.001$), while clusters 1, 2 and 3 were depleted ($p < 0.001$ to 0.05), for EIN3 target genes (Figure 5D; Supplemental Table 2). This suggests a role of EIN3 in the early response to AA. For the stress marker genes of the MDS, 21 were quantifiable in the RNA-seq data, and 20 genes were part of cluster 6 and one gene (OM66) in cluster 5 (Figure 5E,F). Most of these genes showed a delayed, attenuated and/or early declining induction after AA treatment in the *ein3-1* mutant also suggesting a role for EIN3 in the mitochondrial stress signalling pathway. Exceptions were HSP23.5 and the ETHYLENE RESPONSE FACTOR (ERF) HRE2 having higher transcript levels in *ein3-1* than in the wild type, indicating their upregulation by AA treatment is independent of EIN3.

GO term enrichment analysis for the early responsive genes in clusters 5 revealed an enrichment for terms related to defence response, protein phosphorylation, response to ethylene and leaf senescence (Figure 5G; Supplemental Table 4). Associated genes encode the ethylene biosynthesis enzyme ACS6, the ERF transcription factors ERF#011, ERF100 and HRE2, and the MAP kinase kinase MKK9. The latter is part of a signalling cascade, also involving MITOGEN-ACTIVATED PROTEIN KINASE (MPK) 3 and MPK6, that leads to enhanced ethylene production and signalling via phosphorylation of ACS6 and ERFs, respectively (Liu and Zhang, 2004; Meng et al., 2013). Among the enriched GO terms for late responsive genes in cluster 6 were several related to hormone response and indole metabolism (Figure 5G; Supplemental Table 4). On closer inspection of the corresponding gene list, it was apparent that many genes had relationship to auxin homeostasis through their involvement in the biosynthesis, signalling, transport or conjugation (Casanova-Sáez et al., 2021). Auxin biosynthesis-related genes encoded ANTHRANILATE SYNTHASE ALPHA SUBUNIT 1 (ASA1), ANTHRANILATE SYNTHASE BETA SUBUNIT 1 (ASB1), CYTOCHROME P450 (CYP) 71B6, CYP83B1, INDOLE-3-GLYCEROL PHOSPHATE SYNTHASE (IGPS), NITRILASE 1 and 2, and TRYPTOPHAN BIOSYNTHESIS 1, 2 and 3. Genes associated with auxin-conjugation were GRETCHEN HAGEN (GH) 3.2, GH3.5, GH3.15, IAA-LEUCINE RESISTANT-LIKE (ILL) 6, CYP71A12, CYP71A13, GAMMA-GLUTAMYL PEPTIDASE 1 (GGP1) and the MDS gene URIDINE DIPHOSPHATE GLYCOSYLTRANSFERASE (UGT) 74E2. The genes encoding auxin transporters were

another MDS gene *ATP-BINDING CASSETTE* (*ABC*) *B4* and *PIN-LIKES* (*PILS*) *3*, while auxin signalling-related genes were *INDOLE-3-ACETIC ACID INDUCIBLE* (*IAA*) *4* and S*MALL AUXIN UPREGULATED* (*SAUR*) *36*, *SAUR41* and *SAUR59*.

Taken together, our approach using a time course and three genotypes, showed a sequential response to mitochondrial dysfunction that occurred in an early and a late wave of transcriptional changes. The early response suggested an activation by ethylene-mediated signalling at least partly dependent on EIN3.

A time-resolved gene-regulatory network fine-tuning mitochondrial stress responses

To gain further insight on how the mitochondrial retrograde response to stress leads to changes in the expression of thousands of genes and on what impact a mutation of EIN3 has on this process, we performed time-resolved modelling to obtain a dynamic regulatory network of transcription factors and their target genes using the DREM software (Schulz et al., 2012). This defines groups of genes with similar temporal expression pattern, then determines time points at which the expression of genes sets diverges and predicts transcription factors (TFs) causal for these splits based on their binding to promoters of these genes. Based on this, the final output provides groups of genes on similar temporal trajectories of expression (termed paths) and designates TFs to the underlying activation events. Using our time resolved RNA-seq data, a DREM analysis was performed and identified 16 paths for Col-0 and 11 paths for *ein3-1* that consisted of genes with distinct biological functions (Figure 6A, B; Supplemental Tables 5-10).

The DREM model for Col-0 separated the genes into paths that emanated from the three initial splits (coloured red, blue, green in Figure 6A). Paths 1 and 2 included genes most highly up-regulated by AA (above 8-fold) and were controlled by ANAC013, ANAC016 and ANAC017 (TF set 2 in Supplemental Table 5), the three closely related ER-tethered TFs that are established regulators of mitochondrial retrograde signalling (De Clercq et al., 2013; Ng et al., 2013). Several stress responsive WRKY family TFs are predicted to join these ANACs in the connecting paths, including the senescence regulators WRKY25 and WRKY28 (Figure 6A; TF set 4 and 7 in Supplemental Table 5) (Doll et al., 2020; Tian et al., 2020). The identification of the three ANAC TFs as the earliest regulators in the AA response suggest the validity of the DREM model to predict regulatory relationships. Consistent with that, these two paths contained all but one marker gene of the MDS and were linked to enriched GO terms relating to oxidative stress and hypoxia (Figure 6A; Supplemental Table 7). Path 16 also originated from the same early furcation as paths 1 and 2, but genes included were strongly down-regulated and associated to photosynthesis. This agrees with

evidence that organelles share regulatory pathways depending on ANACs, and their interaction with RADICAL-INDUCED CELL DEATH (RCD) 1, to co-ordinate these responses (Meng et al., 2019; Shapiguzov et al., 2019). From the primary furcation, paths 3 to 9 contain genes that are also up-regulated but to a lesser degree than genes in paths 1 and 2. These genes are associated to oxidative stress, ethylene responses, hormone signalling and senescence among others (Figure 6A, Supplemental Table 7). Early regulators of these genes predicted from the model were several WRKYs, ANAC081, CALMODULIN-BINDING TRANSCRIPTION ACTIVATOR (CAMTA) 1 and ERF1, ERF11 and ERF59. These ERFs are involved in diverse stress-signalling pathways (Müller and Munné-Bosch, 2015), while CAMTA1 belongs to the ethylene-induced calmodulin binding protein family and is also involved in auxin signalling (Reddy et al., 2000; Galon et al., 2010). ANAC081 is a regulator of leaf senescence and also controls developmental processes that are dependent on brassinosteroids and light (Peng et al., 2015; Takasaki et al., 2015). Interestingly, ANAC017 was also a regulator for genes in path 3 resulting from a furcation event at 120 mins, suggesting it is not exclusively regulating the highly induced genes in path 1 and 2 but also with hormonal and growth responses. MYB88 and FOREVER YOUNG FLOWER UP-REGULATING FACTOR1 (FUF1) were regulators of genes in path 5 and 7 at the same furcation. MYB88 a regulator of the expression of the auxin transporters PINFORMED (PIN) 3 and PIN7 and FUF1 is an ERF suppressing senescence via activation of several ethylene response DNA-binding factors (Chen et al., 2015; Wang et al., 2015). While responses to AA treatment have largely focussed on up-regulated genes, here we find several largely uncharacterised MYB DOMAIN PROTEIN (MYB), HOMEOBOX PROTEINs (HBs) and ANACs that are predicted regulators of down-regulated genes. These down-regulated genes are associated to enriched GO terms relating to cytokinesis, photosynthesis, chlorophyll biosynthesis and lipid metabolism (Figure 6A; Supplemental Table 7), suggesting an active inhibition of growth and primary metabolism associated with chloroplast functions in the response to AA. In agreement, the earliest regulators of paths 11 to 15 predicted by the DREM model are ABF2, a promoter of chlorophyll degradation (Gao et al., 2016), and MYB3R1, MYB3R4 and MYB3R5 which are positive regulators of cytokinesis (Haga et al., 2007), with the latter two maintaining a regulatory role for paths 12 and 13. Of the 6 ANACs initiating the split leading to paths 11, 14 and 15, four have an established function: ANAC016 and ANAC078 (together with ANAC013 and ANAC017) belong to the phylogenetically similar mitochondrial dysfunction-regulators (De Clercq et al., 2013). ANAC078 also has a function in supporting protein degradation under stress conditions (Gladman et al., 2016), and ANAC045 and ANAC083 control the differentiation of sieve

elements and xylem vessels, respectively (Yamaguchi et al., 2010; Furuta et al., 2014). DREM model-predicted regulators of the HB transcription factor family for paths 11, 14, 15 are HB5, HB13, HB33, HB34 and HB40 (Figure 6A; Supplemental Table 5). These HBs all have a role in seedling development by regulation cell expansion and proliferation which is mediated by hormonal signalling pathways (including auxin) and stress (Perotti et al., 2017). KUA1 was also a regulator of these paths, and similar to HBs, controls leaf cell expansion and enhances auxin accumulation (Kwon et al., 2013; Lu et al., 2014). Thus, the DREM model established a temporal sequence of regulatory events that extend our knowledge on the known TFs responsible for the induction of genes, such as ANAC017 and ANAC013, to mitigate the impact of AA on mitochondrial function. The results also identified TFs that had not been associated with mitochondrial stress, e.g. ERF1, ERF11, ERF59 or ANAC081, that fine-tune this response and TFs that down-regulate growth and photosynthesis.

We next examined how these regulatory events changed in the *ein3-1* mutant background by generating a DREM model using identical parameters as for Col-0 (Figure 6B). For *ein3-1* the model predicted only 11 paths suggesting a less complex regulatory network than for Col-0 which fits the lower number of DEGs. An obvious similarity was the conservation of ANAC013, ANAC016 and ANAC017 (i.e. the key regulators of mitochondrial stress signalling) at the earliest time point, and their sustained association with the most highly up-regulated genes (paths 1 and 2). Also conserved at the early time points were stress responsive WRKYs and CAMTA1. Notably, and in contrast to Col-0 (Figure 6A), ERFs and ANAC081 were missing from these early regulators, indicative for their regulation by EIN3 (Figure 6B). Inspection of a list of EIN3 target genes identified by chromatin immunoprecipitation followed by sequencing (ChIP-Seq; Chang et al. (2013)) confirmed ethylene-dependent binding of EIN3 to the promoters of ERF1, ERF11 and ANAC081. In contrast to Col-0, down-regulated genes were not enriched for GO terms related to photosynthesis or cytokinesis, but rather for cell wall organisation and cellulose metabolism (paths 8 to 11; Supplemental Table 10). This down-regulation was not driven by ANACs and HBs as in Col-0, instead MYB31, MYB88 and FUF1 were regulators of genes in path 9 and MYB70 and MYB73 of path 11 (Figure 6B; Supplemental Table 8). MYB70 and MYB73 are closely related members of the R2R3 MYB family subgroup 22 (Stracke et al., 2001). While little is known for MYB70, MYB73 and other members of this subfamily are positive regulators of auxin signalling (Zhao et al., 2014; Yang et al., 2020) and MYB31 is an interactor of phytochrome A (Zhao et al., 2014; Yan et al., 2020; Yang et al., 2020). In contrast to their regulation of up-regulated genes in Col-0, MYB88 and FUF1 were predicted

regulators of down-regulated genes in *ein3-1* and at the later time point of 240 mins, thus indicating complexities in timing and TF hierarchies.

In summary, the DREM modelling identified a chronology of regulatory events and expands knowledge on involved transcription factors beyond the well-known key regulators of mitochondrial dysfunction that activate the established stress-response such as ANAC017 and ANAC013. These additional transcription factors, many with a role in ethylene or auxin signalling, fine-tune this response to adjust growth and metabolism when mitochondrial function is restricted.

Ethylene-activated signalling precedes auxin-related pathways in the mitochondrial stress response

Previous work has established an antagonistic relationship between auxin and mitochondrial signalling (Ivanova et al., 2014; Kerchev et al., 2014). More recent evidence has also pointed to a role of ethylene for the regulation of mitochondrial biogenesis and proteotoxic stress (Wang and Auwerx, 2017; Kacprzak et al., 2020; Jurdak et al., 2021). Given that the attenuated AA response in *ein3-1* (Figure 5C,F), enrichment of EIN3 binding sites (Figure 5D), ethylene-related GO term enrichment for AA-responsive DEGs (Figure 5G) and the regulatory events predicted by the DREM model (Figure 6) consistently pointed to a role of auxin and ethylene in the mitochondrial stress response, we further analysed our RNA-seq data to gain an understanding of the transcriptional changes for the two hormonal pathways. To do this, we generated two manually curated lists that encompass genes with auxin or ethylene-related annotations in TAIR10, GO term lists and from recent literature reviews involving biosynthesis, transport, conjugation, signalling, and response (Lavy and Estelle, 2016; Dubois et al., 2018; Casanova-Sáez et al., 2021; Pattyn et al., 2021). Furthermore, we focused only on those genes that were responsive to the AA treatment (Supplemental Tables 11 and 12).

As observed for the whole DEG lists (Figure 5), with only a few exceptions the response of auxin and ethylene-related genes was attenuated in *ein3-1* (Figure 7). For the ethylene-related genes, four were early responsive to both treatments (*ACS11*, *ERF019*, *ERF042* and the ACC conjugase *GAMMA-GLUTAMYL TRANSPEPTIDASE* (*GGT*) *1*) but showed a more pronounced induction after spraying with AA. Three more ERFs were the among earliest AA-induced ethylene-related genes, namely ERF#011, *ERF100* and *ABR1*, indicating an early activation of the ethylene signalling pathway after AA treatment. Also, early responsive was the *ARGOS-LIKE* (*ARL*) gene which encodes a member of the ARGOS family of proteins. *ARL* expression is induced by ethylene in an EIN3-dependent

manner, as confirmed by our RNA-seq data, and controls organ size (Hu et al., 2006; Rai et al., 2015). *RAP2.3* had a late and similar response to both treatments in Col-0, but a stronger response to mock spray in *ogo-1* (Figure 7). *RAP2.3* belongs to the class VII ERF which are part of the N-end rule pathway and regulators of hypoxia responses (Hartman et al., 2019). *HRE2*, another class VII ERF which was a close neighbour to the AOX1a in the co-expression network (Figure 1A), was also up-regulated later in the time course at 120 mins and remained highly expressed. Up-regulated already at 30 mins and throughout the whole time course were *MKK9* and *ACS6*, while *ACS2* was strongly up-regulated above 16-fold beyond 270 mins after AA treatment. Current evidence suggests that stress-induced activation of the MKK9-MPK3/6 module leads to phosphorylation of ACS2 and ACS6. The phosphorylation of these two ethylene biosynthesis enzymes leads to their stabilisation and subsequent enhanced ethylene production. (Liu and Zhang, 2004; Zhao and Guo, 2011). There is also evidence that the activation of MKK9-MPK3/6 pathway results in the phosphorylation and stabilisation of EIN3 (Yoo et al., 2008).

Among the earliest auxin-related genes up-regulated by the AA treatment was *YUCCA5* (*YUC5*) (Figure 7). This gene encodes one of eleven isoforms for the enzyme that catalyses the final step in the main auxin biosynthesis pathway (Casanova-Sáez et al., 2021), and more specifically in roots and young vegetative tissues (Woodward et al., 2005). There is also evidence that YUC5, together with other YUC family members, is localised to the ER membrane (Kriechbaumer et al., 2017). Also early induced is *RUB1 CONJUGATING ENZYME 1* (RCE1) which is part of the SCF^{TIR} complex. This complex targets AUX/IAA proteins for degradation, leading to the subsequent activation of auxin-induced genes. RCE1 has also a role in the regulation of ethylene biosynthesis as mutation leads to ethylene overproduction (Larsen and Cancel, 2004). Many of the auxin genes responding at 120 mins after AA treatment were related to auxin response, i.e. *IAA4*, *IAA10*, *SAUR36* and *SAUR59* (Figure 7). The two IAA genes belong to the family of transcriptional repressors of auxin signalling (Lavy and Estelle, 2016), and their up-regulation might have a function in blocking the repressive impact of auxin on mitochondrial signalling (Ivanova et al., 2014; Kerchev et al., 2014). Both *SAUR* genes have been implicated in the co-ordination of auxin and brassinosteroid signalling in development (Yu et al., 2011), with SAUR36 also promoting leaf senescence (Hou et al., 2013). Another set of genes showing an AA response at this time point relate to auxin conjugation, i.e. *GH3.2*, *GH3.3*, *GGP1*, *ILL6*, *UGT74E2* (Figure 7). These enzymes modulate the concentration of the free active form of auxin, indole acetic acid (IAA), through the (reversible) inactivation of IAA by conjugation to low molecular weight metabolites such as sugars or amino acids (Casanova-Sáez et al., 2021). AA-induced after

180 mins or later were several auxin transporters (*ABCB4*, *ABCB9*, *PILS3*) and genes encoding enzymes of IAA precursor biosynthesis (*TRYPTOPHAN BIOSYNTHESIS* (*TRP*) *1*, *TRP2*, *TRP3*; *ANTHRANILATE SYNTHASE ALPHA SUBUNIT* (*ASA*) *1*; *INDOLE-3-GLYCEROL PHOSPHATE SYNTHASE*; *CYP71B6*; *NITRILASE 2*) (Figure 7). The up-regulation of these genes coincides with the down-regulation of many AA-stress marker genes (Figure 5F) and suggests an increased auxin biosynthesis and altered distribution to inhibit the mitochondrial stress response as observed after external auxin application (Ivanova et al., 2014; Kerchev et al., 2014).

Taken together, these results show a complex interplay of components of the ethylene and auxin signalling pathways to modulate mitochondrial retrograde signalling. The early upregulation of ethylene marker genes, activation of the MKK9-MPK3/6 module and subsequently ethylene biosynthesis genes suggest an initiation of ethylene signalling pathways preceding the activation of auxin. An induction of auxin biosynthesis by ethylene is well documented (Stepanova et al., 2005; Stepanova et al., 2008), and this might be an important mechanism in the regulation of mitochondrial retrograde signalling.

ChIP-seq identifies auxin- and ethylene related genes targeted by ANAC017

The involvement of ethylene and auxin signalling pathways in modulating the mitochondrial retrograde response raised the question how these signalling pathways are activated upon mitochondrial dysfunction. A prime target for further investigation was ANAC017 given that it is a key regulator of mitochondrial stress signalling.

To test this, we conducted ChIP-seq experiments by treating Arabidopsis seedlings expressing a GFP-ANAC017 fusion protein with AA and myxothiazol (MT) to induce a mitochondrial stress response. For controls we used seedlings sprayed with 0.1% Tween solutions and sampling was conducted at 180 mins after treatments. Using the MACS2 software for peak detection from the ChIP-seq data (Gaspar, 2018), we determined the 200 most significant target genes for the AA treatment which had an enrichment factor of at least above 7 and a -log10(q) above 42 (Supplemental Table 13). Out of these, 178 were also highly significant (-log10(q) < 5) in the myxothiazol treatment (Supplemental Table 13). Among the most significant target genes were the MDS genes *AOX1a* and *OGO*, confirming their regulation by ANAC017 and thus validating the ChIP-seq experiment (Figure 8A) (De Clercq et al., 2013). Highly significant ChIP-seq peaks were detected for four auxin-related genes: the auxin transporter ABCB4, the auxin conjugating enzyme UGT74E2, the transcriptional repressor IAA16 and the biosynthesis gene *YUC5* (Figure 8A). These genes were also induced by AA in time course experiment (Figure 7). ANAC017 also binds to the

promoters of the five ethylene-related genes with function in signalling (*MKK9*, *ERF8*, *INFLORESCENCE DEFICIENT IN ABSCISSION* (*IDA*)) and biosynthesis (*ACS2*, *S-ADENOSYLMETHIONINE DECARBOXYLASE* (*SAMDC*)). Their regulation by ANAC017 is further supported by the higher expression of these genes, except for *IAA16*, in plants overexpressing ANAC017 (Figure 8B) (Meng et al., 2019). This was also the case for another ANAC017 target, WRKY25, which was a regulator of the AA response predicted by the DREM model (Figure 6).

Thus, our data provides first evidence that ANAC017 is not only a regulator of genes mitigating mitochondrial stress such as *AOX1a*, but also regulates the expression of several genes involved in the biosynthesis and signalling of ethylene and auxin. Especially the direct targeting of MKK9 and ACS2 by ANAC017 provides a mechanism for ethylene-mediated modulation of retrograde signalling that also involves EIN3 (Figure 9). This explains the contribution of ANAC017 to many stress responses depending on mitochondrial function and ethylene signalling such as senescence, hypoxia or submergence (Kim et al., 2018; Wagner et al., 2018; Meng et al., 2019; Bui et al., 2020; Meng et al., 2020; Broda et al., 2021).

DISCUSSION

Plant responses to adverse growth conditions or more severe stresses require the balancing of resource availability with their allocation. The acclimation to unfavourable conditions is often driven by preserving energy and limiting growth to ensure survival. Although this has been established as an adaptive mechanism to cope with non-optimal conditions, it is a bottleneck to improve crop stress tolerance without impacting growth. Overexpression of key regulators often leads to reduced growth and thus decreases productivity under non-limiting conditions. Hence a more refined manipulation of acclimation pathways is necessary, however understanding of the involved regulatory processes is often still lacking (Zhang et al., 2020). Through their role in providing ATP by oxidative phosphorylation and in turning over substrates for metabolic adjustment, mitochondria are ideally positioned to sense changes in energy demand and metabolism, but also mitigate and drive such changes through plasticity in the involved pathways. Examples are the alternative pathways based on the activities of AOX and NDBs in the mitochondrial electron transport chain allowing for the decoupling of electron flow with ATP production and the non-cyclic fluxes of TCA cycle intermediates (Sweetlove et al., 2010; Millar et al., 2011).

Previous studies also revealed that overexpression of the master regulator of mitochondrial retrograde signalling, ANAC017, leads to retarded growth in Arabidopsis and the up-regulation of senescence-, cell death- and ER unfolded protein response-related genes (Meng et al., 2013; Broda et al., 2021). Furthermore, the MDS gene *OGO* is up-regulated by the ethylene precursor ACC and after ethylene signalling-mediated senescence and submergence treatments. Although this, together with its annotation as ACO-like protein, suggests OGO is part of an ethylene-dependent pathway that links with the MRR, its molecular function in the process still needs further investigation. Together with *AOX1a*, *OGO* is also under transcriptional control by the ERF HRE2 and ANAC017. Deeper understanding on the pathways ANAC017 is directly regulating to exert such an effect was missing. The combination of the RNA-seq and ChIP-seq data set in this study provides a direct mechanism for the dual role of ANAC017 in regulating mitochondrial signalling and growth (Figure 9). The early up-regulation of ethylene pathway genes and the direct binding of ANAC017 to the promoters of some of these genes, especially MKK9 and ACS2, suggests an increase in ethylene biosynthesis promoting the mitochondrial stress response. MKK9 also stimulates the MPK3/6 cascade leading to the phosphorylation and stabilisation of another ethylene biosynthesis enzyme ACS6. Consistent with this, activation of MPK3 and MPK6 after AA or cyanide treatment by triggering mitochondrial ROS production has

been observed before (Chang et al., 2012) and our work suggests MKK9 as the activating kinase after induction by ANAC017 (Figure 9). The activation of MPKs has been observed within minutes of stress imposition which would allow for an immediate initiation of the MRR (Ichimura et al., 2000; Zhao et al., 2017). Apart from ACS6, other components of the ethylene pathway, i.e. ERF6, ERF104 and EIN3 itself (Yoo et al., 2008; Bethke et al., 2009; Meng et al., 2013) are also targets of MPK3/6. A role of ethylene and the master regulator of ethylene signalling EIN3 in the MRR is also supported by the dual control of AOX1a, MKK9 and NDB2 by both ANAC017 and EIN3 (Figure 9). In addition, the auxin efflux carriers PIN1 and PIN6 are also targeted by MPK3/6 (Ditengou et al., 2018; Dory et al., 2018). This may explain the identification of PIN1 as one of the regulators of AOX1a expression (Ivanova et al., 2014). Hence the up-regulation of MKK9, and further activation of the MPK3/6 cascade, by ANAC017 has potentially a broader effect on growth. In agreement with this, increased expression of MKK9 has a similar effect as ANAC017 overexpression in promoting senescence (Xu et al., 2008; Zhou et al., 2009; Meng et al., 2019; Broda et al., 2021).

The interaction of auxin and ethylene signalling pathways is complex and both synergistic and antagonistic relationships have been described depending on the analysed processes and tissues (Muday et al., 2012). Together with other recent studies, our findings suggest that both hormones balance the timing and amplitude of the MRR. This is in agreement with other studies showing an involvement of ethylene in the stimulation of the MRR (Wang and Auwerx, 2017; Jurdak et al., 2021). By contrast, auxin represses the MRR and thus provides a regulatory feedback loop (Ivanova et al., 2014; Kerchev et al., 2014). The diminished AA-response in the *ein3-1* mutant demonstrates that ethylene promotes the MRR and the induction of many genes in the down-stream cascade is dependent of EIN3. Importantly, components of both hormone pathways are under direct control of ANAC017 and the two hormones are also major regulators of plant development (Muday et al., 2012), thus providing a direct mechanism to control mitochondrial stress signalling and growth by action of the same transcription factor. This regulatory interaction could be based on balanced biosynthesis of each hormone as ANAC017, as shown by ChIP-seq here, directly activates genes encoding proteins involved in ethylene biosynthesis (ACS2, ACS6 via MKK) and IAA biosynthesis, transport or conjugation (YUC5, ABCB4, UGT74E2) (Figure 9). Reciprocal regulation of both biosynthetic pathways has been demonstrated. While increased levels of auxin lead to induction of ethylene biosynthesis (Růžička et al., 2007; Stepanova et al., 2007; Swarup et al., 2007), ethylene also induces auxin synthesis (Stepanova et al., 2005; Stepanova et al., 2008). This is further complicated by local

synthesis in, and transport between, tissues for both hormones (Brumos et al., 2018). This, in combination with our results, suggests that two transcriptional waves control the MRR. First an increased ethylene biosynthesis activated by ANAC017 induces the MRR and subsequent elevated auxin biosynthesis, induced by ethylene and ANAC017 in tandem, shuts down the MRR. The severe growth retardation of plants overexpressing ANAC017 might be caused by the constitutive induction of the ethylene pathway as increased ethylene production generally leads to a reduction in growth as observed for ethylene over-accumulating plants. More specifically, ethylene restricts plant growth via the epidermis by controlling local auxin biosynthesis and transport (Vaseva et al., 2018). This tissue-specific regulation increases the complexity of putative ethylene-auxin interaction with the MRR and complicates the interpretation of results obtained by harvesting whole organs (Brumos et al., 2018). A tissue-specific regulation of the MRR is supported by recent evidence from an experiment based on laser capture microdissection of leaves followed by RNA-seq and demonstrating differences in the transcriptional responses, including ethylene- and auxin-related genes, to AA treatment (Berkowitz et al., 2021). Therefore, our suggested model will have to be refined with more detailed spatio-temporally resolved data.

The time-resolved regulatory DREM network indicated that ANAC017 controls the maintained AA-response of highly up-regulated genes. Together with a number of other transcription factors it also regulates genes with moderate up- or down-regulation that are associated to growth responses and diverge early in their regulatory trajectory from the gene directly involved in the mitochondrial stress response. While the former was driven mainly by ANAC and WRKY family transcription factors that are known as the major stress regulatory TF families, the latter was based on MYB and HB transcription factors as regulators of gene down-regulated by AA treatment. The HB family is mainly regulating plant growth and development, and three out of the five AA-responsive HBs identified by the DREM model were from the HD-Zip I subfamily (Perotti et al., 2017). One of them, HB5, is a repressor of the auxin signalling component IAA12 and hence might be involved in the control of auxin regulated growth, whereas HB13 and HB40 are regulating cell proliferation and branching, respectively (De Smet et al., 2013; Ribone et al., 2015; González-Grandío et al., 2017). Among the MYB family transcription factors was KUA1 that controls ROS homeostasis to modulate leaf cell expansion and organ size (Lu et al., 2014). The identified MYB transcription factors belonging to the MYB3R subfamily and these are implicated in cell division to control organ development, hence they function provides another level to adjust plant growth to mitochondrial dysfunction (Kobayashi et al., 2015; Yang et al., 2021). The DREM model suggests that distinct transcription factors drive the primary stress-

response to maintain mitochondrial function, while a more subtle and diverse response to adjust growth is controlled by a different set of transcription factors. This is further supported by the changes in the regulatory events predicted by the DREM model when ethylene signalling is altered as for the *ein3-1* mutant. This opens the possibility that, to a certain extent, the two responses are separable and modifiable to allow for a specific stress response in non-optimal environments without an associated growth penalty under standard growth conditions.

In summary, our findings support a model for the dual control of the MRR by ethylene and auxin controlled by direct activation via ANAC017. In this model, early activation of key genes involved in ethylene signalling and biosynthesis, including EIN3, promotes the MRR to mitigate mitochondrial dysfunction. Subsequent activation of auxin biosynthesis, transport and conjugation, also enhanced by ethylene-induced auxin biosynthesis, increases IAA levels that repress the MRR. This feedback loop allows for finely tuned response to mitochondrial dysfunction and co-ordination with growth.

MATERIALS AND METHODS

Plant Material and Growth Conditions

The *Arabidopsis thaliana* Columbia-0 (Col-0; CS70000) accession was used as the wild type control for all experiments. The *ein3-1* mutant was described previously (Binder et al., 2007). The *ogo-1* mutant was obtained from the Nottingham Arabidopsis Stock Centre (SALK_107806). T-DNA insertion in the gene At5g43450 (OGO) was confirmed by PCR and Sanger sequencing. Additionally, RNA-seq data confirmed T-DNA integration and gene knockout without impacting expression of neighbouring genes (Supplemental Figure 1). GUS reporter lines for OGO were generated by PCR amplification of the 1 kb region upstream of the OGO translation start site and cloning into the vector pGPTV-BAR using Gibson assembly (Gibson et al., 2009). The proANAC017-GFP-ANAC017 line used for ChIP-seq was generated by PCR amplification of the 2kb region of ANAC017 and the coding region of ANAC017 and subsequent assembly ensuring translational fusion of GFP and ANAC017 in the vector pK7m34GW using Gateway methodology (Invitrogen). All constructs were verified by Sanger sequencing. Transgenic lines carrying these construct were generated by the Agrobacterium tumefaciens-mediated transformation using the floral dip method (Clough and Bent, 1998). Representative lines were selected from progeny of 30 independent events.

For experiments on plates, seeds were surface sterilized, stratified at 4°C for 48 h and sown on B5 medium supplemented with 1% sucrose and 0.75% (w/v) agar. Plants were then grown in a 14 h/10 h light/dark photoperiod at 22°C and 100 µmol m^{-2} sec^{-1} photosynthetic photon flux density. For antimycin A treatments, plants grown on plates for 10 days were sprayed with either 50 µM antimycin/0.01% Tween20 solution or for controls with only 0.01% Tween solutions. Plants were harvested at indicated time points in parallel for both treatments. For senescence experiments and submergence treatments plants were grown on soil in controlled environment growth rooms in a 14 h/10 h light/dark photoperiod at 22°C and 120 µmol m^{-2} sec^{-1} photosynthetic photon flux density. Submergence experiments were performed as described previously (Meng et al., 2020). Briefly, 4-week-old plants were completely submerged in water for the indicated time periods in the same light regime and then removed for continued growth for desubmergence.

Biochemical assays

GUS reporter assays were performed as described previously (Bowling et al., 1994). For chlorophyll extraction, leaf material (50 mg) was incubated in pre-chilled 100% methanol overnight in the dark. After complete extraction, chlorophyll in the supernatants was

quantified at 666 nm and 653 nm with a spectrophotometer (BMG, ClarioSTAR) as previously described (Lichtenthaler, 1987). The maximum quantum yield of photosystem II (Fv/Fm) was determined after 20 min of dark acclimation using a Chlorophyll Fluorescence System (Photon Systems Instruments).

Quantitative real-time PCR

Total RNA was isolated from homogenised tissue using the Spectrum™ Plant Total RNA kit (Sigma) according to the manufacturer's protocol. Removal of genomic DNA was performed with the On-Column DNase I (Sigma) digestion kit prior to RNA elution. For qRT-PCR, cDNA was generated using the Tetro cDNA Synthesis Kit (Bioline) and then used to perform qPCR with the SensiFAST SYBR & Fluorescein Kit (Bioline) on a QuantStudio™ 12K Flex Real-Time PCR system (Applied Biosystems). The PCR conditions were 95°C for 2 min; 40 cycles of 95°C for 20 sec; 60°C for 30 sec with primers as listed in Supplemental Table 14. Data was analysed using the QuantStudio™ 12K Flex software (Applied Biosystems). All experiments were performed with at least three biological replicates.

RNA-seq and bioinformatic analysis

Total RNA was extracted as described above for three biological replicates for each genotype and sampling time point. RNA-seq libraries were generated with the TruSeq Stranded mRNA Library Prep Kit and sequenced on a NextSeq500 instrument (both Illumina) as 70 bp reads with an average quality score (Q30) of above 93% and an average of 13.2 million reads per sample. Quality control was performed using the FastQC software (https://www.bioinformatics.babraham.ac.uk/projects/fastqc/). Transcript abundances as transcripts per million (TPM) and estimated counts were quantified on a gene level by pseudo-aligning reads against a k-mer index build from the representative transcript models downloaded for the Araport 11 annotation (Cheng et al., 2017) using a k-mer lenth of 31 using the kallisto program with 100 bootstraps (Bray et al., 2016). The program sleuth with a likelihood ratio test was used to test for differential gene expression (Pimentel et al., 2017). Only genes with at least 5 counts in half of all samples per time point were included in this analysis. Differentially expressed genes (DEGs) were called with a false discovery rate FDR < 0.05 and a $|\log2 \text{ (fold change)}| > 1$. Overlaps in the list of DEGs across the different genotypes were identified and represented using UpSet plots (Conway et al., 2017). For further analyses, hierarchical clustering and generation of heat maps the Partek Genomics software suite version 6.16 (Partek Incorporated, http://www.partek.com/) was used. GO term enrichment analysis was performed using the ClueGO plugin for Cytoscape (Bindea et al., 2009). The DREM analysis was performed as described with default parameters (Schulz et al., 2012).

ChIP-seq

The ChIP experiments were performed as described (Bowler et al., 2004; Berckmans et al., 2011) with minor modifications with three biological replicates per treatment. The proANAC017:GFP-ANAC017 line was grown under a 16 h day/ 8 h night photoperiod at 23°C with 100 µmol.$m^{-2}s^{-1}$ photosynthetic photon flux density for 12 days on B5 media with 1% sucrose, 0.8% (w/v) agar. Seedlings were sprayed with 50 µM antimycin A (AA)/0.01% Tween20 solution, 50 µM myxothiazol (MT)/0.01% Tween20 solution or 0.01% Tween20 for mock treatment. Three hours post-treatment, seedlings were harvested, rinsed twice with 10 mM HEPES-NaOH and vacuum-infiltrated with 10 mM HEPES-NaOH/1% (v/v) formaldehyde solution. Formaldehyde was quenched by adding 67 µl of 2 M glycine per ml of fixation buffer and vacuum-infiltration for 2 min. Seedlings were then washed with 10mM HEPES-NaOH, dried with paper tower and snap-frozen. Chromatin was isolated from nuclei of 2 g of seedlings and fragmented into ~500 bp by sonication with a Bioruptor sonicator (Diagenode). Samples were pre-cleared with 80 µl Dynal Protein A magnetic beads (Thermo Fisher Scientific) for at least 2 h at 4ºC with gentle agitation. Ten µg of anti-GFP antibody were coupled to 50 µl Dynal Protein A Dynabeads (Thermo Fisher Scientific) overnight at 4ºC and equal amounts of sonicated chromatin subsequently added for overnight incubation at 4ºC. A mock sample without antibody input was used as control. Beads were washed twice with low salt buffer (50 mM Tris-HCl pH7.4, 150 mM NaCl, 2 mM EDTA, 0.5% Triton X-100), high salt (50 mM Tris-HCl pH 7.4, 500 mM NaCl, 2 mM EDTA, 0.5% Triton X-100), and final wash buffer (50 mM Tris-HCl pH 7.4, 50 mM NaCl, 2 mM EDTA). Samples were decross-linked and digested with proteinase K digestion before the DNA was purified using QIAquick PCR Purification Kit (Qiagen).

ChIP-Seq libraries were generated with the Accel-NGS® 2S Plus DNA Library Kit following the manufacturer's instructions (Swift Biosciences) and sequenced on a NextSeq500 platform (Illumina) with an 84 bp read length. Reads were mapped to the Arabidopsis reference genome (TAIR10) using Bowtie2 (Langmead and Salzberg, 2012). ChIP-seq peaks were called with the MACS2 software using default parameters (Zhang et al., 2008).

Data availability

RNA-seq read data and ChIP-seq read data are deposited at the NCBI SRA database under project ID PRJNA745499 and PRJNA699617, respectively.

FIGURES

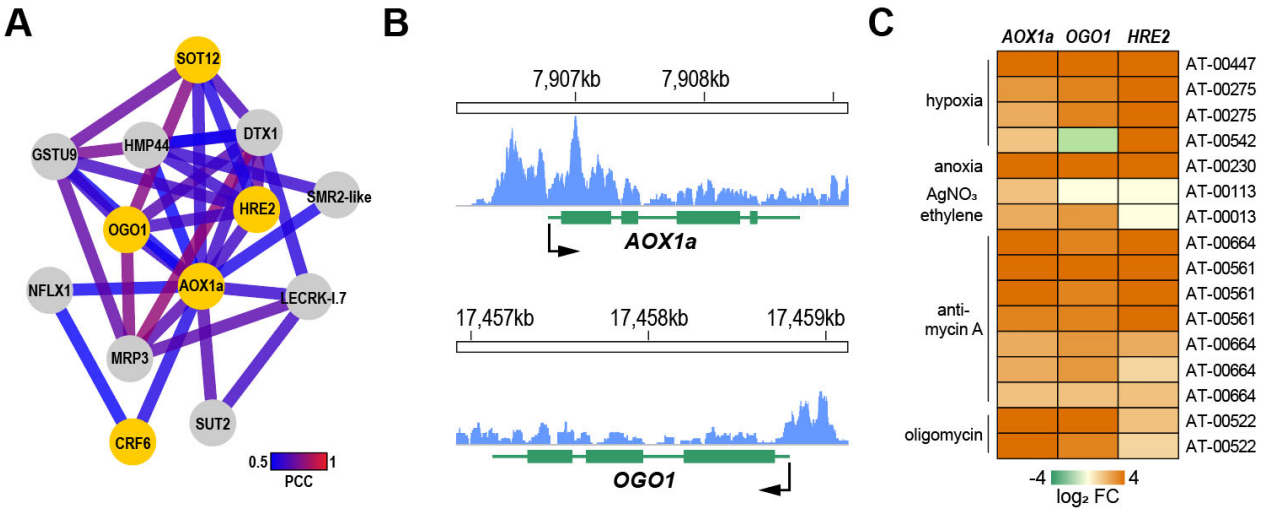

Figure 1. A co-expression network of *AOX1a* involves ethylene-signalling related genes
A. A co-expression network analysis for *AOX1a* with the CoNekT tool kit (Proost and Mutwil, 2018) identified twelve genes with highly correlated gene expression patterns. In the resulting network two genes close to *AOX1a* were related to ethylene signalling, i.e. the *ETHYLENE RESPONSE FACTOR ERF71/HRE2* and *OGO*. Edge color represents the Pearson correlation coefficient (PCC). Genes of the mitochondrial dysfunction stimulon are represented by orange circles (De Clercq et al., 2013). B. HRE2 binds to the promoters of *AOX1a* and *OGO*. Shown are genome browser views of the ChIP-seq read coverage at the promoters of the two genes. ChIP-seq data was downloaded from the NCBI SRA database (SRR8234099) and aligned to the TAIR10 Arabidopsis genome release. Both genes were among the significant peak calls as identified previously by Lee and Bailey-Serres (2019). C. Heatmap showing induced expression of *AOX1a*, *OGO* and *HRE2* in various experiments involving ethylene-dependent signalling (hypoxia, anoxia), altering ethylene tissue-concentrations (ethylene gas, $AgNO_3$) or induce mitochondrial stress (antimycin A, oligomycin). Publicly available gene expression data was retrieved using the Genevestigator platform and data set IDs are indicated (Hruz et al., 2008).

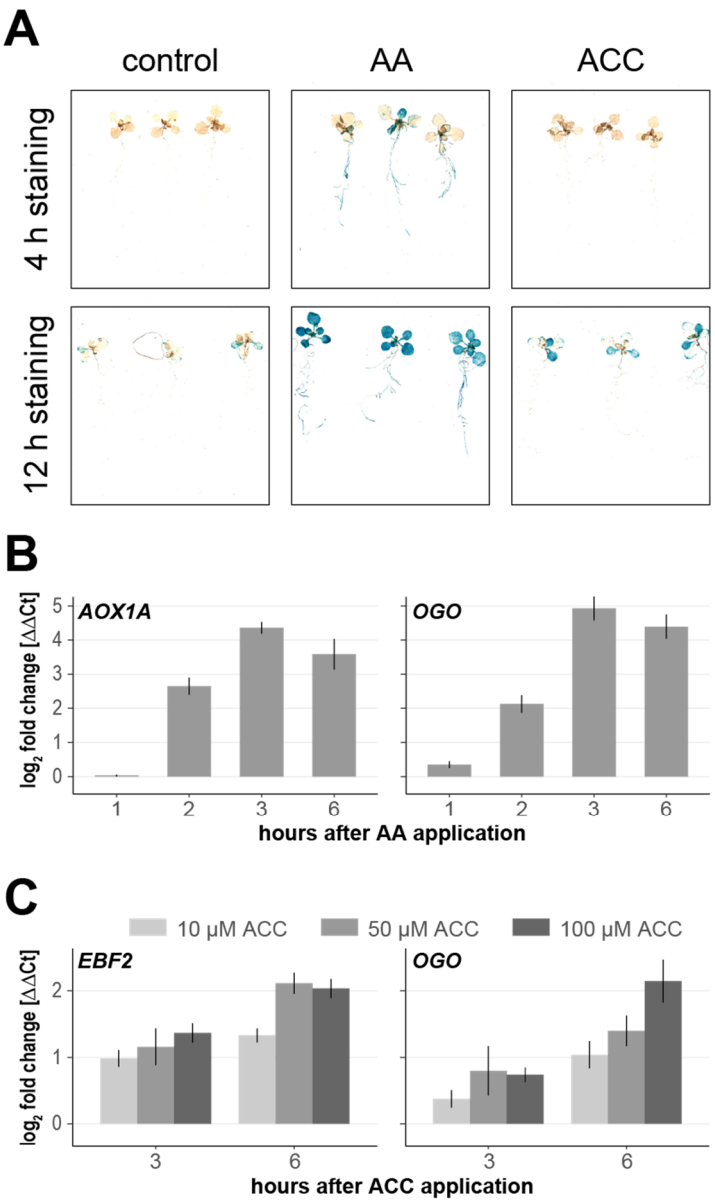

Figure 2. Induced expression of *OGO* by ACC and AA treatment

OGO expression is up-regulated by 1-aminocyclopropane-1-carboxylic acid (ACC) and antimycin A (AA) treatment. A. *proOGO-GUS* reporter lines were treated with AA to induce mitochondrial dysfunction or ACC to increase ethylene tissue concentrations. For both treatments an increased GUS activity was detected after 4 h and 12 h of staining, respectively. Shown are representative images of three biological replicates. B. Increased expression of OGO after AA and ACC treatments in wild type Col-0 was also quantified by qRT-PCR. *AOX1a* and *EBF2* were used as known response genes for the treatments, respectively. Seedlings were grown on plates for 10 d, sprayed with 50 µM AA or varying ACC concentrations as indicated and harvested 3 h post treatment. Shown are the means ± SE for three biological replicates.

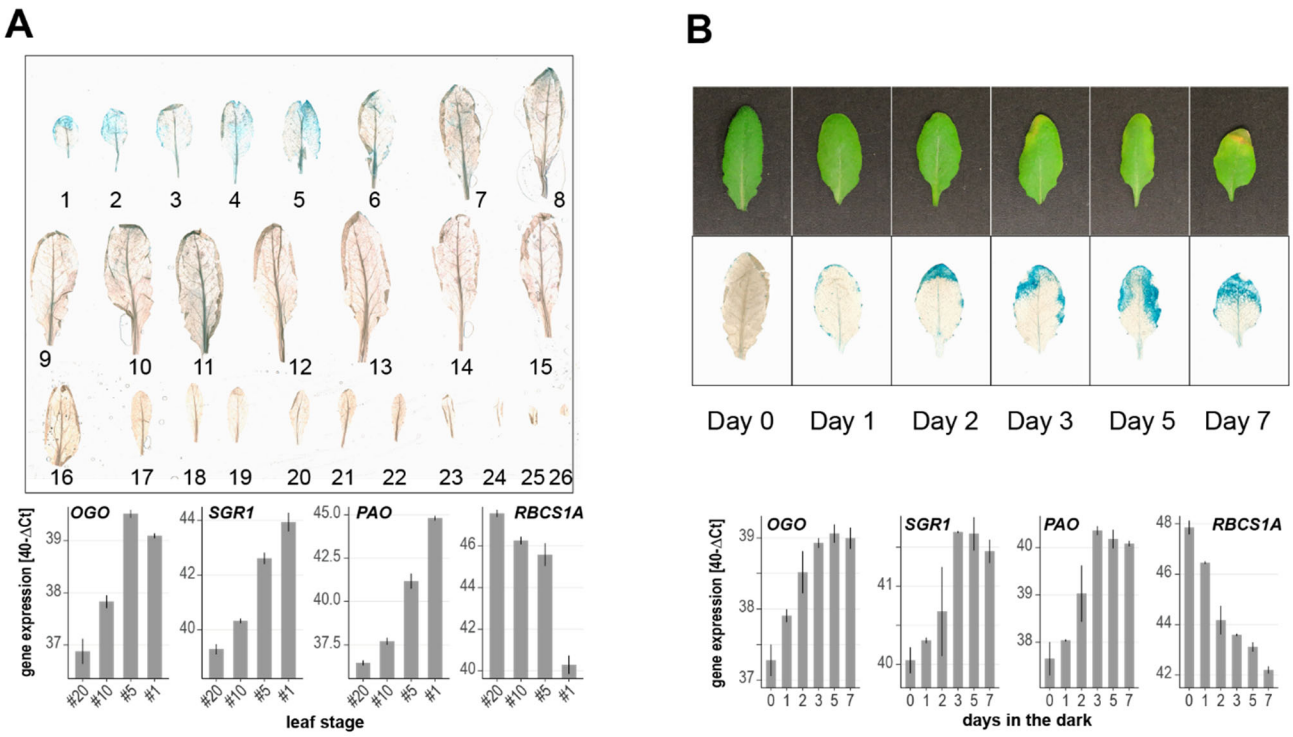

Figure 3. Expression of *OGO* is increased in senescing leaves

The expression of *OGO* is induced during age-dependent and dark-induced senescence in leaves. A. GUS activity in rosette leaves of a representative *proOGO-GUS* reporter line. Leaves are numbered by the sequence of their occurrence through development. GUS staining was highest in the oldest, senescing leaves and not detectable in young leaves. *OGO* expression was also quantified by qRT-PCR in wild type Col-0 for the indicated leaf developmental stages. The expression of the senescence marker genes *SENESCENCE-RELATED GENE 1* (*SRG1*), *PHEOPHORBIDE A OXYGENASE* (*PAO*) and *RIBULOSE BISPHOSPHATE CARBOXYLASE SMALL CHAIN 1A* (*RBCS1A*) was also determined. Shown are the means ± SE for three biological replicates. B. *OGO* promoter activity in reporter lines was also increased by dark-induced senescence. Plants were kept in the dark for up to seven days as indicated before GUS staining. Expression of genes was also quantified by qRT-PCR as described in (A).

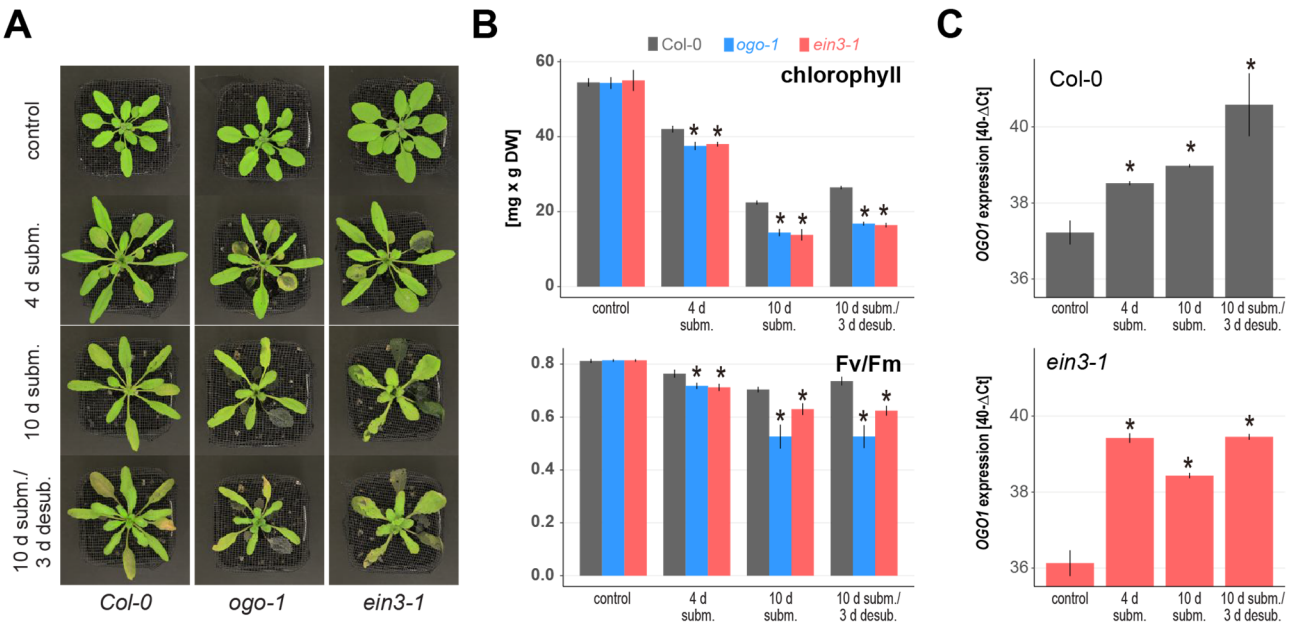

Figure 4. Mutation of *OGO* and *EIN3* decreases tolerance to submergence

The mutant lines for *OGO* (*ogo-1*) and *EIN3* (*ein3-1*) showed a similar reduction in submergence tolerance. Shown are (A) representative images, (B) chlorophyll concentrations and maximum quantum efficiency of photosystem II (Fv/Fm) and (C) the expression of *OGO* in wild type (Col-0), *ein3-1* and *ogo-1* mutant lines before submergence (control), after four- and ten-days submergence and three days after desubmergence as indicated. For mutants, asterisks indicate statistically significant differences (*, $P < 0.05$) from Col-0. Significant differences were identified by one-way ANOVA followed by Tukey's multiple comparison test. Shown are the means ± SE for three biological replicates.

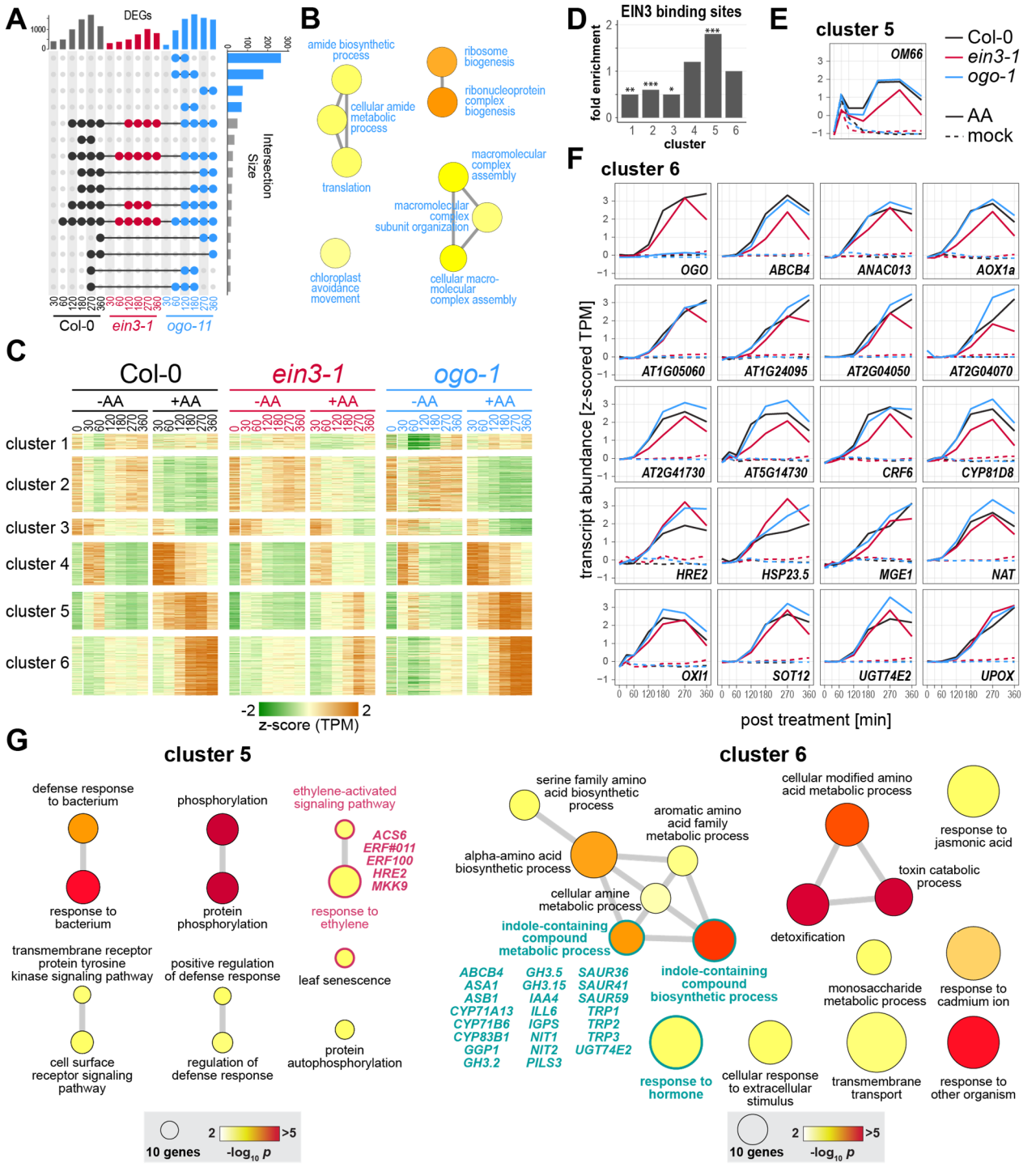

Figure 5. Impaired ethylene-signalling in the *ein3-1* mutant attenuates the transcriptional response to mitochondrial dysfunction. A time course RNA-seq experiment was performed by treatment of Col-0, *ein3-1* mutant and *ogo-1* mutant lines with antimycin A (AA) to induced mitochondrial stress or with water as control treatment. Samples of three biological replicates were taken at the indicated timepoints for RNA-seq analysis. A. UpSet plot representation of overlaps in differentially expressed genes (DEGs; |log2(fold change AA vs control)| > 1, FDR < 0.05) for the comparisons of AA and control treatments at the same time point (Conway et al., 2017). The vertical bar chart gives the number of DEGs in the three genotypes at the different time points and the horizontal bar chart the number of overlapping DEGs in the intersects indicated by connected dots. B. GO terms enriched (p<0.001 after Bonferroni correction) for the *ogo-1*-specific DEGs in the four largest intersects (indicated by blue, horizontal bars) as shown in (A). C. A self-organism maps algorithm identified six clusters of DEGs with shared expression patterns across the three genotypes and time points. D. Enrichment of EIN3 binding sites in promoters of genes in clusters 1 to 6. The gene lists for the six clusters were cross-referenced with a list of identified promoter binding sites for EIN3 (Chang et al., 2013). Enrichment was calculated by a hypergeometric test with asterisks indicating statistical significance (* p < 0.05, ** p < 0.01, ***p < 0.001). E, F. Expression profiles in the AA and control treatments across Col-0, *ein3-1* and *ogo-1* for the mitochondrial dysfunction stimulon genes (De Clercq et al., 2013). These genes were included in cluster 6 except for *OM66* in cluster 5. G. Enriched GO terms (p<0.001 after Bonferroni correction) for DEGs in clusters 5 and 6, respectively. Genes related to ethylene signalling in cluster 5 (magenta) or auxin signalling in cluster 6 (turquoise) are listed. Circle sizes represent the number of genes included in the GO term and circle colour the significance of enrichment as indicated.

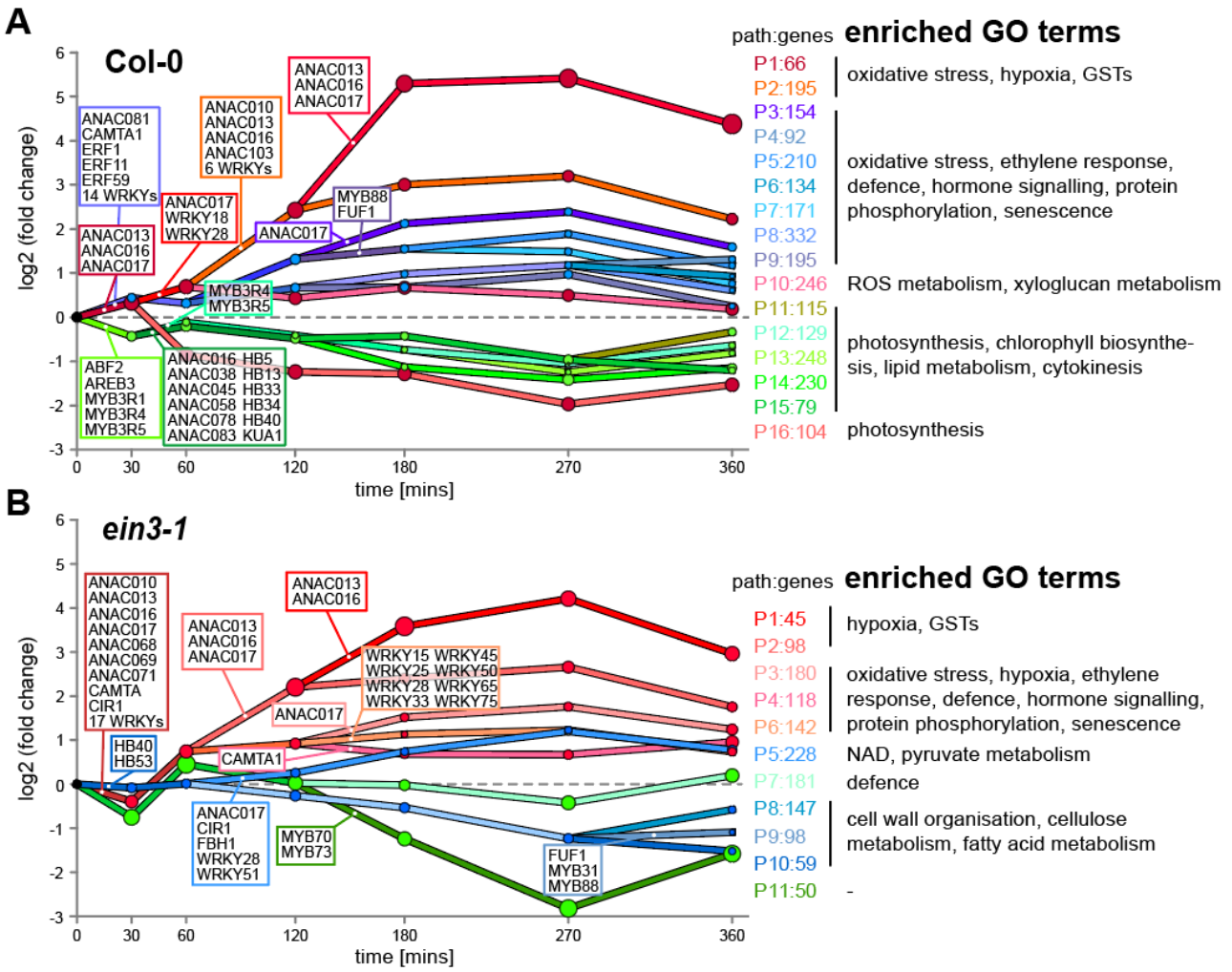

Figure 6. DREM analysis for the AA response in wild type and *ein3-1*

DREM modelling reveals differences in the sequence of regulatory events that govern the transcriptional response to mitochondrial stress in wild type and *ein3-1*. DREM models for Col-0 (A) and *ein3-1* (B) show groups of co-expressed genes in 16 and 11 paths, respectively, with transcription factors underlying the separation of genes into different paths indicated for major furcation events. Paths emanating from the three primary paths are coloured in red, blue or green. The y-axis gives the average expression of genes in the paths and node areas are proportional to the standard deviation of the distribution of genes associated with them. Number of genes in each path and a summary of enriched GO terms ($p<0.001$ after Bonferroni correction) are indicated on the right (see Supplemental Table 5-10 for all genes, TFs associated with regulatory events and details for GO term enrichment for all paths).

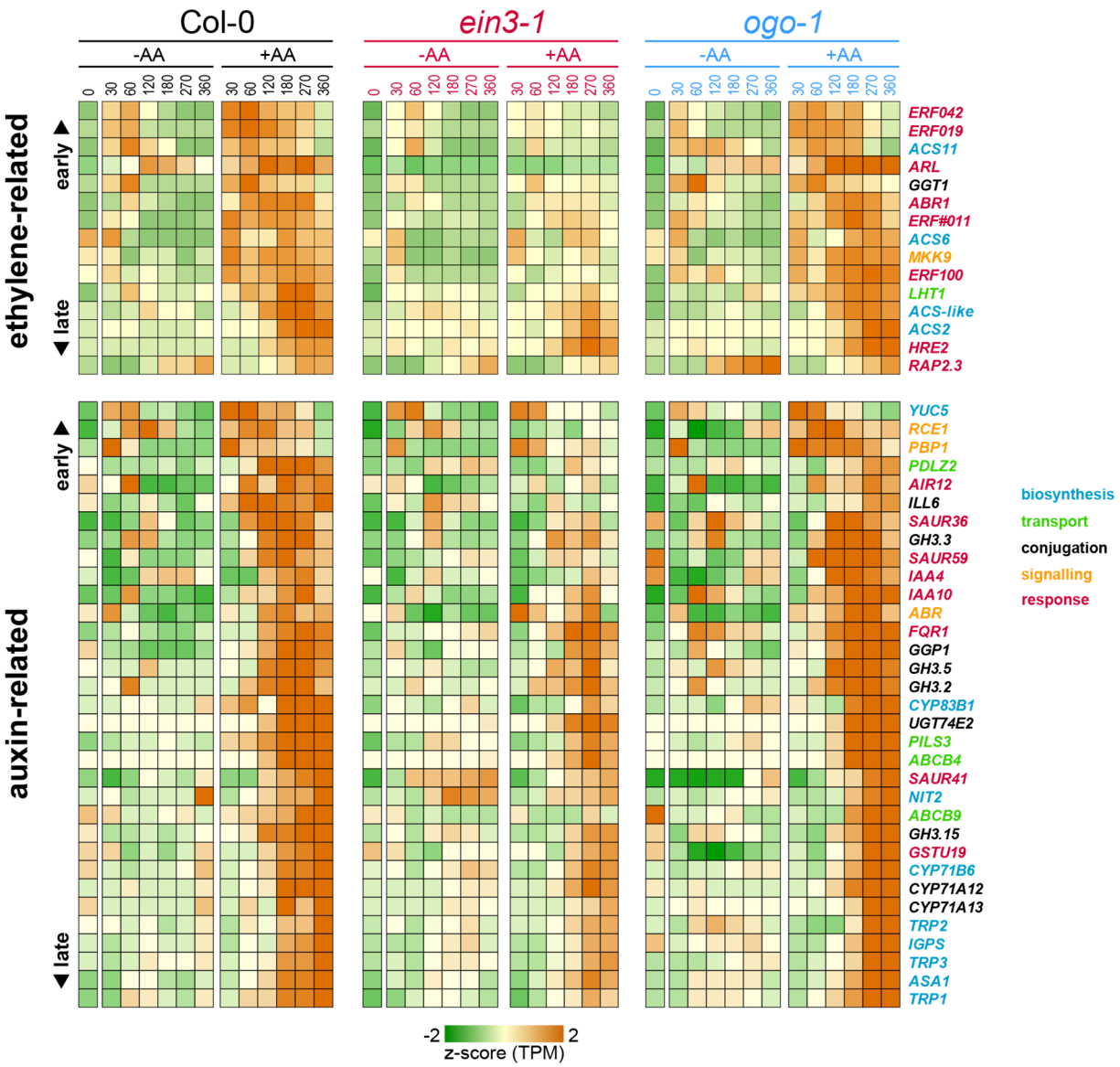

Figure 7. Changes in gene expression of genes associated with ethylene- and auxin signalling or homeostasis

From the list of DEGs responsive those related to ethylene or auxin biosynthesis, transport, conjugation, signalling or response were identified and manually curated based on their annotations in TAIR10, GO term lists and from recent literature reviews (Supplemental Table 11 and 12) (Lavy and Estelle, 2016; Dubois et al., 2018; Casanova-Sáez et al., 2021; Pattyn et al., 2021). A heatmap of their expression over the time course experiments is shown with gene names coloured according to their function. Genes responding early to treatment are at the top of each heatmap, while late-responsive genes are at the bottom.

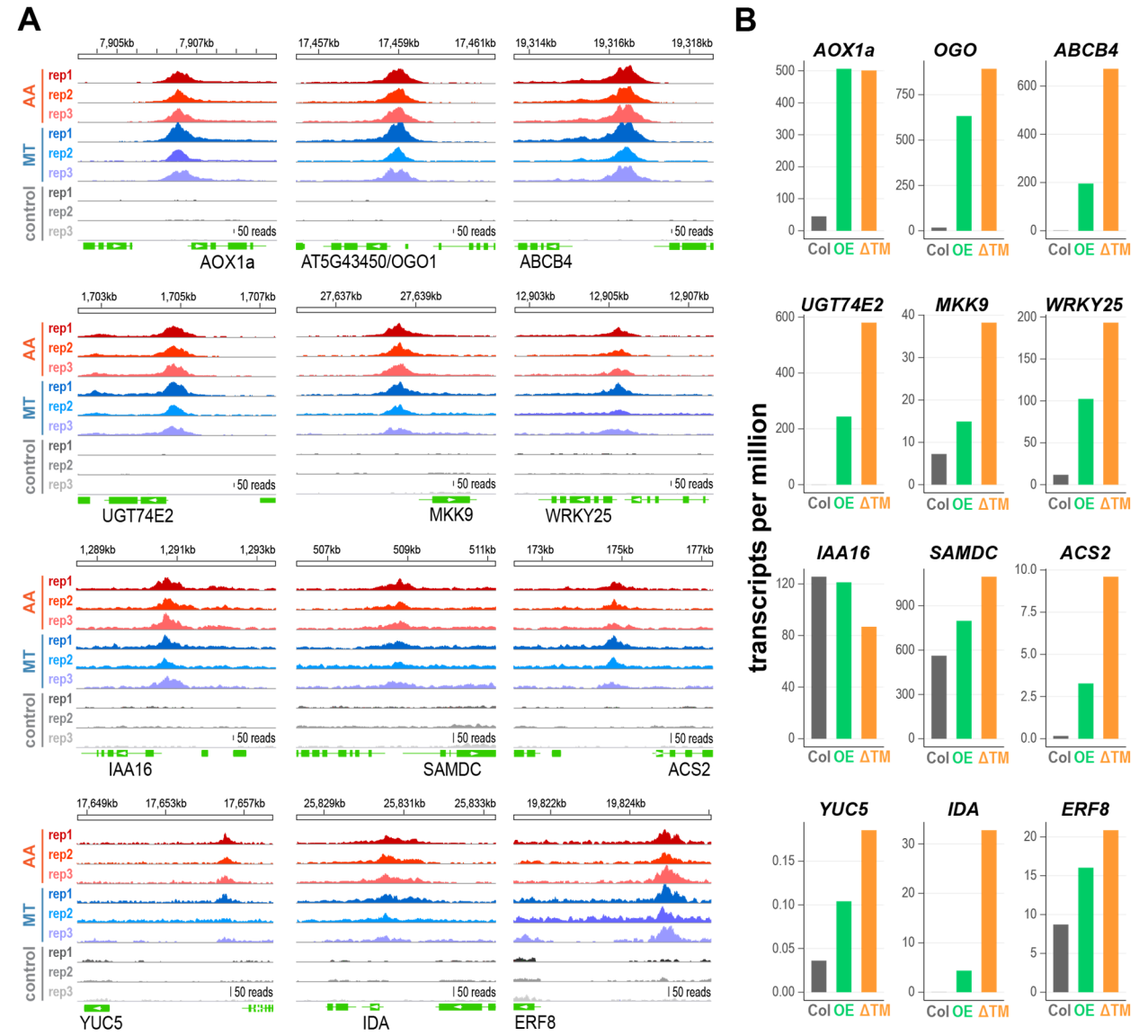

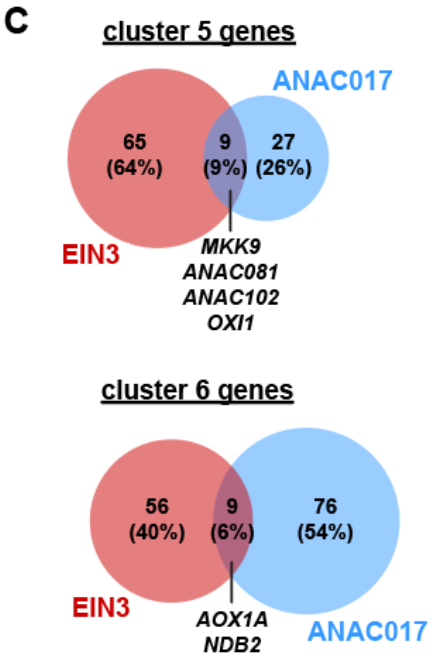

Figure 8. ANAC017 binds to the promoters of several ethylene and auxin-related genes

A. Binding of ANAC017 to the promoters of target genes was determined by ChIP-seq experiments using a transgenic line expressing a GFP-ANAC017 fusion protein under the control of the native *ANAC017* promoter. ChIP-seq was performed after induction of mitochondrial stress by spraying with antimycin A (AA) or myxothiazol (MT), or with water as control treatment. Shown are read coverages around the promoter of associated genes for three biological replicates. *AOX1a* also given for comparison as a known ANAC017 target (De Clercq et al., 2013). B. Expression of the ANAC017 target genes identified by ChIP-seq as shown in (A) in two *ANAC017* overexpression lines (*ANAC017OE3, OE; ANAC017ΔTMOE3, ΔTM*). Data was retrieved from a previously published experiment (Meng et al., 2019). C. Regulation of mitochondrial stress-responsive genes by ANAC017 and EIN3. The Venn diagram shows the overlaps in the AA responsive genes in clusters 5 and 6 (Figure 5c) for which their promoters bind ANAC017 and EIN3. The target gene list of EIN3 has been retrieved from a previously published ChIP-seq experiment (Chang et al., 2013). Relevant genes regulated by both transcription factors are indicated.

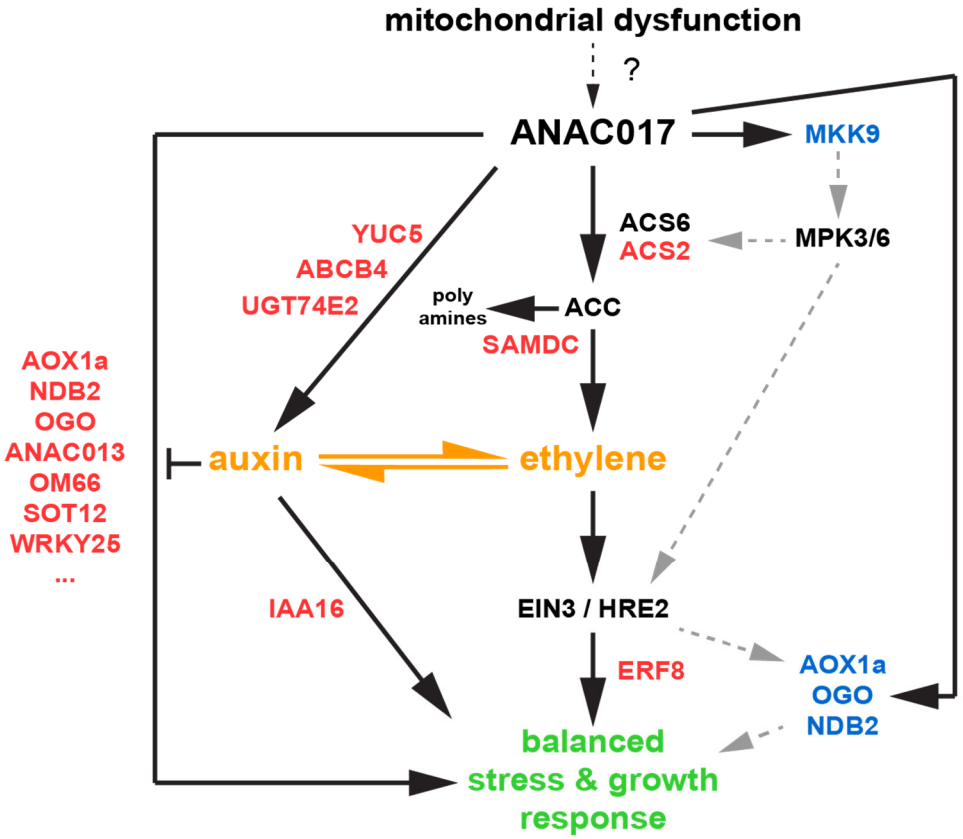

Figure 9. Model for the ANAC017-dependent regulation of the mitochondrial dysfunction response involving ethylene and auxin

While ANAC017 directly induces the expression of stress genes such as *AOX1a*, *NDB2* or *OGO,* it also activates in parallel components of ethylene (*MKK9*, *ACS2*, *ERF8*, *SAMDC*) and auxin (*YUC5*, *UGT74E2*, *ABCB4*, *IAA16*) pathways to fine-tune and balance the acute stress response with plant growth. EIN3 also targets *AOX1a*, *NDB2* and *MKK9*, allowing for dual regulation by the two transcription factors, while HRE2 bind to the promoters of *AOX1a* and *OGO*. Genes associated with steps in the pathway and directly targeted by ANAC017 are highlighted in red, while genes dually targeted by ANAC017 and EIN3 or HRE2 are highlighted in blue. Reciprocal interaction of ethylene and auxin is indicated by orange arrows. See text for details.

SUPPLEMENTAL MATERIAL

Supplemental Figure 1: Characterisation of *ogo-1* mutant

A. Schematic representation of T-DNA insertion site in the ogo-1 mutant (SALK_107806). Primer binding site used for the characterisation of the insertion site are indicated.

B. Genome browser view for read alignments of RNA-seq data for antimycin A treated plants. No reads could be detected beyond the confirmed T-DNA insertion site, confirming the non-functionality of the OGO gene in the ogo-1 mutant

Supplemental Tables for review of this thesis are available under this link:

https://cloudstor.aarnet.edu.au/plus/s/83LUtu4DKzu5EsL

Password: HECunman!2021

Supplemental Table 1: Differentially expressed genes for the comparison of antimycin A versus mock treatments. Given are the log2 values (AA vs mock) for statistically signifcant genes (FDR < 0.05) with an at least two-fold change

Supplemental Table 2: z-scored TPM values for differentially expressed genes (Supplemental Table 1) after clustering using a self-organising maps algorithm (Figure 5C)

Supplemental Table 3: GO term enrichment (p<0.001) for OGO-specifc DEG as shown in Figure 5B

Supplemental Table 4: GO term enrichment (p<0.001) for cluster 5 and 6 genes as shown in Figure 5G

Supplemental Table 5: Output of the DREM model for Col-0 (Figure 6A)

Supplemental Table 6: Gene in each path for the DREM model of Col-0 (Figure 6A)

Supplemental Table 7: GO term enrichment (p<0.001) for genes in Col-0 DREM model paths

Supplemental Table 8: Output of the DREM model for ein3-1 (Figure 6B)

Supplemental Table 9: Gene in each path for the DREM model of ein3-1 (Figure 6B)

Supplemental Table 10: GO term enrichment ($p<0.001$) for genes in ein3-1 DREM model paths

Supplemental Table 11: Ethylene-related DEGs responsive to AA treatment (Figure 7)

Supplemental Table 12: Auxin-related DEGs responsive to AA treatment (Figure 7)

Supplemental Table 13: ChIP-seq peaks for ANAC017 target genes. Given is the significance for each detected peak for the antimycin A and myxothiazol treatments as the -log10(q-value)

Supplemental Table 14: Primers used in this study

ACKNOWLEDGEMENTS

We thank Asha Haslem for technical assistance with RNA-seq library generation and the La Trobe University Genomics Platform for access to next-generation sequencing equipment.

.

LITERATURE CITED

Berkowitz O, Xu Y, Liew LC, Wang Y, Zhu Y, Hurgobin B, Lewsey MG, Whelan J (2021) RNA-seq analysis of laser microdissected Arabidopsis thaliana leaf epidermis, mesophyll and vasculature defines tissue-specific transcriptional responses to multiple stress treatments. The Plant Journal, in press, DOI: 10.1111/tpj.15314

Bethke G, Unthan T, Uhrig JF, Pöschl Y, Gust AA, Scheel D, Lee J (2009) Flg22 regulates the release of an ethylene response factor substrate from MAP kinase 6 in Arabidopsis thaliana via ethylene signaling. Proceedings of the National Academy of Sciences **106:** 8067-8072

Bindea G, Mlecnik B, Hackl H, Charoentong P, Tosolini M, Kirilovsky A, Fridman WH, Pagès F, Trajanoski Z, Galon J (2009) ClueGO: a Cytoscape plug-in to decipher functionally grouped gene ontology and pathway annotation networks. Bioinformatics **25:** 1091-1093

Binder BM, Walker JM, Gagne JM, Emborg TJ, Hemmann G, Bleecker AB, Vierstra RD (2007) The Arabidopsis EIN3 binding F-Box proteins EBF1 and EBF2 have distinct but overlapping roles in ethylene signaling. Plant Cell **19:** 509-523

Bowling SA, Guo A, Cao H, Gordon AS, Klessig DF, Dong X (1994) A mutation in Arabidopsis that leads to constitutive expression of systemic acquired resistance. The Plant cell **6:** 1845-1857

Braam J (2005) In touch: plant responses to mechanical stimuli. New Phytol **165:** 373-389

Broda M, Khan K, O'Leary B, Pružinská A, Lee CP, Millar AH, Van Aken O (2021) Increased expression of ANAC017 primes for accelerated senescence. Plant Physiology

Brumos J, Robles LM, Yun J, Vu TC, Jackson S, Alonso JM, Stepanova AN (2018) Local Auxin Biosynthesis Is a Key Regulator of Plant Development. Developmental Cell **47:** 306-318.e305

Bui LT, Shukla V, Giorgi FM, Trivellini A, Perata P, Licausi F, Giuntoli B (2020) Differential submergence tolerance between juvenile and adult Arabidopsis plants involves the ANAC017 transcription factor. The Plant Journal **104:** 979-994

Casanova-Sáez R, Mateo-Bonmatí E, Ljung K (2021) Auxin Metabolism in Plants. Cold Spring Harbor Perspectives in Biology **13**

Chang KN, Zhong S, Weirauch MT, Hon G, Pelizzola M, Li H, Huang S-SC, Schmitz RJ, Urich MA, Kuo D, Nery JR, Qiao H, Yang A, Jamali A, Chen H, Ideker T, Ren B, Bar-Joseph Z, Hughes TR, Ecker JR (2013) Temporal transcriptional response to ethylene gas drives growth hormone cross-regulation in Arabidopsis. eLife **2:** e00675-e00675

Chang R, Jang CJH, Branco-Price C, Nghiem P, Bailey-Serres J (2012) Transient MPK6 activation in response to oxygen deprivation and reoxygenation is mediated by mitochondria and aids seedling survival in Arabidopsis. Plant Molecular Biology **78:** 109-122

Chen W-H, Li P-F, Chen M-K, Lee Y-I, Yang C-H (2015) FOREVER YOUNG FLOWER negatively regulates ethylene response DNA-binding factors by activating an ethylene-responsive factor to control Arabidopsis floral organ senescence and abscission. Plant Physiology **168:** 1666-1683

Cheng CY, Krishnakumar V, Chan AP, Thibaud-Nissen F, Schobel S, Town CD (2017) Araport11: a complete reannotation of the Arabidopsis thaliana reference genome. Plant J **89:** 789-804

Clifton R, Millar AH, Whelan J (2006) Alternative oxidases in Arabidopsis: A comparative analysis of differential expression in the gene family provides new insights into

function of non-phosphorylating bypasses. Biochimica et Biophysica Acta (BBA) - Bioenergetics **1757:** 730-741

Clough SJ, Bent AF (1998) Floral dip: a simplified method for Agrobacterium-mediated transformation of Arabidopsis thaliana. Plant J **16:** 735-743

Conway JR, Lex A, Gehlenborg N (2017) UpSetR: an R package for the visualization of intersecting sets and their properties. Bioinformatics **33:** 2938-2940

Crawford T, Lehotai N, Strand Å (2018) The role of retrograde signals during plant stress responses. J Exp Bot **69:** 2783-2795

De Clercq I, Vermeirssen V, Van Aken O, Vandepoele K, Murcha MW, Law SR, Inzé A, Ng S, Ivanova A, Rombaut D, van de Cotte B, Jaspers P, Van de Peer Y, Kangasjärvi J, Whelan J, Van Breusegem F (2013) The Membrane-Bound NAC Transcription Factor ANAC013 Functions in Mitochondrial Retrograde Regulation of the Oxidative Stress Response in Arabidopsis The Plant Cell **25:** 3472-3490

De Smet I, Lau S, Ehrismann JS, Axiotis I, Kolb M, Kientz M, Weijers D, Jürgens G (2013) Transcriptional repression of BODENLOS by HD-ZIP transcription factor HB5 in Arabidopsis thaliana. Journal of experimental botany **64:** 3009-3019

Ditengou FA, Gomes D, Nziengui H, Kochersperger P, Lasok H, Medeiros V, Paponov IA, Nagy SK, Nádai TV, Mészáros T, Barnabás B, Ditengou BI, Rapp K, Qi L, Li X, Becker C, Li C, Dóczi R, Palme K (2018) Characterization of auxin transporter PIN6 plasma membrane targeting reveals a function for PIN6 in plant bolting. New Phytologist **217:** 1610-1624

Doll J, Muth M, Riester L, Nebel S, Bresson J, Lee H-C, Zentgraf U (2020) Arabidopsis thaliana WRKY25 Transcription Factor Mediates Oxidative Stress Tolerance and Regulates Senescence in a Redox-Dependent Manner. Frontiers in Plant Science **10**

Dopp IJ, Yang X, Mackenzie SA (2021) A new take on organelle-mediated stress sensing in plants. New Phytologist **230:** 2148-2153

Dory M, Hatzimasoura E, Kállai BM, Nagy SK, Jäger K, Darula Z, Nádai TV, Mészáros T, López-Juez E, Barnabás B, Palme K, Bögre L, Ditengou FA, Dóczi R (2018) Coevolving MAPK and PID phosphosites indicate an ancient environmental control of PIN auxin transporters in land plants. FEBS Letters **592:** 89-102

Dubois M, Van den Broeck L, Inzé D (2018) The Pivotal Role of Ethylene in Plant Growth. Trends in Plant Science **23:** 311-323

Furuta KM, Yadav SR, Lehesranta S, Belevich I, Miyashima S, Heo J-o, Vatén A, Lindgren O, De Rybel B, Van Isterdael G, Somervuo P, Lichtenberger R, Rocha R, Thitamadee S, Tähtiharju S, Auvinen P, Beeckman T, Jokitalo E, Helariutta Y (2014) Arabidopsis NAC45/86 direct sieve element morphogenesis culminating in enucleation. Science **345:** 933-937

Galon Y, Aloni R, Nachmias D, Snir O, Feldmesser E, Scrase-Field S, Boyce JM, Bouché N, Knight MR, Fromm H (2010) Calmodulin-binding transcription activator 1 mediates auxin signaling and responds to stresses in Arabidopsis. Planta **232:** 165-178

Gao S, Gao J, Zhu X, Song Y, Li Z, Ren G, Zhou X, Kuai B (2016) ABF2, ABF3, and ABF4 Promote ABA-Mediated Chlorophyll Degradation and Leaf Senescence by Transcriptional Activation of Chlorophyll Catabolic Genes and Senescence-Associated Genes in Arabidopsis. Mol Plant **9:** 1272-1285

Gasch P, Fundinger M, Müller JT, Lee T, Bailey-Serres J, Mustroph A (2015) Redundant ERF-VII Transcription Factors Bind to an Evolutionarily Conserved cis-Motif to Regulate Hypoxia-Responsive Gene Expression in Arabidopsis. The Plant Cell **28:** 160-180

Gaspar JM (2018) Improved peak-calling with MACS2. bioRxiv**:** 496521

Gibson DG, Young L, Chuang R-Y, Venter JC, Hutchison CA, Smith HO (2009) Enzymatic assembly of DNA molecules up to several hundred kilobases. Nature Methods **6:** 343-345

Gladman NP, Marshall RS, Lee K-H, Vierstra RD (2016) The Proteasome Stress Regulon Is Controlled by a Pair of NAC Transcription Factors in Arabidopsis. The Plant Cell **28:** 1279-1296

González-Grandío E, Pajoro A, Franco-Zorrilla JM, Tarancón C, Immink RGH, Cubas P (2017) Abscisic acid signaling is controlled by a BRANCHED1/HD-ZIP I cascade in Arabidopsis axillary buds. Proceedings of the National Academy of Sciences **114:** E245-E254

Haga N, Kato K, Murase M, Araki S, Kubo M, Demura T, Suzuki K, Müller I, Voß U, Jürgens G, Ito M (2007) R1R2R3-Myb proteins positively regulate cytokinesis through activation of KNOLLE transcription in Arabidopsis thaliana. Development **134:** 1101-1110

Hartman S, Liu Z, van Veen H, Vicente J, Reinen E, Martopawiro S, Zhang H, van Dongen N, Bosman F, Bassel GW, Visser EJW, Bailey-Serres J, Theodoulou FL, Hebelstrup KH, Gibbs DJ, Holdsworth MJ, Sasidharan R, Voesenek LACJ (2019) Ethylene-mediated nitric oxide depletion pre-adapts plants to hypoxia stress. Nature Communications **10:** 4020

Hou K, Wu W, Gan SS (2013) SAUR36, a small auxin up RNA gene, is involved in the promotion of leaf senescence in Arabidopsis. Plant Physiol **161:** 1002-1009

Hruz T, Laule O, Szabo G, Wessendorp F, Bleuler S, Oertle L, Widmayer P, Gruissem W, Zimmermann P (2008) Genevestigator V3: A Reference Expression Database for the Meta-Analysis of Transcriptomes. Advances in Bioinformatics **2008:** 420747

Hu Y, Poh HM, Chua N-H (2006) The Arabidopsis ARGOS-LIKE gene regulates cell expansion during organ growth. The Plant Journal **47:** 1-9

Ichimura K, Mizoguchi T, Yoshida R, Yuasa T, Shinozaki K (2000) Various abiotic stresses rapidly activate Arabidopsis MAP kinases ATMPK4 and ATMPK6. Plant J **24:** 655-665

Ivanova A, Law SR, Narsai R, Duncan O, Lee JH, Zhang B, Van Aken O, Radomiljac JD, van der Merwe M, Yi K, Whelan J (2014) A Functional Antagonistic Relationship between Auxin and Mitochondrial Retrograde Signaling Regulates Alternative Oxidase1a Expression in Arabidopsis. Plant Physiol **165:** 1233-1254

Jurdak R, Launay-Avon A, Paysant-Le Roux C, Bailly C (2021) Retrograde signalling from the mitochondria to the nucleus translates the positive effect of ethylene on dormancy breaking of Arabidopsis thaliana seeds. New Phytologist **229:** 2192-2205

Kacprzak SM, Dahlqvist A, Van Aken O (2020) The transcription factor ANAC017 is a key regulator of mitochondrial proteotoxic stress responses in plants. Philosophical Transactions of the Royal Society B: Biological Sciences **375:** 20190411

Kerchev PI, De Clercq I, Denecker J, Mühlenbock P, Kumpf R, Nguyen L, Audenaert D, Dejonghe W, Van Breusegem F (2014) Mitochondrial Perturbation Negatively Affects Auxin Signaling. Molecular Plant **7:** 1138-1150

Kim HJ, Park J-H, Kim J, Kim JJ, Hong S, Kim J, Kim JH, Woo HR, Hyeon C, Lim PO, Nam HG, Hwang D (2018) Time-evolving genetic networks reveal a NAC troika that negatively regulates leaf senescence in Arabidopsis. Proceedings of the National Academy of Sciences **115:** E4930-E4939

Kim J, Kim JH, Lyu JI, Woo HR, Lim PO (2017) New insights into the regulation of leaf senescence in Arabidopsis. Journal of Experimental Botany **69:** 787-799

Kobayashi K, Suzuki T, Iwata E, Nakamichi N, Suzuki T, Chen P, Ohtani M, Ishida T, Hosoya H, Müller S, Leviczky T, Pettkó-Szandtner A, Darula Z, Iwamoto A, Nomoto M, Tada Y, Higashiyama T, Demura T, Doonan JH, Hauser M-T,

Sugimoto K, Umeda M, Magyar Z, Bögre L, Ito M (2015) Transcriptional repression by MYB3R proteins regulates plant organ growth. The EMBO Journal **34:** 1992-2007
Kong S-G, Wada M (2014) Recent advances in understanding the molecular mechanism of chloroplast photorelocation movement. Biochimica et Biophysica Acta (BBA) - Bioenergetics **1837:** 522-530
Kriechbaumer V, Botchway SW, Hawes C (2017) Localization and interactions between Arabidopsis auxin biosynthetic enzymes in the TAA/YUC-dependent pathway. Journal of Experimental Botany **68:** 4195-4207
Kwon Y, Kim JH, Nguyen HN, Jikumaru Y, Kamiya Y, Hong S-W, Lee H (2013) A novel Arabidopsis MYB-like transcription factor, MYBH, regulates hypocotyl elongation by enhancing auxin accumulation. Journal of Experimental Botany **64:** 3911-3922
Langmead B, Salzberg SL (2012) Fast gapped-read alignment with Bowtie 2. Nature Methods **9:** 357-359
Larsen PB, Cancel JD (2004) A recessive mutation in the RUB1-conjugating enzyme, RCE1, reveals a requirement for RUB modification for control of ethylene biosynthesis and proper induction of basic chitinase and PDF1.2 in Arabidopsis. The Plant Journal **38:** 626-638
Lavy M, Estelle M (2016) Mechanisms of auxin signaling. Development **143:** 3226-3229
Lee TA, Bailey-Serres J (2019) Integrative Analysis from the Epigenome to Translatome Uncovers Patterns of Dominant Nuclear Regulation during Transient Stress. The Plant Cell **31:** 2573-2595
Licausi F, Van Dongen JT, Giuntoli B, Novi G, Santaniello A, Geigenberger P, Perata P (2010) HRE1 and HRE2, two hypoxia-inducible ethylene response factors, affect anaerobic responses in Arabidopsis thaliana. The Plant Journal **62:** 302-315
Lichtenthaler HK (1987) [34] Chlorophylls and carotenoids: Pigments of photosynthetic biomembranes. *In* Methods in Enzymology, Vol 148. Academic Press, pp 350-382
Liu Y, Zhang S (2004) Phosphorylation of 1-aminocyclopropane-1-carboxylic acid synthase by MPK6, a stress-responsive mitogen-activated protein kinase, induces ethylene biosynthesis in Arabidopsis. Plant Cell **16:** 3386-3399
Liu Y, Zhang S (2004) Phosphorylation of 1-Aminocyclopropane-1-Carboxylic Acid Synthase by MPK6, a Stress-Responsive Mitogen-Activated Protein Kinase, Induces Ethylene Biosynthesis in Arabidopsis[W]. The Plant Cell **16:** 3386-3399
Loreti E, van Veen H, Perata P (2016) Plant responses to flooding stress. Current Opinion in Plant Biology **33:** 64-71
Lu D, Wang T, Persson S, Mueller-Roeber B, Schippers JHM (2014) Transcriptional control of ROS homeostasis by KUODA1 regulates cell expansion during leaf development. Nature Communications **5:** 3767
Meng X, Li L, De Clercq I, Narsai R, Xu Y, Hartmann A, Claros DL, Custovic E, Lewsey MG, Whelan J, Berkowitz O (2019) ANAC017 Coordinates Organellar Functions and Stress Responses by Reprogramming Retrograde Signaling. Plant Physiology **180:** 634-653
Meng X, Li L, Narsai R, De Clercq I, Whelan J, Berkowitz O (2020) Mitochondrial signalling is critical for acclimation and adaptation to flooding in Arabidopsis thaliana. The Plant Journal **103:** 227-247
Meng X, Xu J, He Y, Yang KY, Mordorski B, Liu Y, Zhang S (2013) Phosphorylation of an ERF transcription factor by Arabidopsis MPK3/MPK6 regulates plant defense gene induction and fungal resistance. Plant Cell **25:** 1126-1142
Merendino L, Courtois F, Grübler B, Bastien O, Straetmanns V, Chevalier F, Lerbs-Mache S, Lurin C, Pfannschmidt T (2020) Retrograde signals from mitochondria reprogramme skoto-morphogenesis in Arabidopsis thaliana via alternative oxidase 1a. Philosophical Transactions of the Royal Society B: Biological Sciences **375:** 20190567

Millar AH, Whelan J, Soole KL, Day DA (2011) Organization and Regulation of Mitochondrial Respiration in Plants. Annual Review of Plant Biology **62:** 79-104
Muday GK, Rahman A, Binder BM (2012) Auxin and ethylene: collaborators or competitors? Trends Plant Sci **17:** 181-195
Müller M, Munné-Bosch S (2015) Ethylene Response Factors: A Key Regulatory Hub in Hormone and Stress Signaling. Plant Physiology **169:** 32-41
Ng S, Ivanova A, Duncan O, Law SR, Van Aken O, De Clercq I, Wang Y, Carrie C, Xu L, Kmiec B, Walker H, Van Breusegem F, Whelan J, Giraud E (2013) A membrane-bound NAC transcription factor, ANAC017, mediates mitochondrial retrograde signaling in Arabidopsis. Plant Cell **25:** 3450-3471
Noh B, Murphy AS, Spalding EP (2001) Multidrug resistance-like genes of Arabidopsis required for auxin transport and auxin-mediated development. Plant Cell **13:** 2441-2454
O'Malley Ronan C, Huang S-shan C, Song L, Lewsey Mathew G, Bartlett A, Nery Joseph R, Galli M, Gallavotti A, Ecker Joseph R (2016) Cistrome and Epicistrome Features Shape the Regulatory DNA Landscape. Cell **165:** 1280-1292
Pattyn J, Vaughan-Hirsch J, Van de Poel B (2021) The regulation of ethylene biosynthesis: a complex multilevel control circuitry. New Phytologist **229:** 770-782
Peng H, Zhao J, Neff MM (2015) ATAF2 integrates Arabidopsis brassinosteroid inactivation and seedling photomorphogenesis. Development **142:** 4129-4138
Perotti MF, Ribone PA, Chan RL (2017) Plant transcription factors from the homeodomain-leucine zipper family I. Role in development and stress responses. IUBMB Life **69:** 280-289
Pimentel H, Bray NL, Puente S, Melsted P, Pachter L (2017) Differential analysis of RNA-seq incorporating quantification uncertainty. Nat Meth **14:** 687-690
Proost S, Mutwil M (2018) CoNekT: an open-source framework for comparative genomic and transcriptomic network analyses. Nucleic Acids Research **46:** W133-W140
Rai MI, Wang X, Thibault DM, Kim HJ, Bombyk MM, Binder BM, Shakeel SN, Schaller GE (2015) The ARGOS gene family functions in a negative feedback loop to desensitize plants to ethylene. BMC Plant Biology **15:** 157
Reddy AS, Reddy VS, Golovkin M (2000) A calmodulin binding protein from Arabidopsis is induced by ethylene and contains a DNA-binding motif. Biochem Biophys Res Commun **279:** 762-769
Ribone PA, Capella M, Chan RL (2015) Functional characterization of the homeodomain leucine zipper I transcription factor AtHB13 reveals a crucial role in Arabidopsis development. J Exp Bot **66:** 5929-5943
Růžička K, Ljung K, Vanneste S, Podhorská R, Beeckman T, Friml Ji, Benková E (2007) Ethylene Regulates Root Growth through Effects on Auxin Biosynthesis and Transport-Dependent Auxin Distribution. The Plant Cell **19:** 2197-2212
Schulz MH, Devanny WE, Gitter A, Zhong S, Ernst J, Bar-Joseph Z (2012) DREM 2.0: Improved reconstruction of dynamic regulatory networks from time-series expression data. BMC Systems Biology **6:** 104
Shapiguzov A, Vainonen JP, Hunter K, Tossavainen H, Tiwari A, Järvi S, Hellman M, Aarabi F, Alseekh S, Wybouw B, Van Der Kelen K, Nikkanen L, Krasensky-Wrzaczek J, Sipari N, Keinänen M, Tyystjärvi E, Rintamäki E, De Rybel B, Salojärvi J, Van Breusegem F, Fernie AR, Brosché M, Permi P, Aro E-M, Wrzaczek M, Kangasjärvi J (2019) Arabidopsis RCD1 coordinates chloroplast and mitochondrial functions through interaction with ANAC transcription factors. eLife **8:** e43284
Smith C, Barthet M, Melino V, Smith P, Day D, Soole K (2011) Alterations in the mitochondrial alternative NAD(P)H Dehydrogenase NDB4 lead to changes in

mitochondrial electron transport chain composition, plant growth and response to oxidative stress. Plant Cell Physiol **52:** 1222-1237

Stepanova AN, Hoyt JM, Hamilton AA, Alonso JM (2005) A Link between Ethylene and Auxin Uncovered by the Characterization of Two Root-Specific Ethylene-Insensitive Mutants in Arabidopsis. The Plant Cell **17:** 2230-2242

Stepanova AN, Robertson-Hoyt J, Yun J, Benavente LM, Xie D-Y, Doležal K, Schlereth A, Jürgens G, Alonso JM (2008) TAA1-Mediated Auxin Biosynthesis Is Essential for Hormone Crosstalk and Plant Development. Cell **133:** 177-191

Stepanova AN, Yun J, Likhacheva AV, Alonso JM (2007) Multilevel Interactions between Ethylene and Auxin in Arabidopsis Roots. The Plant Cell **19:** 2169-2185

Stracke R, Werber M, Weisshaar B (2001) The R2R3-MYB gene family in Arabidopsis thaliana. Current Opinion in Plant Biology **4:** 447-456

Swarup R, Perry P, Hagenbeek D, Van Der Straeten D, Beemster GTS, Sandberg Gr, Bhalerao R, Ljung K, Bennett MJ (2007) Ethylene Upregulates Auxin Biosynthesis in Arabidopsis Seedlings to Enhance Inhibition of Root Cell Elongation. The Plant Cell **19:** 2186-2196

Sweetlove LJ, Beard KF, Nunes-Nesi A, Fernie AR, Ratcliffe RG (2010) Not just a circle: flux modes in the plant TCA cycle. Trends Plant Sci **15:** 462-470

Takasaki H, Maruyama K, Takahashi F, Fujita M, Yoshida T, Nakashima K, Myouga F, Toyooka K, Yamaguchi-Shinozaki K, Shinozaki K (2015) SNAC-As, stress-responsive NAC transcription factors, mediate ABA-inducible leaf senescence. The Plant Journal **84:** 1114-1123

Tian T, Ma L, Liu Y, Xu D, Chen Q, Li G (2020) Arabidopsis FAR-RED ELONGATED HYPOCOTYL3 Integrates Age and Light Signals to Negatively Regulate Leaf Senescence. The Plant Cell **32:** 1574-1588

Tognetti VB, Van Aken O, Morreel K, Vandenbroucke K, van de Cotte B, De Clercq I, Chiwocha S, Fenske R, Prinsen E, Boerjan W, Genty B, Stubbs KA, Inzé D, Van Breusegem F (2010) Perturbation of Indole-3-Butyric Acid Homeostasis by the UDP-Glucosyltransferase UGT74E2 Modulates Arabidopsis Architecture and Water Stress Tolerance. The Plant Cell **22:** 2660-2679

Trentmann SM, Kende H (1995) Analysis of Arabidopsis cDNA that shows homology to the tomato E8 cDNA. Plant Molecular Biology **29:** 161-166

Van Aken O, De Clercq I, Ivanova A, Law SR, Van Breusegem F, Millar AH, Whelan J (2016) Mitochondrial and Chloroplast Stress Responses Are Modulated in Distinct Touch and Chemical Inhibition Phases. Plant Physiology **171:** 2150-2165

Van Aken O, Ford E, Lister R, Huang S, Millar AH (2016) Retrograde signalling caused by heritable mitochondrial dysfunction is partially mediated by ANAC017 and improves plant performance. Plant J **88:** 542-558

Vandenbussche F, Vriezen WH, Smalle J, Laarhoven LJJ, Harren FJM, Van Der Straeten D (2003) Ethylene and Auxin Control the Arabidopsis Response to Decreased Light Intensity. Plant Physiology **133:** 517-527

Vaseva II, Qudeimat E, Potuschak T, Du Y, Genschik P, Vandenbussche F, Van Der Straeten D (2018) The plant hormone ethylene restricts Arabidopsis growth via the epidermis. Proceedings of the National Academy of Sciences **115:** E4130-E4139

Wagner S, Van Aken O, Elsasser M, Schwarzlander M (2018) Mitochondrial Energy Signaling and Its Role in the Low-Oxygen Stress Response of Plants. Plant Physiol **176:** 1156-1170

Wang H-Z, Yang K-Z, Zou J-J, Zhu L-L, Xie ZD, Morita MT, Tasaka M, Friml J, Grotewold E, Beeckman T, Vanneste S, Sack F, Le J (2015) Transcriptional regulation of PIN genes by FOUR LIPS and MYB88 during Arabidopsis root gravitropism. Nature Communications **6:** 8822

Wang X, Auwerx J (2017) Systems Phytohormone Responses to Mitochondrial Proteotoxic Stress. Molecular Cell **68:** 540-551.e545

Wang Y, Berkowitz O, Selinski J, Xu Y, Hartmann A, Whelan J (2018) Stress responsive mitochondrial proteins in Arabidopsis thaliana. Free Radical Biology and Medicine **122:** 28-39

Wang Y, Lyu W, Berkowitz O, Radomiljac Jordan D, Law Simon R, Murcha Monika W, Carrie C, Teixeira Pedro F, Kmiec B, Duncan O, Van Aken O, Narsai R, Glaser E, Huang S, Roessner U, Millar AH, Whelan J (2016) Inactivation of Mitochondrial Complex I Induces the Expression of a Twin Cysteine Protein that Targets and Affects Cytosolic, Chloroplastidic and Mitochondrial Function. Molecular Plant **9:** 696-710

Wang Y, Selinski J, Mao C, Zhu Y, Berkowitz O, Whelan J (2020) Linking mitochondrial and chloroplast retrograde signalling in plants. Philosophical Transactions of the Royal Society B: Biological Sciences **375:** 20190410

Wolfe CJ, Kohane IS, Butte AJ (2005) Systematic survey reveals general applicability of "guilt-by-association" within gene coexpression networks. BMC Bioinformatics **6:** 227

Woodward C, Bemis SM, Hill EJ, Sawa S, Koshiba T, Torii KU (2005) Interaction of Auxin and ERECTA in Elaborating Arabidopsis Inflorescence Architecture Revealed by the Activation Tagging of a New Member of the YUCCA Family Putative Flavin Monooxygenases. Plant Physiology **139:** 192-203

Wu Q, Li Y, Lyu M, Luo Y, Shi H, Zhong S (2020) Touch-induced seedling morphological changes are determined by ethylene-regulated pectin degradation. Science Advances **6:** eabc9294

Xu J, Li Y, Wang Y, Liu H, Lei L, Yang H, Liu G, Ren D (2008) Activation of MAPK Kinase 9 Induces Ethylene and Camalexin Biosynthesis and Enhances Sensitivity to Salt Stress in Arabidopsis*. Journal of Biological Chemistry **283:** 26996-27006

Yamaguchi M, Ohtani M, Mitsuda N, Kubo M, Ohme-Takagi M, Fukuda H, Demura T (2010) VND-INTERACTING2, a NAC Domain Transcription Factor, Negatively Regulates Xylem Vessel Formation in Arabidopsis The Plant Cell **22:** 1249-1263

Yan Y, Li C, Dong X, Li H, Zhang D, Zhou Y, Jiang B, Peng J, Qin X, Cheng J, Wang X, Song P, Qi L, Zheng Y, Li B, Terzaghi W, Yang S, Guo Y, Li J (2020) MYB30 Is a Key Negative Regulator of Arabidopsis Photomorphogenic Development That Promotes PIF4 and PIF5 Protein Accumulation in the Light. The Plant Cell **32:** 2196-2215

Yang W, Cortijo S, Korsbo N, Roszak P, Schiessl K, Gurzadyan A, Wightman R, Jönsson H, Meyerowitz E (2021) Molecular mechanism of cytokinin-activated cell division in Arabidopsis. Science **371:** 1350-1355

Yang Y, Zhang L, Chen P, Liang T, Li X, Liu H (2020) UV-B photoreceptor UVR8 interacts with MYB73/MYB77 to regulate auxin responses and lateral root development. The EMBO Journal **39:** e101928

Yoo SD, Cho YH, Tena G, Xiong Y, Sheen J (2008) Dual control of nuclear EIN3 by bifurcate MAPK cascades in C2H4 signalling. Nature **451:** 789-795

Yu X, Li L, Zola J, Aluru M, Ye H, Foudree A, Guo H, Anderson S, Aluru S, Liu P, Rodermel S, Yin Y (2011) A brassinosteroid transcriptional network revealed by genome-wide identification of BESI target genes in Arabidopsis thaliana. The Plant Journal **65:** 634-646

Zhang H, Zhao Y, Zhu J-K (2020) Thriving under Stress: How Plants Balance Growth and the Stress Response. Developmental Cell **55:** 529-543

Zhang Y, Liu T, Meyer CA, Eeckhoute J, Johnson DS, Bernstein BE, Nusbaum C, Myers RM, Brown M, Li W, Liu XS (2008) Model-based Analysis of ChIP-Seq (MACS). Genome Biology **9:** R137

Zhao C, Wang P, Si T, Hsu C-C, Wang L, Zayed O, Yu Z, Zhu Y, Dong J, Tao WA, Zhu J-K (2017) MAP Kinase Cascades Regulate the Cold Response by Modulating ICE1 Protein Stability. Developmental Cell **43:** 618-629.e615

Zhao Q, Guo H-W (2011) Paradigms and Paradox in the Ethylene Signaling Pathway and Interaction Network. Molecular Plant **4:** 626-634

Zhao Y, Xing L, Wang X, Hou Y-J, Gao J, Wang P, Duan C-G, Zhu X, Zhu J-K (2014) The ABA Receptor PYL8 Promotes Lateral Root Growth by Enhancing MYB77-Dependent Transcription of Auxin-Responsive Genes. Science Signaling **7:** ra53-ra53

Zhou C, Cai Z, Guo Y, Gan S (2009) An arabidopsis mitogen-activated protein kinase cascade, MKK9-MPK6, plays a role in leaf senescence. Plant physiology **150:** 167-177

4. CHAPTER IV- GENERAL DISCUSSION

The overall aims of this project were to identify and characterise further molecular components involved in mitochondrial retrograde signalling. Prior to this study, the induction of *AOX1a* has been widely used as the main model in Arabidopsis, along with bio-informatic approaches, to dissect and understand the role of mitochondrial signalling. While informative, these studies have some limitations, one being that the induction of *AOX1a* also occurs with perturbation of chloroplast function. This has led to the important finding of links between mitochondrial and chloroplast signalling. However, it also raises the question if there are mitochondria-specific pathways or if there are specific branches in the ANAC017-mediated pathway, as it is a high-level regulator.

Mitochondria maintain plant energy homeostasis and are direct targets, sensors and initiators of signalling pathways under adverse environmental conditions. In this role they change the expression of nuclear gene to optimize their own function but also to preserve cellular homeostasis (Woodson and Chory, 2008; Kmiecik et al., 2016; Crawford et al., 2018; Wang et al., 2018; Meng et al., 2020; Pfannschmidt et al., 2020). In this study I identified several genes that are induced by the treatment with Antimycin A, but not by high light. These were then tested for their suitable to further study, based on the ability of their promoter to drive the expression of a marker genes, namely luciferase. A 2-oxoglutarate and Fe(II)-dependent oxygenase (OGO, AT5G43450) with sequence similarity to the ethylene generating 1-aminocyclopropane-1-carboxylic acid (ACC) oxidase is a mitochondrial dysfunction-specific inducible gene (Chapter II). I showed this gene is regulated by novel mitochondrial retrograde response components ROG2 (SIN3) encoding an enhancer of ETHYLENE RESPONSE FACTOR 7 activity and ROG4 encoding a acyl-CoA N-acyltransferase (Chapter II). My work further demonstrated that part of the mitochondrial dysfunction transcriptional cascade was mediated by the ethylene-signalling regulator ETHYLENE INSENSITIVE 3 (EIN3) and that the transcription factor ANAC017 regulates mitochondrial retrograde signalling by controlling the transcriptional response to mitochondrial dysfunction by directly targeting ethylene- and auxin-related signalling components (Chapter III). Together, these results expand on the knowledge of mitochondrial signalling and how it interacts with hormone signalling pathways.

4.1 Plant growth and stress tolerance

Tolerance to adverse environmental conditions and growth are antagonistic. While tolerance to adverse conditions is an important survival feature in plants, it results in a

slowing or complete cessation of plant growth, which is undesirable for crop productivity (Zhang et al., 2020). Plant growth and productivity can be substantially reduced under abiotic stress caused by excesses or deficiencies in environmental factors such as water, light, temperature, and nutrients (Urano et al., 2010; Zhu, 2016). Up to 70% of potential yield can be lost in key agricultural crops under adverse environment (Boyer, 1982; Vij and Tyagi, 2007; Zurbriggen et al., 2010; Zhang et al., 2020). Severe weather events causing flooding, drought or freezing are likely to increase with climate change (Bailey-Serres et al., 2012). In addition, biotic stress such as rust fungi are responsible for a global loss of 5 million tons for wheat alone (Beddow et al., 2015; Zhang et al., 2020). With the increasing global population, a sustainable intensification of agriculture is needed in which crop yields are increased under adverse environmental conditions, as there is no more arable land available, and with finite resources such as water and phosphorus fertiliser.

Mechanistically the reduction of plant growth under stress is a result of the inhibition of growth process, including both cell expansion and division. This is due to altered resource allocation, favouring preservation of resources and even build-up of reserves when the growth environment becomes unfavourable (Zhang et al., 2020). For instance, plant growth is inhibited under drought treatment with the lack of water needed for cell turgor that drives cell expansion (Tardieu et al., 2011; Nelissen et al., 2018). On the other hand, cell signalling is triggered by adverse environment to prevent and repair cellular damages and allow acclimation to stress conditions (Zhu, 2016; Fu et al., 2020). This is well established in plant defence responses against pathogens. The adaptation to biotic stresses optimises the balance between defence and growth, with the extremes being plants with a constitutively active defence response or plants that induce resistance mechanisms only when needed. This adaptation is driven by the prevalence of pathogens in the environment, with the former being favourable when pathogen pressure is high and the associated growth penalty is the lesser of two evils, while the latter allows faster growth when pathogen attack is rare but with the intrinsic risk of a lower survival rate (Baldwin, 1998; Paul-Victor et al., 2010; Alcazar et al., 2011). A number of studies have shown that growth retardation due to strong stress responses can be repressed by mutation and propose that growth retardation under stress is due to antagonistic transcriptional networks (Züst and Agrawal, 2017). Thus, mutants that have constitutive defence pathways and display a growth penalty can be rescued by additional mutations, without losing the defence activation (Hemm et al., 2003; Vila-Aiub et al., 2009; Paul-Victor et al., 2010; Joseph et al., 2013; Campos et al., 2016; Kliebenstein, 2016).

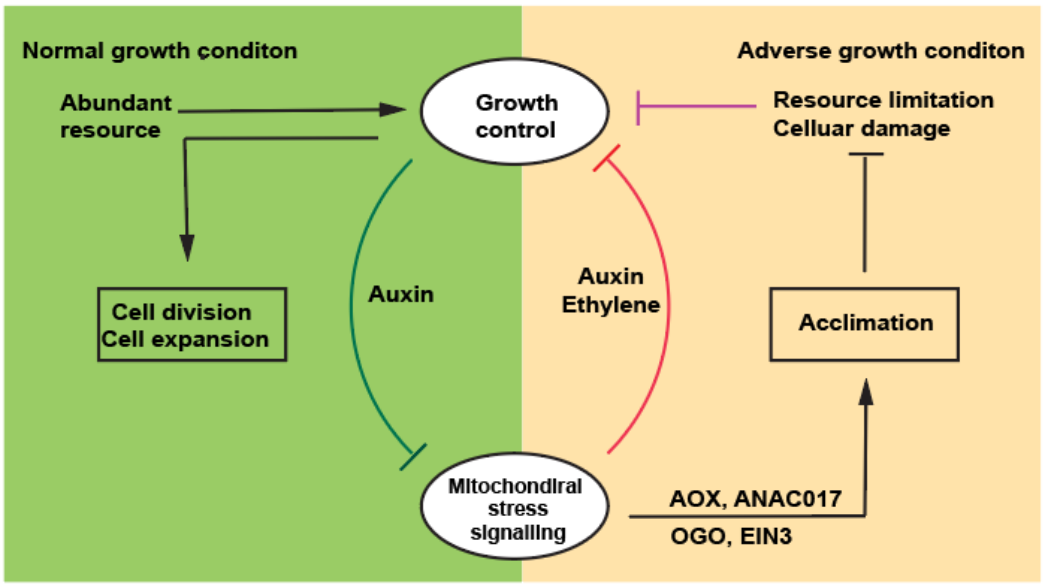

Figure 1. The relationship between plant growth and mitochondrial stress response
Plant growth is inhibited under adverse environmental conditions with limited resource and cellular damage (purple path). Mitochondria stress signalling are trigged with growth inhibition (red path) and activates stress response and acclimation. Under normal growth conditions with abundance resource, growth signalling is activated and partially repress the mitochondrial stress signalling (green path) besides promoting growth. Positive regulation is indicated by arrows, and negative regulation is indicated by blunt ends. Adapted from Ivanova et al (2014); Zhang et al (2020).

Similarly, the growth versus abiotic stress tolerance dilemma is also well established and has traditionally been ascribed to a resource partitioning issue, i.e. energy and metabolites are used to support either growth or tolerance mechanisms (Zhang et al., 2020). This was apparent in early studies using key up-stream regulators of stress signalling in transgenic approaches. Although the overexpression of transcription factors led to increased tolerance to stresses such as cold or drought, these plants had severe growth retardation under non-stress conditions and hence this approach is not viable in agriculture (Kasuga et al., 1999). An activation of tolerance mechanisms under standard growth conditions will be wasteful as it uses energy needlessly that could be funnelled into growth, and at the same time it is likely that energy is needed to mitigate this process in a futile cycle. Hence plants need to strike a delicate balance to prevent either process to take over. The mitochondrial master regulator of mitochondrial signalling ANAC017 is a good example in this respect. Under standard growth conditions knock-out mutants show increased biomass production and accelerated growth, while overexpressing lines show retarded growth (Meng et al., 2019). Thus, a mechanism by which ANAC017 is released from the ER under mitochondrial stress suggests this allows for a tighter regulation than transcriptional activation alone (Ng et al., 2013). The mechanisms of this growth control via ANAC017 were so far unknown but

thought to be rather indirect through the activation of the downstream stress-related signalling cascades leading to programmed cell death and early senescence (Meng et al., 2019).

The results presented in this thesis showed that ANAC017 directly targets genes of the auxin and ethylene pathway (Chapter III), a yet unknown and direct mechanism to regulate the mitochondrial dysfunction response with overall plant growth (Figure 1). The transcriptional cascades suggested that the activation of the ethylene pathways precedes the activation of the auxin pathway. The latter has a known antagonistic relationship with mitochondrial signalling and thus provides a feedback loop to prevent a detrimental effect of sustained activity of stress-related genes such as AOX1a (Ng et al., 2013). An increased production of ethylene and its signalling cascade triggered by ANAC017 might explain the growth-retarding effect of ANAC017 overexpression. Indeed, a direct target of ANAC017 is ERF8 (Chapter III) for which increased expression leads to inhibition of growth (Koyama et al., 2013). This is a generally observed phenotype after overexpression of components of the ethylene signalling pathways, which includes biosynthesis and transcription factors that are also part of the ANAC017-dependent mitochondrial signalling pathway (Dubois et al., 2018).

Hence, to improve plant performance an uncoupling of this ethylene-signalling branch from the primary mitochondrial stress response might allow for sustained growth under mild stress conditions. This could however lead to failing crops under severe stress or necessitate substantial mitigation strategies by growers. Thus, this approach will depend on cost-benefit evaluation for prevailing seasonal growth conditions. Achieving better crop performance while sustaining or even improving crop yields will need a better understanding of the involved processes. Results presented in this work are therefore contributing towards this goal.

4.2 Location and function

It is well established in biology that the location of a process is critical to function. This is relevant on the cellular level for communication between different organelles, but also important on the tissue or whole plant level. Across different tissues, mitochondria vary substantially in their morphology, number and function (Logan, 2006). In Arabidopsis, cold treatment leads to increased total mitochondrial number and volume in epidermal cells, whilst the ratio of cristae to matrix ratio increases in the mesophyll (Armstrong et al., 2006). Also, in the epidermis mitochondrial numbers decrease faster than in the mesophyll under dark induced senescence (Keech et al., 2007). The phenomenon of dual targeting of

proteins is now well established and accepted in plant biology, yet clearly the same protein carrying out the same biochemical reaction in different locations has different functions. Also, there are well over 100 proteins dually targeted to mitochondria and chloroplasts that fall into this category (Carrie and Small, 2013). In addition, some proteins are proposed to have regulatory functions, in addition to their well characterised biochemical activities, sometimes referred to as moonlighting proteins (Su et al., 2019). Likewise, the location of production of any signal molecules is critical and this also established for retrograde signalling. While it is widely accepted that various ROS species or Ca^{2+} are produced in response to adverse conditions and emanating from mitochondria, their signalling is further specified by their spatiotemporal variation in concentrations based on the identity of the protein or molecule that interacts with certain ROS species or Ca^{2+} (Kmiecik et al., 2016; Castro et al., 2021). In addition, the action of plant hormones is also highly dependent on the location of their synthesis and transport across cellular compartments and within tissues (Anfang and Shani, 2021). As a gaseous hormone, ethylene might also have a function in signalling mitochondrial dysfunction away from the direct location of stress impact. A role for mitochondria in the adaptation to submergence has been established in our lab and depends on the retrograde signalling pathway (Meng et al., 2020). Ethylene is the major hormone regulating the response to submergence and therefore a direct interconnection of the two signalling pathways explains the close relationship of the transcriptional responses to inhibition of mitochondrial function and hypoxia/submergence (Wagner et al., 2018; Meng et al., 2020).

Expression of OGO showed a defined expression pattern within leaves, flowers and roots suggesting a role of this protein in distinct parts of the plant. An increased expression during senescence also suggests a function at different stages throughout the plant's development (Chapter II). It has been reported by colleagues in our laboratory that interaction of auxin and ethylene mediates retrograde signalling during mitochondrial dysfunction specifically in the epidermis (Berkowitz et al., 2021). This data set, based on laser capture dissection followed by RNA-seq, suggests a higher expression of OGO in the mesophyll under standard growth conditions, while AA treatment leads to an increase in expression to similar levels across all three analysed tissues (epidermis, mesophyll, vasculature). This suggests a more generalised role for OGO in different tissues under stress treatments and highlights its importance when mitochondrial function is impaired.

4.3 Conclusions and perspectives

An important outstanding question relates to the molecular function of the OGO protein. Although my attempts to obtain native protein with activity have been unsuccessful, a bacterial expression system yielded substantial amounts of protein that were not soluble and accumulated in inclusion bodies (Chapter II, Supplemental Figure 1). This provides confidence that optimisation or changes in expression system will lead to the purification of active OGO protein for subsequent analyses in the future. This will allow to ascertain the specific role of OGO in the mitochondrial stress response but would also contribute to the characterisation of the 2-oxoglutarate (2OG) and Fe(II)-dependent oxygenase family. The latter is one of the largest protein families in plants and with only few family members investigated in detail. Elucidation of OGO function would be a further step to understand the variety of activities across this protein family and its evolution.

In this study a combination of approaches was used to gain further understanding of mitochondrial retrograde signalling. Combined these approaches showed that downstream of ANAC017 ethylene is involved in a branch of the response when ANAC017 is activated (Chapter III). While in this study OGO was not induced by high light like AOX1a, there are a variety of studies that suggest that ethylene may be involve or interact with chloroplast retrograde signalling. It has been proposed that ethylene signalling is involved in the suppression of photomorphogenesis (Gommers et al., 2021) and ethylene response factors have also been shown to be involved in a fast response to high light (Vogel et al., 2014). Also, it has been shown that PAP/SAL1 signalling is involved in iron deficiency response, that also involved ethylene signalling. SAL1 is present in both mitochondria and chloroplasts, although no studies exist on the signalling role for mitochondria (Balparda et al., 2020; Balparda et al., 2021). As with ROS, ethylene may be involved in a variety of pathways produced in different cells, or alternatively the convergence of signalling pathway may mean that these components are shared. The elucidation of the factors involved in ethylene mediated mitochondrial signalling outlined here will help identify the overlap, if any, with the role of ethylene in mitochondrial and chloroplast retrograde signalling.

As outlined above the cell specific nature of organelle retrograde signalling has not been studied to date. However, initial studies suggest that cell specificity does exist with respect to organelle signalling, as well as hormonal signalling, and this interaction needs to be explored further (Berkowitz et al., 2021). With the techniques emerging for single cell transcriptomics, the cell specific nature of stress responses will become clearer and allow greater insight into how different cells/tissues respond to adverse conditions. This has potential for translational research to improve the resilience of crops to adverse growth conditions and increase their performance to sustain yields.

4.3 LITERATURE CITED

Alcazar R, Reymond M, Schmitz G, de Meaux J (2011) Genetic and evolutionary perspectives on the interplay between plant immunity and development. Curr Opin Plant Biol **14:** 378-384

Anfang M, Shani E (2021) Transport mechanisms of plant hormones. Curr Opin Plant Biol **63:** 102055

Armstrong AF, Logan DC, Tobin AK, O'Toole P, Atkin OK (2006) Heterogeneity of plant mitochondrial responses underpinning respiratory acclimation to the cold in Arabidopsis thaliana leaves. Plant Cell Environ **29:** 940-949

Bailey-Serres J, Fukao T, Gibbs DJ, Holdsworth MJ, Lee SC, Licausi F, Perata P, Voesenek LA, van Dongen JT (2012) Making sense of low oxygen sensing. Trends Plant Sci **17:** 129-138

Baldwin IT (1998) Jasmonate-induced responses are costly but benefit plants under attack in native populations. Proc Natl Acad Sci U S A **95:** 8113-8118

Balparda M, Armas AM, Estavillo GM, Roschzttardtz H, Pagani MA, Gomez-Casati DF (2020) The PAP/SAL1 retrograde signaling pathway is involved in iron homeostasis. Plant Mol Biol **102:** 323-337

Balparda M, Armas AM, Gomez-Casati DF, Pagani MA (2021) PAP/SAL1 retrograde signaling pathway modulates iron deficiency response in alkaline soils. Plant Sci **304:** 110808

Beddow JM, Pardey PG, Chai Y, Hurley TM, Kriticos DJ, Braun HJ, Park RF, Cuddy WS, Yonow T (2015) Research investment implications of shifts in the global geography of wheat stripe rust. Nat Plants **1:** 15132

Berkowitz O, Xu Y, Liew LC, Wang Y, Zhu Y, Hurgobin B, Lewsey MG, Whelan J (2021) RNA-seq analysis of laser microdissected Arabidopsis thaliana leaf epidermis, mesophyll and vasculature defines tissue-specific transcriptional responses to multiple stress treatments. Plant J

Boyer JS (1982) Plant productivity and environment. Science **218:** 443-448

Campos ML, Yoshida Y, Major IT, de Oliveira Ferreira D, Weraduwage SM, Froehlich JE, Johnson BF, Kramer DM, Jander G, Sharkey TD (2016) Rewiring of jasmonate and phytochrome B signalling uncouples plant growth-defense tradeoffs. Nature communications **7:** 1-10

Carrie C, Small I (2013) A reevaluation of dual-targeting of proteins to mitochondria and chloroplasts. Biochim Biophys Acta **1833:** 253-259

Castro B, Citterico M, Kimura S, Stevens DM, Wrzaczek M, Coaker G (2021) Stress-induced reactive oxygen species compartmentalization, perception and signalling. Nat Plants **7:** 403-412

Crawford T, Lehotai N, Strand A (2018) The role of retrograde signals during plant stress responses. J Exp Bot **69:** 2783-2795

Dubois M, Van den Broeck L, Inze D (2018) The Pivotal Role of Ethylene in Plant Growth. Trends Plant Sci **23:** 311-323

Fu L, Wang P, Xiong Y (2020) Target of Rapamycin Signaling in Plant Stress Responses. Plant Physiol **182:** 1613-1623

Gommers CMM, Ruiz-Sola MA, Ayats A, Pereira L, Pujol M, Monte E (2021) GENOMES UNCOUPLED1-independent retrograde signaling targets the ethylene pathway to repress photomorphogenesis. Plant Physiol **185:** 67-76

Hemm MR, Ruegger MO, Chapple C (2003) The Arabidopsis ref2 mutant is defective in the gene encoding CYP83A1 and shows both phenylpropanoid and glucosinolate phenotypes. The Plant Cell **15:** 179-194

Ivanova A, Law SR, Narsai R, Duncan O, Lee JH, Zhang B, Van Aken O, Radomiljac JD, van der Merwe M, Yi K, Whelan J (2014) A Functional Antagonistic Relationship

between Auxin and Mitochondrial Retrograde Signaling Regulates Alternative Oxidase1a Expression in Arabidopsis. Plant Physiol **165:** 1233-1254

Joseph B, Corwin JA, Li B, Atwell S, Kliebenstein DJ (2013) Cytoplasmic genetic variation and extensive cytonuclear interactions influence natural variation in the metabolome. Elife **2:** e00776

Kasuga M, Liu Q, Miura S, Yamaguchi-Shinozaki K, Shinozaki K (1999) Improving plant drought, salt, and freezing tolerance by gene transfer of a single stress-inducible transcription factor. Nat Biotechnol **17:** 287-291

Keech O, Pesquet E, Ahad A, Askne A, Nordvall D, Vodnala SM, Tuominen H, Hurry V, Dizengremel P, Gardestroem P (2007) The different fates of mitochondria and chloroplasts during dark-induced senescence in Arabidopsis leaves. Plant, cell & environment **30:** 1523-1534

Kliebenstein DJ (2016) False idolatry of the mythical growth versus immunity tradeoff in molecular systems plant pathology. Physiological and Molecular Plant Pathology **95:** 55-59

Kmiecik P, Leonardelli M, Teige M (2016) Novel connections in plant organellar signalling link different stress responses and signalling pathways. J Exp Bot **67:** 3793-3807

Koyama T, Nii H, Mitsuda N, Ohta M, Kitajima S, Ohme-Takagi M, Sato F (2013) A regulatory cascade involving class II ETHYLENE RESPONSE FACTOR transcriptional repressors operates in the progression of leaf senescence. Plant Physiol **162:** 991-1005

Logan DC (2006) The mitochondrial compartment. J Exp Bot **57:** 1225-1243

Meng X, Li L, De Clercq I, Narsai R, Xu Y, Hartmann A, Claros DL, Custovic E, Lewsey MG, Whelan J, Berkowitz O (2019) ANAC017 Coordinates Organellar Functions and Stress Responses by Reprogramming Retrograde Signaling. Plant Physiol **180:** 634-653

Meng X, Li L, Narsai R, De Clercq I, Whelan J, Berkowitz O (2020) Mitochondrial signalling is critical for acclimation and adaptation to flooding in Arabidopsis thaliana. Plant J **103:** 227-247

Nelissen H, Sun XH, Rymen B, Jikumaru Y, Kojima M, Takebayashi Y, Abbeloos R, Demuynck K, Storme V, Vuylsteke M, De Block J, Herman D, Coppens F, Maere S, Kamiya Y, Sakakibara H, Beemster GTS, Inze D (2018) The reduction in maize leaf growth under mild drought affects the transition between cell division and cell expansion and cannot be restored by elevated gibberellic acid levels. Plant Biotechnol J **16:** 615-627

Ng S, Ivanova A, Duncan O, Law SR, Van Aken O, De Clercq I, Wang Y, Carrie C, Xu L, Kmiec B, Walker H, Van Breusegem F, Whelan J, Giraud E (2013) A membrane-bound NAC transcription factor, ANAC017, mediates mitochondrial retrograde signaling in Arabidopsis. Plant Cell **25:** 3450-3471

Paul-Victor C, Zust T, Rees M, Kliebenstein DJ, Turnbull LA (2010) A new method for measuring relative growth rate can uncover the costs of defensive compounds in Arabidopsis thaliana. New Phytol **187:** 1102-1111

Pfannschmidt T, Terry MJ, Van Aken O, Quiros PM (2020) Retrograde signals from endosymbiotic organelles: a common control principle in eukaryotic cells. Philos Trans R Soc Lond B Biol Sci **375:** 20190396

Su B, Qian Z, Li T, Zhou Y, Wong A (2019) PlantMP: a database for moonlighting plant proteins. Database (Oxford) **2019**

Tardieu F, Granier C, Muller B (2011) Water deficit and growth. Co-ordinating processes without an orchestrator? Curr Opin Plant Biol **14:** 283-289

Urano K, Kurihara Y, Seki M, Shinozaki K (2010) 'Omics' analyses of regulatory networks in plant abiotic stress responses. Curr Opin Plant Biol **13:** 132-138

Vij S, Tyagi AK (2007) Emerging trends in the functional genomics of the abiotic stress response in crop plants. Plant Biotechnol J **5:** 361-380

Vila-Aiub MM, Neve P, Powles SB (2009) Fitness costs associated with evolved herbicide resistance alleles in plants. New Phytol **184:** 751-767

Vogel MO, Moore M, Konig K, Pecher P, Alsharafa K, Lee J, Dietz KJ (2014) Fast retrograde signaling in response to high light involves metabolite export, MITOGEN-ACTIVATED PROTEIN KINASE6, and AP2/ERF transcription factors in Arabidopsis. Plant Cell **26:** 1151-1165

Wagner S, Van Aken O, Elsasser M, Schwarzlander M (2018) Mitochondrial Energy Signaling and Its Role in the Low-Oxygen Stress Response of Plants. Plant Physiol **176:** 1156-1170

Wang Y, Berkowitz O, Selinski J, Xu Y, Hartmann A, Whelan J (2018) Stress responsive mitochondrial proteins in Arabidopsis thaliana. Free Radic Biol Med **122:** 28-39

Woodson JD, Chory J (2008) Coordination of gene expression between organellar and nuclear genomes. Nat Rev Genet **9:** 383-395

Zhang H, Zhao Y, Zhu JK (2020) Thriving under Stress: How Plants Balance Growth and the Stress Response. Dev Cell **55:** 529-543

Zhu J-K (2016) Abiotic stress signaling and responses in plants. Cell **167:** 313-324

Zurbriggen MD, Hajirezaei MR, Carrillo N (2010) Engineering the future. Development of transgenic plants with enhanced tolerance to adverse environments. Biotechnol Genet Eng Rev **27:** 33-56

Züst T, Agrawal AA (2017) Trade-offs between plant growth and defense against insect herbivory: an emerging mechanistic synthesis. Annual review of plant biology **68:** 513-534